The Palaeo-Ecology and Geochemistry of Potential Source and Reservoir Microbialites in the Ediacaran-Cambrian Sirab Formation, Sultanate of Oman.

Volume 1 of 2.

Karrer Kazyumba Mbayo

Degree of Msc. research

University of Dublin, Trinity College

Department of Geology

Supervisor: Dr Christopher Nicholas

Submitted to the University of Dublin, Trinity College,

July 2022.

Declaration

I hereby declare that this is entirely my own work and that it has not been submitted as an exercise for the award of a degree at this or any other university. I agree that the library may lend or copy this dissertation on request._____

KARRER KAZYUMBA MBAYO ___/07/2022

Summary

Oil has made the geology of Oman a scientific feature for geological research. The lithostratigraphy of the Huqf Supergroup of Oman, incorporates the Ara Group which is a geological Formation representing the Ediacaran-Cambrian time interval of the South Oman Salt Basin (SOSB) due to its intrasalt petroleum reserves, the production of which has been active in this region for many years. However, the Ara Group does not outcrop on the surface and the only means of its investigation has been made using various drilling and geophysical data. An outer Platform section (Birba) with a carbonate ramp interspersed with evaporite levels and a Basin section consisting of shale at the base (U) interspersed with a silicilyte level (Athel) then closed at the top by a shale level (Thuleilat) are recognized for the Ara Group and the evaporite levels meet from the base to the top of the Basin. The Ara Group is currently defined as a thick set of at least six carbonate-evaporite rings which are each informally labeled A0 to A6 and subdivided into carbonate "C" or evaporite "E" units such as A4C and A4E while volcanic ash was reported to be located in A3C, which geochronologically dated U-Pb to 542 ± 0.6 Ma or nearly identical to the biostratigraphic age of ancient calcareous-tabular fossils *Claudina* and possibly *Namacalathus* found in A4 (542 ± 0.6 Ma). But as there is no direct observation of the Ara Group, the drilling well of the Platform was named birba (well BB-3) while those of the Basin are (ALNR-1 and MM NW-7). Along with the Ara Group, it has been reported that the Sirab Formation which outcrops on the surface in

Oman in the Al-Huqf region is a stratigraphic age equivalent to the Ara Group. Although this Formation is accessible at the surface and promising for evaluating the architecture of sedimentary facies of intrasalt reservoirs Oil and Gas encountered in the subsurface for the Ara Group, given that the two geological Formations are mainly carbonates with a high content of dolomite whose the facies are similar, however it is worth noting that there is no presence of volcanic ash or even tabular *Claudina* fossils and possibly of *Namacalathus* recognized to date in the strata of the Sirab Formation. Nevertheless, the geochemical analysis available from the Ara Group drill cores in the Platform and the Basin allows them to be correlated chemostratigraphically.

Here in this thesis, the chemostratigraphy of the Major Geochemical Elements (Ca, Mg, Fe. Al, Mn, P in weight as well as K_2O%, Na_2O% in percentage) combined with REEs and Trace Elements (Th, Ti, Zr, V, Mo, $U_{authigen}$) made it possible to compare these two Formations. It appears from the results obtained that the palaeo-ecology of the Sirab environment is largely dominated by anoxic conditions similar to the Ara Group, with regard to the real anomalies in Ce*. The majority of Y/Ho ratios indicate less marine influence and/or viewed from another angle, loss of marine signal similar to the Ara Group while REEs concentrations in the Sirab Formation that would otherwise have shown more affinity with the chondrites of the crust according to their Y/Ho ratios are indeed depleted with respect to the PAAS as in the rocks of the Birba Platform. The Manganese concentrations present in

the carbonates of Sirab do not seem to have been enriched by diagenesis whereas the restriction of the circulation of M^{2+} ions seems to result from an endorheic capture of the structure of the paleo-relief which would have been devoid of marine bonding permanently in the south, east and west of the Al-Huqf region with regard to the results of Y/Ho analyzes in the localities of Wadi Shital and Wadi Shuram, while Infinitely small evidence of a brief marine connection can be recognized through the uppermost strata of the Sirab Formation which lie north of the Al-Huqf region in the locality of Wadi Aswad, in the Aswad Member. The entire Formation of Sirab has been divided itself into three main Member which are form bottom to the top: Ramayli Member, Shital Member and Aswad Member and due to time to time litle change to the sedimentaries facies observed throughout the Formation, internal subdivisions in unite as lower and upper Ramayli or again lower, middle and upper Shital Member, have been also admitted for this Formation. However, in relation with the Oman region where Sirab Formation spreads visible outcrops, there was recognize that there is structural change between crossing Nafum Group which is more old in age than Sirab Formation which overlains it with Ramayli Member. Indeed, Buah Formation belongs to the top of Nafum Group and it is overlain in the majority areas studies here by Sirab Formation while this rests confortably at top of Buah. However, where such as palaeo-topographic high dominating the region of Sirab Formation would has been actived before the setting of Sirab, discordante angular was reported on the stratigraphy continuity between both Buah Formation on the bottom and Sirab Formation to

the top whilst the rocks facies sedimentary has just litle or not change. This areas such as in locality nammed Wadi Salutiyyat; were seen as a lateral variable of Ramayli Member which was called Salutiyyat Member.

The details of the petrographic and geochemical analyzes carried out in this thesis make it possible to summarize the palaeo-ecology of Sirab Formation in the light of that of the Ara Group in the drillings of the Platform and the Basin. Here is after this brief summary of the objective pursued in this thesis; the development, argumentation and scientific contributions to the exploration of the Sirab Formation which are presented in the following chapters.

Table of Contents

Table of Figure

Table of Tables

Acknowledgements

Above all, I thank God for the life and well-being that I have for free and that I use as I will, to guide my life in one way or another.

This research project started with the support of the Ministry of Hydrocarbons of the DRC, but due to the abandonment of the partner, its realization was self-financed. Here I want to thank Dr Christopher Nicholas for his tremendous contribution and support to enable me to achieve this Msc. research program after so many difficulties encountered in finalizing this study. I thank the Dean of Graduate Studies for his authorization to allow me to move the initial funding of the project by the DRC Ministry of Hydrocarbons to self-funding and for having accepted my request for a free extension of the academic fees to submit this thesis.

I thank Dr Robbie Goodhue for his rich ideas which allowed me to deepen the development of my thesis and for having been personally assisted in the petrographic laboratory during my XRD analyses. I express great gratitude to Cora McKenna for her contribution to my ICP-MS at the geochemical laboratory at Trinity College Dublin as well as for all the many scientific information she was able to bring to my knowledge to finally help me develop my thesis.

My thanks go to all the technical staff of the Geology department including, in particular, Franc, Maura and Noel for the realization of my thin blades, the maintenance of my computer tool as well as for the many advice of use received from them during my research period.

Thank you to all the postgraduate friends with whom I had a wonderful time and thank you also to my colleagues Sylvain Mangoni and Joel Fumbwe.

And I couldn't close this chapter of thanks without saying a word of thanks to all my family. My parents, sisters and brothers whose consideration of love they have for me, make me a happy man.

1 ***First chapter:*** *Overview of Sirab Formation in Huqf Supergroup.*

1.1 Introduction.

The Sirab Formation represents the approximate age of the Ara Group in Oman. The Ara Group represents a thick package of at least six carbonate-evaporite cycles deposited between the late Ediacaran and early Cambrian in the South Oman salt Basin also known as the SOSB (Gorin et al., 1982; Clarke, 1988; Amthor et al., 2003), see figure 1-1. The carbonate rings making up the Ara Group are informally referred to as A0 to A6 and are subdivided into carbonate "C" or evaporite "E" units; for example A4C and A4E. The evaporite units are composed of intervals of gypsum and anhydrite approximately 10 to 20 m thick, associated with halite deposits. The salt is on the order of 10 to 100 meters thick before subsequent halokinesis. The evaporites accumulated during low water periods in the basin with circulation and restricted marine exchanges. Carbonate cycles occur as isolated platforms called "stringers", thought to be a variation of low slope ramps with cyclic fill levels. This carbon pattern may be the result of repeated transgressions from sea level to the basin, which may result in periodic connection of the basin environment with the open sea, Grotzinger and Amthor (2002). Due to its thalweg structure which will be developed in this thesis and the demonstration of tectonic halokinesis, the Sirab Formation can be considered as a gradual evaporite-carbonate transition operating along a saline environment, dating approximately from the Precambrian - Cambrian (more or less equivalent in age to the Oman Ara Group).

The typical shallow carbonate "stringer" facies consists of ooidal grains usually trapped at the base of waves in fair weather, and oncolite packstones with microbial barrier accumulations of stromatolites as well as layered thrombolites with tissues " clots" characteristics (Grotzinger and Amthor, 2002; Amthor et al., 2003). The high primary porosity in the intervals of the microbial framestone thrombolite means that, the Ara salt carbonates and the Sirab stringers, form a system of hydrocarbon plays of which notably the Ara Group, is the one of the oldest in the world to provide Oman's largest hydrocarbon reserves, Al-Siyabi (2005).

The Ara Group and its facies have been defined in the SOSB using underground exploration wells. In the SOSB, this group overlaps the Buah Formation of the Nafun Group and is located below the Nimr group in the regional lithostratigraphic scale of Oman, Droste (1997). With the SOSB buried at a depth of more than 2 km below the desert in southern Oman, the only probable real exposures of Ara carbonates are fragments contained in perforating Domes in central Oman. Thus, the lithostratigraphic unit says Ara Group was long considered as having no stratigraphic equivalence to the surface units found in Oman and this, despite the importance of the hydrocarbon plays of the Ara Group. However, the late recognition as a possible surface equivalence to the Ara Group, of a set of scattered outcrops in the Haushi-Huqf desert region located slightly northeast of the south Oman salt basin by Gold (2010), has hypothesized that the outcrops of the Sirab Formation lithostratigraphic unit, which was once thought to

be younger than the Ara Group, did indeed have more or less approximate ages. So that the surface accessibility of a geological Formation close to that of the Ara Group, known for its economic interest, would have made it possible to deepen the evolution of the architecture and geometry of the sedimentary facies, which contain a source potential for hydrocarbon reservoirs of Oil and gas.

In the Al-Jabal al-Akhdar of the mountains of Oman, the Buah Formation is covered with approximately 600 m of carbonate olistostomes, volcaniclastics and siliciclastics known as the Fara Formation, see figure 1-1 [UTM 547358, 2575519]. Following by work of (McCarron et al., 2000), reconnaissance work on the Fara Formation by sampling a volcanic interval, gave a U-Pb age date of 544.5 ± 3.3 Ma. This confirmed that the Fara Formation straddles the Ediacaran/Cambrian boundary and is a chronostratigraphic equivalent of the subsurface Ara Group. However, the lithofacies of the Ara Group in the SOSB show little similarity to those of Fara. The beginning of the Ara deposition across the region of Oman being marked by a period of tectonic activity and subdivision into saline Basin deposits, may be the basis of this difference which exists between the Ara Group and the Fara Formation located about 400 km north of SOSB.

Thus, the Haushi-Huqf region of east-central Oman (about 130 km northeast of the present boundary of SOSB) where the geological

outcrops belonging to the Sirab Formation are scattered (outcrops grouped locally and geographically in terms of field sections), appears to date and at the stage of the studies in progress, to be a promising zone for its sedimentary facies with possibly a potential in hydrocarbon plays, equivalent to the Ara Group.

1.2 Preliminary studies of the Sirab Formation.

The geological survey of Al-Huqf by the Bureau of Geological and Mining Research, Rabu (1988) was not originally carried out at a scale that would recognize an Ara equivalent. On geological maps published at that time, the Buah Formation is taken up at the top of the Huqf Supergroup, truncated by the regionally extensive Angudan Unconformity, at the base of the Haima Supergroup, and is overlain by the Thumaylah Formation now called Formations Amin and Miqrat in Petroleum Development Oman - AOP - nomenclature.

Research on the Buah Formation in Al-Huqf in the late 1990s sparked interest in the deposit environments of the upper Buah. In a detailed field study of the Nafun Group as a whole, (McCarron et al., 2000) summarized and rationalized previous work on internal facies and subdivisions within the Buah Formation. She admitted that the Al-Huqf appeared to be made up of two Members. The lower extremity is composed of dolomites passing through stromatolites and grainstone, and is generally of uniform thickness throughout the region. The upper Member consists of peritidal cycles - sabkha. Each member generally forms a prominent topographic ridge above the otherwise generally low topography.

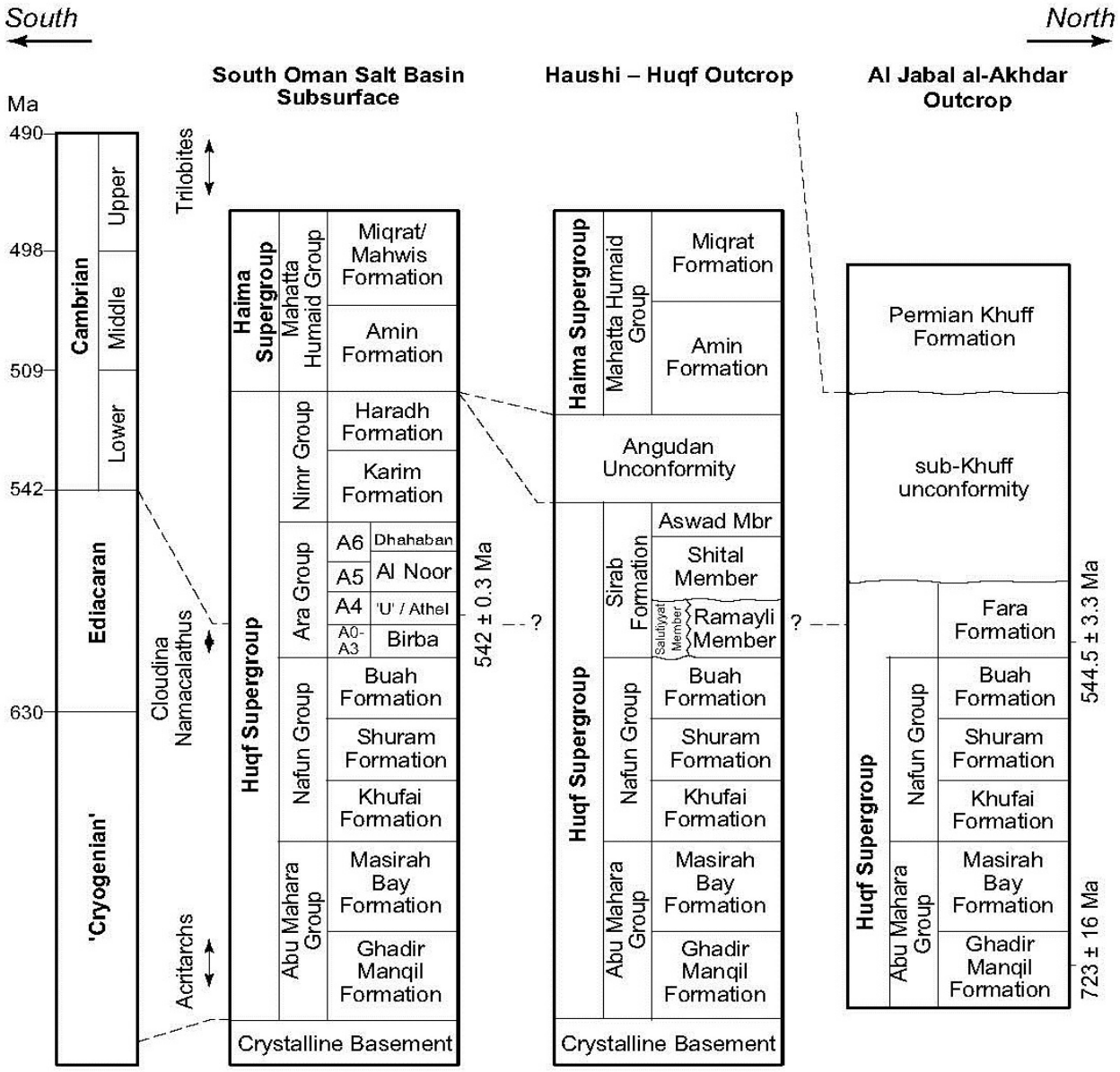

Figure 1-1: *Stratigraphic nomenclature of the Neoproterozoic and Cambrian subsurface and outcrops of Oman. The current Petroleum Development Oman (PDO) lithostratigraphic scheme for the South Oman Salt Basin (SOSB) subsurface is that summarized by Al-Siyabi (2005), with chronostratigraphic and biostratigraphic data from (Amthor et al., 2003). The Sirab Formation is shown superimposed on the litho - and chrono-stratigraphy of the outcrops of the Al-Huqf and Oman mountains, Gold (2010). The infra-Cambrian dates come from (Davidek et al., 1998). Note that the Sirab Formation occupies the same lithostratigraphic position than Ara Group (in subsurface) and the Fara Formation (of the Oman Mountains).*

Subsequent studies on the Buah Formation in Al-Huqf by Cozzi and Al-Siyabi (2004) confirmed that the two McCarron Members of the Buah Formation could be recognized in Al-Huqf. Later, Cozzi (2009) wrote a communication which correspond to previously publish of Nicholas and Brasier (2000), in which the top of the Buah Formation is defined at the top of the lower Member of McCarron, under the first unit d peritidal evaporites. Indeed, this lower Member is now recognized as the Buah Formation sensu stricto, with a thickness of about 130 to 190 m below potential Ara equivalent. This redefinition also led to aligning the Al-Huqf lithofacies with the laterally persistent facies of the entire thickness subsurface of Buah and in Al-Jabal al-Akhdar to the north. In this diagram, there are no recorded occurrences of evaporite beds in the Buah Formation.

(Gold, 2010; Nicholas and Gold, 2012) present the results of the original unpublished survey of potential Ara equivalents. This work was conducted between 1999 and 2001 plus new field data from a survey resumption in 2006. A reassessment of the old sections combined with localities surrounding the Al-Huqf, provided a robust regional lithostratigraphic framework for the recognition of a new unit at the top of the Huqf Supergroup. This Formation is what is now known as the Sirab Formation. As such, it occupies the corresponding litho-stratigraphic position of the Ara Group in the subsurface; overlying the Buah Formation, but underlying to the Middle Cambrian Angudan unconformity which is a basal regional unconformity of the Haima Supergroup clastics.

1.3 Overview of Huqf supergroup.

The Huqf Supergroup covers the crystalline basement of the Proterozoic and represents the oldest known sedimentary sequences in the south Oman Salt Basin "SOSB". While the geographical location of Oman may lie along the southeastern margin of the Arabian Plate whose geographical limits are: the area of propagation of the Gulf of Aden to the south, the Masirah transformation fault as well as Owen's fracture zone to the east, and the margin of the converging Zagros Makrarem plate, giving rise to the mountains of Oman to the north. The Haushi-Huqf region from which the name of the Huqf Supergroup is derived is therefore located towards the south of Oman, covering a vast desert area of which the outcrops of the Huqf Supergroup alone represent a neoproterozoic layer that extends over 180 km to the northeast and about 40 km wide. As for the stratigraphic presentation of the Huqf Supergroup, it was drilled along its surface of the Dome of Khuafai and the borehole had penetrated the crystalline basement about 0.5 km near the center of Inlier, (Gorin et al., 1982). The data collected during the drilling showed that from the bottom up, the Huqf Supergroup is made up of the following different geological groups: Abu-Mahara, Nafun, Ara and Nimr. Four groups in total recognized on the basis of geological outcrops and drilling data.

The Neproterozoic (~870 to ~730 Ma) basal assemblage is part of the collage of Archaeo-Proterozoic microcontinents (terranes), Pan-African mobile belts, island arcs, subduction complexes, ophiolites

and molasse basins; assembled during African orogeny in the Neoproterozoic to form the Arabian plate. This timeline of tectonic event precedes the expansion of the first Abu-Mahara sedimentary package which forms the basis of the Huqf Supergroup. Hussein (1989) recognized five distinct terranes amalgamated during the Neoproterozoic in western Saudi Arabia. These are the Asir, Hijaz, Midyan, Afif and Ar-Rayn terranes. There is a strong diachrony of accretion between the five different terranes identified by Husseini. The terranes located towards the west would have been accreted first (780-700 Ma), followed by the large Afif terrane at 720-680 Ma and finally, terranes located towards the eastern part like that of Ar-Rayn which would have been accredited around 640-640 Ma (Hargrove et al., 2006; Johson and Kattan, 2001; Johnson, 2003). The main phase of closure and coalescence was followed by transpressional tectonics and extension along the megatrends and differ in detail.

The post-collisional Neoproterozoic-Cambrian (~ 730 to ~ 520 Ma) collapse and extension mark the early compression fold that was overprinted by sinister transpression along the NS trending strike-slip faults active at 700-650 Ma in Arabia, Allen (2007); and this tectonic event almost spans the entire Huqf Supergroup. At the end of the Neoproterozoic (~ 680 Ma), the Pan-African deformation associated with the final accumulation of terranes along the western margin of the eastern Arabian craton marks the Formation of gneiss domes. The uplift and Formation of mountain ranges have a major N to NE trend within lithological and structural grains, Stuart-Smith (2003). The

sutures of the island arch are also cut by N and NW directional senestral structures, called “Najd structures”, whose movement synchronization can range from 650 to 550 Ma, Al-Husseini (2000).

The Najd Faults formed on the continental shear scale of Gondwana, comprising a set of crustal-scale subvertical northwest shear zones, which cut through northern Gondwana, cross-sections of Europe North Africa, Arabia, Oman, India and southern Australia (Stuart-Smith and Romine, 2003), see figure 1-2. The “Najd event” is also marked by a major thermal event reflected in radiometric data from Abu Mahara and in basement rocks, Romine (2004). The Nafun, Ara and Nimr Groups are part of a series of basins developed in post-tectonic intrusions (~ 610 to 565 Ma) in Oman. They constitute platform deposits and are associated with weak tectonism in which deposition of marine clastics, carbonates, evaporites and possibly continental sediments took place in spreading basins trending N to NE (for example the salt basin of Ghaba 550 to 540).

At 540 to 520 Ma, it is the episodic deformation period (Angudan event) to which correspond folds and northeast thrusts affecting the sediments of the Huqf supergroup in southwest Oman. The Angudan is considered to be an angular offset at the edges of the basin (such as: the eastern limit of Ghaba, the western limit of the Fahud terrane and the salt basin of southwestern Oman). The internal structures of the

northern Oman sub-basin network have been reversed such as: Makarem High (Romine, 2004).

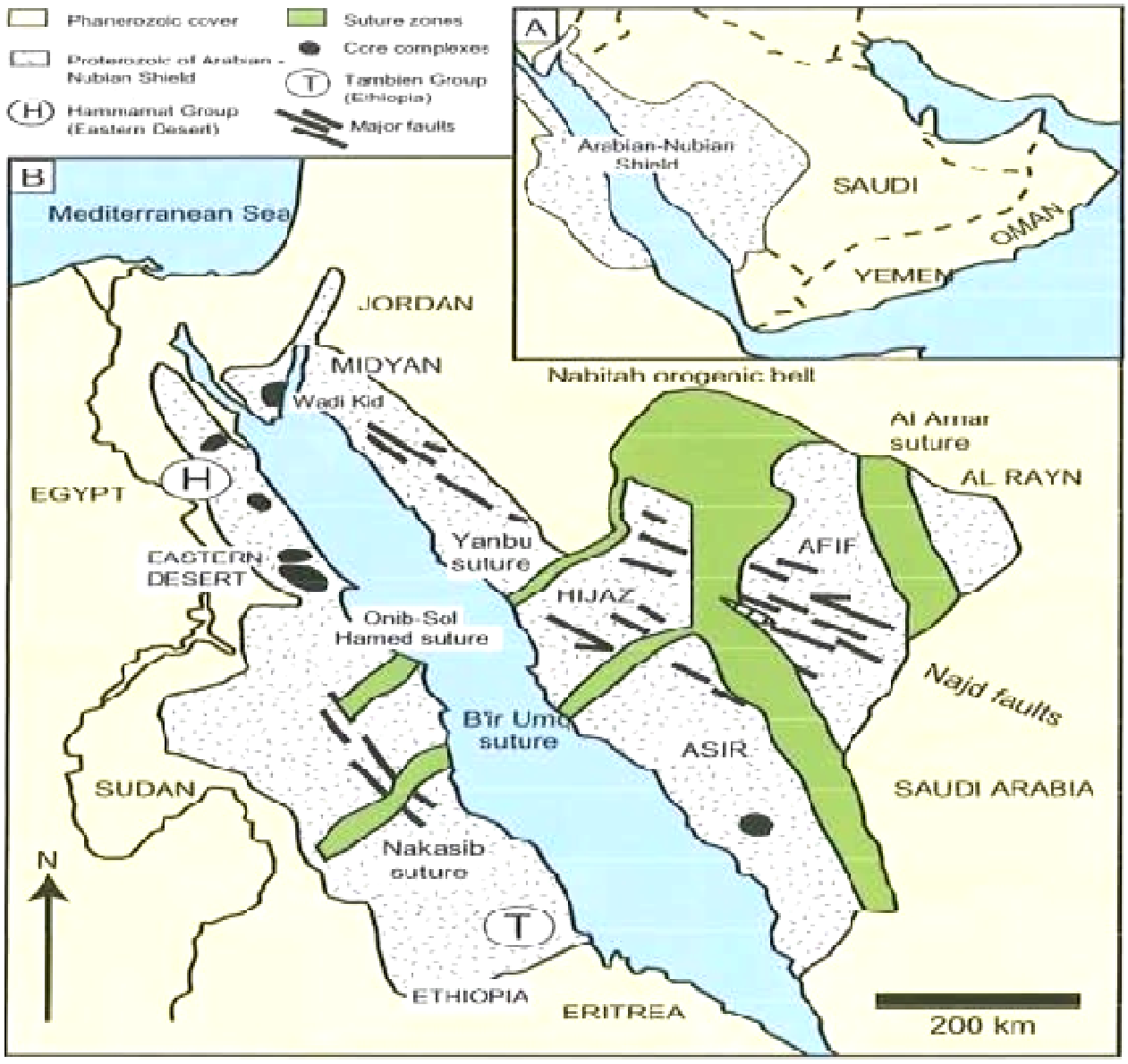

Figure 1-2: *The Arab-Nubian shield. A) Location map of Arabia - Nubian Shield. B) Main tectonic terranes, ophiolite belts (sutures) and NW - SE Najd structures, modified from Quick (1991), Allen (2007) and Gold (2010).*

The shape, character and extent of deformation of these sub-basins are linked to a particular subterranean terrane, the accretion terrane of southern Oman and its border with the Arab terrane (Romine, 2003). As along the western edge of the southern Oman saline basin, the "western deformation front" thrust structures take over the Huqf Supergroup, but these are eroded and truncated by the Angudan shift and display then the mark of a deformation of contraction which corroborates at the base of Haima (beginning of the upper Cambrian). In some places, continental siliciclastics of western origin (Nimr group of Cambrian age) show the appearance of a tectonic uplift and the generation of source zones of sediments in the west, before the actual birth of the unconformity Angudan (Allen, 2007).

Thus and in general, the Neoproterozoic to Cambrian age in Oman is represented by the Huqf Supergroup. This Supergroup covers the Proterozoic crystalline basement and represents the oldest known sedimentary sequences in the south Oman salt basin (SOSB) which hosts from the bottom to the top of its stratigraphy: the Abu-Mahara Group, the Nafun Group, the Ara and the Nimr Group, plus in the new setup after work by Gold (2010), the Sirab Formation as almost the equivalent time to Ara Group within Huqf Supergroup.

1.4 Comparative age of the Sirab Formation.

The age of Ara Group subsusrface is well constrained (Amthor et al., 2003; Bowring, 2007). U-Pb zircon geochronology, carbon isotope chemostratigraphy and biostratigraphy together indicate that the Ara Group extends from the most recent Ediacaran to the oldest Cambrian, with the Ediacaran/Cambrian boundary at or near of the base of cycle A4 which is dated 542 ± 0.6, see figure 1-1. Ash from the underlying A3C carbonate also gave an age date of 542.6 ± 0.3 Ma. The presence of the oldest *Cloudina* tabular limestone fossil and also possibly *Namacalathus* in the Ara below A4 also supports the conclusion that the lower units of the Ara Group are of late Neoproterozoic age. The top of the underlying Buah Formation sensu stricto both below the surface and in outcrop has therefore been estimated to be approx. 550 Ma (Cozzi and Al-Siyabi, 2004).

On the other hand, *Cloudina* and *Namacalathus* are intimately associated with thrombolite facies encountered in the carbonates of Ara Group subsurface, as is also the same for some exposed Ediacaran reefs seen in Namibia (Schroder, 2000; McCormick, 2001; Grotzinger, 2005). Although the discovery of this type of fossil biomarker has not yet been elucidated in the Sirab Formation, Gold (2010); nevertheless, there remains the presence of coagulated thrombolytic frameworks and stromatolytic thrombolite in the upper Members of Sirab, namely: Shital and Aswad, whose fossil

preservation in good condition throughout the Al-Huqf region, makes it possible to simulate the two geological Formations.

On the other hand, even the absence of clear and direct observation of the calcareous fossils characteristic of the A4 (Ara Group) in the upper thrombolitic units of the Sirab Formation, can suppose a Cambrian age or younger because, *Cloudina* became extinct at the Ediacaran-Cambrian boundary in Oman (Amthor et al., 2003). Alternatively to limestone fossils, the Ediacaran/Cambrian boundary may still appear in some horizons not yet studied in detail in the Haushi-Huqf region (Sirab Formation). But also, a restricted depositional environment, for example with varying salinity, with changing levels of evaporation and chemical exchanges of the composition of the water at the water-sediment interface, can also be likely to modify the initial ecology of calcareous fossils presence and drive during the evolution of sediment deposits, to their extinctions.

Prior to Gold (2010), the presence of thrombolite in Oman was only known in the perforating domes of central Oman and the underground of Ara Group in the SOSB. Seen under angle of thrombolite fossils conserved shapes, we may suggest equivalent ages between Ara Group and upper Members of Sirab. However, strictly speaking, thrombolite do not determine stratigraphic criteria for age. They range from Neoproterozoic to Phanerozoic and are particularly common in

the Paleozoic, James (1986). We find them aslo present in the Permian-Triassic Saiq Formation of the Saiq plateau in Oman

The age of Haima Supergroup units on display at Al-Huqf is still unresolved. It was reported to be limited by a rare occurrence of upper Cambrian trilobites in the Al-Bashair and Lower Barik sandstone Formation of the Andam Group (Fortey, 1995; Droste, 1997; Forbes, 2010), see figure 1-1. The non-fossiliferous Haima units under the Andam Formation could therefore be of any age from the Early Cambrian to the early Late Cambrian. Droste (1997) or Husseini (2010) correlated the sandstones of the Amin Formation with the Lalun sandstone sequence of Iran, which is covered by Middle Cambrian sea beds. If this was the case, then the basal Group of Nimr will be early Cambrian age. The regional Angudan unconformity is indicated to lie between the Nimr Group and the Amin Formation, as the former is clearly truncated and overlapped by the latter below the surface. In the exhibits around the Dome of Buah in the Al-Huqf, this major angular mismatch can clearly be seen as underlying the conglomerates and this suggests that there is no unequivocal Nimr group exhibited in the Al-Huqf.

From then on, the approximate age for the summit of the Buah Formation sensu stricto was ca. 550 Ma, and the base of the Haima Supergroup in the early Cambrian around ca. 530-520 Ma, constrain the age of the Sirab Formation to a ca. Interval of 20 to 30 Ma;

covering the end of the Ediacaran to the beginning of the Cambrian, Gold (2010).

1.5 Location of outcrops of the Sirab Formation.

Geographically speaking, the Al-Huqf region in Oman contains several scattered sections of the Sirab Formation. Starting from the south of this region to its north, several outcrops belonging to different lithostratigraphic units (also called Members) of the Sirab Formation appear troughout the desert of east-central Oman, without necessarily showing an unbroken continuity between the gradual passage of one sedimentary unit to another, as observed on the field from the base of Formation located between Buah transition and lower part of Ramayli Member to the most upper unit (sommital) called Aswad Member which is actual the top Sirab Formation.

The reassessment of the lithostratigraphic context of the Sirab Formation in the geological map of Oman by Gold (2010), led to the identification of three main Members for the whole Formation. In particular, the first Member rests concordantly on the Formation of Buah in the majority exposure localities shown in figure 1-3. However, in some localities where remnants of a paleotopographic high are exposed such as at Wadi Salutiyyat, the earliest Member of the Sirab Formation unconformably overlies either the Buah Formation or the older Shuram Formation. Thus, for these particular localities from the point of view of the lithostratigraphic succession of the Members of the Sirab Formation, a fourth Member representing a lateral variation from the geographical point of view were added, see figure 1-3.

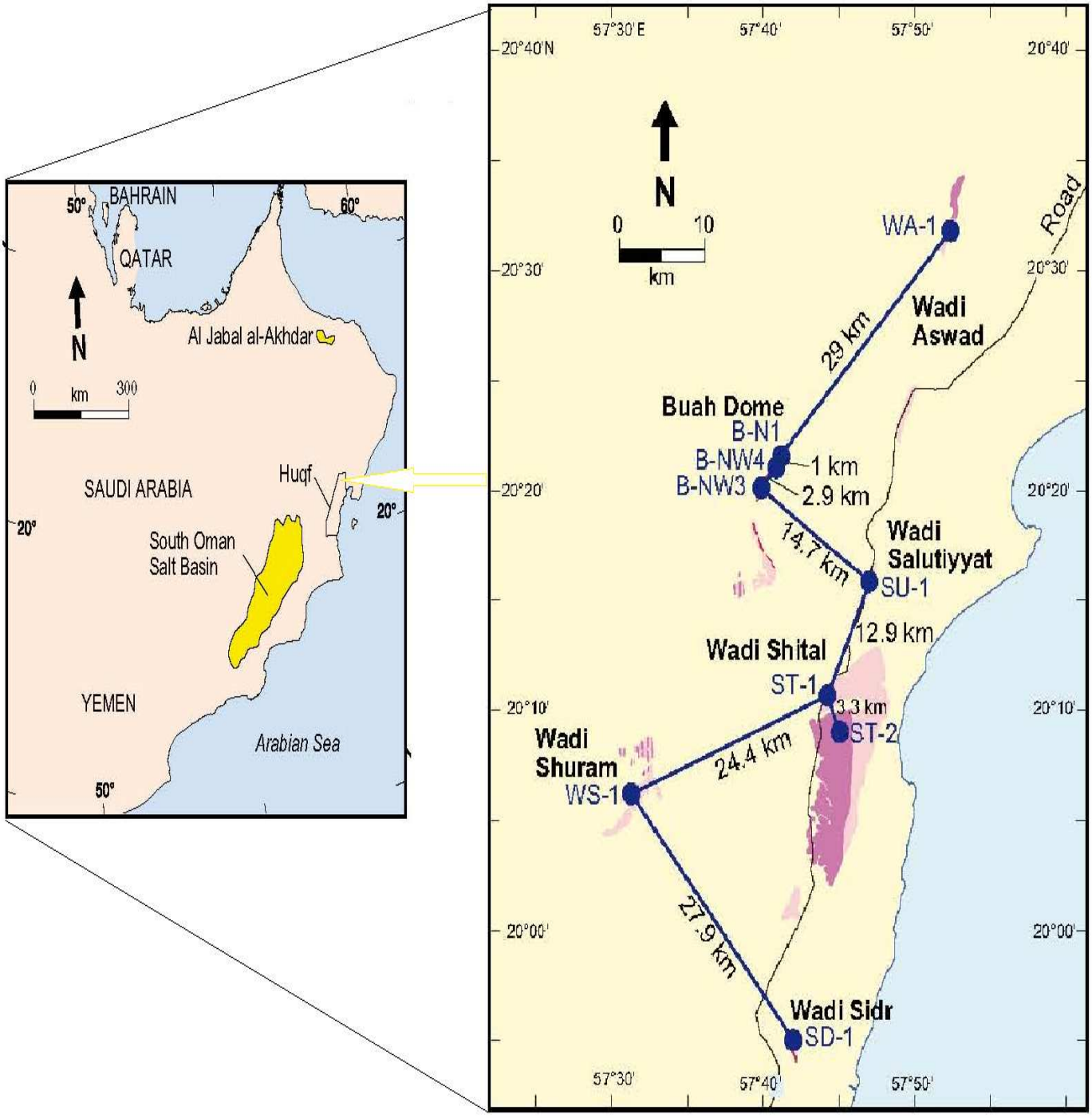

Figure 1-3: *Geolocation map of the field sections of Sirab Formation such as located in Oman and among different localities where outcrops are exposed, according to Gold (2010).*

1.6 Principal characteristics of Members' lithofacies.

Sirab Formation				
Unit	**Geographic occurrences in Al-Huqf**	**stratotype section (type section)**	**key facies of member**	**Variable facies within member through Al-Huqf**
Aswad Member	The Member outcrops in the locality of Wadi Aswad and to the NW of Wadi Shital (section ST-2).	In the locality of Wadi Aswad (base of section WA-1 [UTM 591131, 2277591]	Thrombolite - oncolites carbonates articulated with well-preserved primary dolomite precipitation ribbon in the lower Member horizons as well as thrombolite - oncolites facies disarticulated as cauliflowers shape in the upper Member horizons.	No change of facies in the localities where it is observed. Unless the same facies are altered.
Shital Member	The Member outcrops in Wadi Sidr, Wadi Shuram, Wadi Shital, Wadi Salutiyyat, and Wadi Aswad as well as around the Domes of Buah (B-N1, B-NW4 and B-NW3).	In the locality of Wadi Shital (base of section ST-1 [UTM 576808, 2234196].	Lower unit of the Member: rhythmic deposits of carbonates - evaporites (evaporite unit 2), carbonates finely laminated in its basal part and rising in a fenestral zone with pockets of breccia (facies α and β); middle Member: dominated by the facies of red dolospar, transition to the upper unit of the member by a sandstone horizon (sandstone unit 1 - evaporite); higher unity of the Member: Appearance of conophyton Reefs.	No change in the character of this Member's facies and in their deposit styles. Except alteration of same ’facies. The depocentre of this Member occur the Wadi Shuram section.
Ramayli Member	The Member outcrops in Wadi Sidr, Wadi Shital, Wadi Salutiyyat, and Wadi Aswad as well as around the Domes of Buah (B-N1, B-NW4 and B-NW3).	In the Buah Dome based on section B-NW3 [UTM 569371, 2253038]	The lower unit of carbonates is composed of the fine-grained ones that enter lagoon and peritidal environments, ascending into beds of dissolution and evaporite collapse. The upper unit is typically composed of red and purple mudstones, siltstones and dolomicrites with common beds of evaporite dissolution and collapse and emerging silcrete crusts and breccias.	No change of facies in the localities where it is observed. Unless the same facies are altered.
Saluttiyyat Member	The Member mainly outcrops in Wadi Salutiyyat and "Wadi Shuram"	In the locality of Wadi Salutiyyat, base of section SU-1 [UTM 582329, 2245812]	Lateral variation of the facies of fine-grained carbonates of lagoon and peritidal environments, ascending in beds of dissolution and collapse of evaporites (lower part of the Ramayli Member, discordantly resting on the Buah Formation or on the Shuram formation at Wadi Salutiyyat).	No change of facies

Table 1-1: *The main lithofacies characteristics identified within carbonates of Sirab Formation in each Member.*

The table 1-1 shows the three main Members (carbonate sedimentary units) of the Sirab Formation lithostratigraphy. Below here, are presented internal subdivision of each member as well as the pseudo fourth Member which is particularly found along the lateral variation that is occurred in certain localities. This variation lateral is only situated on the oldest first Member of the Formation. Going from the base to the top of Formation by lithostratigraphy order, we have:

- Ramayli Member (comprising a lower unit and an upper unit);
- Shital Member (comprising a lower unit and an upper unit. In the context of this study, the facies called “red dolospar” defined between the lower and upper unit of Shital Member was considered as ± middle unit);
- Aswad Member (the only Member not to host any internal subdivision).

An example paleotopographic locality hosting Salutiyyat Member (informal fourth unit of Sirab Formation) has been described in the locality having the same name: of Wads Salutiyyat, see Figure 1-3 such as published by Nicholas and Gold (2012).

The three main Members of the Sirab Formation always rest in conformity with the Buah Formation while the Salutiyyat Member

discordantly rests on either the Buah Formation or the Shuram Formation (figure 1-4 and figure 1-5).

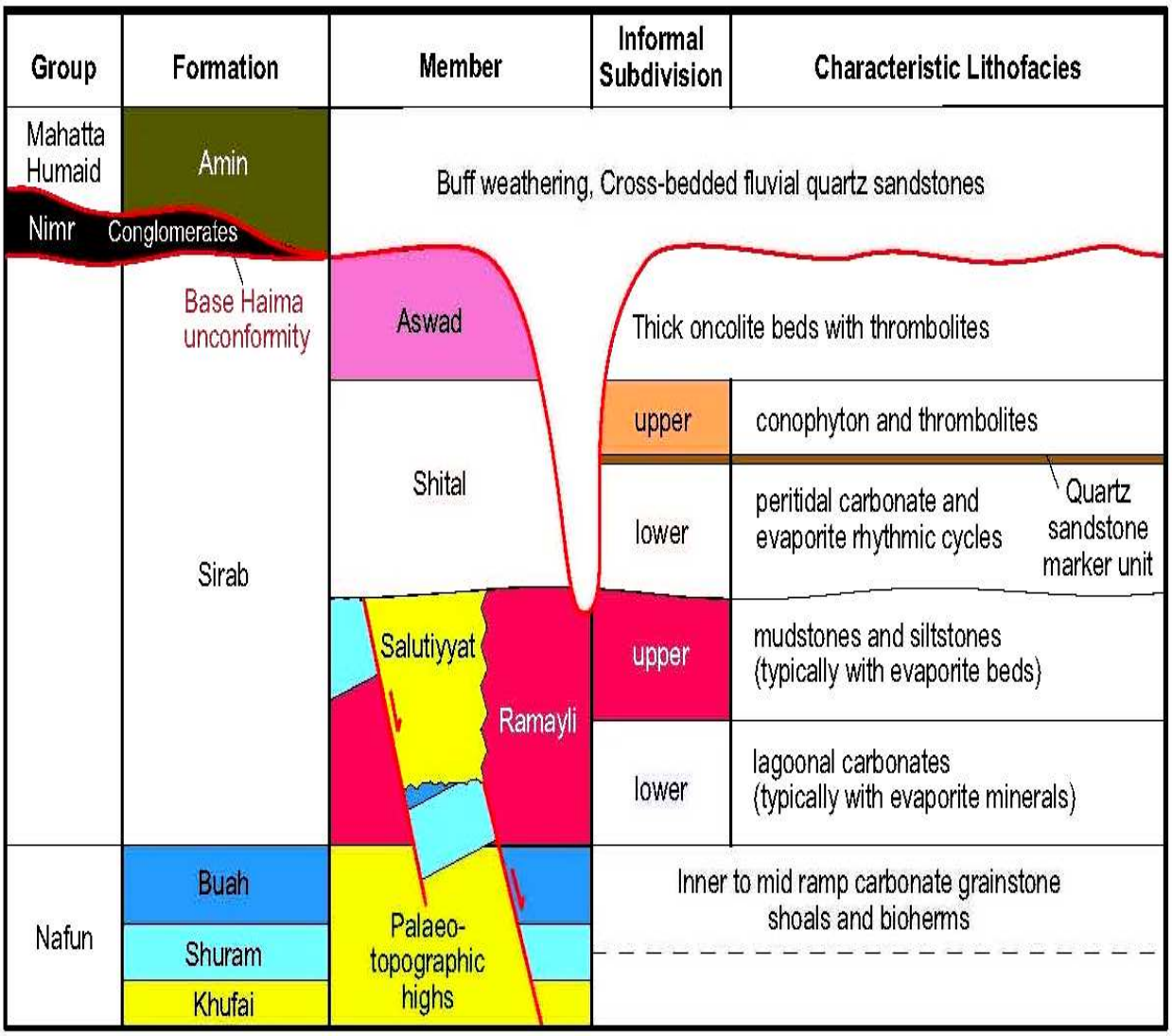

Figure 1-4: *Internal stratigraphic nomenclature of the Sirab Formation. The Formation is based both on the Buah Formation of the Nafun group and on the eroded paleotopographic high of Nafun. Discordantly covered by the Nimr group and the Amin Formation of the Haima Supergroup. Internally, the Formation can be subdivided into four Members, with the Shital Member being separated from the Ramayli or Salutiyyat Members below of it by a gap, for more reference, see Gold (2010).*

1.7 Location of Members through field sections in Al-Huqf.

The ranges of the field sections where the various Members of the Sirab Formation outcrop in the Al-Huqf region run from south to north (figure 1-3). In several field sections, the lithostratigraphic succession of the Formation going from the base to the summit is discontinuous. For example in the locality of Wadi Shuram where the base of Formation starts with Salutiyyat Member instead of Ramayli Member or again in the locality of Wadi Aswad where the base Ramayli Member is not exposed. It is the same for field sections discovered around Buah Domes where Aswad Member is missing, see figure 1-5). According to the Member which is most outcropping in places and whose sediment unit thickness is both large and well preserved, the sections typical for the member concerned have been established. These are called stratotype sections. Strictly speaking, the conjunction of the words “section and stratotype” designates an outcrop which serves as a reference to define a geological unit. For example towards the southeast of the Al-Huqf region of Oman, the locality of Wadi-Salutiyyat displays a discordant angular contact between the Sirab Formation and either the Buah or Shuram Formation. As such, since this field section outcrop differs markedly in the stratigraphic contact of the different Formations from other generalized sections of the Sirab Formation; it has been described as a stratotype of Salutiyyat Member (bearing the type name of the locality in Al-Huqf where this part of the outcrop is exposed).

In the investigations of Nicholas and Gold across the Al-Huqf region in Oman, six geographic locations between the south and the north of Al-Huqf provided a number of field sections where the outcrops are exposed. However, breaks in the stratigraphic continuity of exposures are frequent occurred in large majority of sections. Discontinuity of exposures along the field sections makes difficult to study the whole Sirab Formation by easier way. But some main localities hosting more than one section with different sedimentary units have allowed to group according to altitude of exposures, different units for build a logical stratigraphy of formation. For example, the stratotype section of the Aswad Member includes field sections WA-1 and WA-2, ranging from the base of the section at WA-1 [UTM 591131, 2277591]. As such, for a better understand of lithostratigraphic study of Formation, the aim of study must select the most significant horizons where maximum of palaeo-ecology information can be analyzed. This exercise of selecting main field sections gives the advantage to preserve during final interpretation, the global understand of the genesis of the Formation (see table1-1, details of characteristic facies of the Sirab Formation).

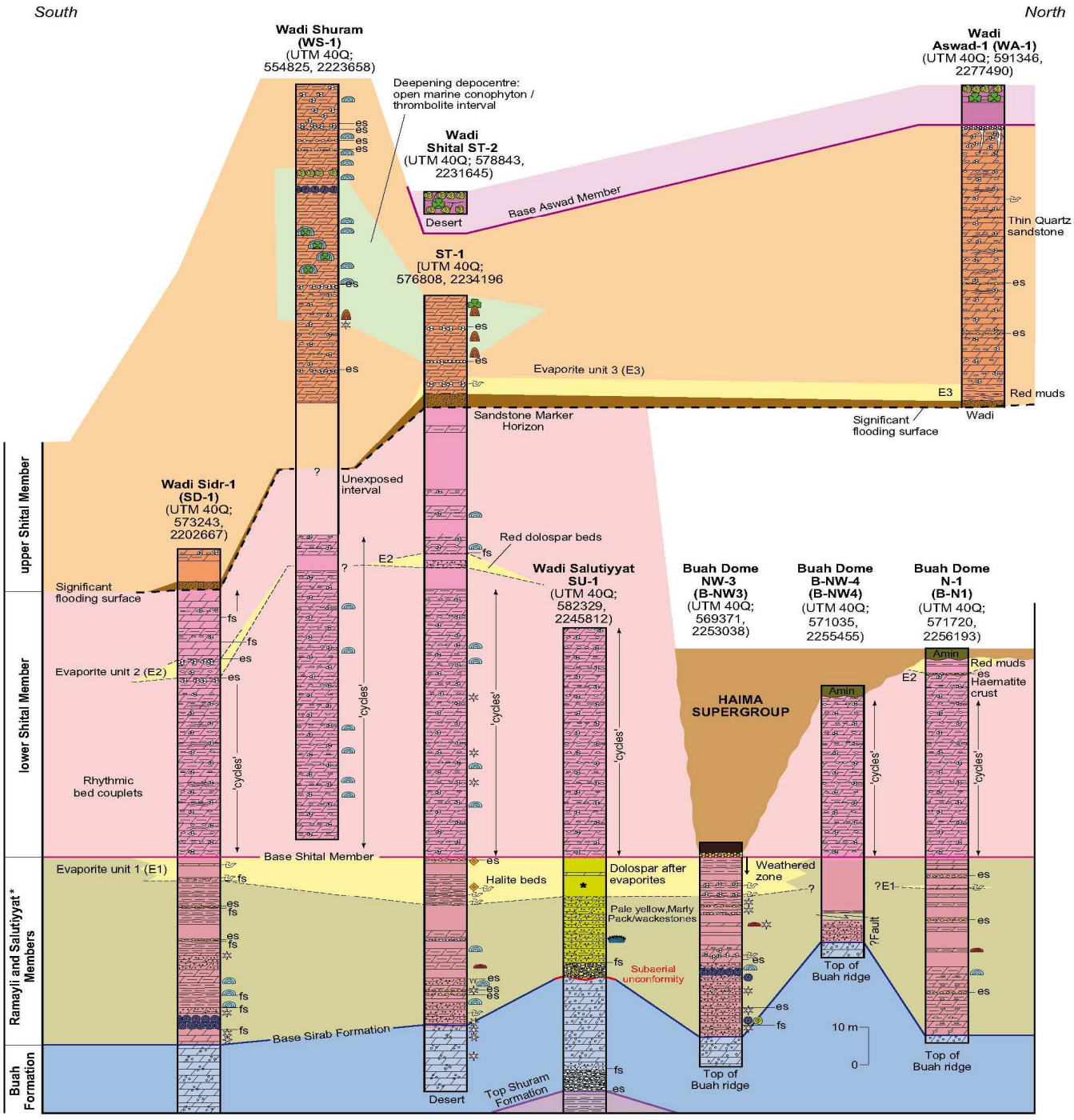

Figure 1-5: *Regional correlation of the main sections of Sirab Formation. The Sirab Formation can be traced laterally from north to south in the Al-Huqf area at approx. 85 km, by Nicholas and Gold (2012).*

From the Wadi Shital ST-1 section (UTM 40Q 576808, 2234196) and crossing the entire lithostratigraphic Formation between ~ 215 m at upper part of the Shital Member above the base Formation, a loss of outcrop is observed. Getting up on the same section Wadi Shital ST-1, a small thickness of the lithofacies of the Thrombolite and Oncolite mats appears. This level of Thrombolite-Oncolite mats was correlated with the level of Thrombolite - Oncolite mats which are located in the stratotype locality of Wadi Aswad. Field investigation suggests that the microbial mats shifted slightly above the section Wadi Shital ST-1 would indeed be a part of the Aswad Member itself, separated and/or exposed in the vicinity of ST-2 by the movements of the faults that affected the Aswad Member, Gold (2010) and see figure 1-4. As such, this field section represents therefore a general exception since it allows rebuilding all the Members of the lithostratigraphy Formation. Definitively, the combination of sections Wadi Shital ST-1 and a part of Wadi Shital ST-2, led to the section Wadi Shital ST-1 & ST-2, see figure 1-5.

By the way, strictly speaking, the section of Wadi Shital ST-1 is stratotype of Shital Member. Erosion in the Haima Supergroup has deeply affected the exposed sedimentary units in the Buah Dome locality at B-NW3 which is the stratotype section of the Ramayli Member. The zone appears to exhibit an interaction between in situ breccia and partial dissolution of fault fracturing and upward movement of fluids from the underlying Shuram Formation, Nicholas and Gold (2012) and see figure 1-4. This make more or less

ambiguous on bounding surface at the base of the Sirab Formation that may defined at the point of lithostratigraphic changes, taken either on level where clear section of shallow depth appears and indicates a change from grainstone to packstone and wackstone or where the first beds of evaporite appear. Therefore, in rapport to clear evidence of succession of grain facies (grainstone to packstone andwackstone), and evaporite beds exposed, the section of Wadi Shital ST-1 made possible to better delimit the base of the Sirab Formation. The Wadi Aswad section is a stratotype of the Aswad Member. The Wadi Shuram section does not stratotype for any Member but however, the depot centre of the Shital Member is found in this section at Wadi Shuram, taking into account thickness of the sediments in the upper sedimentary unit of the Shital Member (Conophyton Reefs) exposed in the section at Wadi Shuram (WS9). This section appears to have a much larger water slice rather than its similar facies within stratotype section of Wadi Shital ST-1, see figure 1-5.

1.8 Composite stratotype section and origin of name Sirab.

The name Sirab derives from the Arabic word "Sirab" (or spelled "Sarab") which loosely means "no life here". As a geographical name, it is used locally in the central region of Al-Huqf to include the Wadi Shital desert just west of the Al-Maha gas station on the main road, east and south to 'to the sprawling village of Sirab by the coast, and is labelled on some tourist maps of Oman. Before the construction of the asphalt road and the gas station, a small gasoline dump was located at the exit of Sirab [UTM 576098, 2233244]. This is close to the base of the most complete single stratigraphic section through the Formation defined at [UTM 578843, 2231645]. The Sirab is the only area discovered to date in which all three Members are exposed in close proximity and with minimal fault disturbance. This is why the name “Sirab” was given to the Formation, Nicholas and Gold (2012). The desert region it covers and is considered the type zone, with a composite stratotype section consisting of the type locality of Wadi Shital ST-1 combined with the short section above ST-2. The meaning of the name "Sirab" also highlights the current absence of traces or bodily fossils within the Formation.

1.9 Sedimentary logs and field Sections studied.

As elucidated above and supported in figure 1-5; the composite stratotype section of Sirab (Wadi Shital ST-1 & ST-2) is the main study section. It contains the stratotypes of the Shital Member and makes it possible to better delimit the base of the Sirab Formation (Ramayli Member) in gradual transition with the outcrops of the Buah Formation. However, not being itself a stratotype of the Aswad Member, the addition of the stratotype section of the Aswad Member primarily for outcrops that are exposed to the Aswad Member, is necessary in the Paleo-ecology analysis. In addition, the depot centre of the Shital Member located in the deep flood zone at upper part of the Shital Member (Conophyton Reefs) that we encounter in the section of Wadi Shuram (WS-9), was judged essential to be incorporate in this study.

The stratotype section of Wadi Salutiyyat has been seen as of little interest to this study of palaeo-ecology as a large part of the outcrops exposed at its base are belong to the Buah Formation or to Shuram Formation. More again, the first levels of outcrop beds in section of Wadi Salutiyyat that may be relate to the Sirab Formation are in fact a lateral variation of Ramayli Member which is best exposed in the stratotype section of Wadi Shital ST-1. Therefore, excluding the base outcrops that belong to the Buah Dome or the older Shuram, the best way to study the lithostratigraphic transition of the Huqf Supergroup

within the Sirab Formation, is to expose it in the stratotype section Wadi Shital ST-1, such decided in this thesis.

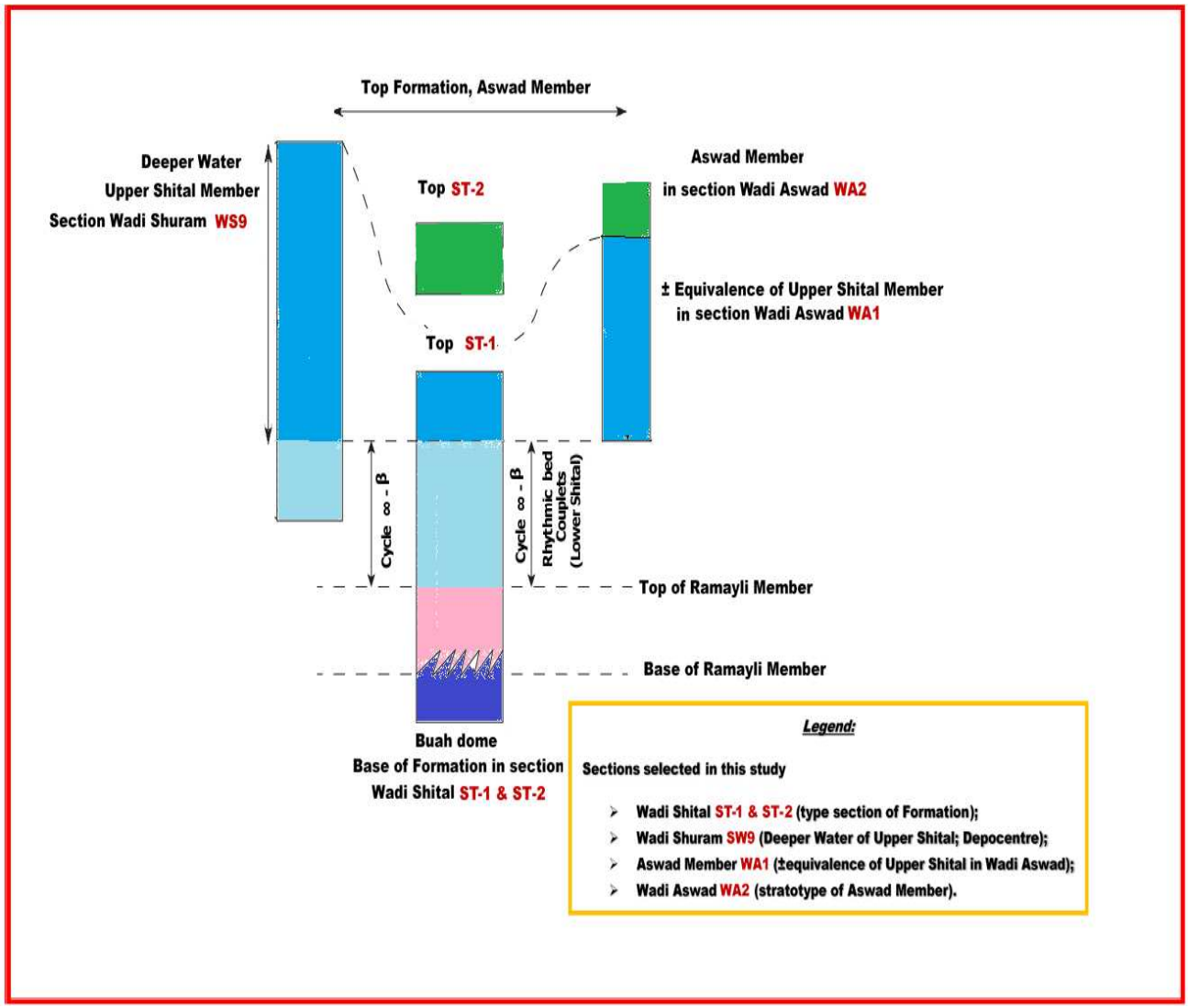

Figure 1-6: *Field sections exploited in this Palaeo-ecology study of Sirab Formation.*

1.10 Sedimentary logs and field description.

The Sirab Formation represents a discrete sedimentary package composed of lagoonal to peritidal carbonates, sabkhas and evaporites associated with a component of continental clastic origin, Gold (2010). The Sirab Formation differs from the grainstone dominating interior and mid-slope facies of the underlying Buah Formation, and also from the ferruginous river conglomerates and sandstones of the overlying Haima Supergroup. The Sirab Formation is separated from the overlying Haima Supergroup by a regional angular mismatch which cuts it into many places. Due to carbonates facies abundant rather than clastics sediments like the overlying Haima, the entire Formation has been incorporated into the upper part of the lithostratigraphic diagram of Huqf Supergroup, figure 1-1.

1.10.1 Lithostratigraphy of section Wadi Shital ST-1 & ST-2.

Wadi Shital ST-1 & ST-2 represents the type section of Sirab and can also be called as composite stratotype section. The base of the Sirab Formation (transition Buah Formation to Ramayli Member boundary) is well exposed in the stratotype section Wadi Shital ST-1 (figure 1-5). However, this transitional zone between the sedimentary units of the summit of Buah and the overlying lower part of the Ramayli Member is best exposed to a series of outcropping sections around the western flanks of the Buah Dome fault pericline. The structure of Buah Dome consists to an inner area with prominent dolomite ridges of the Khufai Formation that dipping away from the core of the fold and an outer area on the western flank where a single prominent ridge forms the only true topography above the desert. This ridge is composed of the predominantly ooidal / peloidal grainstone and interbedded silts of the upper transitional facies of the Shuram Formation, with full thickness of the Buah Formation sensu-stricto as defined above, McCarron (2000).

In the stratotype section of the Ramayli Member at B-NW3, the upper layers of the Buah Formation slope ~ 30˚ west-northwest of the main topographic ridge at [UTM 569371, 2253038]. The facies seen consist of medium dolomitic grained cross-bed stones of inland to medium tidal shoals, which form massive weathering low and rounded exposures at about waist height. As the topography disappears from

the granular ridge towards the west-northwest, there is a change from lithofacies to finer-grained dolomites, with a mud component. Exposures become less massive and more irregular. This facies change into packstones and wackstones suggests a model of progression towards the sea with a deposit of facies closer to the paleo-shore and from shallower lagoon environments such as originally defined by Nicholas and Gold (2012), after field observation. Pseudomorphic gypsum slats are common in some horizons, overlain by at least hard soil and this is followed by a transition to calcarenites with a scattered detrital quartz component.

There is evidence at B-NW3 of karst-filled cracks, breccias and hollows around lower Ramayli interval. This zone appears to exhibit an interaction between in situ breccia and partial dissolution of fault fracturing, as well upward movement of fluids from the underlying Shuram Formation and sporadic karst troughs penetrating downward from the surface of Angudan discordance located above. Hematite cementation appears to be a peculiar feature of the Amin at the base of the Haima, and crusts of hematite can be found on the surface of these presumed karst hollows. This karst penetration into the Huqf Supergroup can be observed in several larger scale locations around the outer Buah Dome. The Buah/Ramayli boundary was considered compliant and transitional.

The boundary surface at the base of the Sirab Formation could be defined either at the level where shallow clear section appears, indicated by facies change from grainstones to packstone or wackstone. This shallow depth trend does not appear to have reversed significantly at any time in the Ramayli Member and therefore constitutes a reliable surface. But, the boundary of lower Ramayli could also be defined by the first occurrence of dispersed evaporite pseudomorphic minerals that we encounter on the field, such as gypsum or anhydrite.

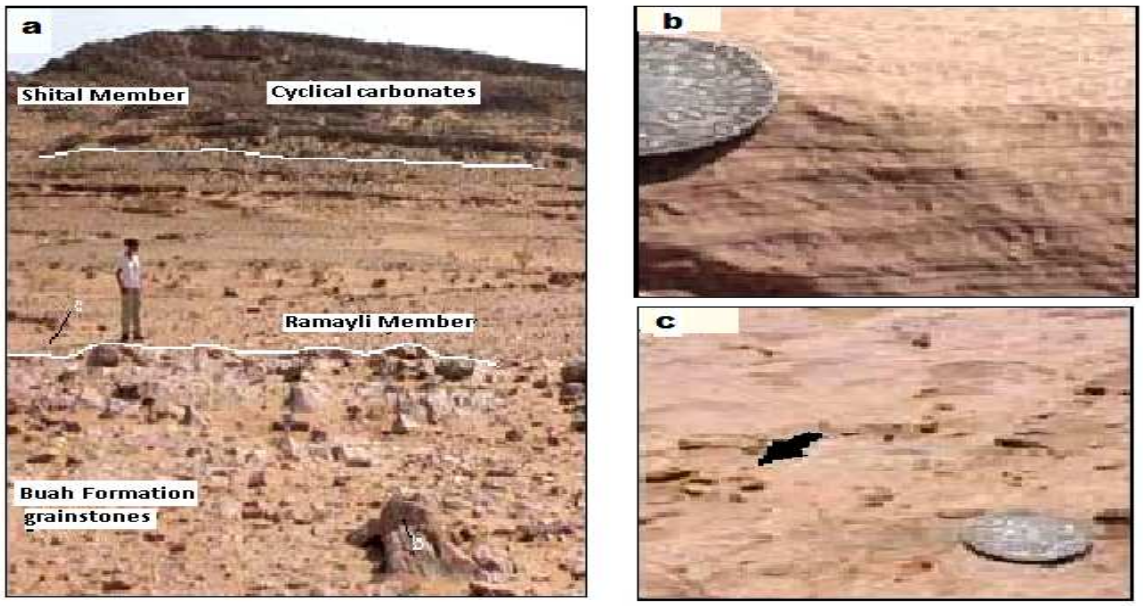

Figure 1-7: *(a) Looking southeast up-section through the Buah/Ramayli boundary and the lower part of the section up to the first prominent beds of the Shital Member at Wadi Shital. The position of photographs (b) and (c) are also shown. (b) Cross-bedded grainstone in the upper few beds of the Buah Formation, with dispersed pseudomorphed gypsum laths. (c) Partly chert-replaced dolomicrite rip-up clasts (arrowed) set in a packstone-wackstone that marks the Buah/Ramayli boundary at Wadi Shital, from Nicholas and Gold (2012).*

In the Sirab type area, the Buah/Ramayli boundary is exposed at the base of the ST-1 section near the asphalt road. The transition is similar to B-NW3, but identifies where to place the base of Formation. Cross-bedded grainstone of the upper Buah Formation are overlain by little weathered packstone. However, the change is on a single bedding surface at the base of Wadi Shital ST-1 which is marked by dolomicrite peel clasts partially replaced by chert. As such, it may represent a minor non-sequence. About 9 m below this surface, scattered pseudomorphic gypsum slats and anhydrite rosettes can be seen in the grainstone of the Buah Formation. This suggests that restriction of the inner ramp and lagoon area had begun before a change in sediment supply there. However, since the growth of evaporitic minerals from the seabed could penetrate through thick unconsolidated beds of the seawater-sediment interface, the first appearance of evaporitic minerals at ST-1 could be more recent than the bed in which they are observed. This sedimentological criterion was not enough to prove the basis of the Formation, Nicholas and Gold (2012).

The base of the Sirab Formation (Ramayli Member) was definitely adopted from the lithostratigraphic surface which marks the transition from grainstone to packstones or wackstones. This surface is relatively easy to locate through the Al-Huqf area where the stratigraphic outcrops are exposed. On the western flank of Buah Dome, the base of Formation boundary is always within a ca. 5 m west of the outer surface of the main topographic ridge. It can be tracked almost

continuously from north to southwest and this transition interval has been recorded at various points to confirm its presence. There is an ascending section of topographic change in Wadi Shital that descends from the heavily weathered Buah to the Ramayli Member. This easily forces the limit to a distance of a few meters on the ground. In an additional section just south of the Mukhaibah Dome structure at Wadi Sidr, the Buah/Ramayli transition is also exposed and the transition from grainstone to packstone occurs on a single bedding surface [UTM 573243, 2202667], Gold (2010). This demonstrates that the basal boundary surface of the Sirab Formation can be successfully located in sporadic exposures from the northern tip of Buah Dome south of Wadi Sidr at a distance of about 56 km.

Figure 1-8: *Example of chert replacement in lower unit of Ramayli Member around B-NW3. View of chert concretion marker bed at 27 m. The size and shape of the chert suggests that they are replacing small stromatolites Domes (Gold, 2010).*

Thus, the Ramayli Member is the oldest of the three main Members that make up the Sirab Formation. It represents a marked shift to shallower, lagoonal, and sabkha depositional environments in the Al-Huqf region and the first evidence in the Huqf Supergroup that exhibits widespread evaporite deposition. The base of the Member has already been defined above as the base of the Sirab Formation. The top of the Member is the base of the first carbonate-evaporite peritidal cycle of the overlying Shital Member, which generally forms prominent topographic ridges. The Ramayli Member can be informally divided into lower and upper units, depending on the quality of exposure from locality to locality. The lower unit is composed of fine-grained carbonates that intrude the lagoonal and peritidal environments, rising in dissolution beds and evaporite collapse. The upper unit is generally composed of red and purple mudstones, siltstones and dolomicrites with common beds of dissolution and collapse of evaporites, emergent silcrete crusts and breccias.

Figure 1-9: *Example of dissolution and collapse in lower unit of Ramayli Member around B-NW3.View of dissolution and collapse unit at 30 m. The base of this unit is marked by increased brecciation overlying a chert horizon and it is suggested that evaporite have been withdrawn from between the two, Gold (2010).*

The western flank of Buah Dome in the center of the stratotype section at B-NW3 provides excellent exposure of the Ramayli Member which clearly demonstrates the characteristics of this unit. Since there were few geographical names that could be used to define a new lithostratigraphic unit in this area since the construction of the asphalt road through Al-Huqf; the turnoff to the structure of Buah Dome was marked with a sign saying "Ar-Ramayli". This name refers to the quicksand area that must be negotiated when entering the Buah Dome outcrop area [UTM 578848, 2248639]. Thus, the same name of Ramayli marking the access to the stratotype section was then adopted for the conformal basal unit of the Sirab Formation.

Transition to Shital Member: The Shital Member is the central unit of the Sirab Formation and is by far the largest Member in terms of stratigraphic thickness. This represents a significant change in the classification style of the underlying Members Ramayli or Salutiyyat. The characteristic feature of Shital Member tends towards an extensive repetition of coupled beds over large stratigraphic intervals. In the Wadi Shital ST-1 stratotype section, 1-2 meter thick beds of fenestrated bedded dolomicrite are overlain by thin 10-20 cm intervals of replaced anyhydrite or wired dolomicrite that usually repeat several times (up to 100 m across the section). Similar intervals are present in other sections of the Ramayli Member while in the field, the ridges made up of these "cycles" are perhaps one of the most obvious features of the Sirab Formation to identify from a distance. The base of the Shital Member can be defined as the stratification surface at the base of the first carbonate-evaporite peritidal rhythm. This important border area seems easy to trace along the Al-Huqf region. And this is especially clear at the northern end of Buah Dome (B-N1).

The presence of a buff quartz sandstone unit in the Shital Member, particularly in section ST-1, was used to determine the marker horizon at [UTM 576839, 2233696]. The beds immediately encountered above this sandstone are the earliest occurrences of Conophyton bioherms in the section. Progressive stratification reduces conophyton exposure in the ST-1 section, localized in the upper parts where the exposure becomes a series of mounds some of which are entirely composed of Conophyton accumulations, for example [UTM 577525, 2233831].

The presence of the sandstone unit as well as the development of the Conophyton beds in the upper Shital informally show subdivisions of lower and upper units separated by a qualified sandstone marker horizon in this study of the intermediate zone of the Shital Member (where facies red dolospath appears in the stratigraphy). In the ST-1 section, well-developed Conophyton beds are rare and rarely found below the sandstone marker horizon. But the deep flood zone of Shital Member seems to have been present in Wadi Shuram section where upper conophyton facies of Shital are well developed and the whole unit shows thicker height than in section ST-1 (figure 1-5).

The top of the Shital Member is a more difficult boundary due to its low exposure above the Sirab stratigraphy at the ST-1 type section. The dip of this section becomes sub-horizontal and the overlying Aswad Member is exposed across the road from Sirab to the southeast, but a low sandy area covers the boundary between the two. Strictly speaking, the only locality where Shital and Aswad (two upper Members of Sirab located above Ramayli) are in direct contact with each other is at Wadi Aswad, along the northern part of WA-1. The summit of the Shital Member at this location locally develops sub-Haima karst pockets at [UTM 591131, 2277591] which are apparently conformably overlain by oncolite and thrombolite beds of the Aswad Member.

The most complete exposure of Shital Member which overlies Ramayli Member can be identified in the roadside section towards the eastern end of Wadi Shital in the center of this region of Al-Huqf. Wadi Shital itself is the sandy area to the west of the main tarmac road that crosses the Sirab region near the Al-Maha gas station. The name of this locality does not appear on any road signs but is marked on a tourist map of Oman as "Wadi Shital". The arbitrary base of Wadi Shital section ST-1 [UTM 576808, 2234196] is embedded in granular rocks of the Buah Formation about 300 m northeast of Al-Maha gas station on the main asphalt road towards Duqm and Salalah. The low-grained stone ridges of the Buah Formation near the roadside are capped to the southeast by low exposures of Ramayli Members. This flat area is mostly covered with desert sands. The Ramayli/Shital boundary is located where the topography begins to rise from the desert floor halfway up the first prominent ridge visible from the road. The base of the stratotypical section of the Shital Member is 63.3 m above the base of ST-1 at [UTM 576903, 2234116].

Exposure of an evaporite bed unit to the upper Ramayli occurs at the bottom of the first topographic ridge between 50.25 and 58.5 m above the base of ST-1. This includes beds of dark yellowish orange (10YR 6/6) and light brown (5YR 5/6) coarse dolospar which still retain some preserved halite patches. This set passes up to 3m of non-exposure. From 61.5 to 62.1 m, two thin beds of large lozenges of light brown dolomite, with grains of halite, outcrop. After another 0.6 m thin opening without exposure, a 0.3 m thick bed of pink-orange-

grey (5YR 7/2) coarse laminated dolospar contains a thin horizon of dissolution breccia and collapse in its center. After another 0.3 m without exposure, the base of the first cyclic peritid unit is at 63.3 m. Over the next 5.5 m of stratigraphy, these cyclic layers remain eroded into the ridge in the same way as the upper layers of the Family dispatch below. Above 68.5m the deposits are rather altered. Despite the weathering, the exposure of the sediment beds is continuous upward from the base of the Shital Member defined at 63.3 m.

The basal bed of Shital Member 63.3 to 64 m is composed of a very pale orange dolomicrite (10YR 8/2). It is finely fluffy in its basal half on a scale of 1-2 cm, but it rises to the top of the bed where the flakes are less pronounced and are replaced by bird eye windows. Small rupture plates that dissolve and collapse are scattered throughout the bed. There is a small eroded split between the top of this bed and the next exposed one at 64.1 m. This 10 cm interval was interpreted as the presence of a coupled evaporite bed, well present and visible in certain localities such as the Buah Dome. The 63.3 to 64.1 m interval represents a carbonate-evaporite rhythm characteristic of the lower unit of the Shital Member. The evaporitic top of the couplets has not always been developed or preserved, and the 64.1-67.9 m interval consists of three dolomicrite beds all identical at the base but without anhydrite or dolomicrite networks between them.

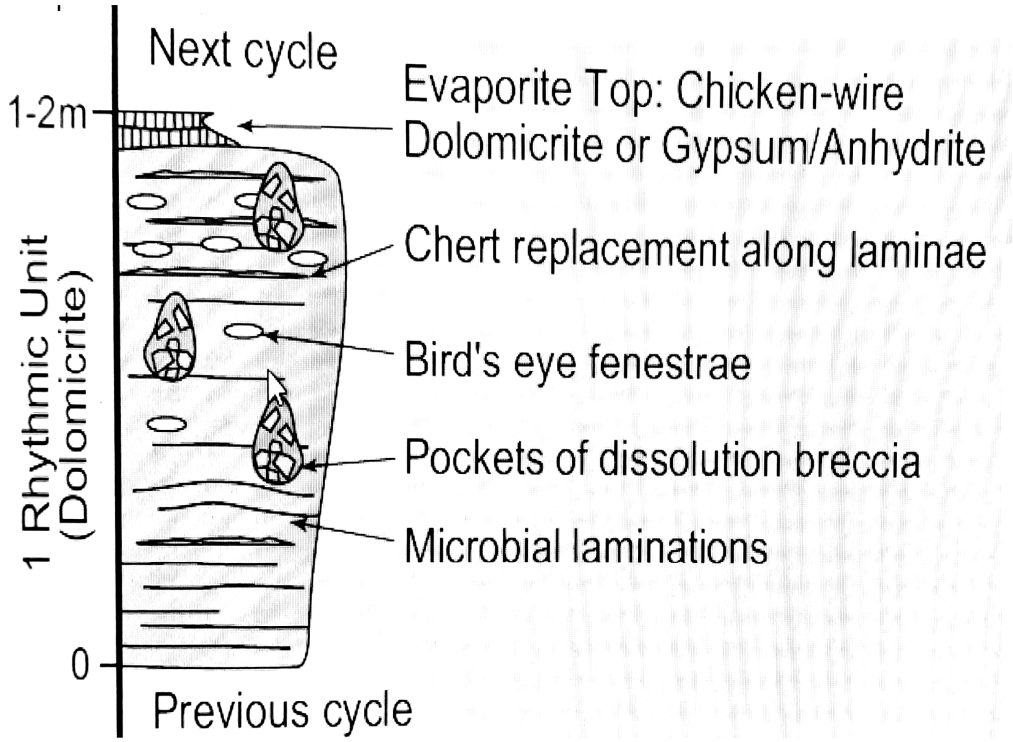

Figure 1-10: *Cartoon showing the cyclical rhythm of evaporation-carbonate as a typical character for the lower Shital, from Nicholas and Gold (2012), modified.*

Frequently, in the stratigraphy of the lower part of this Member, one observes beds of dolomicrite inside a well-laminated couplet whose base rises in a fenestral zone with pockets of breccias. These beds have been unofficially recognized as α facies, forming the typical carbonate unit. Alongside these beds, a second subtle variation of the carbonate unit has also been observed and is called β facies. The 67.9 to 69.75 m interval at ST-1 contains three such beds. These consist of a very pale orange (10YR 8/2) mixture of coarsely crystalline interbedded dolomite with chert replacement along the laminae and irregular chert concretions, with ca. 2-5 cm thick sandwiched in

between. Dissolution-reprecipitation of dolomite has been identified as being associated with pseudomorphs of gypsum lamellae and may suggest that the β-facies was deposited in a smaller water body than the α-facies, promoting evaporite mineral growth, Nicholas and Gold (2012). From 69.75 to 70 m, a thin 25 cm thick layer of powdery white dolomicrite rises on the ridge and probably represents the upper evaporite unit of the upper bed.

From 70 to 136.2 m, repetitive beds of facies α and β and occasional choppy and weathered interbeds of fissile-grid dolomicirite which continue with only a slight loss of exposure on this ridge to the next prominent topography at the south-east. The monotonous character of the cyclicity of this unit of the Shital Member at its lower level is the most characteristic feature of the outcrop. Also in this interval, it can be observed that the cut lamellae in many beds are undulating microbial mats that have developed into recognizable stromatolite Domes.

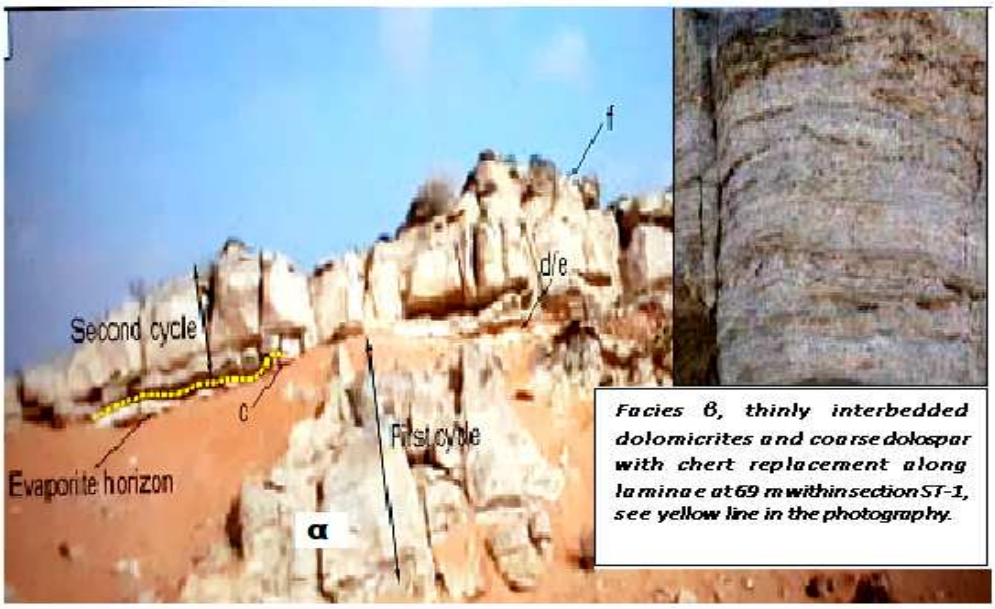

Figure 1-11: *Example within Shital Member of two typical rhythmic cycles occurring in the section B-NW4 (figure 1-5), according to the cartoon presented in figure 1-9. (d/e= dissolution – evaporite and f= conophyton facies), from Gold (2010), modified.*

The interval between 136.2 and 142 m marks a certain break in exposure (figure 1-13). Above this interval is a 0.5 m thick layer of pale red (5R 6/2) coarse dolospar, well bedded, interbedded and with fine dolomicrites. In the description of this thesis, the level of the stratigraphy of the Shital Member where the red dolospath facies occurs at the sandstone horizon has been called the middle part of the Shital Member.

Between 142.5 and 143.25 m there is still a lack of exposure before a similar bed of red dolospar reappears in the stratigraphy. Another Red dolospar lies between 144 and 144.25 m. This younger bed is

brecciated. Similar red dolospar beds are reported at the top of the underlying Ramayli Member in ST-1, and these are intimately associated with halite. Thus, these layers of Red dolospar located in the middle part of the Shital Member were reasonably inferred to be part of the same facies as the evaporites between 136.2 and 144.25 m (evaporite unit 2). These levels correspond to an interval roughly similar to the stratigraphy of the Buah Dome (B-N1) and Wadi Sidr (SD-1) sections; figure 1-5. Between 146 m and 163.1 m, the continuity of the stratigraphic outcrop appears intermittently until the outcrop disappears through the desert sand which coincides with the leveling of the topography into a wide flat desert plain.

The outcrop reappears at the base of the next ridge to the south-east 178.8 m above the base of ST-1 and shows a rhythm of poorly exposed dolomicrite 1.5 m thick, overlain by 4 .5 m more without outcropping. From 184.8 to 188.4 m, there is an abrupt change in lithology in the stratigraphy at ST-1. in such Layered fine quartz arenites of moderate reddish brown to yellowish brown color (10R 4/6 to 10YR 5/4) found in the lower 2 m, are overlain by more massive quartz arenites with a bimodal fine grain size distribution and moderately coarse on the upper 1.6m. These quartz arenites consist mainly of cemented silica and hematite, but there is a minor dolomitic component. The tallest and most massive unit was defined as having undergone localized deformation of soft sediments, reminiscent in places of biortubation. This sediment unit represents the buff sandstone marker horizon. It can be traced at this stratigraphic level

from Wadi Aswad north of Al-Huqf to Wadi Sidr south, a distance of approx. 85 kilometers. It also occurs west towards Wadi Shuram as part of a Shital Member fault fragment.

The buff sandstone has a surprising strike length from north to south of the Haushi-Huqf region (figure 1-5). But in the field representation of the Sirab Formation, there is only one stratigraphic marker of this unit which lies between the red dolospath and the appearance of the Conophyton reefs in the Shital Member; the sandstone horizon is interposed between the middle part and the upper part of the Shital Member. The buff sandstone marker is covered by a thin outcrop of 0.6 m. The level between 189 and 192 m displays a laterally extending breccia unit east 3 m of this interval consists of an irregular lower zone of brecciated and collapsed dolomicrites, which is overlain by thin beds of more coherent pale yellowish orange stratified dolospar (10YR 8/6). A few relics of halite cross a second breccia zone between this interval. This upper unit also contains the first recognizable fragments of brecciated Conophyton. Given similarities to dolospar beds associated with evaporites and breccias, the interval was defined as another level of evaporites exhibiting dissolution and withdrawal of coherent evaporite beds, leading to breccias and evaporites d collapse covering the dolospar beds. The unit is labeled as evaporite unit 3, correlated with the fine red mud present in the Wadi Aswad interval to the north (figure 1-5). The upper surface of the evaporitic breccia 3 at ST-1 forms a low ridge and shows patches of Conophyton in situ, developed directly on the irregular upper

surface of the breccia. This indicates that although evaporite dissolution was post-lithification, it took place at the very beginning of sediment burial, Nicholas and Gold (2012). Transgressive drowning of the evaporitic unit would have allowed Conophyton accumulations to begin to settle on its upper bed. Dissolution and collapse can also result directly from the drowning of this unit?

Viewed in this sense, earlier Conophyton Domes would have been brecciated before larger Conophyton mounds re-established themselves above the brecciated come horizons below. The remaining 23 m of the Shital Member 192-215 m consist of undulating and stratified microbial dolomicrites, pale yellowish orange to pinkish orange gray (10YR 8/6 to 10R 8/2) whose regular intervals can develop into conical Domes (pointed about 10 to 20 cm high). Beds often have sporadic pockets of solution breccia that have developed within them, and many upper-layer surfaces are marked by a thin breccia horizon. Farther in the southeastern part upstream, the topography stabilizes as the bedding dips become sub-horizontal. The stratotypical section of the Shital Member at this location terminates among the dissected mounds of the most exposed beds, and there are large exhumed paleomicrobial mounds or Conophyton "reefs" often flanked by a breccia apron. Some of the weathered surfaces within and around these mounds also appear to show crypto-coagulated or mottled tissue similar in size and scale to the thrombolite of the overlying Aswad Member.

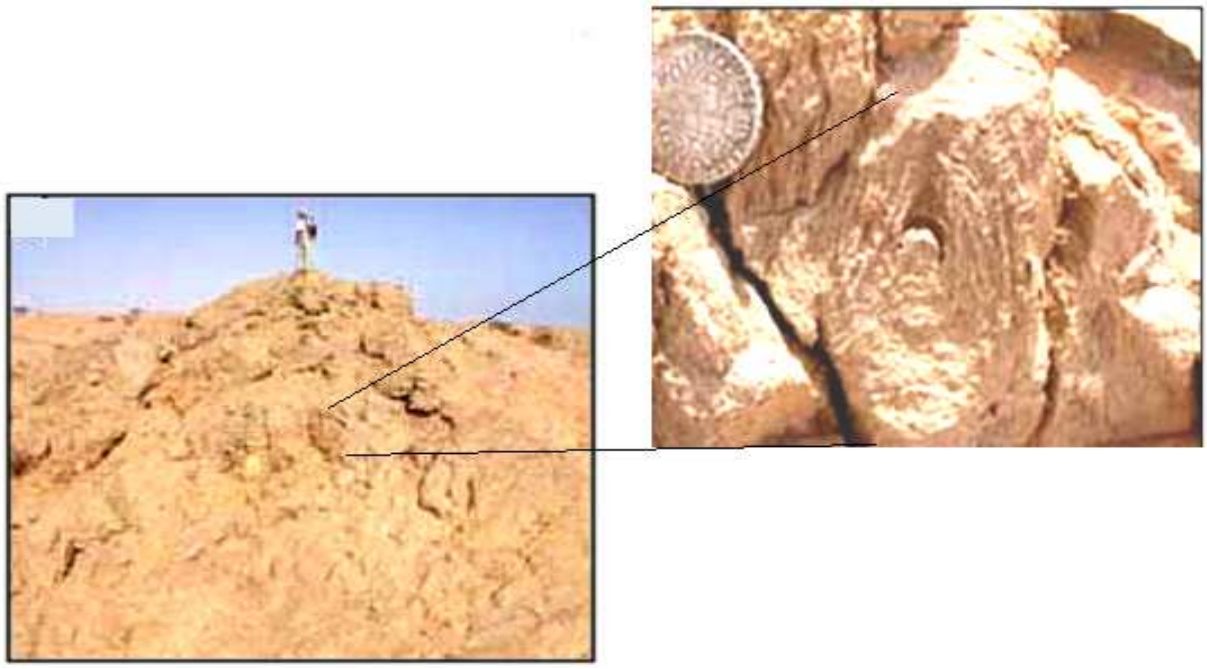

Figure 1-12: *Sophia Gold looking northst in cross section a conophyton reef in the exposed upper layers of section ST-1 and enlarging an oblique cut through one of the characteristic steep-walled conophyton columns composing the bioherm, from Gold (2010), modified.*

The transition to the Aswad Member in the composite stratotype section known as Wadi Shital ST-1 and ST-2: The Aswad Member is the youngest unit in the Sirab Formation. In the stratotypical composite section of the Sirab Formation, the dip of the beds at the top of the ST-1 section gradually stabilizes and the exposure ends north of the Sirab asphalt road in a series of low mounds with mounds of well-developed Conophyton. Southeast of the road, there is a plateau of low hills which is slightly higher in relation to the topography and stratigraphy of Sirab, in comparison with the outcrops in the section ST-1. These hills are composed of horizontal intersections of Thrombolite and oncolite. In general, Oncolite beds

are 0.5 to 1.0 cm in diameter. As these beds have little or no tilt, their subaerial exposures are excellent (less eroded). Only problem, their weak dips as well as the thickness of the Aswad Member in this section (ST-1) remain unreliable (figure 1-13).

Definitively, it is towards the north of the region, along the contact of the Shital Member and the Haima Supergroup, that the Thrombolite and Oncolite mounds identical in lithofacies as those in the south-east of the Sirab road will be incorporated into the stratigraphy of the composite stratotype section of the Sirab, as the ST-2 section. The faults of Wadi Aswad intersect and truncate the stratigraphy of the ST-2 section into a series of fault breakouts. Nevertheless, a coherent fragment of the Aswad Member which includes the marker sandstone unit of the Shital Member at its base and which was correlated with the Oncolite mounds in section section WA-1, was identified north of Wadi Aswad, Gold (2010). Just below the first occurrence of Oncolite. The dolomicrites of the Shital Member form a prominent ridge about 2 m thick, consisting of about two to three massive beds. These are crossed by karstic fissures which fill with breccias and dolomitic matrix at [UTM 591131, 2277591]. It most closely resembles modern karst ground development, certainly with some modern wind influence cementing the surface of some of these rocks. The karst seems to develop locally along this ridge, from the upper surface of the beds that compose it. Considering that in this area the basal Haima sandstones sunk in troughs develop on a paleo-karst surface at the top of the Sirab Formation, the typical karst surface has

been interpreted as a development that depends on the Angudan unconformity while the Aswad Member concordantly overlays the base of Shital Member (Gold, 2010).

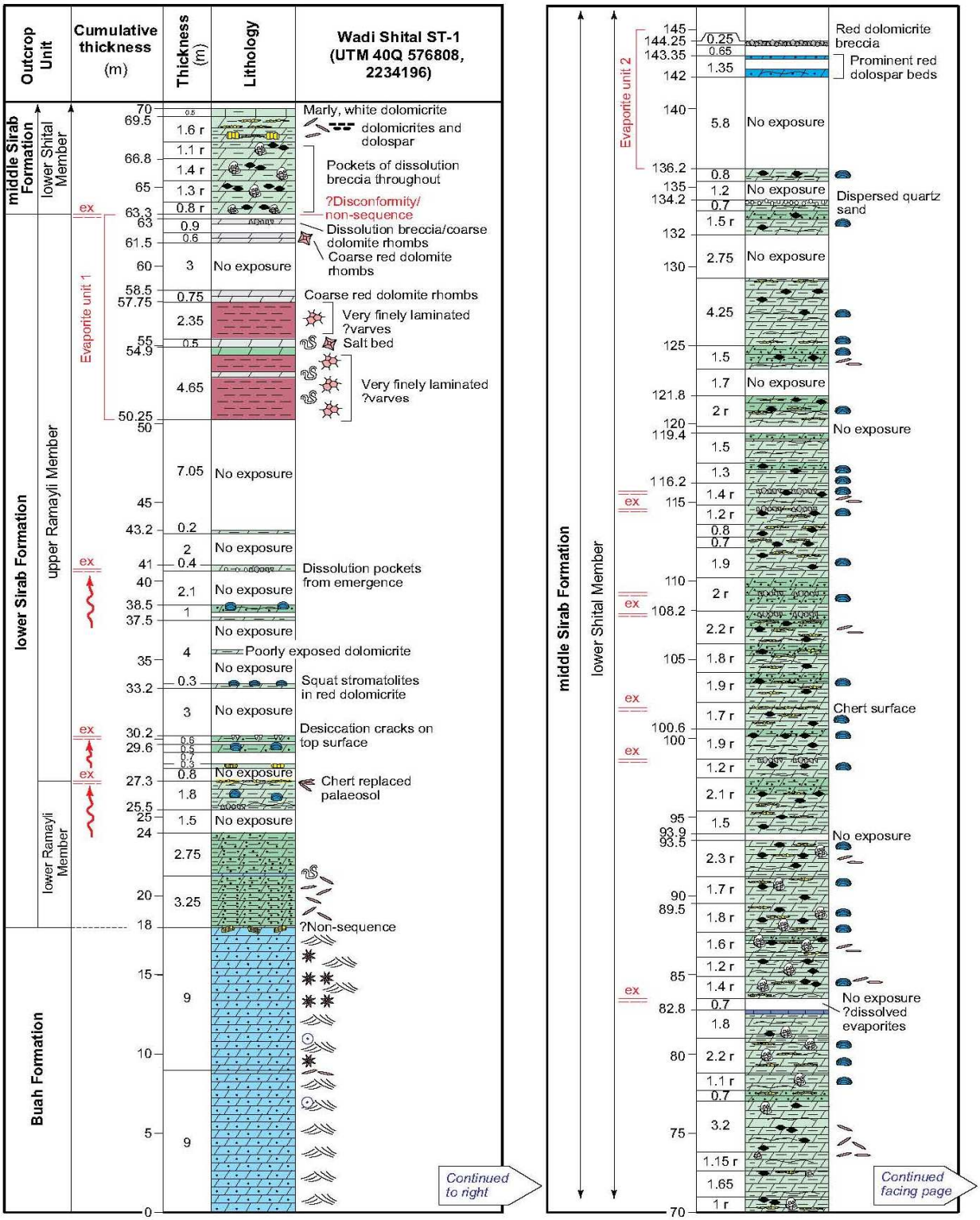
Outcrop Unit
Cumulative thickness (m)
Thickness (m)
Lithology
Wadi Shital ST-1 (UTM 40Q 576808, 2234196)
middle Sirab Formation
lower Shital Member
lower Sirab Formation
upper Ramayli Member
lower Ramayli Member
Buah Formation
Evaporite unit 1
ex
Marly, white dolomicrite
dolomicrites and dolospar
Pockets of dissolution breccia throughout
?Disconformity/ non-sequence
Dissolution breccia/coarse dolomite rhombs
Coarse red dolomite rhombs
No exposure
Coarse red dolomite rhombs
Very finely laminated ?varves
Salt bed
Very finely laminated ?varves
Dissolution pockets from emergence
Poorly exposed dolomicrite
Squat stromatolites in red dolomicrite
Desiccation cracks on top surface
Chert replaced palaeosol
?Non-sequence
Continued to right
middle Sirab Formation
lower Shital Member
Evaporite unit 2
Red dolomicrite breccia
Prominent red dolospar beds
Dispersed quartz sand
Chert surface
No exposure ?dissolved evaporites
Continued facing page

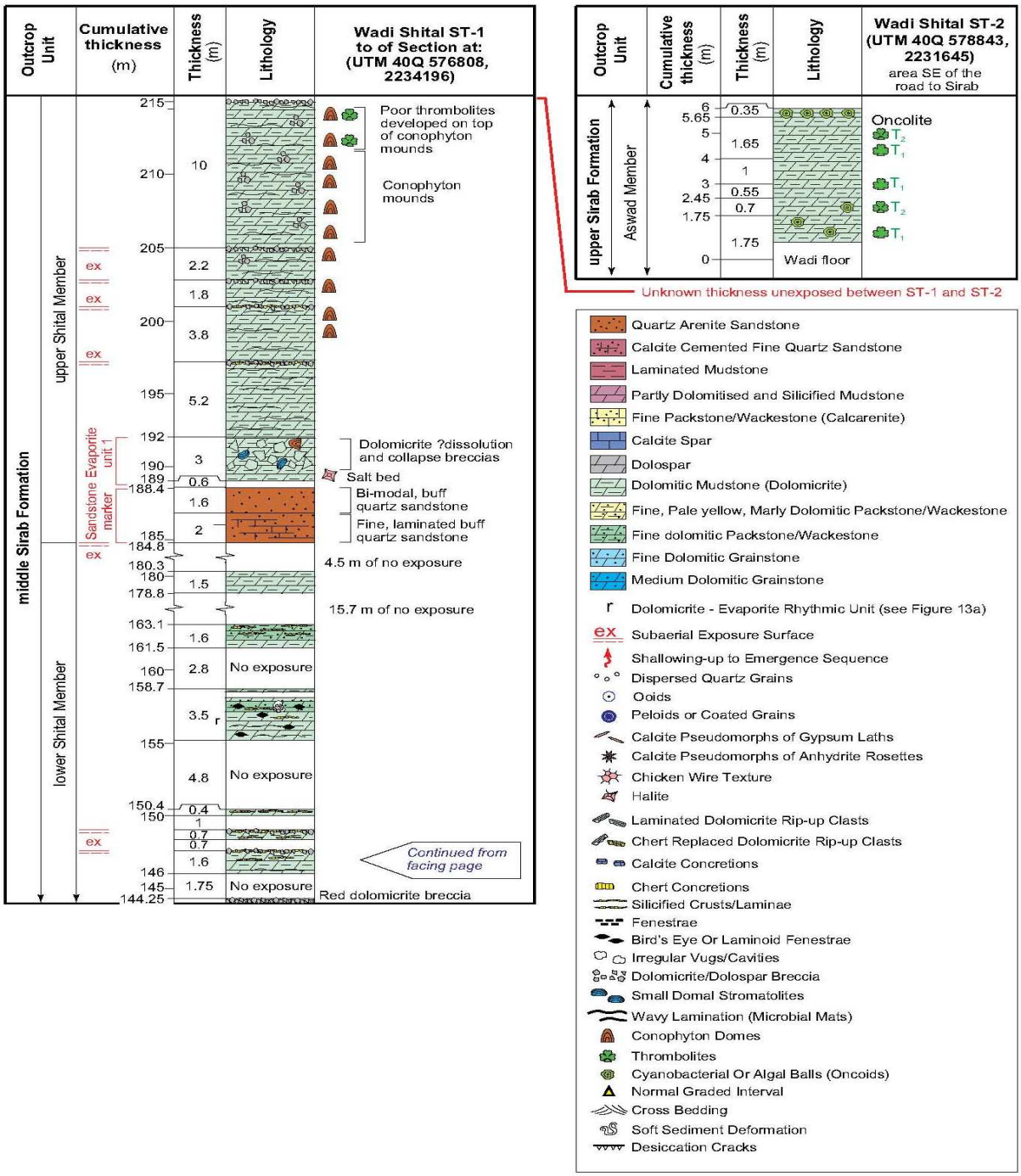

Figure 1-13: *Detailed sedimentary log of the stratotype section of the Sirab Formation, at Wadi Shital, ST-1 and ST-2. Section ST-1 also contains the type section through the Shital Member (middle Sirab Formation). Coordinates refer to the base of the section at ST-1 [UTM 576808, 2234196] in which Transitional zone between Buah and Ramayli Member occurred, from Nicholas and Gold (2012).*

1.10.2 Lithostratigraphy of section Wadi Aswad.

The base of the WA-1 section at [UTM 591131, 2277591] incorporates the stratotypical section of the Aswad Member. It begins at the base of the buff sandstone marker horizon exposed at the center of the ridges forming the western flank of the locality of Wadi Aswad. The stratigraphic succession covers a sandstone boundary and is dominated by thin monotonous and repetitive dolospathic beds. The monotonous and repetitive dolospath beds represent minor dissolution and recrystallization events in the ancient dolomicrites of the upper Shital Member. A fault shard of the upper part of this section repeats west of the oncolite mounds of the Aswad Member and contains tufted mats and Conophyton mounds which are a feature of this upper sedimentary unit of the Shital Member in Wadi Shital. The base of the Aswad Member is defined by the first occurrence of thrombolite/oncolite lithofacies at Wadi Aswad WA-2. The stratigraphic continuity occurs in a relatively abrupt transition of approximately 4.5 m from the facies of the Aswad Member, outcropping in section WA-2, above the base WA-1 of the Aswad Member and this, before that the bedding troughs flatten out horizontally to become a series of dissected mounds across the plain. The 4.3 m base of the Aswad Member consists of light gray to medium gray (very pale fresh orange; 10YR 8/2) weathered dolomicrites, stratified on a scale of 20 to 40 cm. Within these beds there are intervals of undulating, coherent microbial stratification as well as intra-bed breccia pockets.

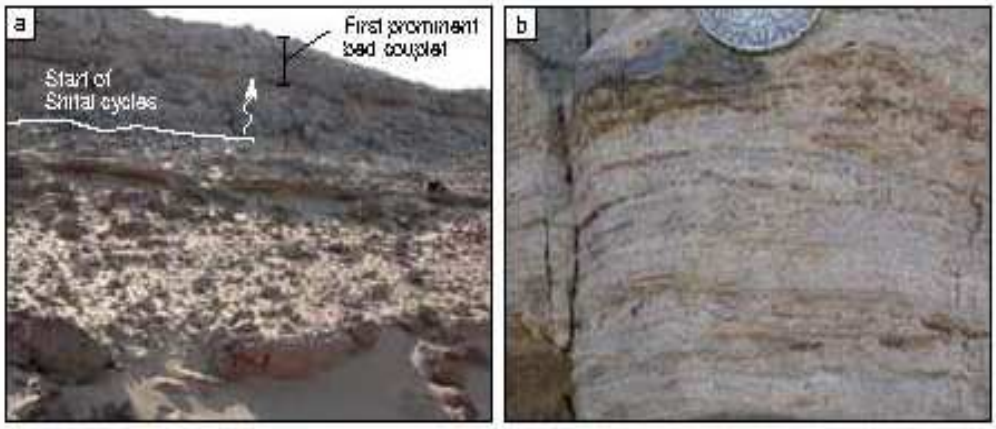

Figure 1-14: a*) Looking northeast along the Shital Member/Aswad Member boundary at WA-1. A prominent ridge dissected by karst fissures and chert replacement appears to pass up without faulting into an overlying succession of oncolite mounds that may dip more gently. b) Organic-rich oncoids in beds at the top of WA-1 (specifically on section WA-2), from Nicholas and Gold (2012).*

The characteristic bed tissues are the Thromboid mesoclots that appear in the areas between the brecciated pockets (figure 1-14). At approx. 4.3-4.5 m, the "cauliflower" Thrombolite heads begin to morph into more cohesive, disarticulated balls so that, the upper beds in this unit consist entirely of oncoids, with diameters similar to the width of the thrombolite heads. One of these oncoid beds marks the top of the stratotype section of the Aswad Member at WA2.

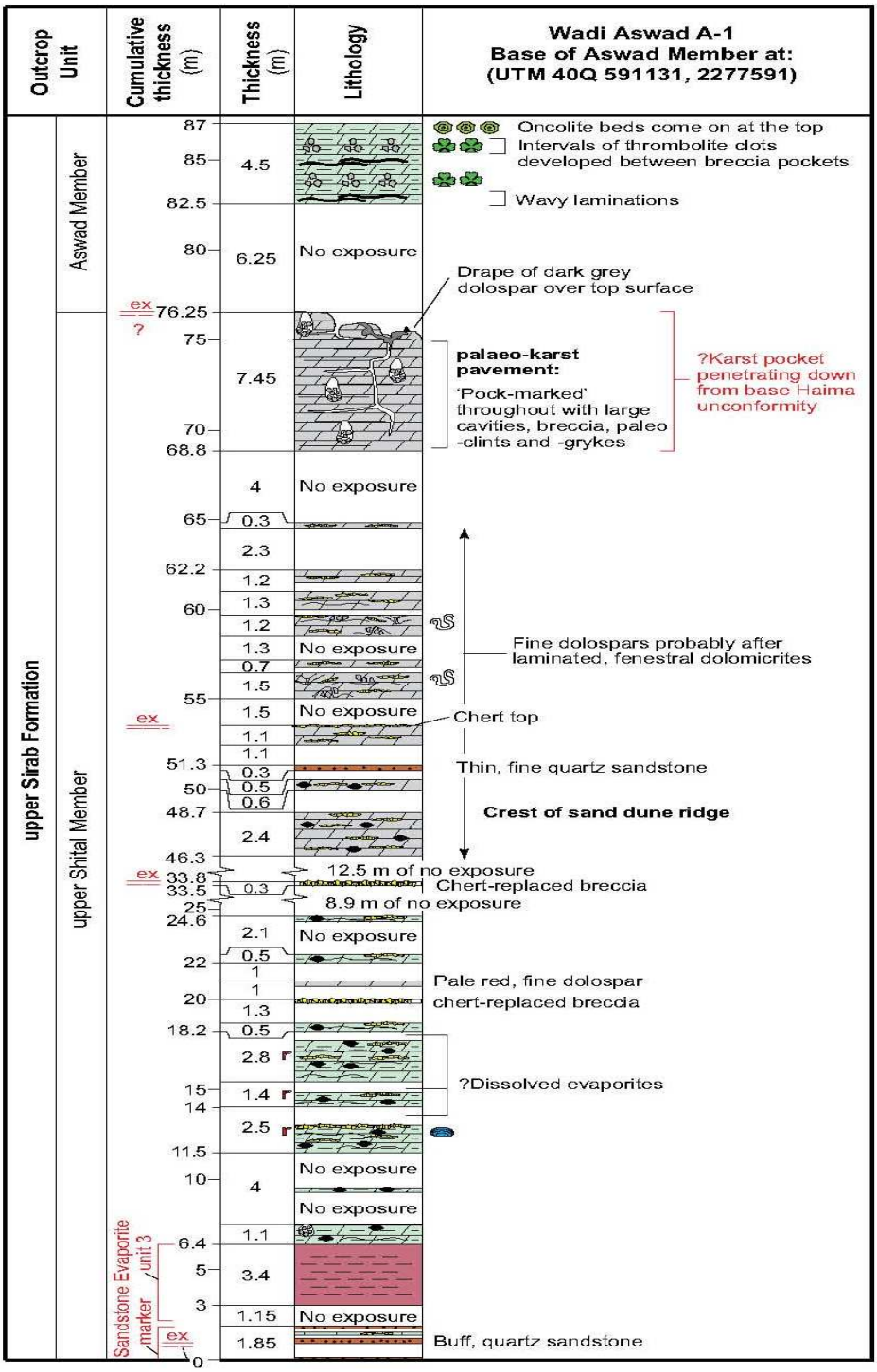

Figure 1-15: *Detailed sedimentary log of section Wadi Aswad WA-1, including the short stratotype section of the Aswad Member (upper Sirab Formation). UTM coordinates refer to the base of the Aswad Member, See figure 1-3 for localisation areas, from Gold (2010).*

Stratigraphically speaking, the lateral correlation of the Aswad Member was made in the type zone of the Sirab Formation (Wadi Shital ST-1) by incorporating the ST-2 add-on section. This latter section is slightly more extensive through the dissected mounds of the Aswad Member and overlaps horizontally for about 2 km southeast of the beds of the Shital Member which outcrop beneath ST-2, in the Sirab-type zone. Mounds below this level south of the Sirab Road have less than 30 m of Aswad Member stratigraphy. Although the Aswad unit is thin in the add section (ST-2), it still offers the opportunity to examine lateral facies changes within the Aswad Member. Oncoid beds higher than WA-1 consist of a medium gray matrix that suggests a reasonable component of preserved organic matter. Viewed as such, Aswad Member sediments (oncolites) may be potential hydrocarbon source rocks (figure 1-14b). Compared to the type section of the Aswad Member (WA-1), in the type area of Sirab (Wadi Shital ST-1 & ST-2), the Oncoid beds are creamy white in color and do not appear to be well preserved from organic matter (figure 1-16). The alteration of the oncoid bioherm in this zone seems particularly accentuated. In this way, the ST-2 addition section would make sense to be called a para-stratotype of Aswad's member [UTM 578843, 2231645], Nicholas and Gold (2012).

Figure 1-16: *Characteristics of Aswad Member at Wadi Shital ST-2, south of Sirab. The parastratotype section of the Aswad Member southeast of the road from Sirab to Wadi Shital ST-2, has an estimated mound height of 6 m, from Nicholas and Gold (2012).*

The ST-2 section was recorded through a mound representative of the many exposures. The base of the log is pinned to the desert sand where there is no exposure for the first 0.7m (figure 1-13). The lowest unit of the ST-2 section lies between 0.7 to 1.3 m from the beginning of the total length of the Aswad Member at ST-2. These first puts of the unit are altered into pinkish gray to very light gray sediments when the dolomicrite is fresh (5YR 8/1 to N8). Microbial laminations are irregular on a scale of 1–2 mm in the basal 40 cm of the unit. Then they pass laterally to plaques of Thrombotic clots. A gradual vertical change also occurs in this base-layered dolomicrite unit which eventually transitions to 20 cm thick Thrombolytic tissue towards the top of section ST-2.

Between 1.3 to 1.6 m, a highly developed Thrombolite bed appears. And approximately between 1.6 and 1.65 m an apparent mixture of Oncoids and Thrombolytic heads appears to be a gradation within the thrombolite to higher energy, fully disarticulated microbial balls. The level following the thrombolytic Oncoid beds transitions upwards to the more typical framework tissues at the top of the bed at 1.75m. The Thrombolites appear again between 1.75 and 2.05 m, covered with the more typical clotted thrombolite tissue dominating the rest of the section.

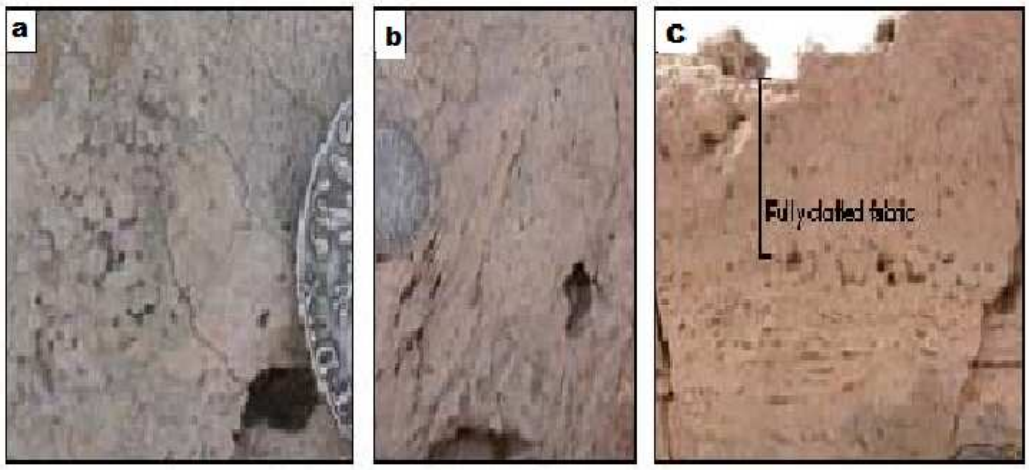

Figure 1-17: *a) The Aswad Member coagulated thrombolite in dolomicrites and fine packstones which are interstratified with thick oncolite horizons in the area southeast of ST-1. b) Large flat block of thrombolite, rolled up, coated and draped with microbial slides, forming a giant oncoid close to ST-2. C) Vertical development of thrombolitic clots from thin, wavy stromatolitic stratifications at the base of an ST-2 bed, as highlighted by the change in porosity of the framework as the clots grow from the bottom up, from Nicholas amd Gold (2012).*

Other dissected lateral equivalent mounds are exposed around ST-2. They show gradual facies between individual oncoids, oncoids microbially bound together in plaques, beded (stromatolytic) Thrombolite, and coagulated textures of well-developed Thrombolite. Partially lithified plates of microbial dolomicrite rolled up by currents and subsequently microbially bound, are also reported (figure 1-17) [UTM 578664, 2231841].

At the origin of previous work on the Sirab Formation, the latter noted the persistent presence of Thrombolites in the Aswad Member. Their presence was interpreted as a possible marine depositional environment, more open than the lower units of the Formation. On the other hand, Gold (2010) believed that Thrombolitic lithofacies could occur lower in the Sirab stratigraphy if there had been localized and sufficient subsidence to cause an increase in water depth and circulation. Since such a deepening event seems plausible to have occurred temporarily in the upper Shital sedimentary unit at Wadi Shuram WS-1 (where an interval of excellent domale stromatolytic Thrombolite occurs, see figure 1-5) . This interval more or less represents the depocenter of the Shital Member through the WS-1 base section of Wadi Shuram. The domed stromatolites of the maximum inundation zone of the Shital Member (figure 1-18) are overlain by a single bed of oncolites approximately 10 cm thick. However, the Oncolites here (maximum inundation zone at Wadi Shuram) are identical in size and in fassily preservation as in the typical facies of the Aswad Member. Farther northeast along the

Shital Member ridges in Wadi Shuram, there are also small isolated Thrombolitic reefs among the Conophyton [UTM 556554, 2226603], (figure 1-18). Field observations in the Wadi Shuram section indicate that the transition of lithofacies from the Shital Member to the Aswad Member is gradual and controlled by the water depth in the lagoon, Nicholas and Gold (2012).

Finally, the Aswad Member across the add section (ST-2) also asserts the increase in water depth through the Formation in relation to the sediment facies. More details concerning the sedimentological data of the Sirab Formation in Oman can be read in the publications of Gold (2010) as well as Nicholas and Gold (2012).

Figure 1-18: *Large domes of stromatolytic thrombolite in the upper Shital (Shital Member) of the Wadi Shuram WS-1 section. These domes are covered with a single bed of thin oncolite, from Gold (2010).*

2 Second chapter: *Samples and Methodology.*

2.1 Introduction.

The palaeo-ecological study of this thesis on the Sirab Formation, of approximately Ediacaran - Cambrian era in Oman in the Huqf Supergroup, required, in addition to the annotation of the outcrops presented at the end of this chapter 2, the methodological use next:

- The selection of field sections likely to record chemostratigraphic variations;
- Selection of outcrops by stratigraphic order on the main Study section (Wadi Shital ST-1 & ST-2) from the base of the Formation to the top as well as, targeted selection of outcrops in the horizon of maximum inonation (Wadi Shuram) and in the thrombolite-oncolite horizon of Wadi Aswad;
- Petrographic study of the outcrops in order to determine the mineralogical trend of the mixed carbonates of the Sirab Formation;
- Diagenetic analysis of outcrops to examine the degree of burial of sediments;
- Analysis of $\delta^{13}C$ and $\delta^{18}O$ isotopic ratios to examine the horizons of evolution of isotopic values which are indicators of environmental changes;

- Chemostratigraphic analysis of the main inorganic geochemical elements present in the outcrops in order to understand the origin of their enrichments;

- Analysis of REEs from outcrops in order to interpret variations in REEs recording trends likely to lead to a good Paleoecological interpretation of the Sirab Formation.

2.2 Field sections such to reveal chemostratigraphy change.

Three field sections have been selected to lead to the Palaeo-ecological study of the Sirab Formation. These include the composite stratotype section of Wadi Shital ST-1 & ST-2 (main section of the Sirab Formation), the stratotype section of Wadi Aswad (type section of the Thrombolite - Oncolite facies) with the outcrops which lie above the base of section WA-1 (outcrops WA-1 and WA-2), as well as the section of Wadi Shuram with the outcrops above the base of section WS-1 (outcrops WS-9) which are depocenter sedimentary facies, see tables 2-6 and 2-7. The base of the section of Wadi Shuram WS-1 was not retained because the facies of the Ramayli Member was analyzed in the stratotypical section of Wadi Shital ST-1. In addition, only a significant variation of the $\delta^{13}C$ isotopic ratio exists in the upper Shital unit for the entire Formation. And this one was well identified among the samples analyzed in the stratotype section (Wadi Shital ST-1) at the Shital Member. Overall the $\delta^{13}C$ isotope ratio changes towards the upper Shital part within the lithostratigraphy and this for all the different field sections so far revealed by Gold (2010). Moreover, these isotopic variations occur in the horizons of the stratigraphy where the Conophyton reefs begin to develop.

See the following points for more details: Chapter 1.7; chapter 1.8 as well as chapter 1.9 which summarize the choice of field sections likely to record Palaeo-ecological variations.

2.3 Stratigraphy of outcrops analyzed.

The samples collected by Christopher Nicholas and Sophia Gold in the Al-Huqf Supergroup in Oman were subsequently stored in the premises of Trinity College, Dublin. In this thesis, all rock samples submitted for analysis are those collected by Christopher Nicholas and Sophia Gold in the Haushi-Huqf in Oman which is located among rocks within the region of Al-Huqf according to lithostratigraphy of Oman.

However, due to the notion of stratotype section explained in chapter 1.7 (first paragraph), all the sections discovered in the field and by extension the horizons of outcrops within the different Members of the Sirab Formation; do not present the same interest during a historical reconstruction study. Some of the sections including their outcrop levels are particularly important to feature prominently. Indeed, they are either stratotypical (Wadi Aswad) or they exclusively represent a stratigraphic succession as complete as possible of the entire Formation (composite stratotype section Wadi Shital ST-1 & ST-2).

However, in the previous publication of the Sirab Formation as a sedimentary unit at the lithostratigraphic scale of the Al-Huqf Supergroup by Gold (2010), the facies descriptions of the carbonate sediments in the upper part of the Shital Member (Conophyton Reefs) and the Aswad Member (Thrombolite - Oncolite), were identified as a

ramp shift to a more open environment. As such, the change in isotopic signature of $\delta^{13}C$ recorded from the upper Shital can be added to the considerations presented in chapter 1.9 with respect to the sections that are analyzed in this thesis. This finally to identify upstream, what constitutes the horizons of outcrop which make it possible to retrace the markers of ecological change through the study of the Palaeo-filling of the carbonated ramp for the Sirab Formation.

The Wadi Shital section ST-1 & ST-2 being taken as the main section of the study in relation to the almost complete stratigraphy of all the Members; the Thrombolite - Oncolite carbonate beds are explored in detail Palaeo-ecology in the Wadi Aswad section and the same for the beds of the Conophyton Reefs found in the upper unit of the Shital Member which have been better analyzed at through the depocenter in the Wadi Shuram section. The $\delta^{13}C$ isotope ratio of the Formation indicates a characteristic positive peak which appears stratigraphically only after the sandstone horizon or at least from the upper Shital in all sections. This characteristic of the upper Shital is invariable in all sections and marks the beginning of the gradual transition from the upper Shital to Aswad Member. As such, it (positive peak $\delta^{13}C$) served as a reference during the selection of outcrops for the Conophyton Reefs level in the Wadi Shuram section and in the Wadi Aswad section.

Figure 2-1: *Stratigraphy logs and location of samples analyzed as part of this thesis.*

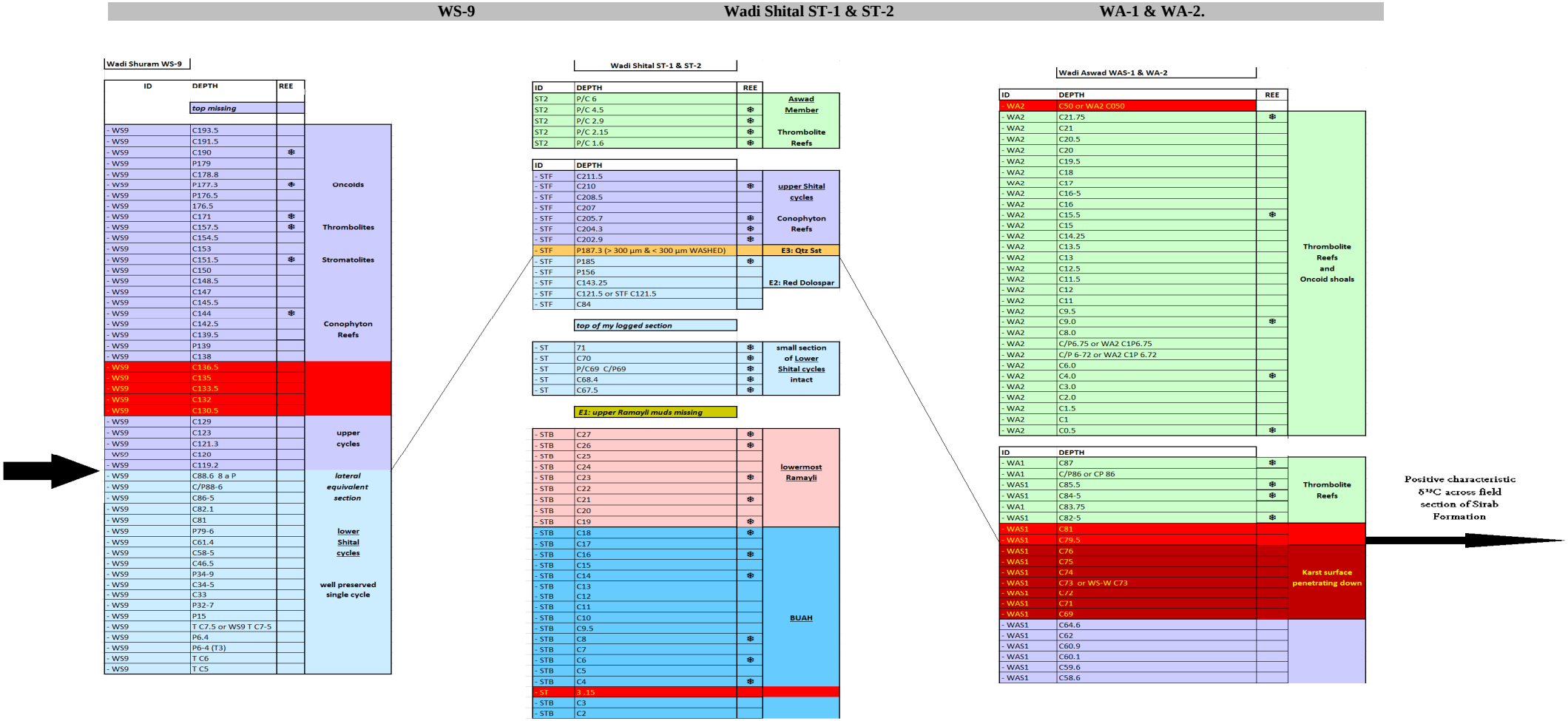

Shart color used in this study to analyse Sirab samples

Aswad member
Upper Shital member
Quartz sandstone horizon
Lower Shital cycles intact plus one sample of Red dolospar included STF 185
Upper Ramayli member samples missing in this study
Lower Ramayli
Buah Formation (Nafun Group)

N.B: Samples listed in yellow with RED background coud not be lacated with certainty on the original logs and so, were left aside. Only samples having cross on left side of their original logs were analysed. On the other hand, sample of Saluttiyat member are not represented in this study due to the raison avoqued to the chapter 1 in point 1.9.

Sections retain are:

- **Wadi Shital ST-1 & ST-2 (type section of Sirab).**
- **Wadi Shuram WS-9 (depocentre/deeper water of upper Shital).**
- **Wadi Aswad WA-1 & WA-2 (stratotype of Aswad member on WA2).**

When examining the bins containing the rock samples of Christopher Nicholas and Sophia Gold (samples used in Sirab's first publication as the surface equivalent of Ara Group (Gold, 2010; Nicholas and Gold, 2012); certain labels of the levels of the outcrops which are stored in the TCD sample bins were no longer recognizable to trace it in the stratigraphy of the sections to which they belong. Other samples such as those from the upper Ramayli unit in the Wadi Shital ST-1 & ST-2 field section could not be precisely located in the storage lot.

Finally, to preserve the originality of the stratigraphic field data as they appear in the figures: figure 1-1; figure 1-5; figure 1-13 and figure 1-15 (all presented in chapter 1); the outcrops whose stratigraphic reconstruction could not be elucidated within the sections to which they belong were simply not included in this study during the analyses.

A total of twenty-five (25) samples were taken from the Wadi Shital section ST-1 & ST-2, of which six samples at the base of the section represent outcrops of the transition zone (Buah Formation at lower Ramayli Member for the Sirab Formation). Five (5) samples were taken from the stratotype section of Wadi Aswad more precisely at the level of the Thrombolite - Oncolite facies (WA-2). Four (4) additional samples were re-collected from Wadi Aswad section at Thrombolite reefs (WA-1) which lies on the upper Shital in this section at Wadi Aswad, prior to the development of the Thrombolite-Oncolite facies. And finally, six (6) samples representing the upper Shital depocenter in the Wadi Shuram section (WS-9) were also incorporated in the analysis of this thesis; see figure 2-1.

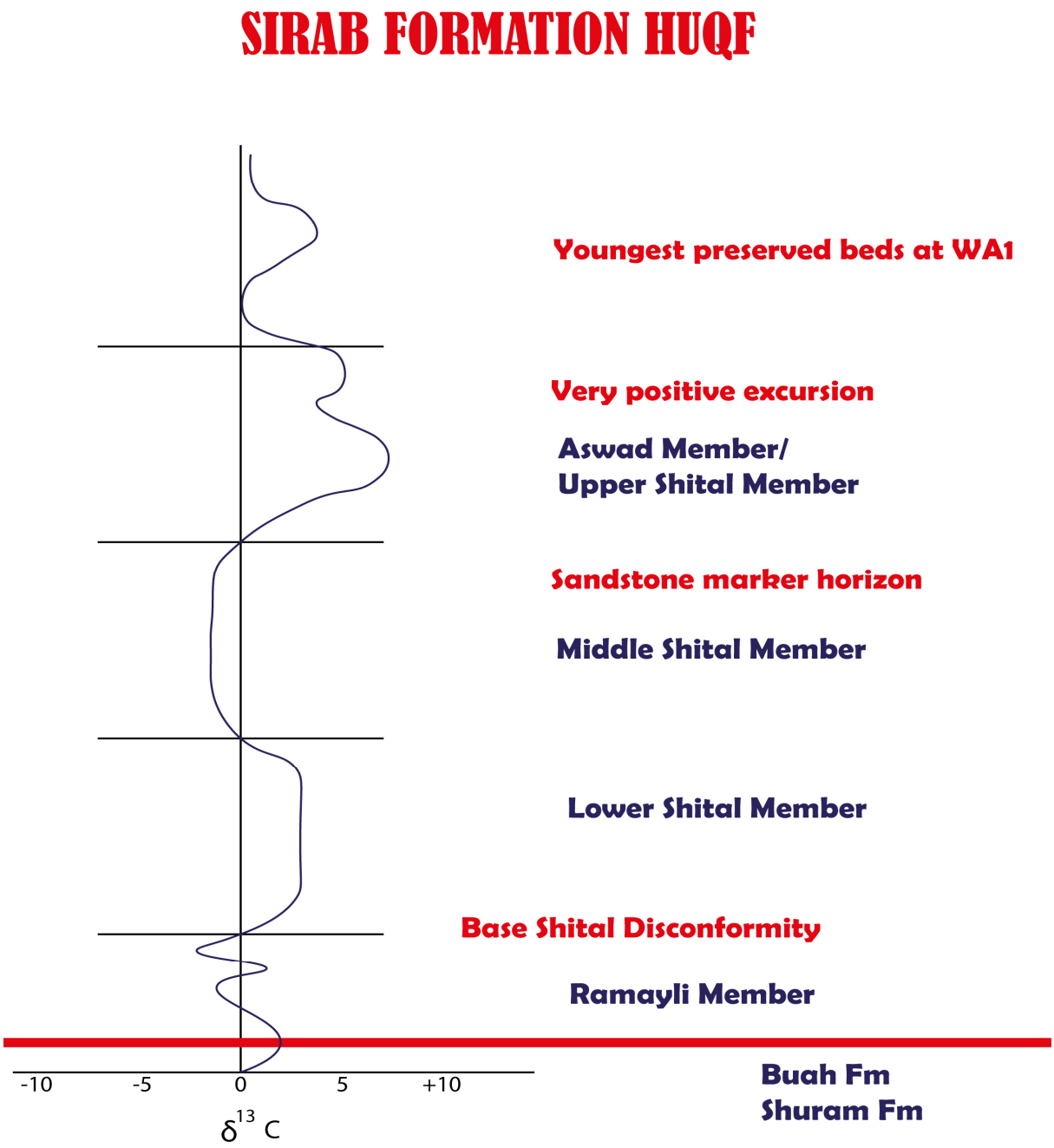

Figure 2-2: *Isotope curve of the carbon composites for the Sirab Formation. The "sandstone marker" can appear at different positions within the central Shital Member. The vertical scale is approximate, with an estimated total thickness for the Sirab Formation of around 300 m, from Gold (2010). Figure 2-2 is used to illustrate more at less $\delta^{13}C$ isotope curve which occurs at upper Shital in the Sirab Formation as seen to the resume of samples in figure 2-1.*

2.4 Petrographic analyzes.

(Folk's, 1952; Dunham, 1962; Klovan, 1971) are the most appropriate and widely used petrographic works for the description of rock samples. The term petrography in itself is the science whose object is the description of rocks, the analysis of their structural, mineralogical and chemical characteristics, and the relations of these rocks with their geological environment. Usually, during the macroscopic examination in the field, the petrographic study is limited to describing the main structural elements, mineralogical, coloration, facies, bedding, etc., which make up the rock. These elements make it possible to define the large family of rocks (endogenous, sedimentary or metamorphic) to which the observed sample belongs. In the case of sedimentary rocks, the structural elements essential to the petrographic description by macroscopic and microscopic observation are: the size of the grains, the shape of the grains, and the presence of figured elements (allochthonous and/or autochthonous), the nature of the cement as well as than the nature of the matrix. This description, which has as a basic indication: the size of the constituent elements of the rock as well as their arrangement in mechanical equilibrium in the matrix, leads to the terms (grainstone, packstone, wackstone, mudstone, etc.).

In the field, the constituent Elements of the rock still identifiable with the naked eye or either with a magnifying glass lend themselves immediately to the description of the sample when this criterion can still be the subject of a macroscopic estimate. Other elements not

taken into account in the classification of Folk's and Dunham such as: the color, the structural characters of the sedimentary beds (finely bedded bed, crossbed, teepee, Hummocky, etc.) can also be supplemented by a macroscopic evaluation. Basically, these elements make it possible to macroscopically describe the lithological data of the environment of the deposit.

Macroscopically, the detail of certain constituent Elements of the rock, such as the matrix and the cement, can be highlighted by the use of thin sections. Thanks to the microscopic observation of the sections made on the rock outcrops that have been collected in the field, it is therefore possible to analyze and describe the discrete lithological aspects that do not appear in macroscopic observation. This additional analysis step makes it possible to build a new set of descriptive information related to the field of the outcrop for a better understanding of the geological environment of the Formation.

2.4.1 Microscopic Analyzes.

Rocks of the Sirab Formation differ markedly from interior and mid-slope facies dominated by grainstone of the underlying Buah Formation and ferruginous fluvial conglomerates and sandstones of the overlying Haima Supergroup. They are all composed of a mixture of dolomite carbonates. Beds of intercalated evaporites are recognized in the stratigraphy of the Sirab Formation. Calcite is generally recognizable in the field. The sedimentological field data mention the abundance of carbonates with dolomite, calcite and evaporite to which is added a fraction of terrigenous sediments (clasts). See sedimentology in chapter 1.

In carbonate and as a rule, calcite and dolomite are the main mineralogical constituents. To differentiate them from each other in our study, our thin sections were mounted using the Alizarin Red S staining technique, used in its modified version of Dickson (1966). A thin section produced by this technique has the advantage of coloring the space occupied by the dolomite in a pink tint so that, by microscopic observation, one can estimate the percentage share occupied by the dolomite over the length of the section. As for their examinations, the thin sections were examined in natural light and in transmitted light.

2.4.2 XRD responses.

X-ray diffraction (XRD for X-ray diffraction) is an analysis technique based on the diffraction of X-rays by matter, especially when it is crystalline. X-ray diffraction is elastic scattering, that is to say without photon energy loss (unchanged wavelengths), which generates interference that is all the more marked as matter is ordered. For non-crystalline materials, we speak rather of diffusion.

The (X-ray) method uses a beam of X-rays which, when it encounters a crystal, is reflected in directions determined by the wavelength of the X-rays and by the dimensions and orientation of the crystal lattice. By measuring the angles and the effect of the diffracted rays, it is possible to obtain the dimensions of the crystal lattice, the symmetries of the crystal structure (space group) and a three-dimensional picture of the electron density in the lattice. From this density, the average position of the atoms in the crystal forming the crystal pattern can be determined as well as the nature of these atoms (to some extent), their chemical bonds, their thermal agitation and other structural information.

Each bulk sample for XRD analysis was predisposed as a flattened powder in a dish, and then was placed in a diffractometer to count the photons and then reveal the mineralogical nature of the sample tested, by the formation of a diagram of diffraction or diffractogram. As part

of the carbonate-type mineralogical identification, only samples from the type region of Sirab (Wadi Shital ST-1 & ST-2) were used for XRD analysis. The entire XRD test was performed at the laboratory of Trinity College Dublin (TTEC), and more details on the results obtained from this analysis can be found in volume 2, appendix 1 of this thesis.

In addition, the analysis of the Major Elements carried out by ICP-MS and ICP-MS/OES made it possible to mineralogically support the carbonate type trend which predominates in the Sirab Formation, by the comparative use of the MgO ratios (%) against CaO (%). This relation was verified for all the samples of analyzes of this thesis contrary to XRD which was only carried out on the composite stratotype section of Wadi Shital ST-1 & ST-2. MgO (%) versus CaO (%) confirmed the main mineralogy of carbonates found at Sirab in the Haushi-Huqf in Oman.

2.5 ICP-MS and ICP-MS/OES data.

For the masses and concentrations of the main Geochemical Elements, Traces and Rare Earth, two series of analyzes were carried out on the samples. The first set of analyzes was carried out on samples from the type section of Sirab at Wadi Shital ST-1 & ST-2. This analysis was carried out at the laboratory of Trinity College Dublin. Concentrations of Elements in chondrites were normalized at MUQ to identify the trace from sea level to the water-sediment interface, from which carbonates were deposited on the ramp. The detection limits of Major Elements were given and evaluated in ppm while those of Trace Elements and Rare Earths were given in ppb. The final laboratory results sheets as well as the entire protocol are presented in volume 2 of this thesis while the summary of the analysis is given as follows:

- Collection of powders from each sample and dissolution in aqueous solution for the ICP-MS laboratory (2-step dilution);
- Step 1: ~10mg of powder sample to be placed in a test tube with the addition of ~1.5ml of 5% HNO_3;
- Storage of the solution for a few days to allow time for the acid to digest the sample in powder;
- Step 2: dilution of ~0.0217 g of the first solution plus addition of ~0.2000 g and ~1.7783 g 5% HNO_3. (Dilution 2) put in a new tube.

The test was repeated identically for all samples analyzed from the standard section of Sirab in Wadi Shital ST-1 & ST-2. In the development of this study, the Y/Ho ratio was also measured in samples from Wadi Shuram WS9 sections as well as Wadi Aswad WA1 and Wadi Aswad WA2. However, the concentrations of Major Elements, Traces and REEs of the samples from these sections were analyzed at the ALs OMAC Laboratories and their chondrites were normalized with respect to the average concentrations in the crust (PAAS). Therefore, the main reference of the palaeo-marine level at the water-sediment interface within the framework of this study was the most developed on the Y/Ho ratios obtained from the samples.

Regarding the batch of 15 samples belonging to the sections of Wadi Shuram WS9, Wadi Aswad WA1 and Wadi Aswad WA2, the latter were sent to the ALs OMAC laboratory to obtain their geochemical concentrations. Chondrites normalized with PAAS made it possible to estimate the average contamination of carbonates with respect to PAAS in these sections of the Sirab. Unlike the analysis carried out at Trinity College Dublin where the concentrations of Major Elements were given in ppm and that of Trace Elements and REEs in ppb, the detection limits for the analyzes carried out at ALs OMAC were all given in ppm. Major elements were estimated in percent (%) ppm units rather than weight (ppm) as in the Trinity lab results. The results sheets of the ALs OMAC laboratory are given in volume 2, appendix 3 of this thesis which also includes the analysis protocol.

Data on the abundance of carbon and oxygen isotopes are reported in a table in Volume 2, appendix 4 of this thesis. These data relate to field sections of the Sirab Formation and were collected at Trinity College, Dublin, after being used in part by Gold (2010) in his lithostratigraphic correlation study. The $\delta^{13}C$ and $\delta^{18}O$ isotope values were determined by the Thermo Deltaplus mass spectrometer at Trinity College Dublin. They were performed with a reproducibility based on international and internal laboratory standard which is between ±0.1‰ (1σ) for C and O isotopes. This instrument separates and detects ions based on the motion of charged particles different masses in the magnetic field. For the field to be effective, they (the particles) must be inside a vacuum with a pressure of $1.8X10^{-6}M$, which ends with three pumps. More information regarding mass spectrometer theory can be found in the works of (Hoefs, 2008; Anderson, 1983 and Corfield, 1995).

For the purpose of comparing the profile of REEs, it has been inserted in this work in chapter 6, the profile of REEs of a sample of freshwater carbonate taken in the south-west of the DRC and whose laboratory analysis was carried out in 2016 at Trinity College Dublin following the same laboratory protocol as that with the samples from the type section of Sirab (Wadi Shital ST-1 & ST-2). The field detail of the Precambrian freshwater carbonate sample collected in south-western DRC is given in volume 2, appendix 5 of this thesis.

The other REEs profiles illustrated in comparison with the final results of the laboratory analyzes mentioned in this thesis are the responsibility of the authors who published them. For each case of data already published and subject to a comparative analysis in this thesis, the names, edition, scientific journal, etc., of the publication that summarizes the previous work (publication taken as a reference for comparison purposes) were cited throughout the text as well as in the bibliography of this study.

2.6 Diagenetic analysis.

In sediments and more particularly in dolomitic carbonates, the hypothesis of the origin of magnesium enrichment can be explained by the phenomenon of sediment diagenesis which occurs during deep burial. However, in certain environments where the concentration of Magnesium ions is high (example of certain lakes hyper saturated with Mg), primary dolomite can form by direct precipitation and completely independently of the diagenetic process. Generally, to differentiate between the two (diagenesis dolomite or primary dolomite), the use of geochemical tracers capable of filtering the variations in the values of the Sr and Mg recordings according to the depth of the sediments is essential. For this reason, Land (1985) believes that the reason for the widespread dolomitization is due to continuous diagenesis which allows the import of sufficient Mg and the rejection of excess Ca and Sr.

Brand (1980) find that the substitution of Ca^{2+} by trace elements such as Sr^{2+}, Mn^{2+}, Fe^{2+}, Pb^{2+}, Zn^{2+} and Na^{+} in the $CaCO_3$ lattice can occur to varying degrees due to different partition coefficients and large differences in composition in marine and meteoric water. As such, these exchanges imply that open or partially closed diagenetic systems and/or single or multiple dissolution-reprecipitation events generally lead to a decrease in the concentrations of the elements in this case, the partition coefficient (Kcalcite-water) < 1 (Sr^{2+}, Na^{+}, Mg^{2+}). However, there is an increase in K > 1 (Mn^{2+}, Fe^{2+}, Zn^{2+}) at the same

time. That is, the greater the deviation of a particular coefficient from unity, the greater the depletion or enrichment for a given degree of diagenesis with meteoric water.

Many Elements, including iron and manganese, reach high threshold concentrations in the Sirab Formation, so that diagenetic alteration can be suspected as a source of (Mn) enrichment in the sediments. To analyze the diagenetic origin or not of the concentration of certain Major Elements including in particular Manganese (Mn), the following correlations were made:

Ratios	Key to determine diagenesis	Positive correlation	Interpretation	Lack of correlation	Interpretation
Mn/Sr	value R^2	$R^2 \geq 6$	Proof of diagenesis.	$R^2 < 5$	Loss of diagenesis signal while Mn enrichment could be considered as inherited from Mn-rich sediments.
Mn/δ^{13}C	value R^2	$R^2 \geq 6$	Evidence of diagenesis and possible evolution of the isotopic signature of carbon.	$R^2 < 5$	Loss of diagenesis signal.
Fe/δ^{13}C	value R^2	$R^2 \geq 6$	Possible evidence for Fe enrichment and carbon isotope evolution resulting from diagenesis.	$R^2 < 5$	Loss of Fe enrichment signal as no diagenesis effect.
δ^{18}O/δ^{13}C	value R^2	$R^2 \geq 6$	Possible primary values of C and O isotopes.	$R^2 < 5$	Evolution of isotopic signatures over time.
Y/Ho	Value of Y/Ho	> 45	Marine signature and possible diagenesis effect on carbonates.	~26	Freshwater signature with less evidence for a possible role of diagenesis.

Table 2-1: *Summary of diagenesis analysis in the type section of the Sirab Formation (Wadi Shital ST-1 & ST-2).*

Ratios	Key to determine diagenesis	Positive correlation	Interpretation	Lack of correlation	Interpretation
Sr/MgO (%)	value R^2	$R^2 \geq 6$	Sr and Mg may have a close origin in the development of dolomite as an effect of diagenesis.	$R^2 < 5$	Loss of diagenesis signal while Mn enrichment could be considered as inherited from Mn-rich sediments.
MnO (%)/Sr	value R^2	$R^2 \geq 6$	Evidence of diagenesis.	$R^2 < 5$	Loss of diagenesis signal while Mn enrichment could be considered as inherited from Mn-rich sediments.
$\delta^{18}O$/MgO (%)	value R^2	$R^2 \geq 6$	Possible modification of isotopic values of oxygen during the development of dolomite; possible effect of diagenesis.	$R^2 < 5$	Possible primary oxygen values unrelated to dolomite development.
$\delta^{18}O/\delta^{13}C$	value R^2	$R^2 \geq 6$	Possible primary values for C and O isotopes.	$R^2 < 5$	Evolution of isotopic signatures over time.

Table 2-2: *Summary of diagenesis analysis within sections of Wadi Shuram (WS9), Wadi Aswad (WA1) and Wadi Aswad (WA2).*

2.7 Analysis of Major Geochimical Elements.

The analysis of the Sirab Formation through this study was particularly important in determining the redox state of the environment at the time of carbonate deposition. Ca and Mg are commonly associated with dolomite mineralogy, followed by Fe, Al, Mn and P, all of which were detected as Major Elements by ICP-MS performed at Trinity College Dublin. These data in relation to the Major Elements were both confirmed by the ICP-MS/OES analyzes carried out in the ALs OMAC laboratories and in addition to the Elements mentioned above, the Na_2O (%) and K_2O (%) analyzes of the ALs OMAC specifically state that sodium is similar in content to manganese and slightly higher than phosphate. Which also makes them (Na and K), other Major Elements. Except that sodium (Na) and potassium (K), not having been measured by ICP-MS in the laboratory of Trinity College Dublin, only Fe, Al, Mn and P are then considered here as Major Elements accompanying the composition of carbonates (Ca and Mg).

Currently, the characteristics of the concentrations of geochemical elements are better and better elucidated for the different environmental types (marine, terrestrial, lacustrine, etc.). As an example, clay is a geochemical element that is more abundant in the continental environment, particularly transported by river sediments which are loaded with clay particles (e.g. the lithostratigraphic correlations of clay levels in the Mandawa Basin by McCabe et al.,

2019). Carbonates still contain in minor proportions Fe and Mn contents of about 10 ppm because these geochemical elements have low concentrations in seawater. Burial effort causes a negative modification of the oxidation-reduction potential (Eh). This has the consequence that the diagenetic pores at the water-sediment interface become enriched in Fe and Mn (Tucker, 1986). High Fe and Mn contents in carbonates generally reflect a redox state of the carbonate environment, undergoing the process of diagenesis.

In addition, depending on the thickness of the sediment, diagenesis can act to varying degrees. Certain horizons (levels by extensions) of the sediment may be more diagenetic than others. The differentiation of a diagenesis characteristic of the entire sediment accounts for the use of the term “general diagenesis”. This term was used in this study to define whether or not, for the entire Formation, there would have been similar redox conditions that lead to Fe and Mn enrichment in the carbonates. Because other conditions other than diagenesis such as, for example, rocks originally rich in Fe and Mn can transmit by inheritance to the sediment, a mineralogical composition of carbonates rich in these Elements; it is therefore important to qualify in the absence of generalized diagenetic evidence (effectiveness) for the whole of the sediment, what are then the reasons or at least the hypotheses of the enrichment in Fe and Mn on the carbonated ramp of Sirab..

Current observations confirm that the exchanges between different types of environments highlight the contamination of the sediments and the original rocks from which they come by the detrital contributions which are then deposited within the sediments in formation. Rare Earths are excellent tracers of the composition of the original sediment (marine, continental by extension or terrigenous by detrital contribution). Because the Rare Earths retain the chemical signatures (mineralogical DNA) of the rocks from which the sediments originate for a long time. Their release from the original mineral framework from which they come is caused by the alteration of the source rocks which contain them before they accumulate within the sediment by fractionation of REEs. Furthermore, the total concentration of a given geochemical element in the sediment can be translated into three independent fractions: detrital, biogenic and hydrogenated (i.e. derived from seawater), see Piper (1994) or Piper and Isaacs (1995). Since the initial content of the concentration of Geochemical Elements in the sediments (enriched Elements) can be modified later by alteration, monitoring of the detrital fraction is necessary to evaluate the redox parameter in relation to the detrital component (LREEs). The geochemical composition of Rare Earths can be decomposed into LREEs, MREEs and HREEs, three categories of total Rare Earth fractions that are associated with distinct environments depending on the composition of the sediment. Taylor and Mclennan (2001) found that PAAS represents the average composition of the crust (enriched in LREEs) and that the siliciclastic detritus which is the main source of REEs production in the sediments

exhibits similar REEs profiles to PAAS. Unlike detritus, authigenic sediments preserved in the marine environment with negligible detrital influence can potentially preserve the Rare Earth composition of seawater that is enriched in HREEs rather than LREEs (Mclennan, 1989).

On the other hand, regarding the redox state of Rare Earth, there are few individual Rare Earth Elements that can provide better information about redox records in sediments. Among the Rare Earth Elements that are part of the redox changes of the environment, Ce and Eu exhibit key oxidation states. These anomalies are of particular interest because they can record redox conditions in the overlying water column and early diagenesis (Elderfield, 1990). However, abnormal La/Nd ratios can lead to miscalculations of Ce anomalies, which are unrelated to Ce geochemistry. Abnormalities are expressed as Ce/Ce*, where Ce* denotes the concentration of Ce in normalized chondrites (McLennan, 1989). True Ce anomalies can be checked by a graph of Ce/Ce* against Pr/Pr* (Bau, 1996).

Eu also exhibits Eu/Eu* anomalies. In strongly reducing environments, Eu can appear in the oxidation state (+2). Seawater shows variable but low Eu positive anomalies (around 1.5). Larger positive Eu anomalies may be present where seawater has mixed with hydrothermal fluids (Meyer, 2012) while apparent Eu anomalies may result from interference with barium oxides formed during analysis

and this can be assessed by measuring Ba concentrations (Jarvis, 1989).

Thus, to relate the enrichments in Major Elements in the carbonates with respect to the detrital or authigenic environment in relation to the redox parameters given by the Ce/Ce* anomalies (apparent and true), the following analytical ratios were used :

Analysis	Interpretation
P; Mn; Fe; Al; $\delta^{13}C$; $\delta^{18}O$	Intersection of the profiles of the Major Elements with each other and with respect to the isotopic abundances of C and O.
REEs / Mg	Determine the upper limit of REEs production concentrations in carbonates below the water level.
Y/Ho / Mg	Determine the development ceiling of the dolomites (sediments) below the water level.
Major Elements / Mg	Determine the correlation of the concentrations of Major Elements with respect to the magnesium (Mg) contained in the dolomites.
Major Elements / Eu/Eu*	Determine the correlation in Major Element with positive anomalies in Eu in possible pores of the sediment pressed by diagenesis during the formation of carbonates.
Major Elements / Ce/Ce*	Determine the correlation in Major Element with the level of oxygenation of the sediment during the development of carbonates.
LREEs ; HREEs, ; Mg/Ca, Al/Fe ; P/Al	Comparison of fractionation of detrital profiles (LREEs) as well as authigenic fractions (HREEs) versus dolomites (Mg/Ca), terrigenic mineralogical substitutions (Al/Fe) and non-authigenic phosphate (P/Al).
REEs / Major Elements	Correlation of REE fractionation in carbonates with Major Elements. It should be noted that the alteration accentuates the process of fractionation of REEs, in particular their abundances in the sediments (Taylor and McLennan 1985).
Al / Cr, Mo, U, V, Ni and Cu	Determine the authigenic or detrital enrichment of aluminum.
P/Th ; P/LREEs ; P/HREEs	Determine authigenic or detrital phosphate enrichment.
LREEs/Fe_2O_3 ;HREEs/FeO ;REEs /Fe_2O_3;REEs/FeO ; Al/Fe_2O_3 as well as Al/FeO	Determine the mineralogy of Fe. Note that the detrital tendency of iron is Fe_2O_3 while the authigenic tendency of iron is FeO.
Mn / Mg/Ca	Determine the correlation of Mn enrichment with the dolomites.

Table 2-3: *Summary of the analysis of the concentration of Major Elements in the type of section of the Sirab Formation (Wadi Shital ST-1 & ST-2).*

Analysis	Interpretation
REEs / Mg	Determine the upper limit of REE production concentrations in carbonates below the water level.
Y/Ho / Mg	Determine the development ceiling of the dolomites (sediments) below the water level.
Major Elements / Mg	Determine the correlation of the concentrations of Major Elements with respect to the magnesium (Mg) contained in the dolomites.
Major Elements / Eu/Eu*	Determine the correlation in Major Elements with positive anomalies in Eu in possible pores of the sediment pressed by diagenesis during the elaboration of carbonates.
Major Elements / Ce/Ce*	Determine the correlation in Major Element with respect to the level of oxygenation of the sediment during the development of carbonates.
REEs / Major Elements	Correlation of REEs fractionation in carbonates with respect to Major Elements. It should be noted that the alteration accentuates the process of fractionation of REEs, in particular their abundances in the sediments (Taylor and McLennan 1985).
Y/Ho / REE+Y; Y/Ho /Th; Y/Ho / Zr	Determine the average values of the concentrations of Elements with respect to the crust (PAAS).

Table 2-4: S*ummary of Major Element concentration analysis in sections of Wadi Shuram WS9, Wadi Aswad WA1 and Wadi Aswad WA2.*

2.8 Traces Elements and REEs analyzes.

As their names suggest, Trace Elements are Geochemical Elements whose concentration in the samples in which they are measured is low compared to the Major Elements. Among the Elements with a low concentration, Rare Earths are also distinguished. These Geochemical Elements are counted among 15 Lanthanide Elements (La, Ce, Pr, Nd, Pm, Sm, Eu, Gd, Tb, Dy, Ho, Er, Tm, Yb, Lu) to which are added the Sc and Y (Mclennan, 1989; Walters and Lusty, 2011). Lanthanide Elements are generally classified into groups according to their atomic weight (Mclennan, 1989; Laveuf and Cornu, 2009; Walters and Lusty, 2011). Commonly abbreviated REEs, the different categories of Lanthanides within the sediment can be grouped into three (3) families: LREEs or light Rare Earth of La - Sm, MREEs or medium Rare Earth of Eu - Dy, and HREEs or heavy Rare Earth of Ho-Lu (McCabe et al., 2019). Due to geochemical similarities, Y is often included in HREEs, while Sc behaves geochemically differently from all other REEs. However, Sc is similar to Elements such as Ni, Cr, V and Co (Mclennan, 1989).

In this study, the analyzes of the Trace Elements Th, Zr, Mo, U, V and Ti were compiled in chapter six (6) in order to determine the chemostratigraphic architecture of the Sirab Formation in association with the Major Elements data analyzed in chapter five (5). The REEs profiles of the carbonates belonging to the Sirab Formation were compared to those of the Ara Group and of different environments and

minerals known throughout the world in order to properly assign and define the palaeo-ecology of the Formation. Apparent Ce/Ce* anomalies persist in the Sirab carbonate samples while the Y/Ho ratios of the majority of the samples show no clear marine involvement in the magnesium enrichment of the carbonates. In order to restore the redox conditions of the circulation of oxygenation in the mass of the sediment during the deposition of the Sirab carbonate ramp, the real Cerium (Ce*) anomalies were checked by plotting the Ce/Ce* ratio in relation to the Pr/Pr*. The result of the analysis is presented in the discussion that summarizes this present study and below relates the summary of the objectives pursued:

Analysis	Interpretation
Ce/Ce* / Pr/Pr*	Monitoring of true Ce* anomalies.
Zr/Th ; Ti/Th ; U/Th ; V/Th ; Mo/Th	Monitoring of detrital inputs. It is one of the elements incompatible with short residence times in seawater which can ideally be adapted to filter contamination of authigenic sediments by the entry of detritus. Because this element (Th) will be transferred almost quantitatively to sediments, and should therefore closely reflect the original composition of the continental crust (Taylor and McLennan 1985, Webb and Kamber 2000). Also, unlike some elements that depend on source zone and grain size (see Taylor and McLennan 1985, Johnson and Grimm 2001), Th is largely independent of factors such as grain size relative to Fe_2O_3, Al_2O_3, MnO as well as P_2O_5. Moreover, a diagenetic modification of Ti, Th and Zr concentrations is unlikely in carbonate rocks, since these elements are mainly associated with non-carbonate components (Veizer 1983a).

Table 2-5: S*ummary of analysis of Trace Elements and REEs concentration in Sirab type section (Wadi Shital ST-1 and ST-2), Wadi Shuram WS9, Wadi Aswad WA1 and Wadi Aswad WA2.*

2.9 Annotation of samples.

A) Wadi Shital ST-1 & ST-2 (type section of Sirab Formation).

SIRAB FORMATION ALONG ITS STRATOTYPE COMPOSITE SECTION (WADI-SHITAL ST-1 & ST-2).							
MEMBER	**FIELD ANNOTATION**	**SUB- MEMBER / NAMES**	**NUMBER OF SUBMEMBERS**	**SAMPLING HEIGHT FROM BASE (B-NW3)**	**SAMPLE ANNOTATION IN THIS STUDY**		**Outcrop limits**
ASWAD	ST2 P/C	None	*0*	Expressed in numerical values after the annotation of each member	ST2 P/C 1.6 ; ST2 P/C 2.9 ; etc.		up to more than 6 m Base ST-2
SHITAL	STF C	Conophyton Reefs; Sandstone horizon; Red Dolospar; Lower Shital cycles intact	*4*		Conophyton Reefs	STF 204.3 ; STF 202.9 ; etc.	~ 215 m between ~ 189 m
					Sandstone horizon	STF	~ 188.4 m between ~ 184.8 m
					Red dolospar	STF	144.25 m between 142.5 m
					Lower Shital	STF 68.4 ; STF 67.5 ; etc.	~ 136.2 m between ~ 61.5 m
RAMAYLI	STB C	Upper Ramayli ; Lower most Ramayli	*2*		Upper Ramayli	missing	~ 56.5 m between ~ 35 m
					Lower Ramayli	STB 14 ; STB 8; etc.	~34.9m to ~8 m
BUAH DOME	STB C	None	*0*		STB 4 and STB 6		~7.9 m between B-NW3

Table 2-6: *Summary table of field annotations for samples from the composite stratotype section of the Sirab Formation at Wadi Shital ST-1 & ST-2, modified from data of Nicholas and Gold (2012).*

Note: In the section of Wadi Shital ST-1 & ST-2, called stratotype composite section of Sirab or type section of the Formation, the sample STF 185 analyzed in this study has the characteristic of Red dolospar (see petrographic description of the Formation in chapter 3 as well as the sample's photo). On the field sketch presented in chapter 1 (figure 1-13), the STF 185 level is located on the sandstone horizon according to the field lithostratigraphy. However, the complete literature description of the Wadi Shital ST-1 & ST-2 section in

chapter 1, point 1.10.1 indicates that the red dolospar occurs about 184.8 m above the base of the section (Buah-Ramayli transition), and outcrops of Red dolospars continue to ~215 m. Although often the observation of these same outcrops (Red dolospars) is lost in the desert. For this reason, even though the sketch section of Wadi Shital ST-1 & ST-2 places the sample (STF 185) at the sandstone horizon, but due to its facies and appearance as shown in figure 3-4, the latter was placed at the interval of red dolospar rather than sandstone in this study.

B) Wadi Shuram WS9, Wadi Aswad WA1 and Wadi Aswad WA2 samples.

SIRAB FORMATION ALONG SECTIONS OF WADI SHURAM (WS9) and WADI ASWAD (WA1 & WA2).						
SECTION	**FIELD ANNOTATION**	**NUMBER SECTION OF FIELD**	**NUMBER OF SECTIONS ON THE FIELD**	**SAMPLING HEIGHT FROM BASE OF SECTION**	**SAMPLE ANNOTATION IN THIS STUDY**	**Outcrop limits**
WADI ASWAD	WA	WA1 & WA2	*2*	Expressed in numerical values after the annotation of each member	WA1 - (87, 85.5, 84.5, 82.5 m) FOR WADI ASWAD FIRST SECTION; WA2 – (21.75, 15.5, 9, 0.5 m) FOR WADI ASWAD SECOND SECTION	~ 87 m between 0 m. ~ 21.75 m between 0 m
WADI SHURAM	WS	WS1, WS2, WS3,….WS10 (All of Shuram sections contain only Shital member)	*10*		WS9-(190, 177.3, 171, 157.5, 151.5, 144 m) FOR WADI SHURAM SECTION 9, DEEPER WATER OF UPPER SHITAL	~ 193.5 m between 0 m

Table 2-7: S*ummary table of field annotations for samples from sections of Wadi Shuram (WS9) and Wadi Aswad (WA1 &WA2), modified from data of Nicholas and Gold (2012).*

3 **Third chapter***: Petrographic Study.*

3.1 Introduction.

As part of this thesis, the petrographic study of rock outcrops (samples) of the Sirab Formation which belong to the field section of Wadi Shital ST-1 & ST-2 (composite stratotypic section of Sirab also called type locality of Sirab), Wadi Shuram (precisely in the upper Shital unit for the Conophyton Reefs facies "depotcenter") as well as Wadi Aswad the stratotypical locality of the Aswad Member, was carried out in a comparative manner. First, the main section of the Formation (Wadi Shital ST-1 & ST-2), was detailed petrographically using the macroscopic description with the cut slab sections, microscopically using the thin sections and then mineralogically using the interpretation XRD results; all these petrographic analyzes were repeated on all the samples.

The ICP-MS/OES analysis performed on the outcrops of the Wadi Shuram and Wadi Aswad sections made it possible to obtain a set of inorganic Geochemical Rlements including in particular, CaO (%), MgO (%), SiO_2 (%), Al_2O_3 (%), Fe_2O_3 (%) as well as the Y/Ho (ppm) ratio, which made it possible to petrographically analyse the Geochemical composition of mixed carbonates (dolomite in majority, calcite and evaporate) of the Sirab Formation.

3.2 Wadi Shital ST-1 & ST-2 (type section of Sirab).

Initially presented in Chapter 1 as well as in chapter 2, the composite stratotype section of Sirab (Wadi Shital ST-1 & ST-2) makes it possible to analyze all the typical facies of Formation. However, given that the outcrops stratigraphically belonging to the upper level of the Ramayli Member were not located in this study, this level (with dolomitic mud) is therefore the only one that would not have been analyzed in this thesis. However, the sedimentological descriptions of the upper Ramayli are taken up in chapter 1 of this thesis and more details can be read from work of Gold (2010).

3.2.1 Presentation of samples analyzed.

A) Transitional Buah – Ramayli Member.

5G 4/1
Dark Greenish
Gray

5G 4/1
Dark Greenish
Gray

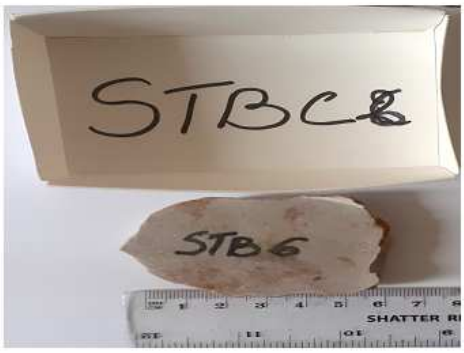

N6+
Medium light
gray
(GSA Rock Color Chart)

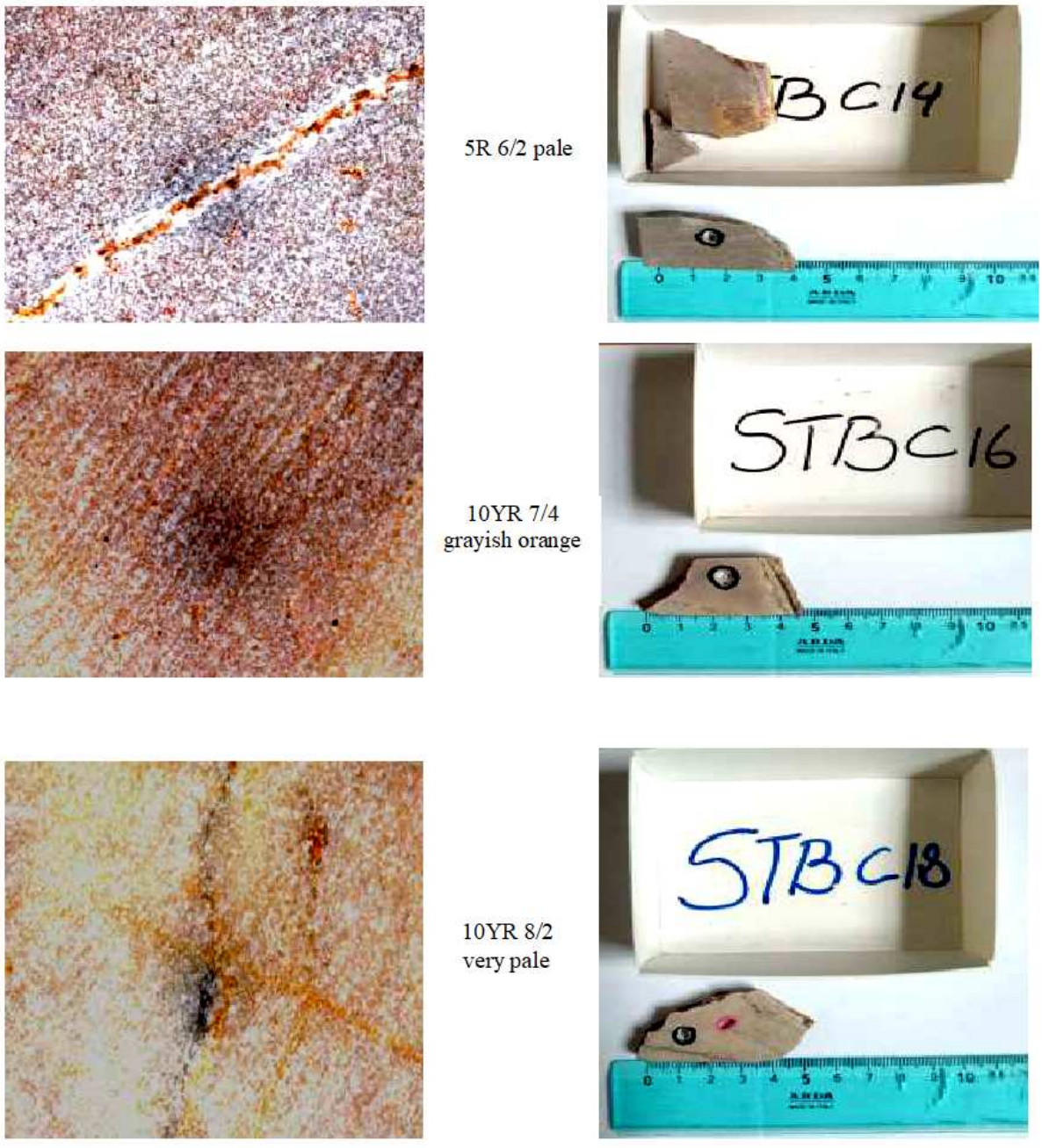

Figure 3-1: *Rocks from Buah-Ramayli (transition zone).*

Observation of rocks: bright colors dominate the rocks belonging to the Buah-Ramayli transition zone. STB 4 and STB 6 levels are dark in

color and shimmering quartz reflections are visible on the surfaces. The levels (STB 8, STB 14 as well as STB 18) are crossed by mini-veins post-filled with quartz. In the petrographic laboratory during the assembly of the thin sections, these samples presented a particularly high hardness when they were cut into thin sections.

B) Ramayli Member (lower unit only).

10 YR 8/2 very pale orange (GSA Rock Color Chart)

10 YR 8/2 very pale orange

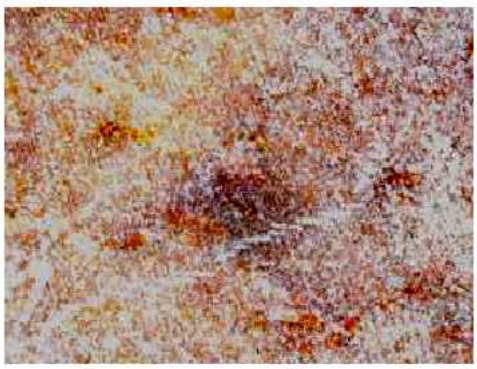

10 YR 7/4 greyish orange

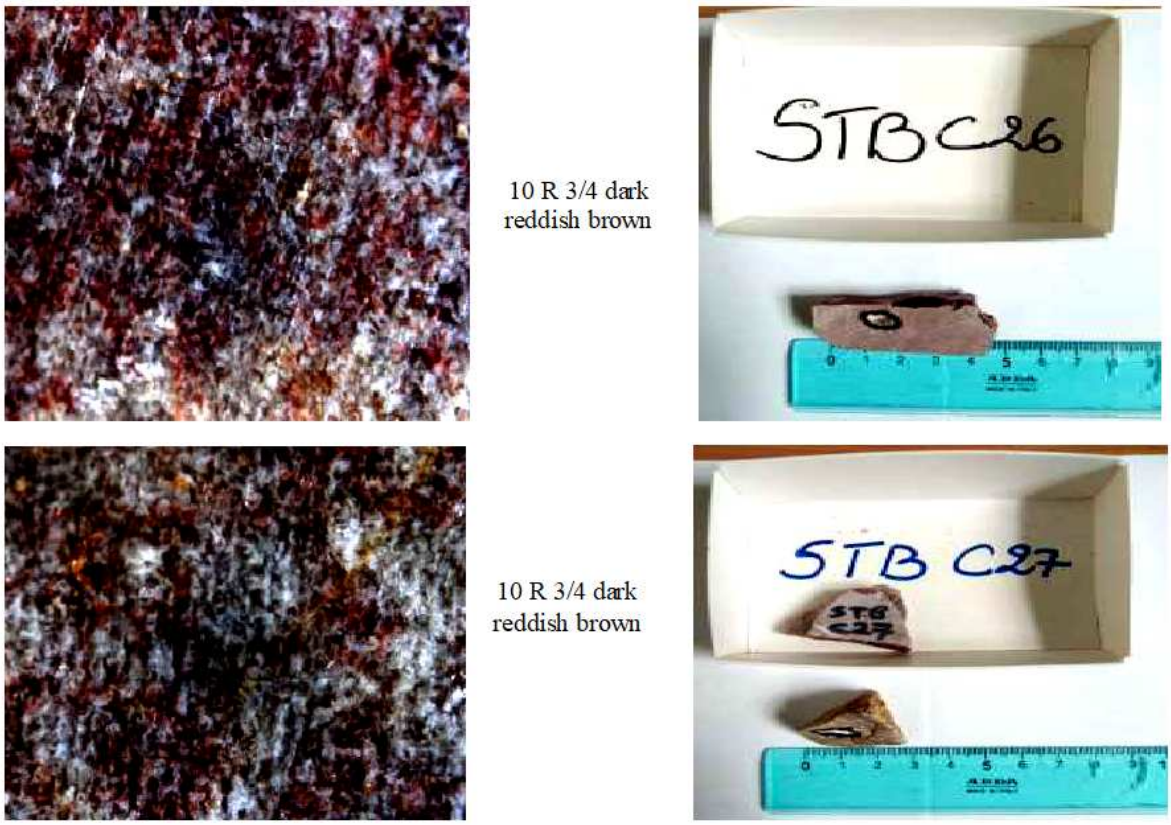

Figure 3-2: *Rocks from lower Ramayli Member*.

Observation of rocks: the bright colors remain dominant among the rocks belonging to the lower Ramayli. Level STB 19 displays an elongated dolomicrite rip clast. The STB 26 and STB 27 levels are dark red in color with shimmering reflections reminiscent of the presence of quartz which appears when the outcrops have been subjected to the mechanical effect of the saw when they are cut. On the other hand, the bright red hues are also an indication of the presence of iron as a major constituent of these rocks. Inconspicuous micro-veins are observed at STB 23. All post-filled and/or cemented

with quartz or calcite. Also the rocks were so hard to cut when mounting them in thin sections.

C) Shital Member (lower unit).

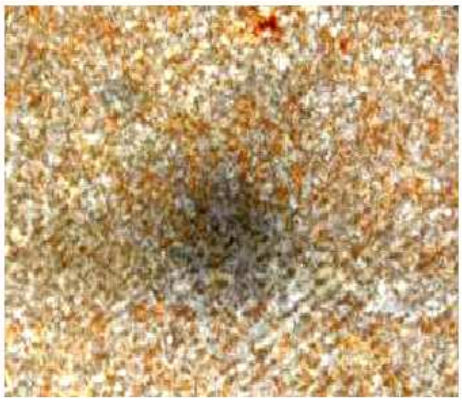

10 YR 8/6 pale yellowish orange (GSA Rock Color Chart)

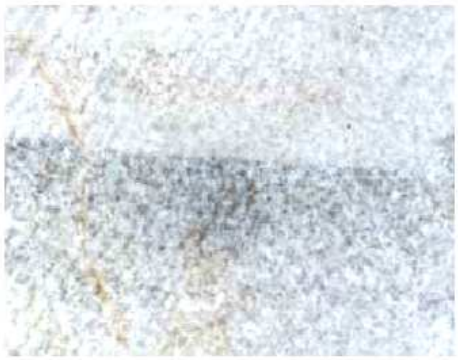

N8
very light gray

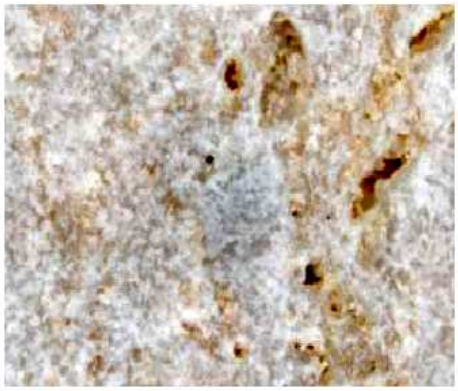

5GY 8/1 light greenish gray

Figure 3-3: *Rocks from lower Shital.*

Observation of rocks: bright colors remain dominant among rocks belonging to lower Shital. They are more vivid than in the lower Ramayli unit and in the Buah-Ramayli transition zone. Probably the lower Shital unit in the Wadi Shital ST-1 section was less preserved from the sub-aerial exposure in the desert at Al-Huqf. The shimmering reflections of the presence of quartz appear on almost every outcrop of this lower unit of the Shital Member. The bird's eye shaps associated to fenestrations which develop in the β facies of the rhythmic carbonate cycle (see chapter 1.10 paragraph 9) are perceptible on the

rock of STF 69 as well as on the rock or sample STF 67.5 with a beautiful vein about a few centimeters, post-filled with quartz. All rocks were hard to cut with saw during assembly.

D) Shital Member (Red dolospar, ± middle Shital).

Figure 3-4: *Rocks from Red sandstone (± middle part of Shital).*

Observation of rocks: The outcrop is a compact, reddish, relatively soft mud with two internal facies (surfaces A and B). The dolomite on surface B appears to be primary. It does not occupy the entire surface of the outcrop, which suggests that the dolomite was post-precipitated in the sediment, on the present surface A. As such, it is unlikely to be diagenetic. Probably, the initial level of magnesium in the environment during the deposition of the sediments on surface A was lower for the dolomite to precipitate. Subsequently, either due to a condition of restricted circulation of magnesium ions, or following a change in the chemical composition of the water at the water-sediment interface, enriched in magnesium; the dolomite would then have precipitated on surface B after breaking its equilibrium constant.

E) Shital Member (upper unit).

N8 very light gray (GSA Rock Color Chart)

5GY 8/1 light greenish gray

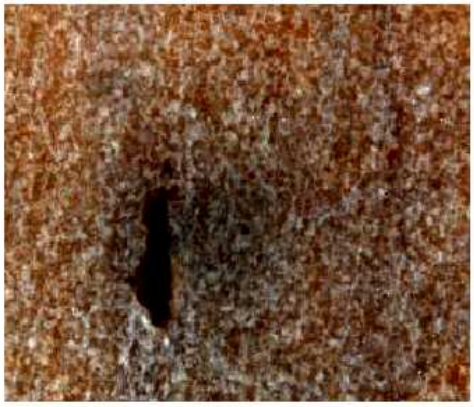

5R 4/6 moderate red

Figure 3-5: *Rocks from upper Shital.*

Observation of rocks: the bright colors remain dominant among the rocks belonging to the upper Shital. Probably the upper Shital unit in the Wadi Shital ST-1 section was less preserved from subaerial exposure in the desert at Al-Huqf like the lower Shital also which precedes it in the same field section. The shimmering reflections of the presence of quartz appear on almost all outcrops of this upper Shital unit. All the rocks were difficult to cut with a saw when assembling.

F) Aswad Member.

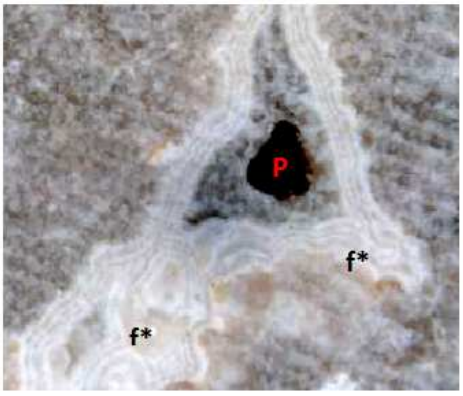

N7
Light gray (GSA Rock Color Chart)

(f*): filamentous forms.
(P): porosity.

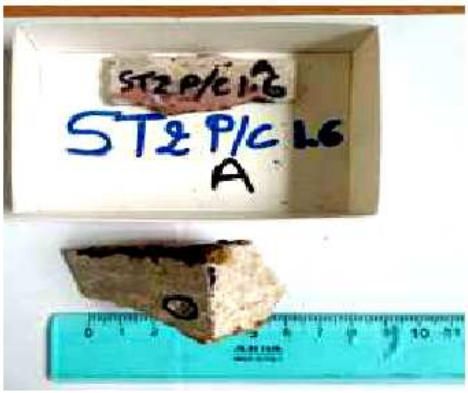

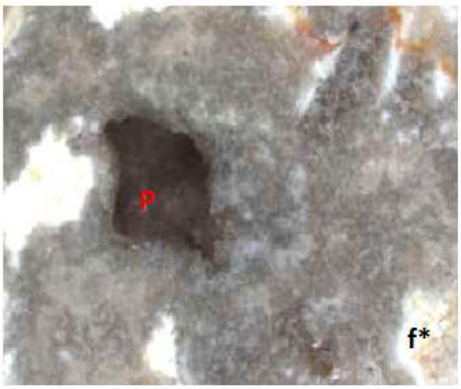

N7
Light gray

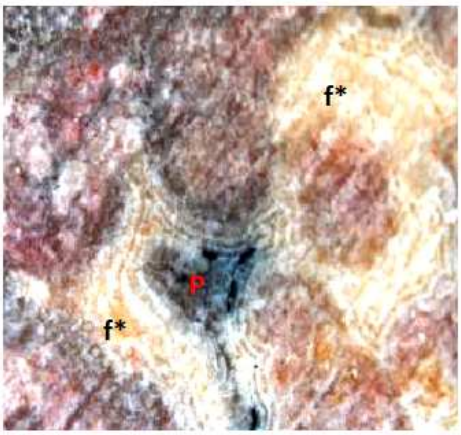

5R 6/6
Light red

Figure 3-6: *Rocks from Aswad Member.*

Observation of rocks: bright colors remain dominant among the rocks belonging to the Aswad Member. Small porous holes are perceptible on the surface of certain outcrops as in the photographs of the ST-2 4.5, ST-2 2.15, etc. These porosities indicated by the letter (P) on the rock sides on the left seem to be due to the release of gas bubbles on the surface of the sediment. Thus, if the bioherm of the Aswad Member had been partially or totally deprived of oxygen, the resulting sulfate-reduction at the time of preservation of the Aswad unit would likely have resulted in the release of gas bubbles. However, the filamentous shaps represented by the letter (f*) seem to be primary dolomite which would have precipitated posterior to the surface of the Aswad Member. If so (post-precipitation of dolomite), probably diagenesis would not had such a decisive effect on the Aswad Member and the evolution of gas bubbles by sulphate-reduction would perhaps be unlikely? Or the geothermal gradient of the basin fill of the Sirab Formation during the Ediacaran-Cambrian era had played some importance given fault movements and the general tectonics at Al-

Huqf. In this last condition, even with a low rate of diagenesis, the bioherm of the Aswad Member would have been subjected to relatively warm temperatures which caused the evolution of gas? Can this also be imagined to be produced in the sediments when the ramp periodically emerged from the surface of the water and simultaneously the primary dolomite precipitated? Moreover, the presence of quartz, already recognized in the lower units of Sirab, persists at all levels of the Formation lithostratigraphy. The ST-2 2.9 level has a characteristic redness indicating the fairly significant presence of iron as one of the major Geochimistry Element of the mineralogy. The REEs analyzes carried out in this study have deepened the geochemical composition of the mixed carbonates of Sirab in the following chapters.

G) Small figures of Aswad Member in stratotype section of Wadi Aswad WA2.

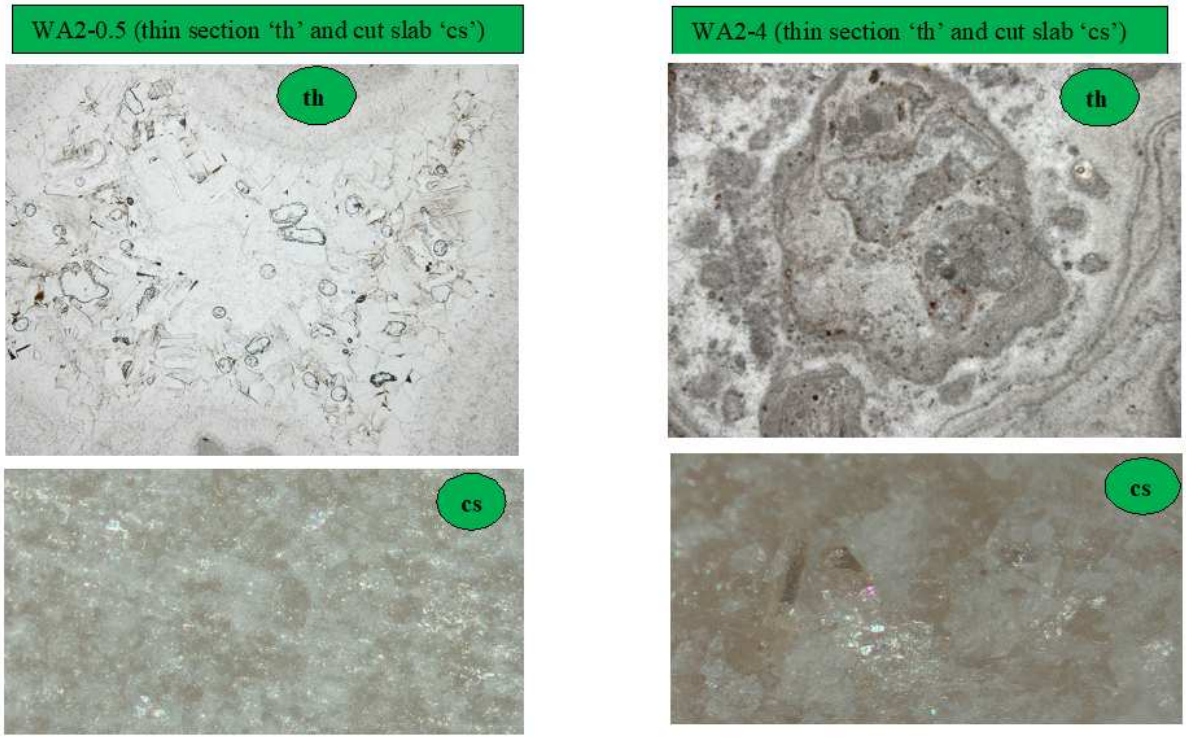

Figure 3-7: *The rocks of Aswad Member outcrops within facies well preserved in Wadi Aswad WA2 (stratotype section of Aswad Member).*

Observation of rocks: Thrombolite-Oncolite facies well preserved in Wadi Aswad WA2 section. Right figure shows development of filamentous shap well preserved and post-filled by dolomite. While left side figure shows development of cauliflowers shaps on the surface of rocks. The dolomite is always abundant and drawn a whitish circumference on the sediment. Wadi Aswad WA2 facies is considered as probably more enriched in O.M as well as more

influenced by palaeo-marine eustatic than the facies of Aswad Member encountered at ST-2 (the top of Formation at composite stratotype section of Sirab).

3.2.2 Thin sections of Wadi Shital ST-1 & ST-2.

A) Transitional Buah – Ramayli Member.

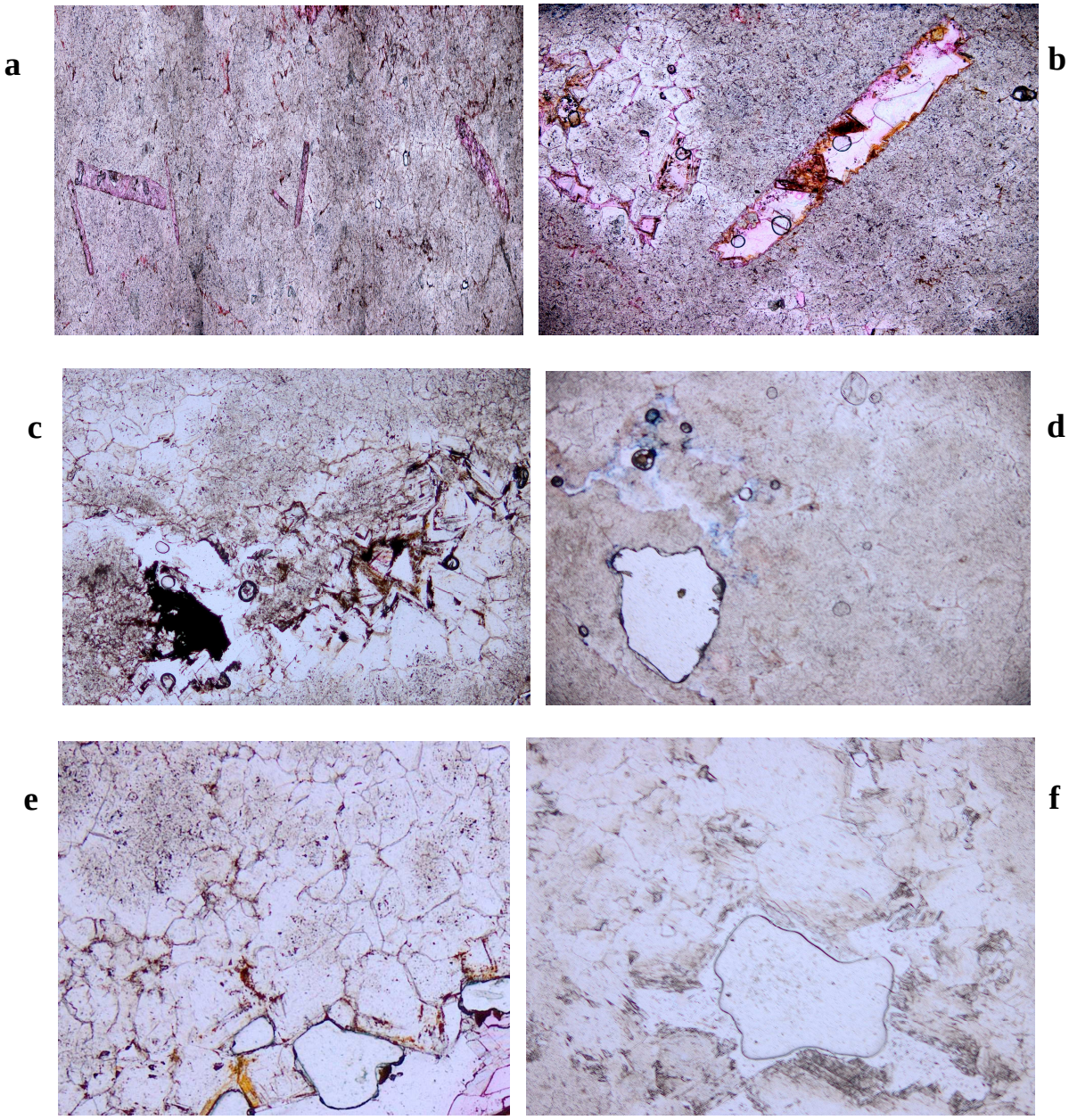

Figure 3-8: *Photographs of thin sections (a, b, c, d, e and f) by using an electron microscope NIKON ECLIPSE LV 100 (Scale 100 μm).*

Dolomite is the major constituent of the thin sections of the above samples belonging to the Buah - Ramayli transition zone. a) Several elongated clasts embedded in a fine matrix of micrite (dolomicrite). It appears in the photograph of the dolomite a slight reflection of white coloring which, together with the pink colored dolomite, paints the thin mosaic section. This mosaic coloration is most visible where the clasts are fused to the micritical matrix. This is an indication of calcite ciment. b) A large sample of clast in the center of the photograph which is accompanied on the left by a pseudo form engulfed by dolomicrite (matrix). The interval of outcrops corresponds to the zone where the first beds of evaporites generally accompanied by clasts and peloids appear, at the transition zone between the Buah Formation and the Sirab Formation. It is likely that this indiscernible shap which is buried in the dolomicrite is either a peloid embedded in the dolomicrite cloud or even a pseudo morph of dolomite next to rosettes of anhydrite crystals in finely crystallized calcite cement. c) Gas bubbles developed around large dolomitic lozenges with increased cement of the calcite due to the coloring relief of the thin section. d) Gas bubbles with observation of an irregular surface (hole or void on the surface of the slide) probably caused by the withdrawal of an evaporite? The dolomitic matrix appears dry and stiff due to compaction and calcite cementing the thin section. e) Dolomite with tightly imbricated anhedral mosaic. The porosity of the grains is reduced or simply cemented by the calcite. f) Dolomitic mosaic of imbricated anhedral crystals with a porous space obstructed by calcite cement (grainstone).

B) lower Ramayli.

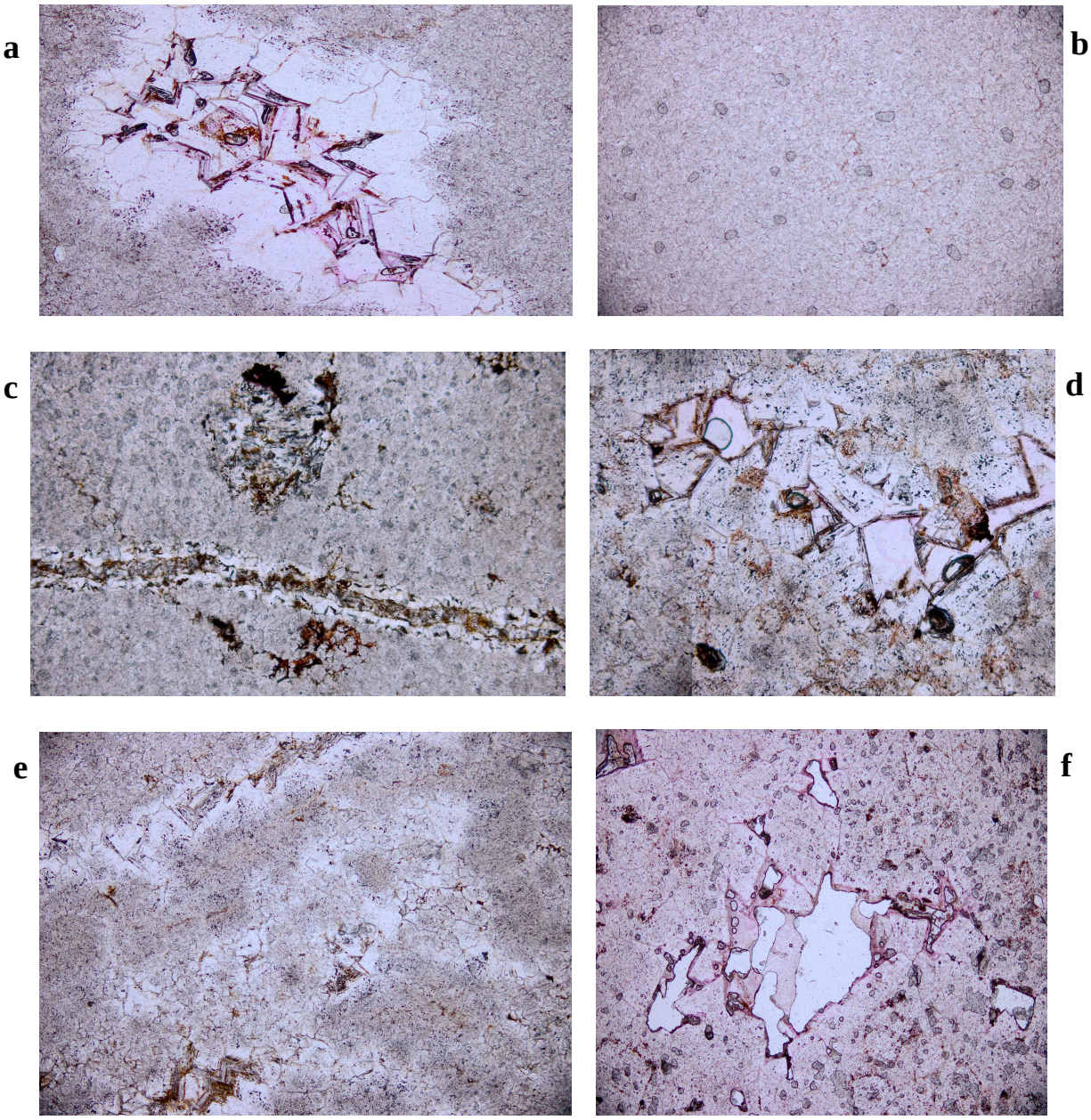

Figure 3-9: *Photographs of thin sections (a, b, c, d, e and f) by using an electron microscope NIKON ECLIPSE LV 100 (Scale 100 μm).*

Photographs showing a range of dolomite textures found in lower Ramayli. a) Replacement of dolomite by calcite which develops around a submerged body (possible clast or evaporitic mineral) in the dolomicritic matrix "Pseudomorphic dolomite with coarse calcite sparite". b) Gas bubbles associated with micrite mud pellets, the whole compacted and embedded in a fine matrix shell with dolomicrite and cemented by calcite. c) Dolomicrite with post-cemented calcite fracturing. The background of the photograph appears speckled because of the small circular shapes which recall the presence of peloids next to the dolomite-calcite replacement within the thin section d) Dolomite replaced by a calcite spar. The calcite cement developed on the spar engulfs the bottom of the dolomite and obstructs the clast shown in the center of the photograph. A few circular shapes marked by a fatty black coloration recall the presence of ooids/peloids encountered in the lower Ramayli (see sedimentology of the Sirab Formation in the composite stratotype section of Wadi Shital ST-1 & ST-2 in chapter 1). e) Poikilotopic fabric represented by the secondary porosity of the calcite filling. It is possible in the case of photograph (e) that the pores are aligned with the direction of elongation of the calcite extinction angle under the crossed poles. Compaction of the outcrop level or any other hydrothermal effect may be the cause of the precipitation of calcite which post-cements the initially precipitated dolomite. Permeability and porosity are reduced in this dolomicritic rock due to cementation by calcite. f) Porous dolomicrite due to shrinkage of evaporite on the center of the photograph, with the presence of numerous peloids.

C) lower Shital.

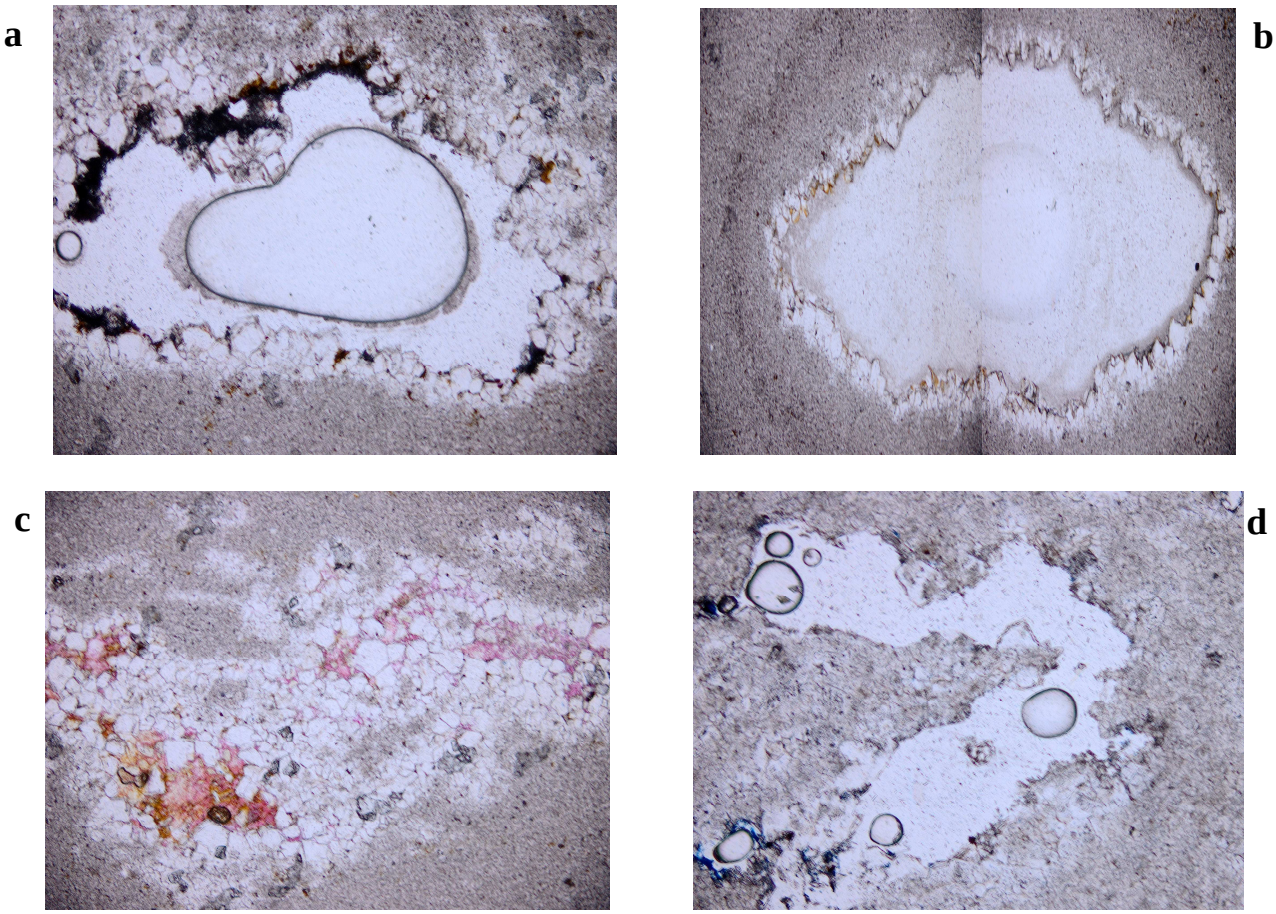

Figure 3-10: *Photographs of thin sections (a, b, c and d) by using an electron microscope NIKON ECLIPSE LV 100 (Scale 100 μm).*

The photographs show a range of dolomite textures found in the lower Shital. Figures a & b show replacement of dolomite by calcite along α & β rhythmic cycles (see presentation of the composite stratotype section of Sirab in chapter 1 for more details). In Figure (a), the shap in bird's eye is collapsed and there are small dolomite rhombuses around and pores developed throughout the calcite replacement. In

figure (b), the replacement of dolomite by calcite is done without the surface of the dolomitic bed being perforated (development of calcite around the shapes of bird's eye without collapse of the dolomitic bed around the calcite). c) Replacement of calcite and plugging of the dolomitic matrix. d) Replacement of calcite within dolomite.

D) Red dolospar (± middle Shital).

a

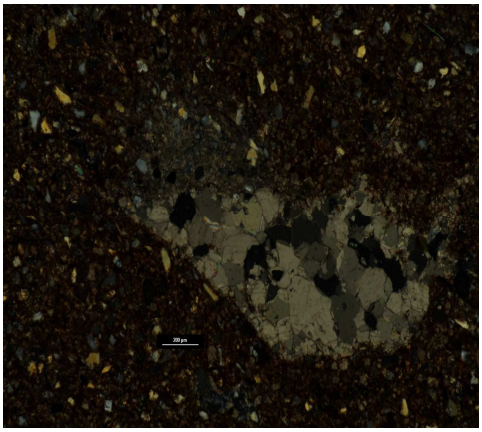

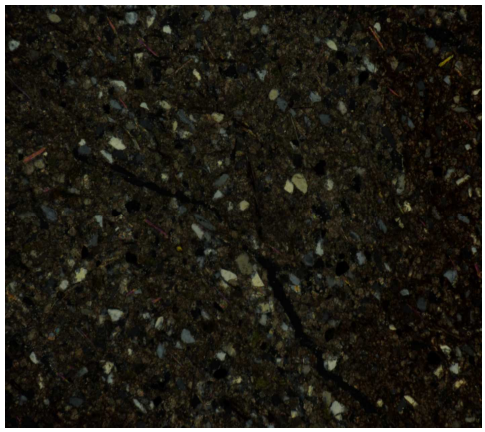

b

Figure 3-11: *Photograph of the thin section of the sample (a and b) using an electron microscope NIKON DS-R12 (Scale of photos: 200 µm).*

The photographs show a darkening of the coloring of the dolomite due to the change of objective of the analyzing microscope. The STF 185 level is a sample of dolomitic mud. The matrix of this outcrop is micritical with the presence of inclusions of small particles (probably impurities in the carbonate) due to terrigenous sediments which are abundant.

E) upper Shital.

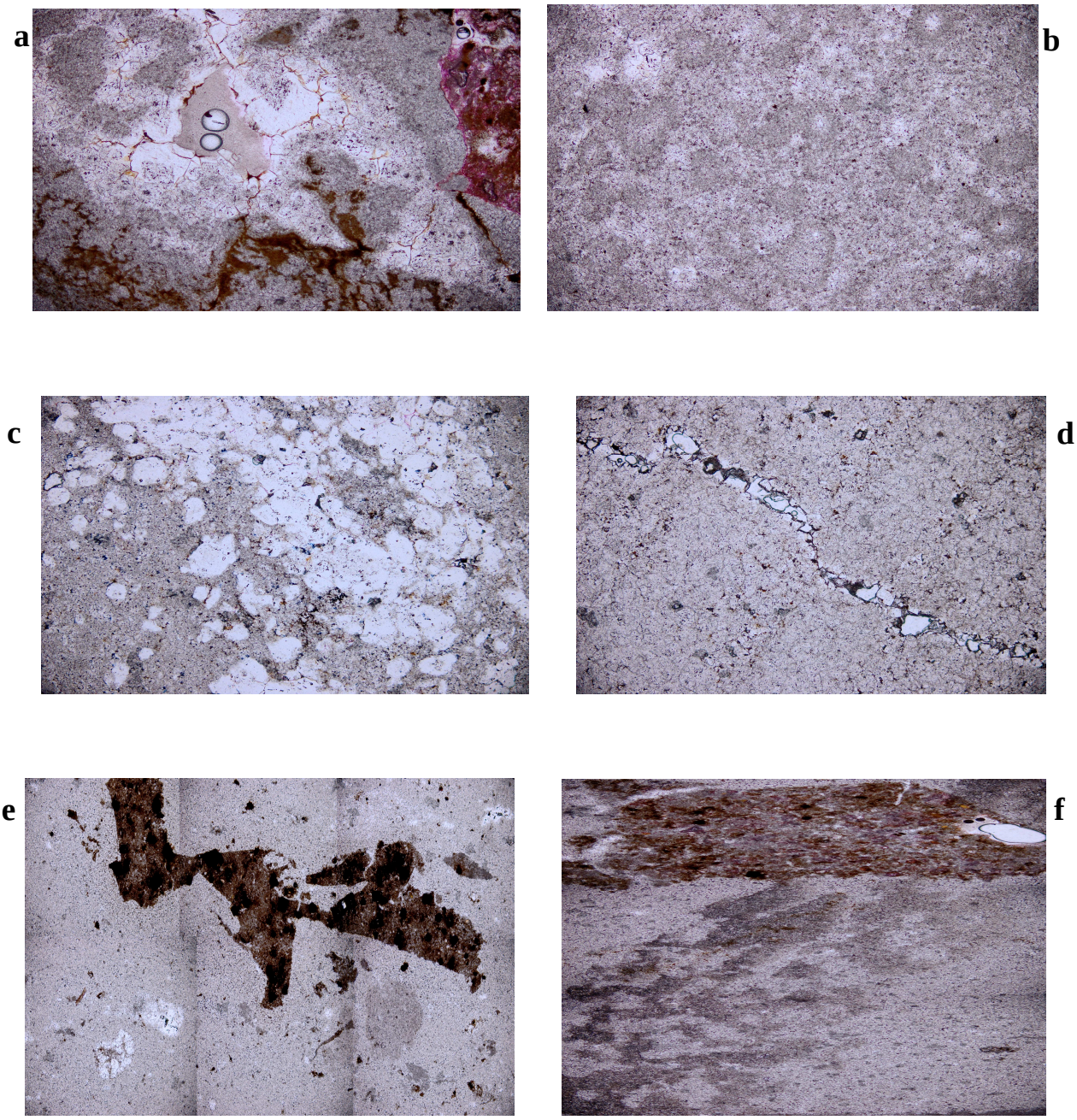

Figure 3-12: *Photographs of thin sections (a, b, c, d, e and f) by using an electron microscope NIKON ECLIPSE LV 100 (Scale 100 μm).*

The photographs show a range of dolomite textures found in the upper part of the Shital. Figures a, b, c as well as d are photographs of compacted dolomite replaced by calcite cement. Particularly a & c shows a white relief characteristic of the substitution of calcite in pink dolomite while photograph b displays a circular grain relief similar to ooids. The permeability and porosity in these photographs of the outcrop levels belonging to the upper Shital are obstructed by the development of calcite cement. Fracturing of the dolomite post-filled with calcite is also noticeable in figure d. As for figures e and f, they make it possible to observe the Conophyton Reefs indices preserved in the dolomitic matrix of the upper Shital level.

F) Aswad Member

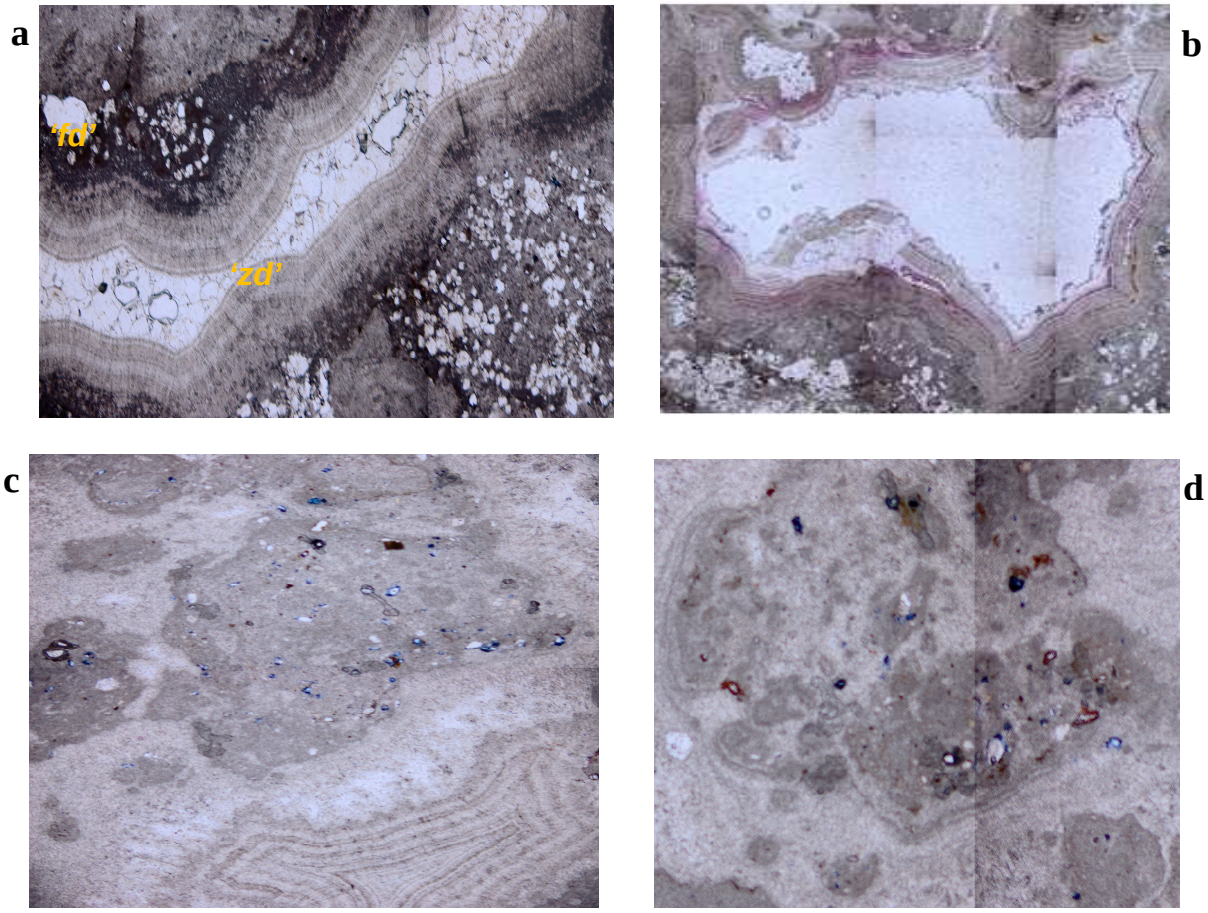

Figure 3-13: *Photographs of thin sections (a, b, c and d) by using an electron microscope NIKON ECLIPSE LV 100 (Scale 100 μm).*

The photographs show a range of dolomite textures found in Aswad Member. a) Thrombotic mesoclots and fringing cement phases in the lower part of the section (ST2 1.6). Primary fringing dolomite "*fd*" and zoned dolomite "*zd*". b) Well developed and larger mesoclots in the main part of the section, at 2.9 m. Cavity cements are younger than zoned dolomites appear to have filled the entire pore space with

carbonate rains before burial. c and d) Progressive development of large, well-developed concentric oncoids in the upper bed of the section (ST2 4.5).

3.3 Summary of Microscopy.

In general, dolomite (within mixed carbonate of Sirab Formation) is dominant in compared to the underlying Buah Formation or to the group of rocks of the overlying Haima Formation. Dolomite in the Sirab Formation is more abundant than other shapes of carbonates (calcite, aragonite, or carbonate beds associated with precipitation of salts such as gypsum, anhydrite or halite). The technique of red alizarin S made it possible to differentiate dolomite from calcite. The former appears in pink (dolomite) and the calcite often leaves a gray reflection whereas in the thin layers of the outcrops which have been examined above, the calcite appears lightly colored in white-gray. For reasons of simplification when describing the various thin sections, the term white or whitish coloring has been used to refer to calcite which often occurs as a cementing phase of the dolomite. Obviously, unlike the photographs taken by a microscope with a more powerful objective like those of the STF 185 level (Red dolospar) above, the coloring of the thin section looks slightly different. This drives that the observations made on outcrops (carbonates with dolomite, calcite and evaporite; Sirab Formation) by the red alizarin s technique are apparently differents. As example of this slightly microscopy difference of dolomite: the photographs of dolomites taken by the NIKON ECLIPSE LV 100 objective (scale 100 μm) for the Buah-Ramayli, lower Ramayli, lower Shital, upper Shital and Aswad Member levels differ from the photographs taken by the NIKON DS-R12 lens (scale of photos: 200 μm, for the Red dolospar). As such, the

use of the microscope objective employed also plays a significant role when viewing thin sections.

In thin sections, the marked presence of dolomite with calcite has often confers a strong dye on the thin section as the pink coloration of dolomite mingles with that of calcite in grayish-white. This rise of dye in the form of relief observed in the thin section has been commonly called a mosaic, thus defining a mosaic of hue between the pink color of dolomite colored by the red alizarin technique and the gray-white colors of calcite.

Notwithstanding the indication given in the two preceding paragraphs above concerning the use of different microscope objectives when describing thin sections, the dolomite or the percentage of dolomite contained in the mixed carbonate of the Formation confers the appellation dolomicrite to sedimentary units, whose sediment particle size is thin while the levels with medium or relatively coarse particle size are qualified as dolostones. This is due to the predominant dolomitic tendency in Sirab in the Haushi-Huqf region. The shapes of dolomite seen in thin sections are contextual. They persist after replacement of the calcite cement in certain outcrops and in this case, the compaction of the sediment has often been mentioned. Furthermore, in the Aswad Member, it is distributed zonally in the form of elongated and/or banded filaments. Dolomite in the Aswad Member appear to be primary dolomite and as such diagenesis is

either suspected or not in the process of dolomite formation. Preservation of the primary form of dolomite in the thin sections of the Aswad Member is indicated by “fd or primary dolomite” as well as “zd or zoned dolomite”. The (zd) is the structuring of primary dolomite in ribbon or ornamental form which appears to have been preserved from the influence of diagenesis.

Usually, diagenesis is believed to be influential in the process of magnesium enrichment in the ancient sediments because it is almost impossible that those sediments remain completely insensitive to diagenetic fluids through geological time. In contrast to this, the well-preserved primary forms of dolomite in the Sirab Formation so limit the importance of diagenesis and, therefore, of the burial process of the Formation. This is particularly the case suspect for the Aswad Member. Perhaps the ramp of these carbonate sediments had not been sufficiently submerged, or at most, some field sections in the Al-Huqf containing the members of the Sirab Formation, would not have been submerged so that the enrichment of the magnesium in the carbonate does not take place by exchange of thermal fluids during diagenesis but rather by direct precipitation of the magnesium on the bottom of the sediment after its saturation level has been reached at the water-sediment interface? It is also conceivable that in such a circumstance that the surface alteration is favorable rather that the burial effect. The assessment of isotopic signatures in the next chapter on diagenetic indices will further help to understand diagenesis process of the Formation.

3.4 XRD analysis data.

The Petrographic study of the Wadi Shital ST-1 section as well as of the addition part ST-2 (composite stratotype section) made it possible to differentiate in the samples of mixed carbonates (calcite/dolomite and evaporites) belonging to the lithostratigraphy of the Sirab Formation, the predominant calcite or dolomite type mineralogy.

For the composite stratotype section of Wadi Shital ST-1 & ST-2 (typical section of the Sirab Formation), a total number of the 25 bulk samples was analysed by XRD. The peaks in yields recorded by the diffractometers as well as the graphical representations shown on the various Camemberts diagrams for each individual case were used with great interest to complete the mineralogical identification of the predominant carbonate type.

A) Transitional Buah – Ramayli

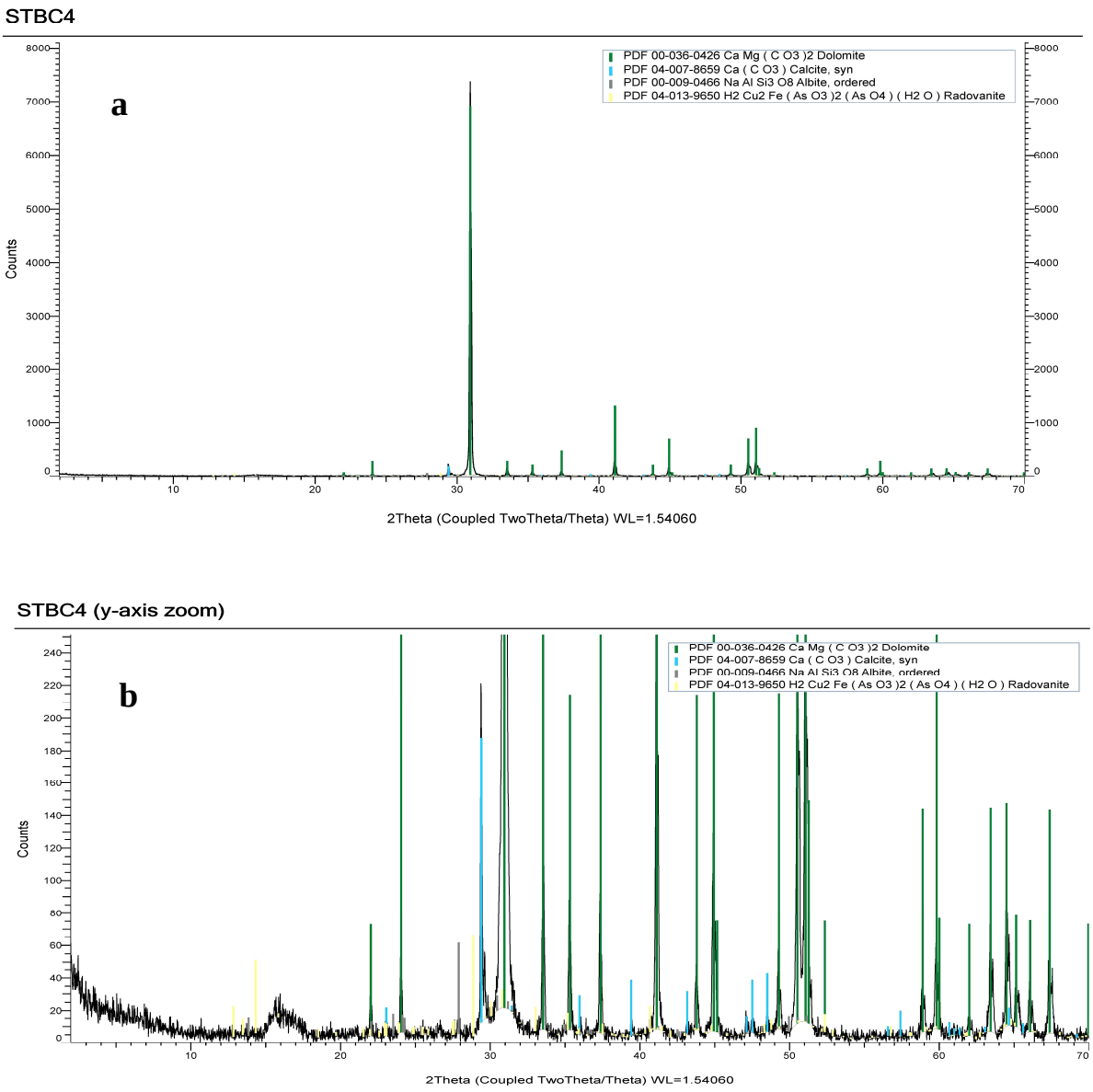

Figure 3-14: *XRD response of STB 4. Diagrams are taken along the X and Y axes to show the dominant mineral tendency for carbonates, plus a circular representation of Dolomite in the sample (photographs a, b and c).*

STBC6

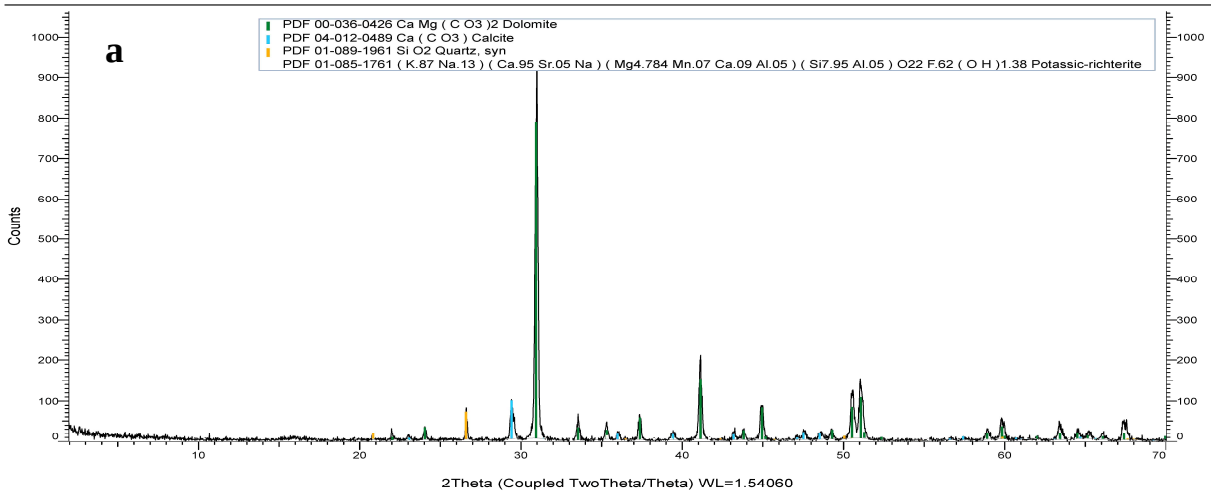

STBC6 (y-axis zoom)

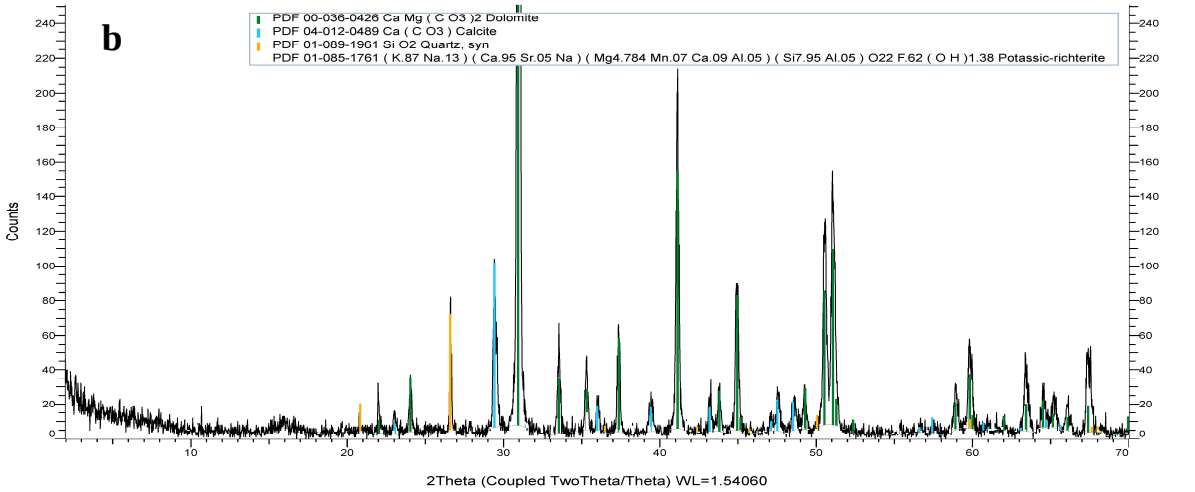

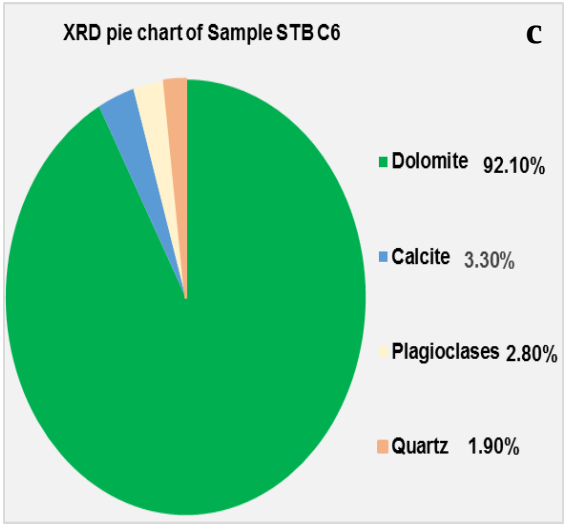

Figure 3-15: *XRD response of STB 6. Diagrams are taken along the X and Y axes to show the dominant mineral tendency for carbonates, plus a circular representation of Dolomite in the sample (photographs a, b and c).*

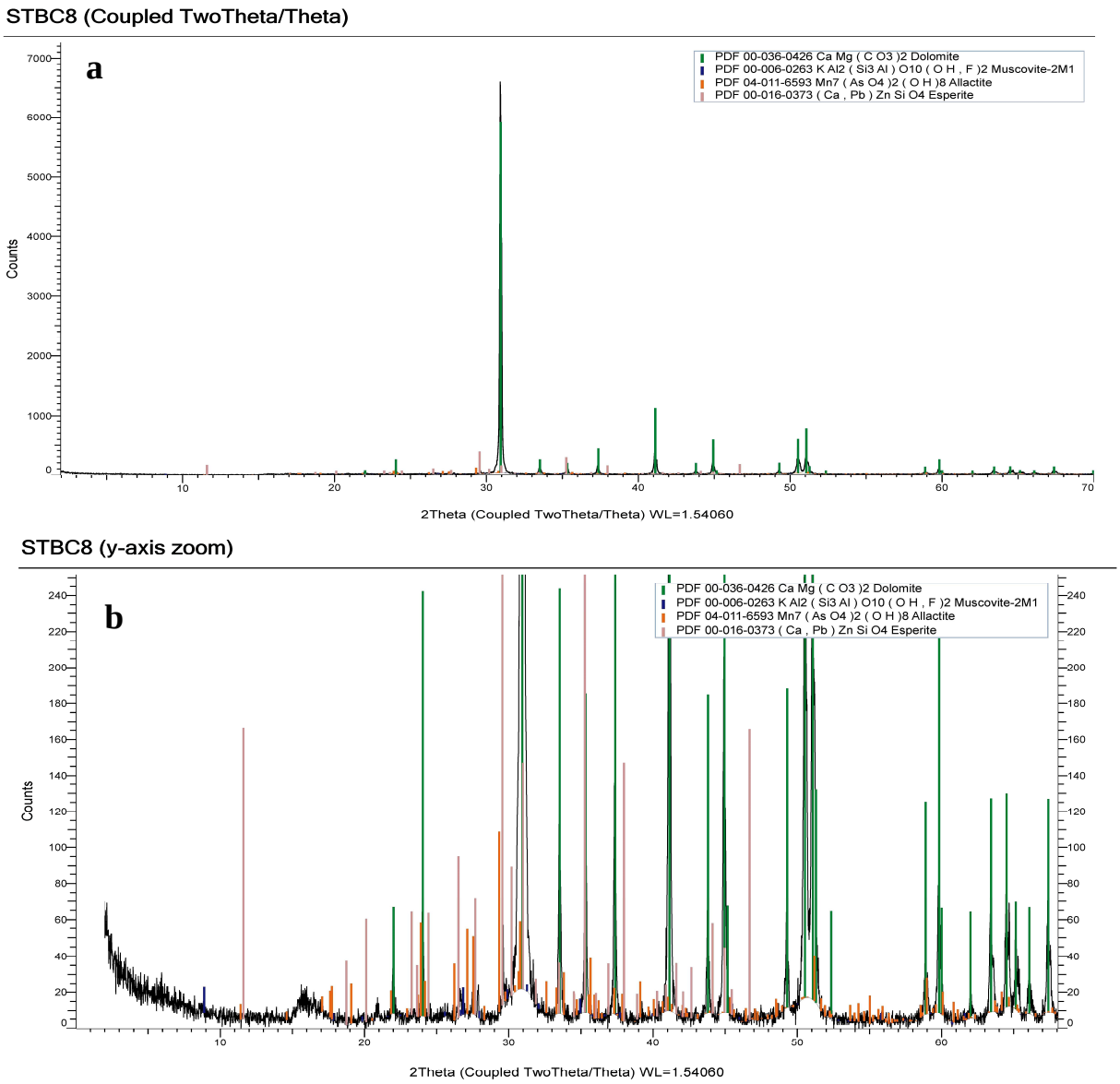

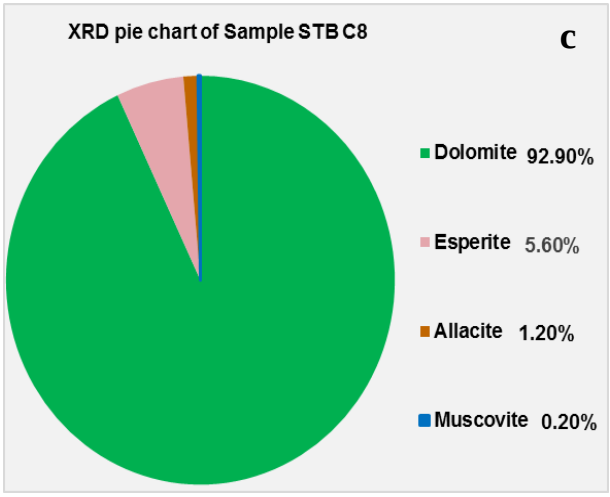

Figure 3-16: *XRD response of STB 8. Diagrams are taken along the X and Y axes to show the dominant mineral tendency for carbonates, plus a circular representation of Dolomite in the sample (photographs a, b and c).*

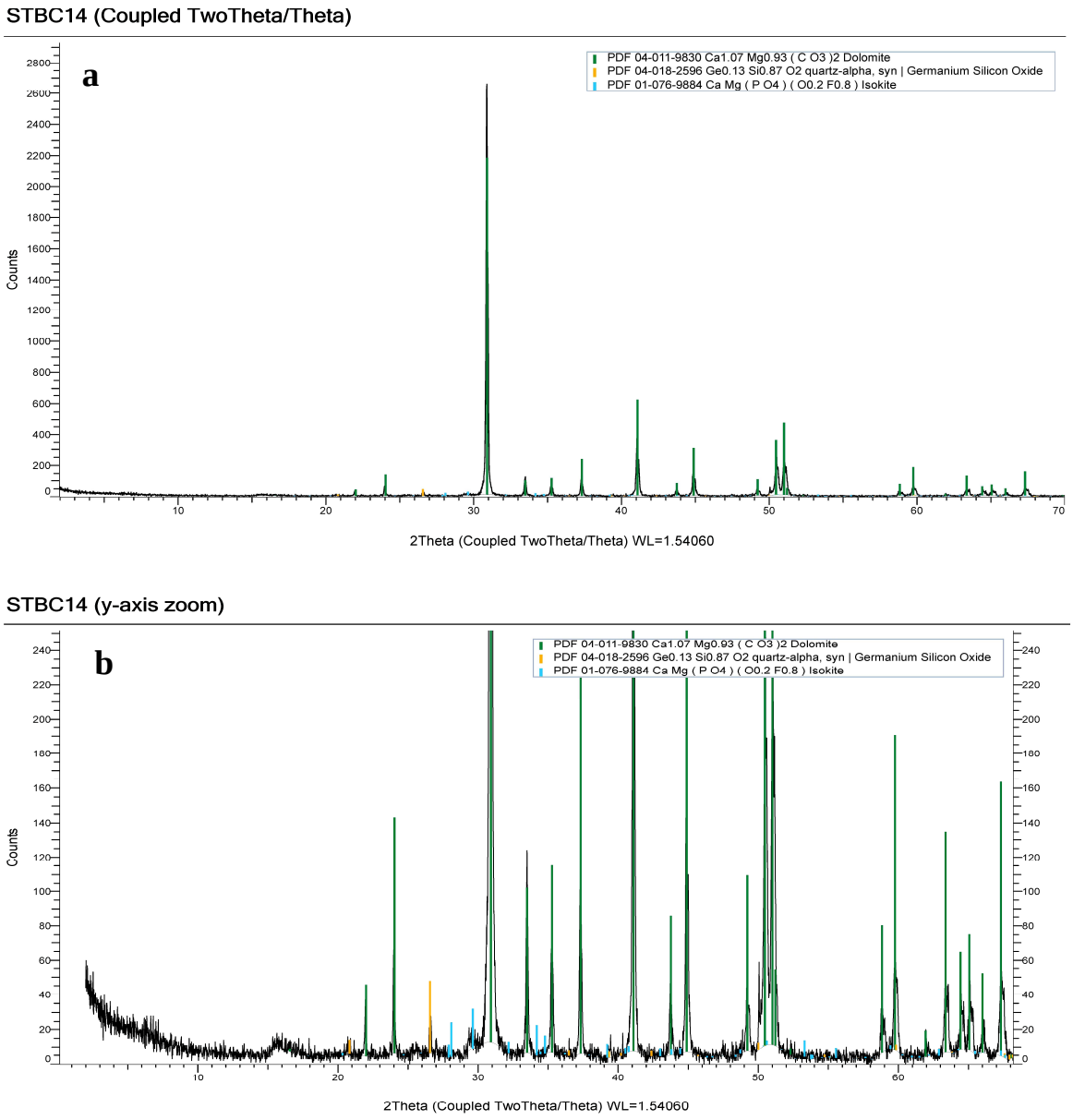

Figure 3-17: *XRD response of STB 14. Diagrams are taken along the X and Y axes to show the dominant mineral tendency for carbonates, plus a circular representation of Dolomite in the sample (photographs a, b and c).*

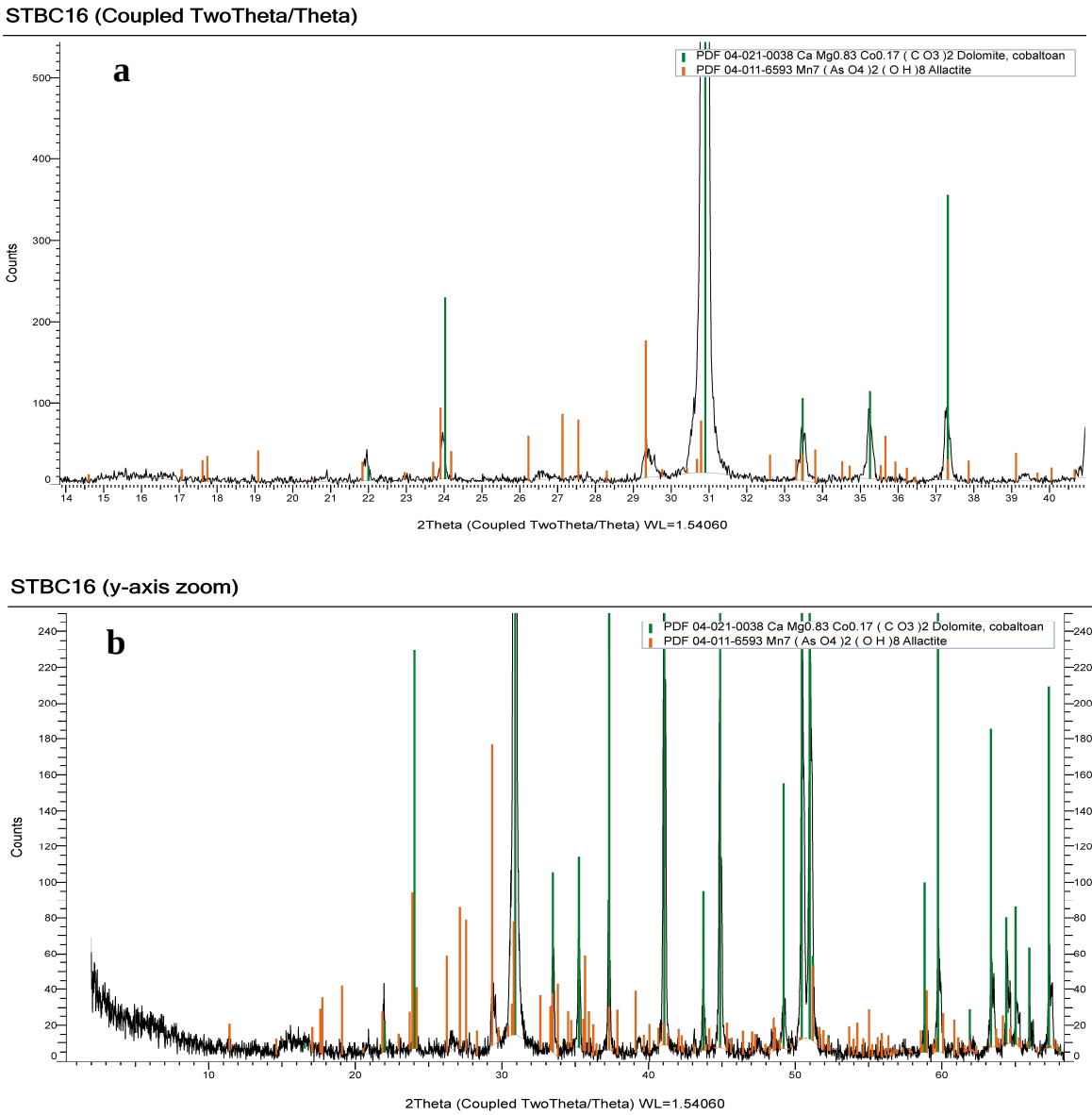

Figure 3-18: *XRD response of STB 16. Diagrams are taken along the X and Y axes to show the dominant mineral tendency for carbonates, plus a circular representation of Dolomite in the sample (photographs a, b and c).*

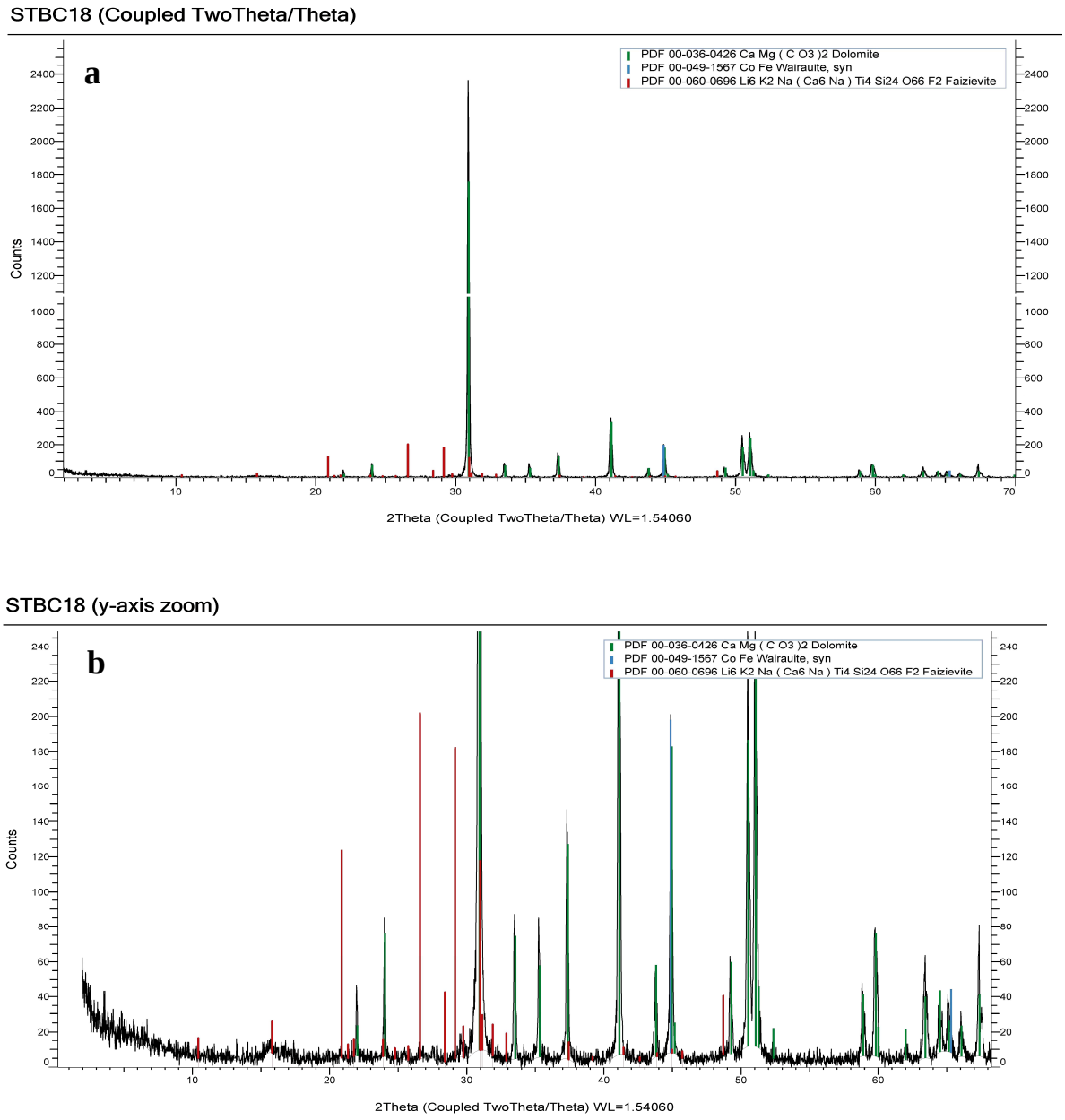

Figure 3-19: *XRD response of STB 18. Diagrams are taken along the X and Y axes to show the dominant mineral tendency for carbonates, plus a circular representation of Dolomite in the sample (photographs a, b and c).*

B) Ramayli Member (lower unit only).

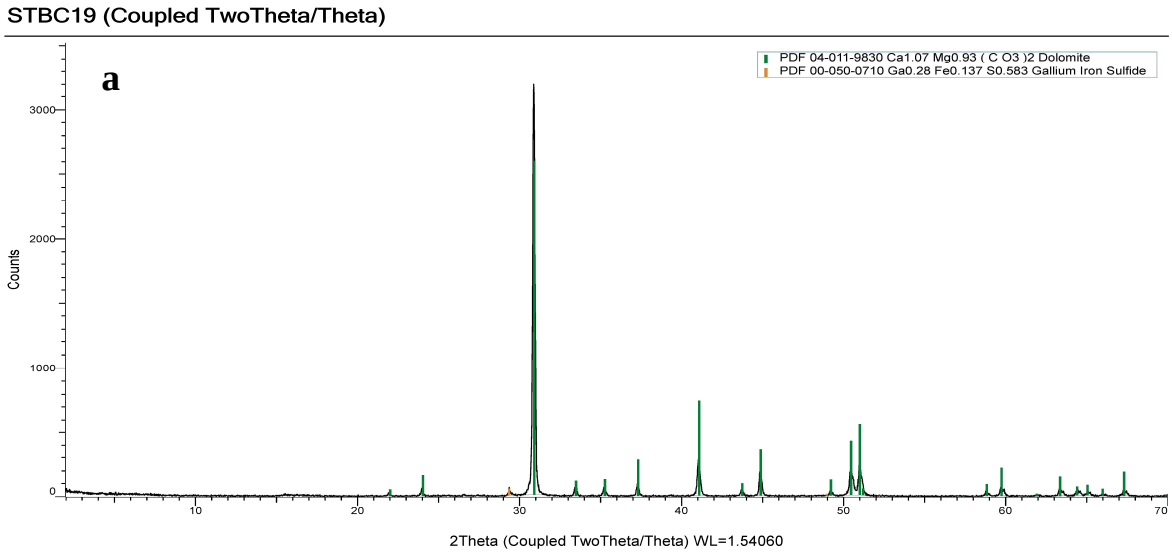

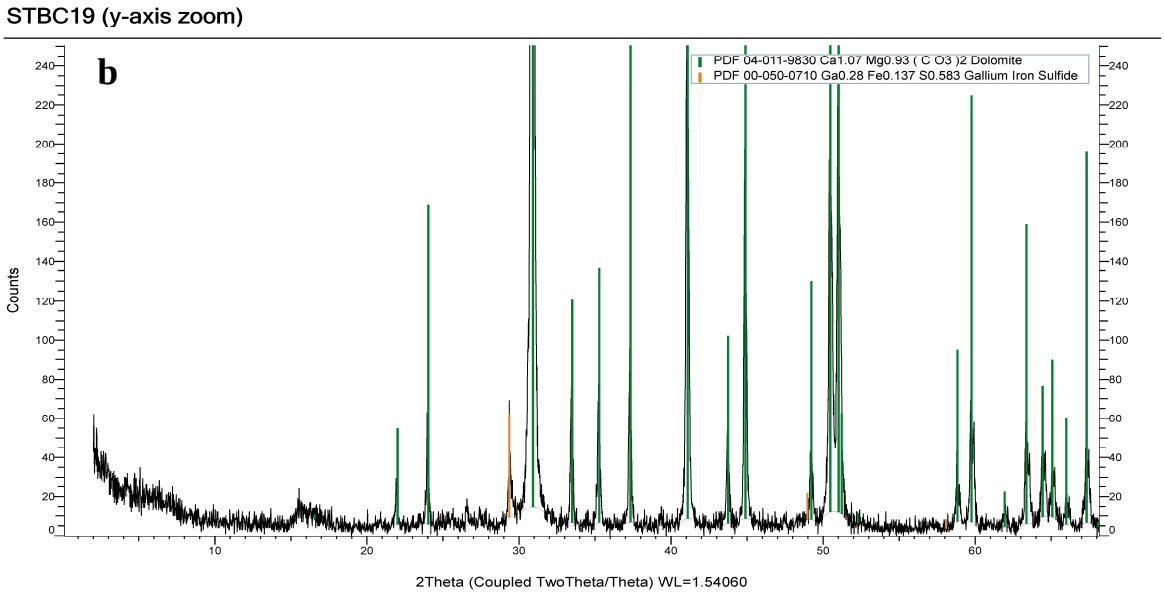

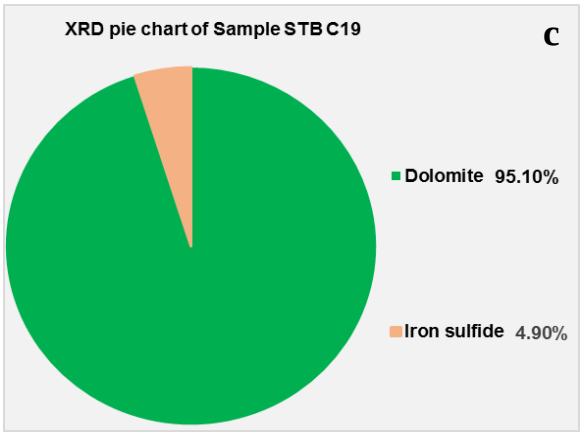

Figure 3-20: *XRD response of STB 19. Diagrams are taken along the X and Y axes to show the dominant mineral tendency for carbonates, plus a circular representation of Dolomite in the sample (photographs a, b and c).*

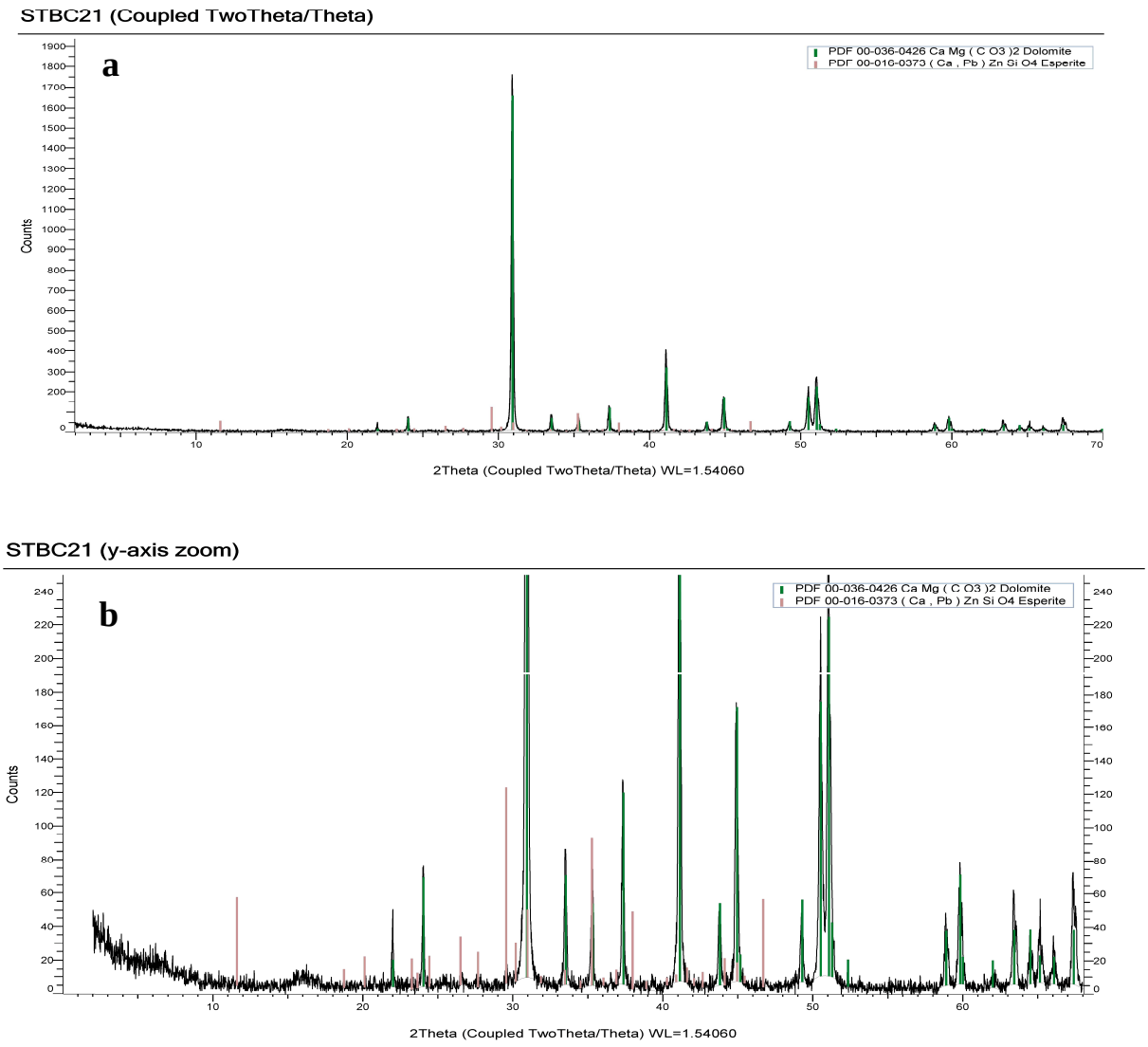

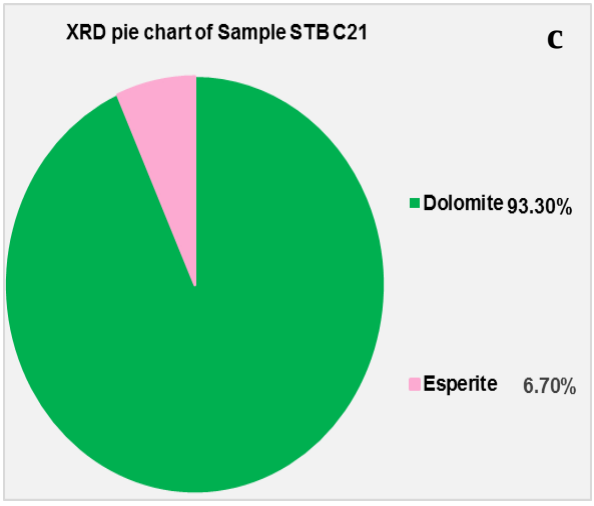

Figure 3-21: *XRD response of STB 21. Diagrams are taken along the X and Y axes to show the dominant mineral tendency for carbonates, plus a circular representation of Dolomite in the sample (photographs a, b and c).*

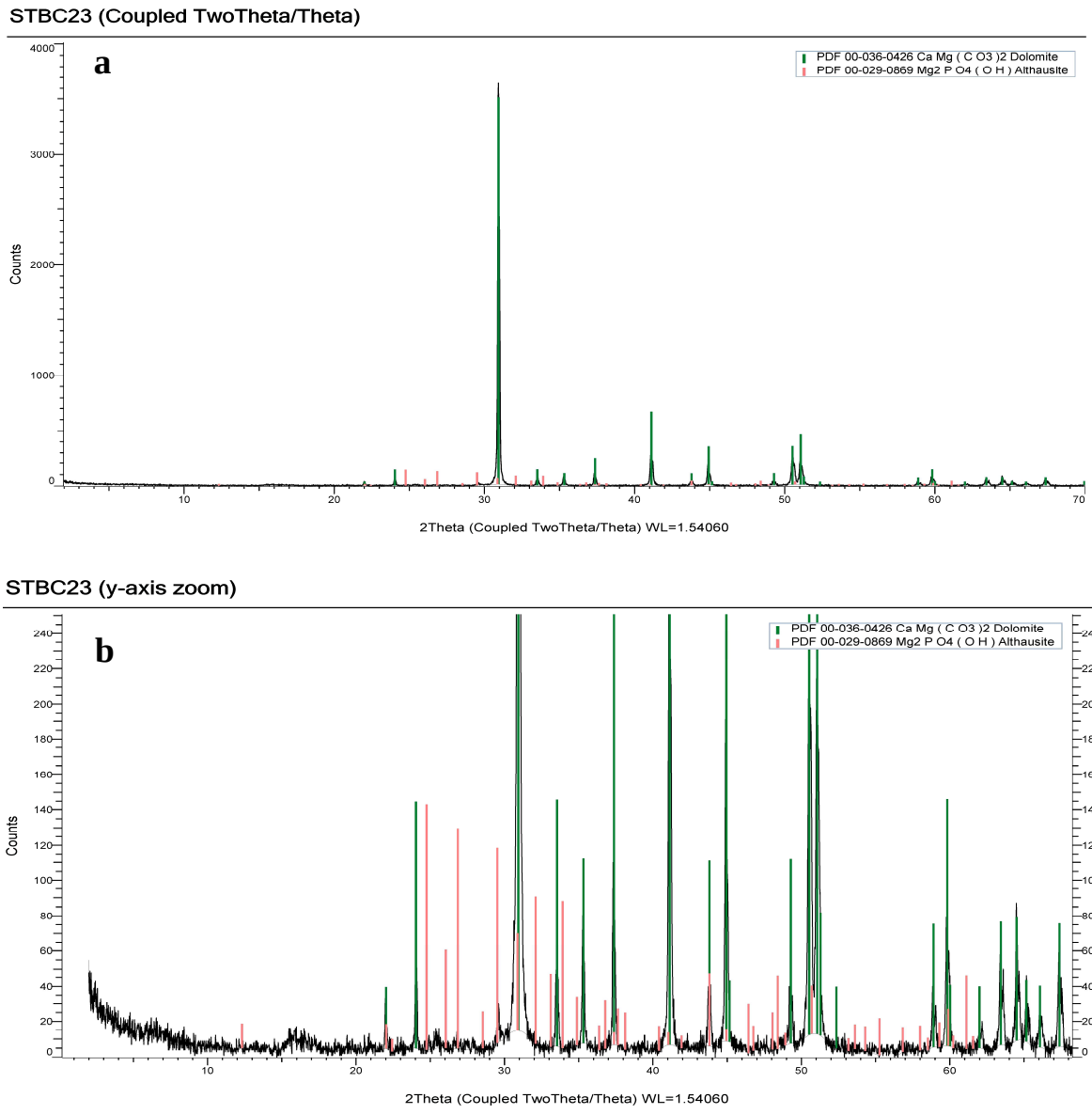

Figure 3-22: *XRD response of STB 23. Diagrams are taken along the X and Y axes to show the dominant mineral tendency for carbonates, plus a circular representation of Dolomite in the sample (photographs a, b and c).*

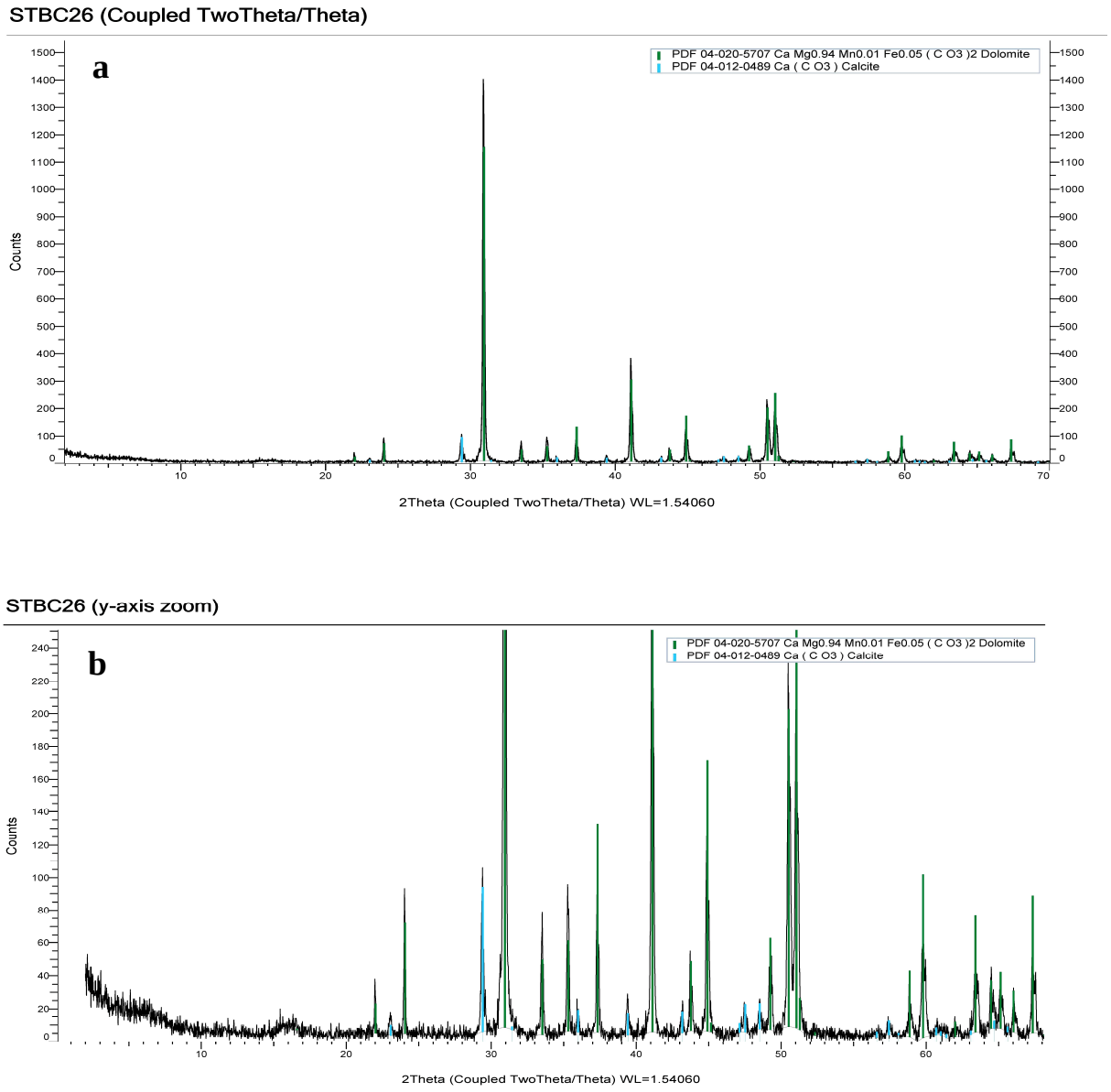

Figure 3-23: *XRD response of STB 26. Diagrams are taken along the X and Y axes to show the dominant mineral tendency for carbonates, plus a circular representation of Dolomite in the sample (photographs a, b and c).*

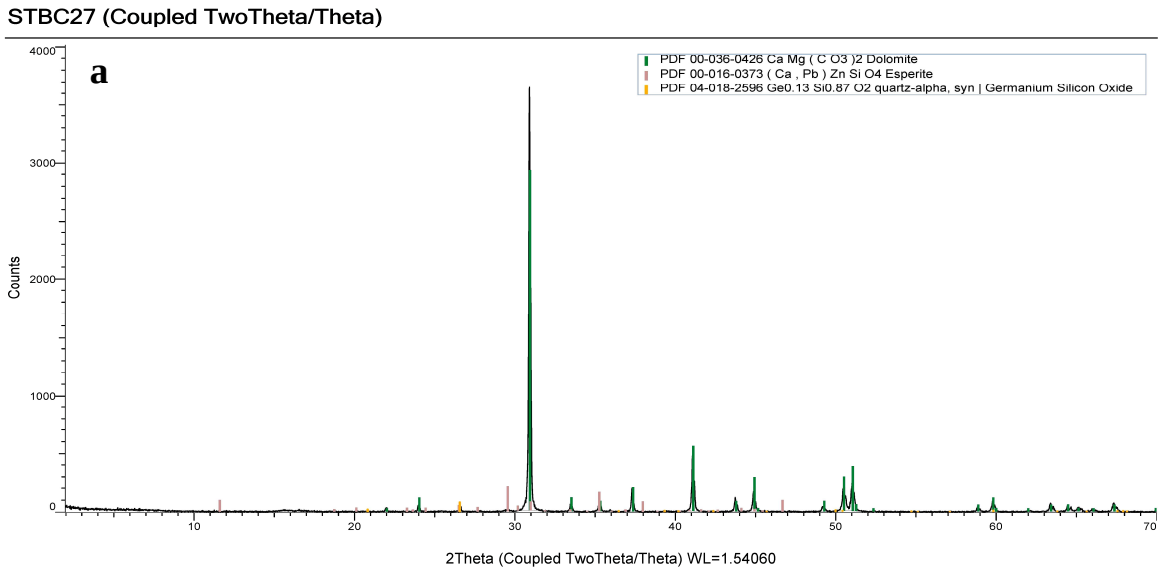

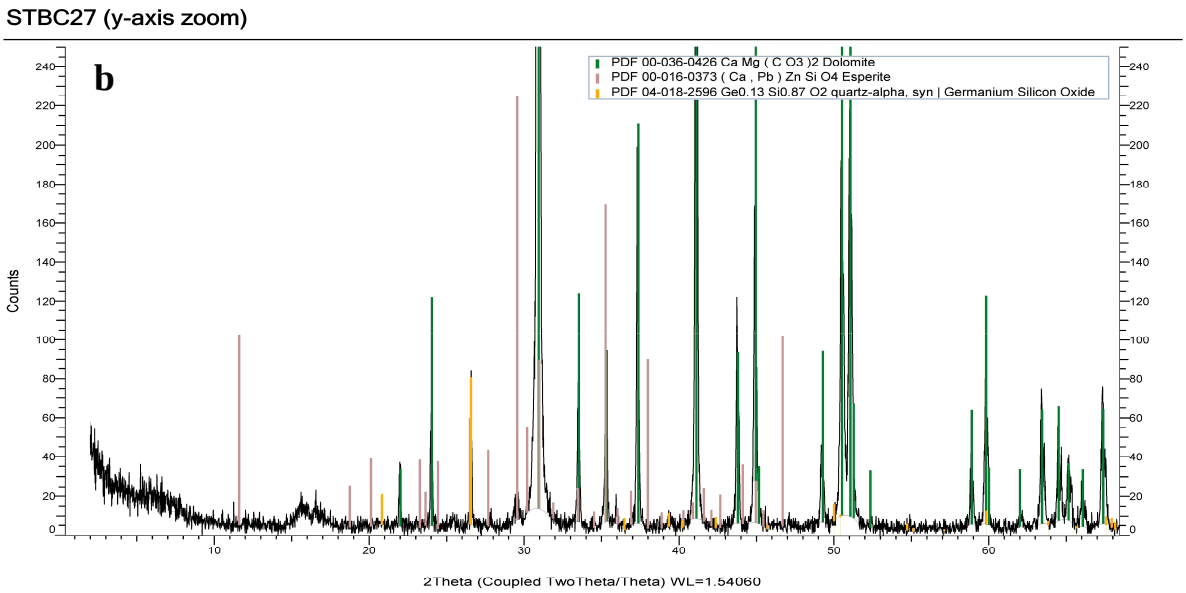

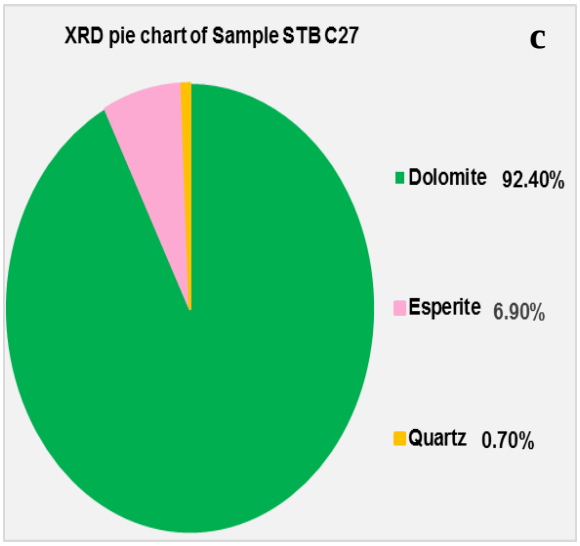

Figure 3-24: *XRD response of STB 27. Diagrams are taken along the X and Y axes to show the dominant mineral tendency for carbonates, plus a circular representation of Dolomite in the sample (photographs a, b and c).*

C) Shital Member (lower unit).

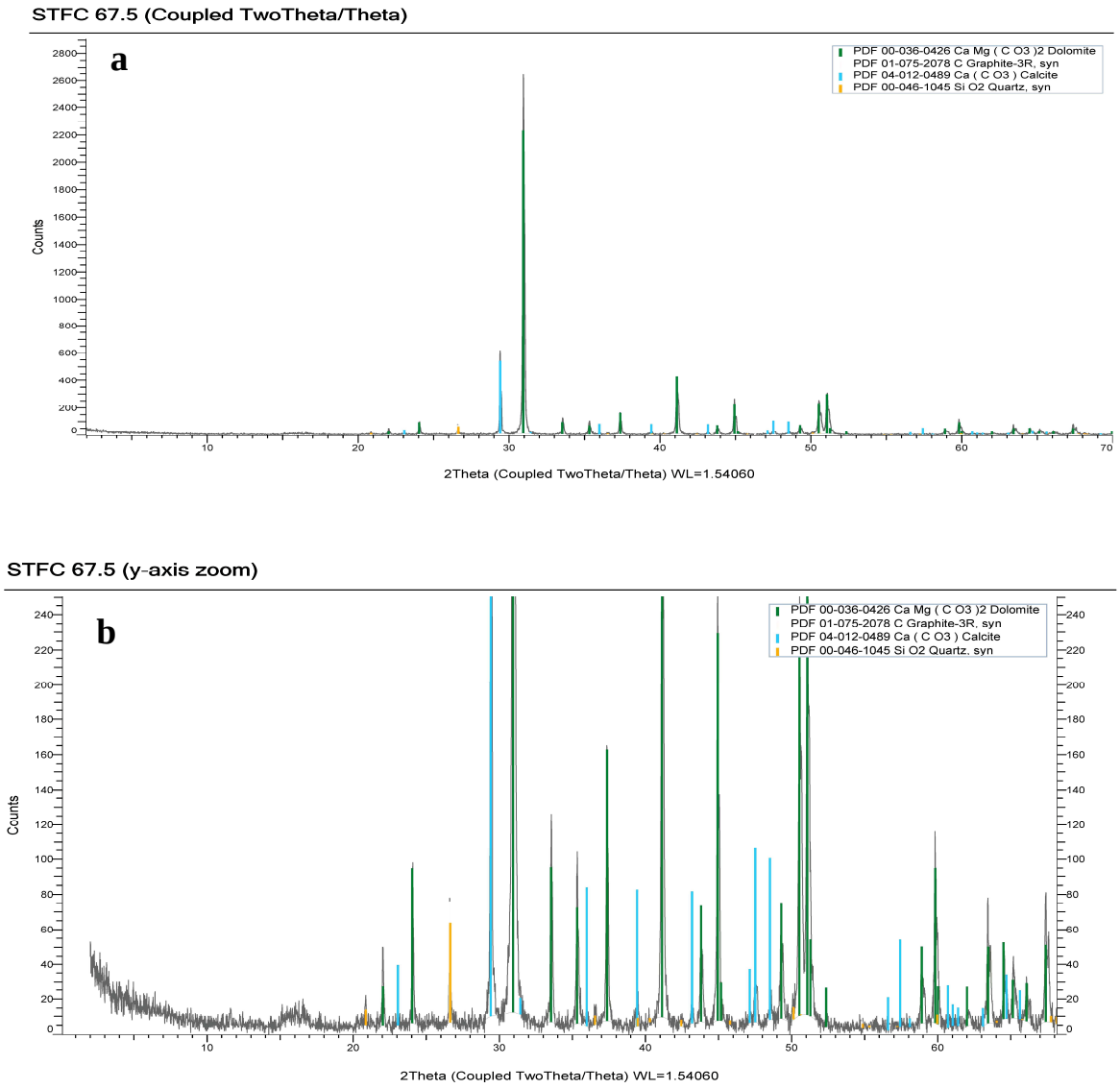

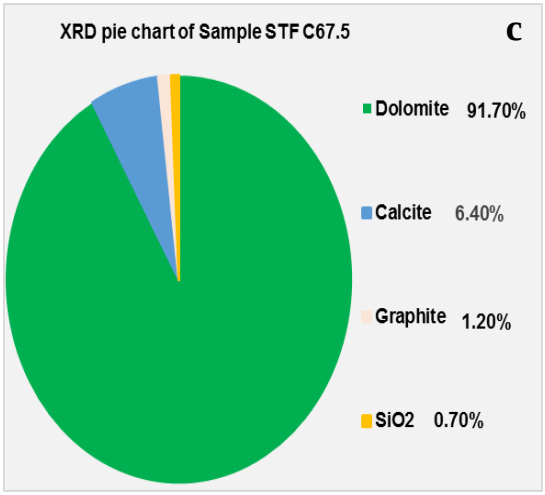

Figure 3-25: *XRD response of STF 67.5. Diagrams are taken along the X and Y axes to show the dominant mineral tendency for carbonates, plus a circular representation of Dolomite in the sample (photographs a, b and c).*

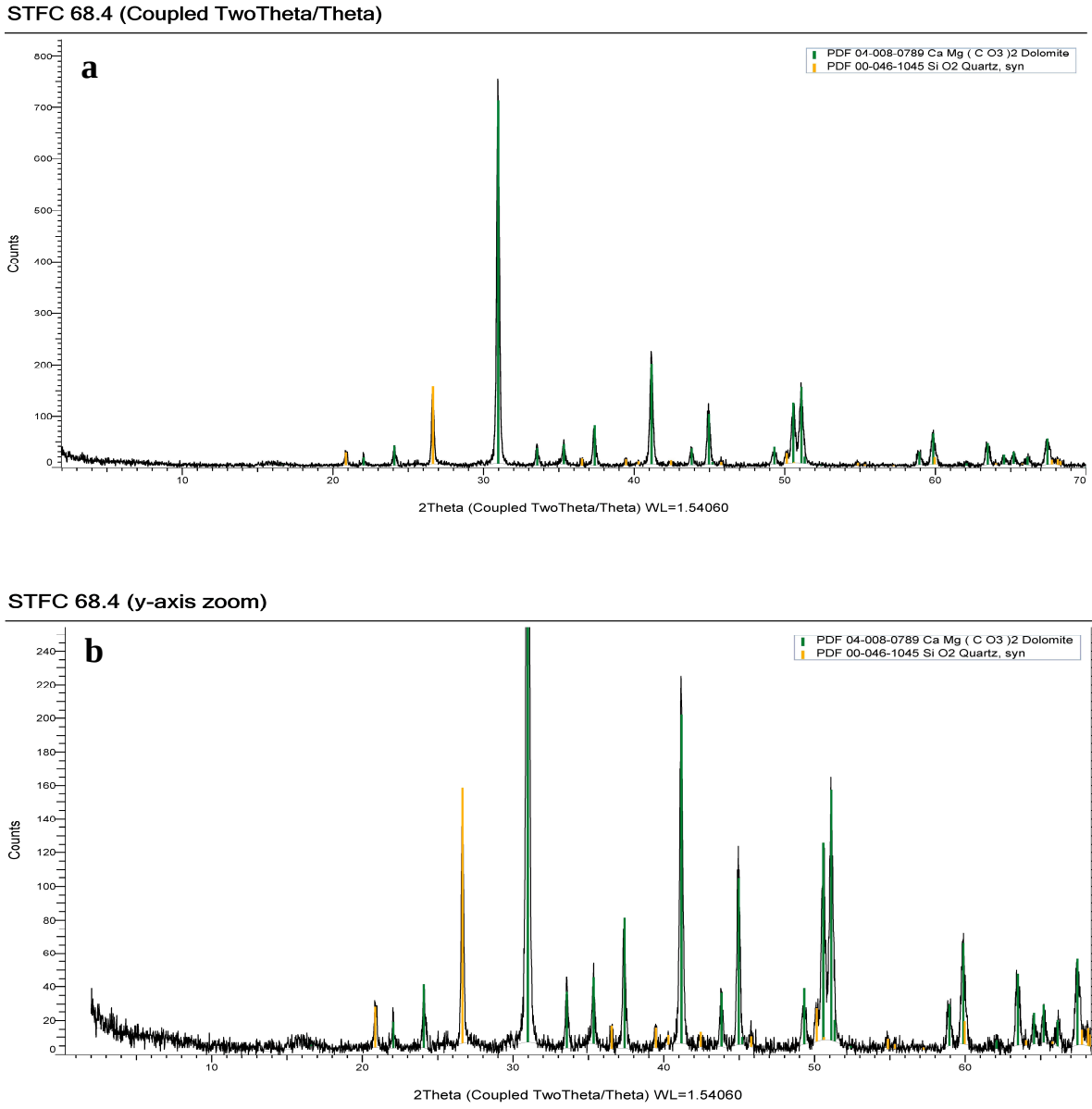

Figure 3-26: *XRD response of STF 68.4. Diagrams are taken along the X and Y axes to show the dominant mineral tendency for carbonates, plus a circular representation of Dolomite in the sample (photographs a, b and c).*

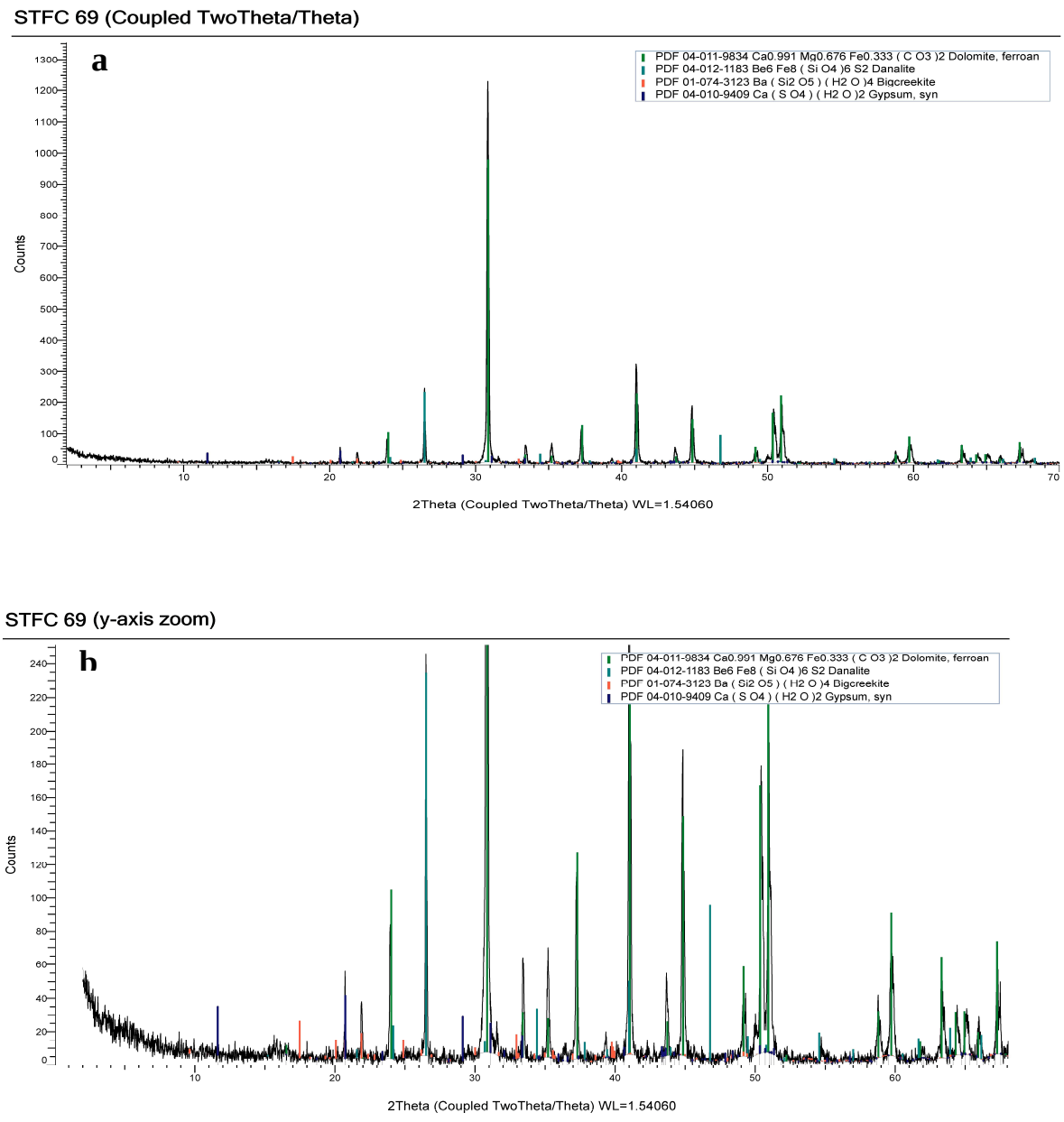

Figure 3-27: *XRD response of STF 69. Diagrams are taken along the X and Y axes to show the dominant mineral tendency for carbonates, plus a circular representation of Dolomite in the sample (photographs a, b and c).*

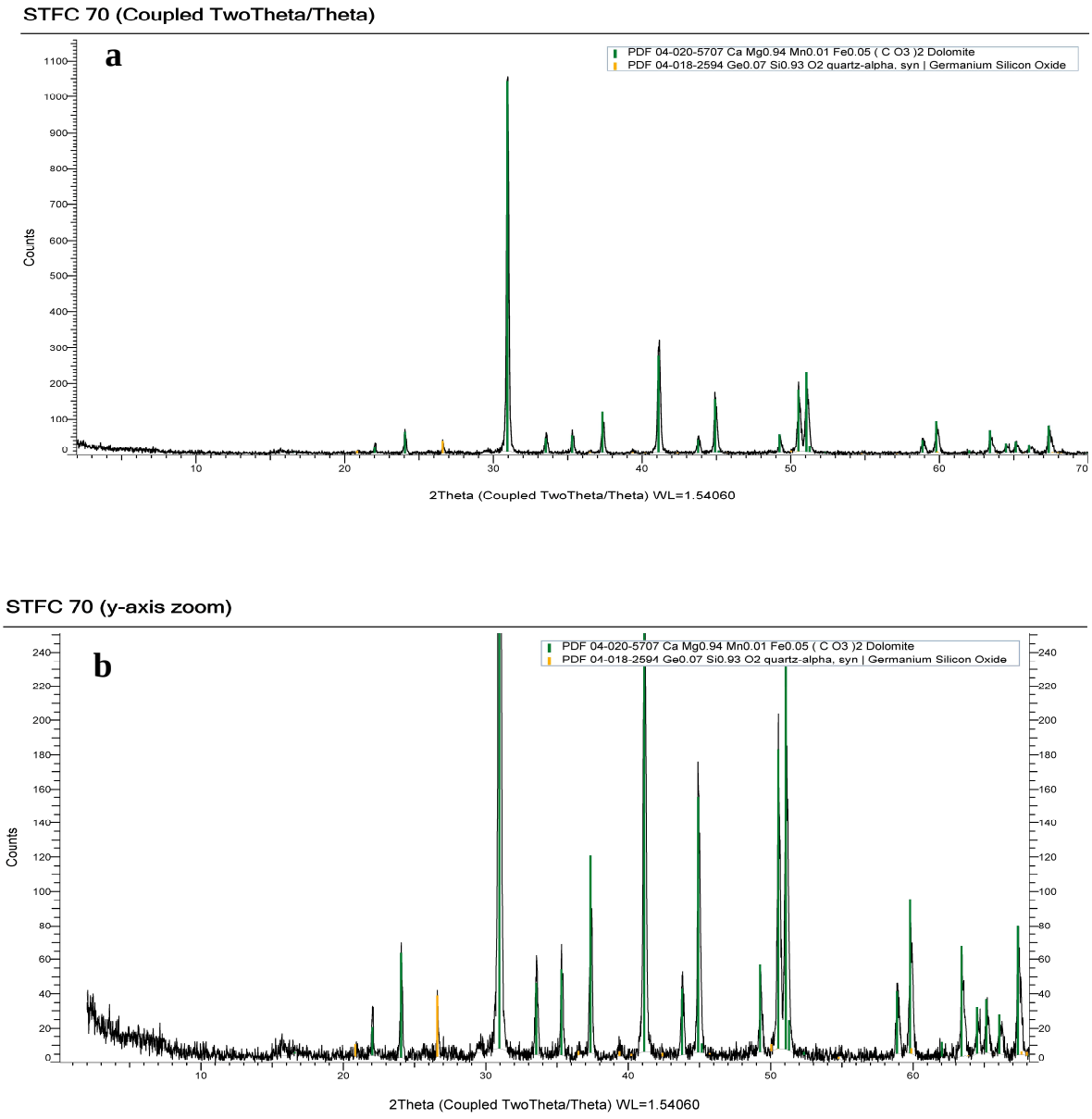

Figure 3-28: *XRD response of STF 70. Diagrams are taken along the X and Y axes to show the dominant mineral tendency for carbonates, plus a circular representation of Dolomite in the sample (photographs a, b and c).*

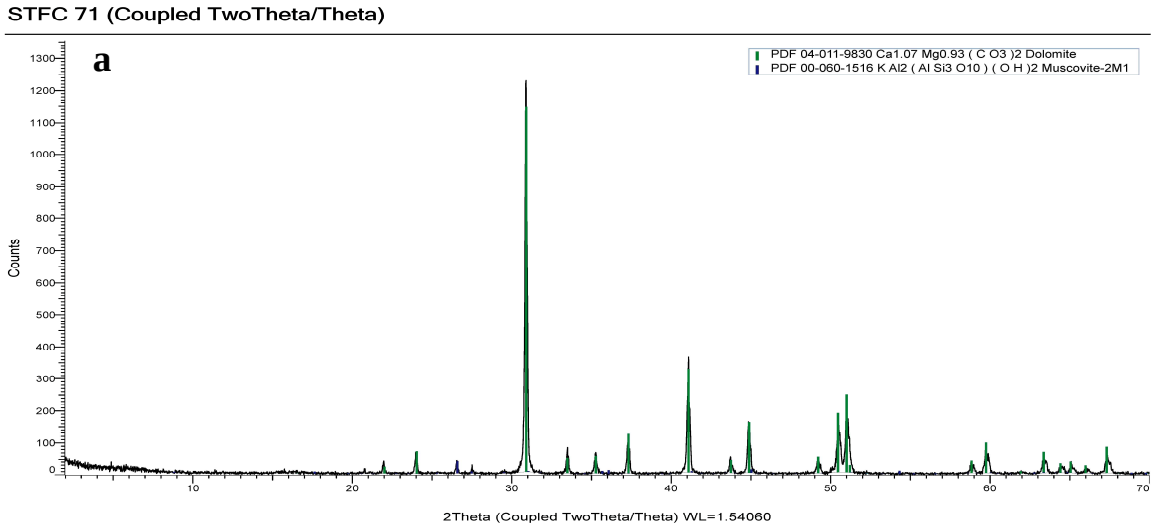

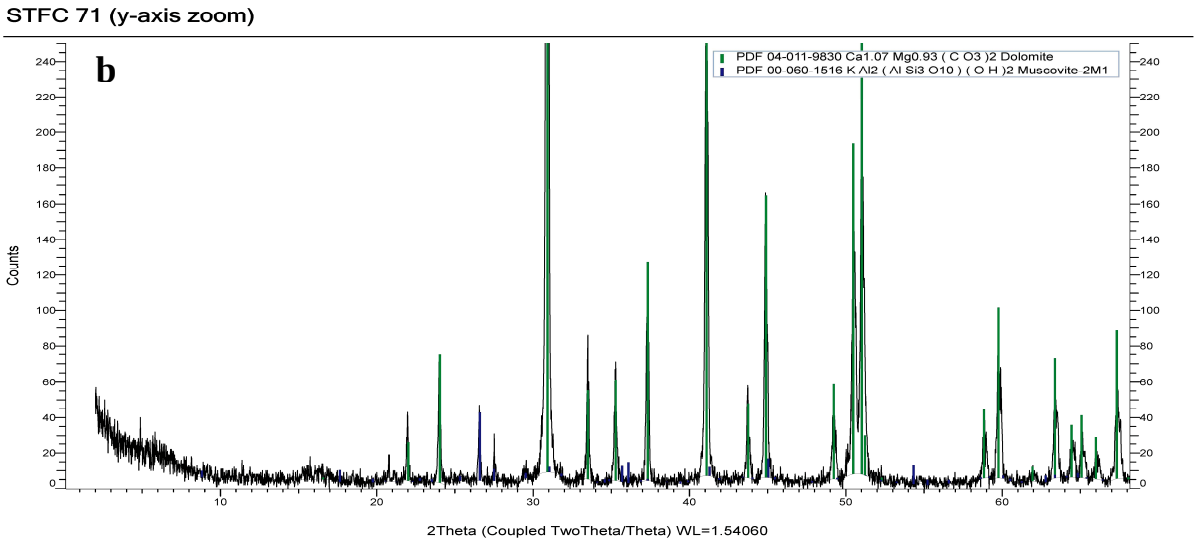

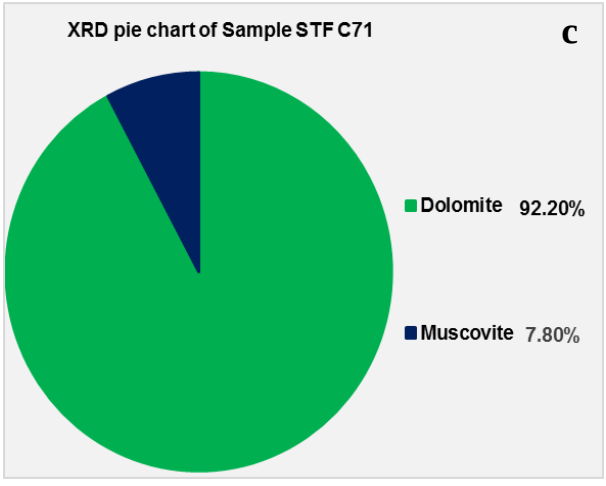

Figure 3-29: *XRD response of STF 71. Diagrams are taken along the X and Y axes to show the dominant mineral tendency for carbonates, plus a circular representation of Dolomite in the sample (photographs a, b and c).*

D) Red dolospar (± middle Shital)

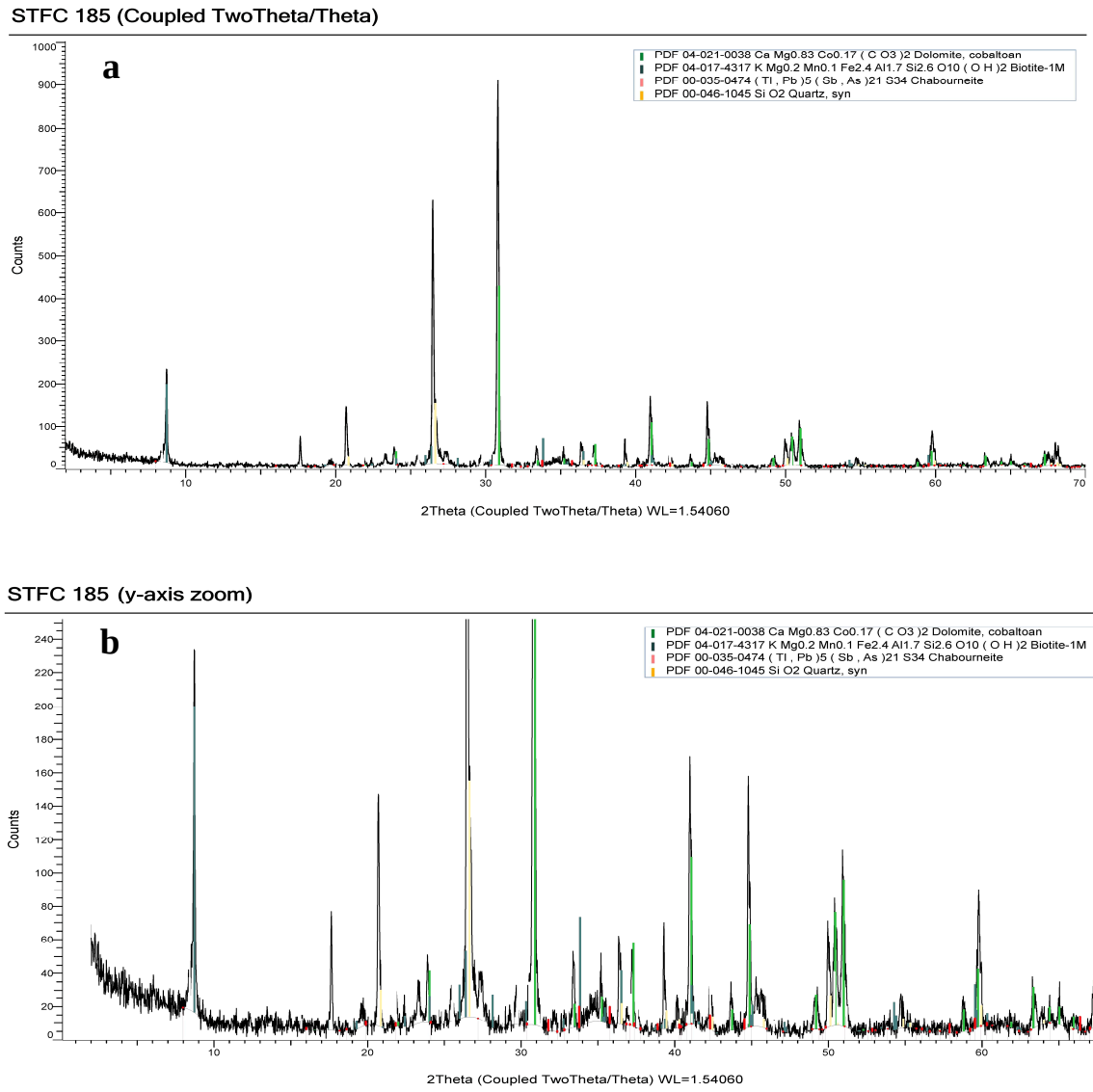

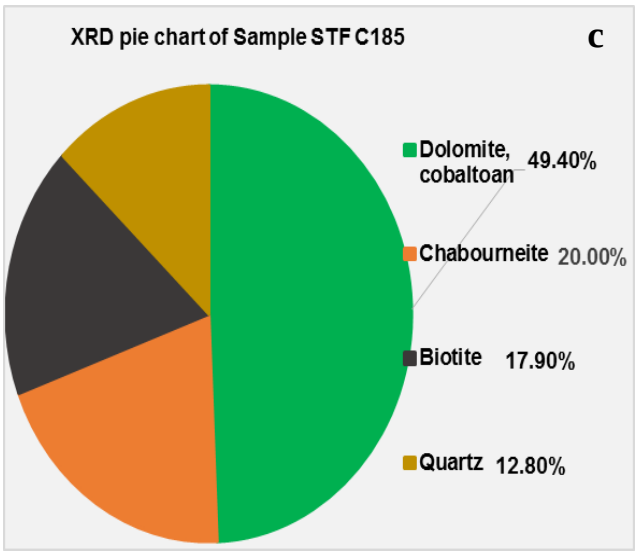

Figure 3-30: *XRD response of STF 185. Diagrams are taken along the X and Y axes to show the dominant mineral tendency for carbonates, plus a circular representation of Dolomite in the sample (photographs a, b and c).*

E) Shital Member (upper unit)

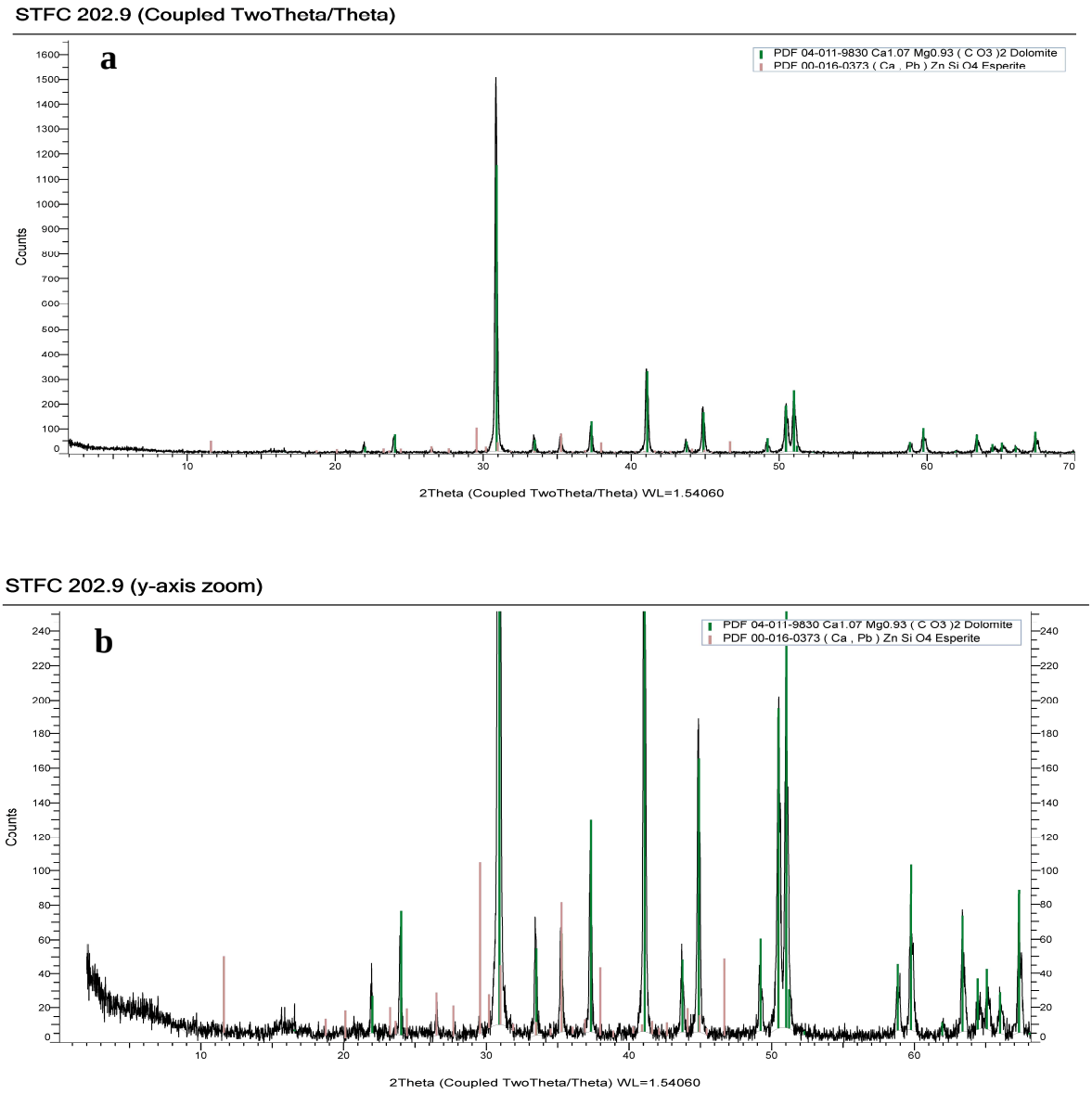

Figure 3-31: *XRD response of STF 202.9 Diagrams are taken along the X and Y axes to show the dominant mineral tendency for carbonates, plus a circular representation of Dolomite in the sample (photographs a, b and c).*

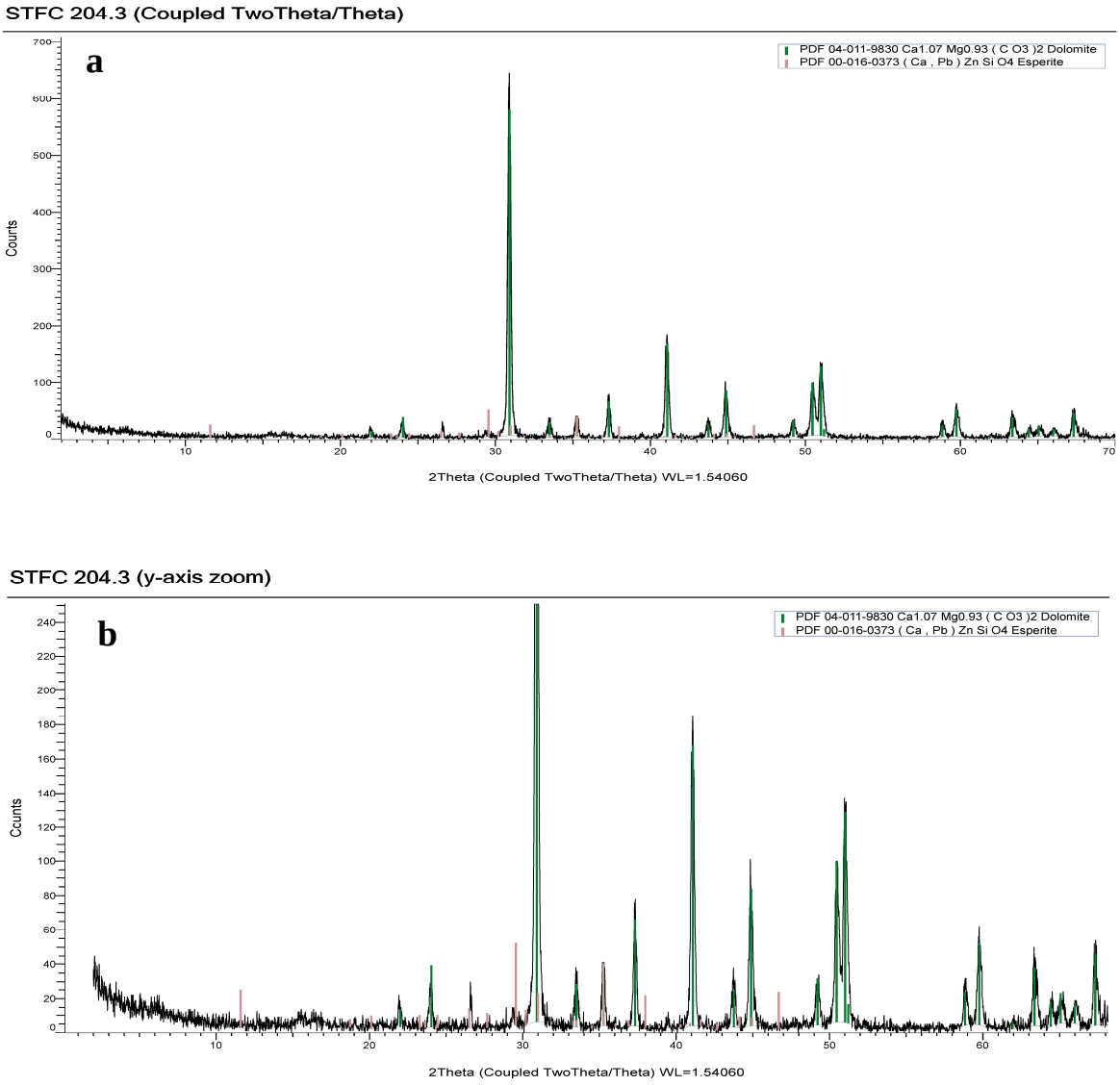

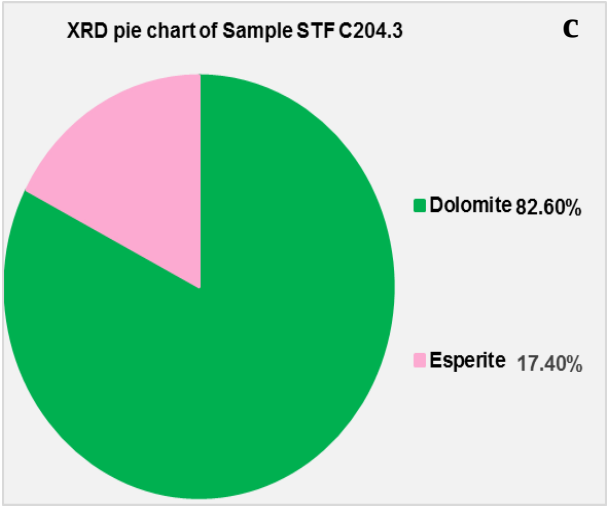

Figure 3-32: *XRD response of STF 204.3 Diagrams are taken along the X and Y axes to show the dominant mineral tendency for carbonates, plus a circular representation of Dolomite in the sample (photographs a, b and c).*

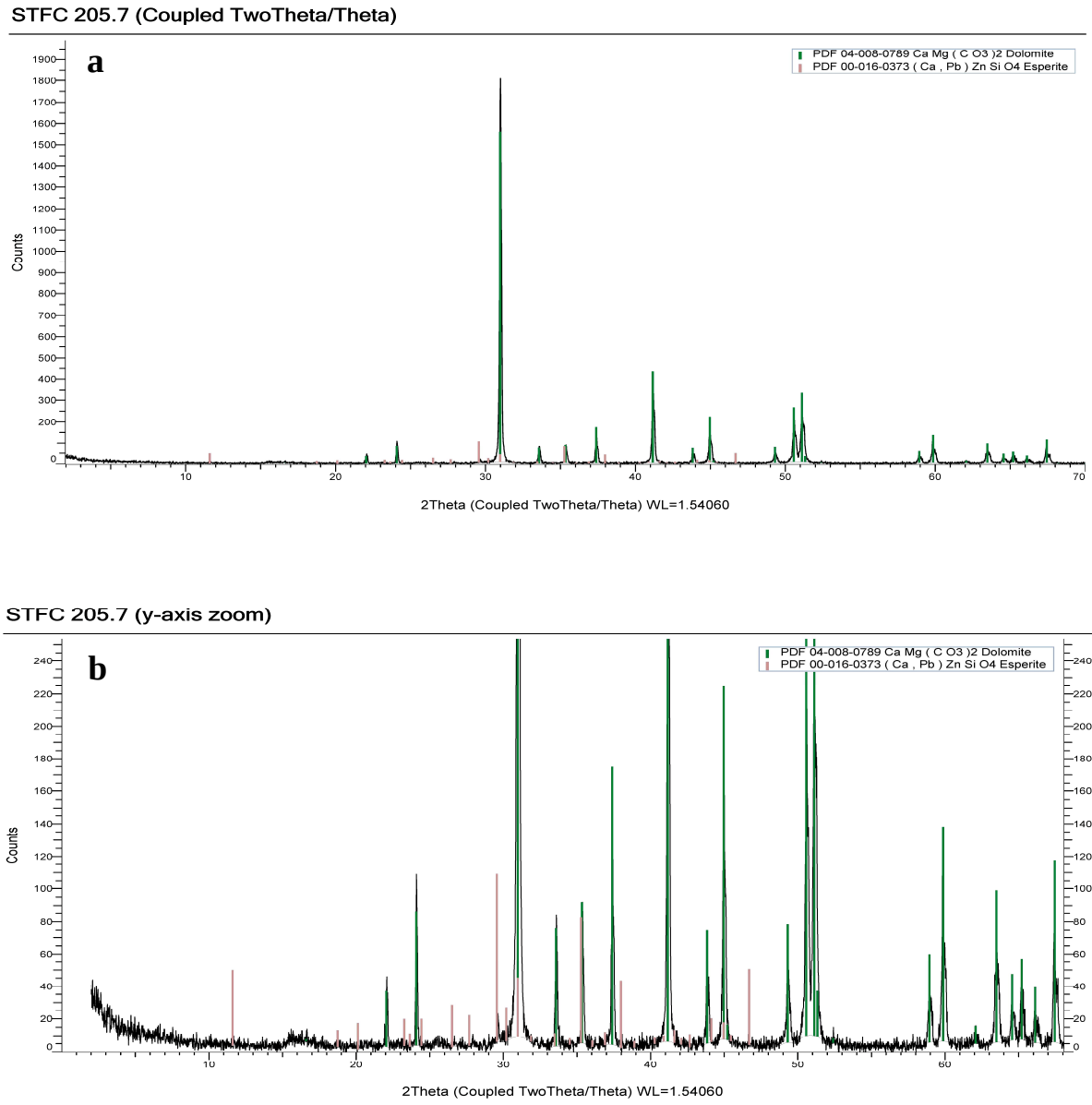

Figure 3-33: *XRD response of STF 205.7 Diagrams are taken along the X and Y axes to show the dominant mineral tendency for carbonates, plus a circular representation of Dolomite in the sample (photographs a, b and c).*

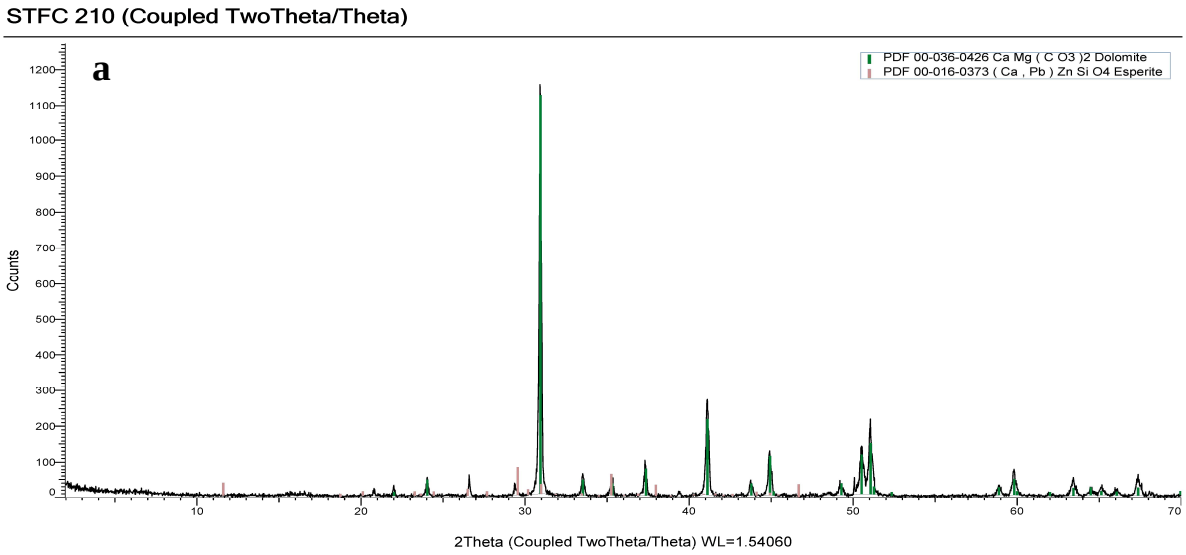

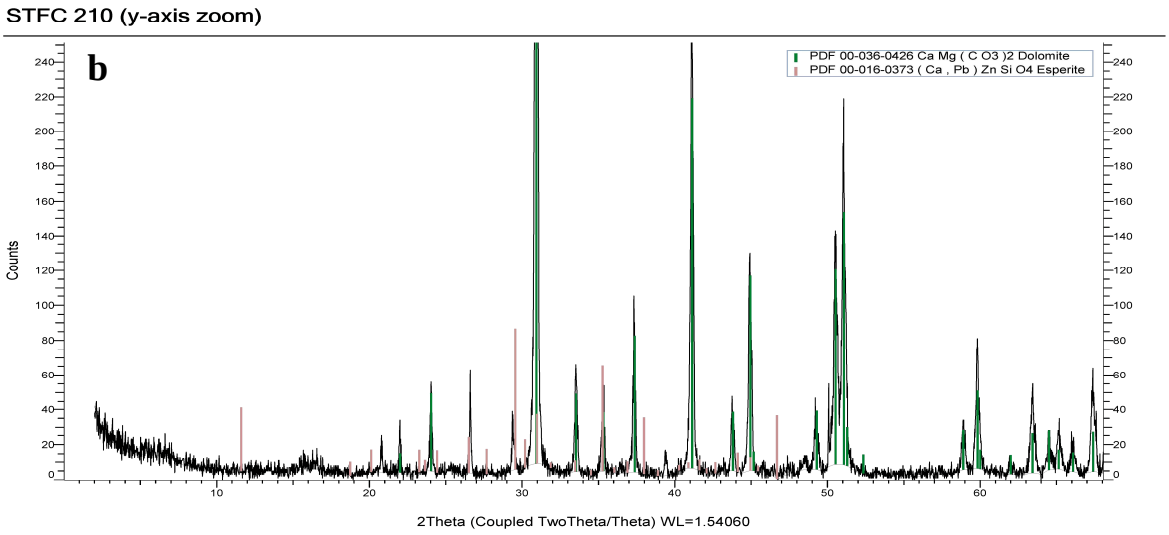

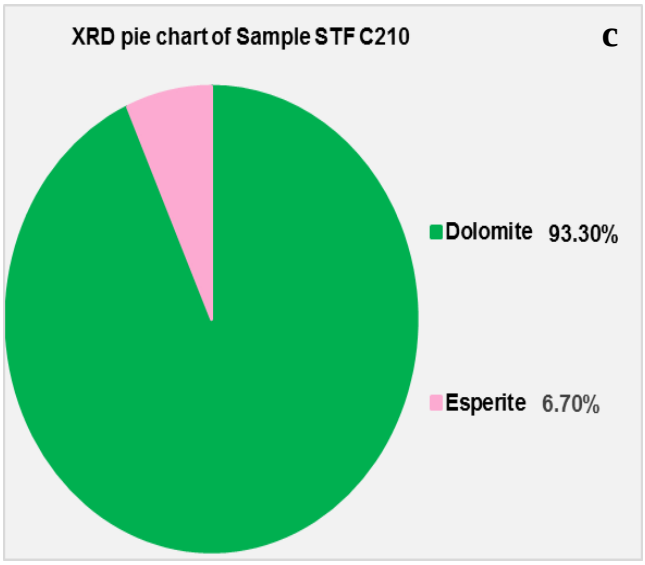

Figure 3-34: *XRD response of STB 21. Diagrams are taken along the X and Y axes to show the dominant mineral tendency for carbonates, plus a circular representation of Dolomite in the sample (photographs a, b and c).*

F) Aswad Member

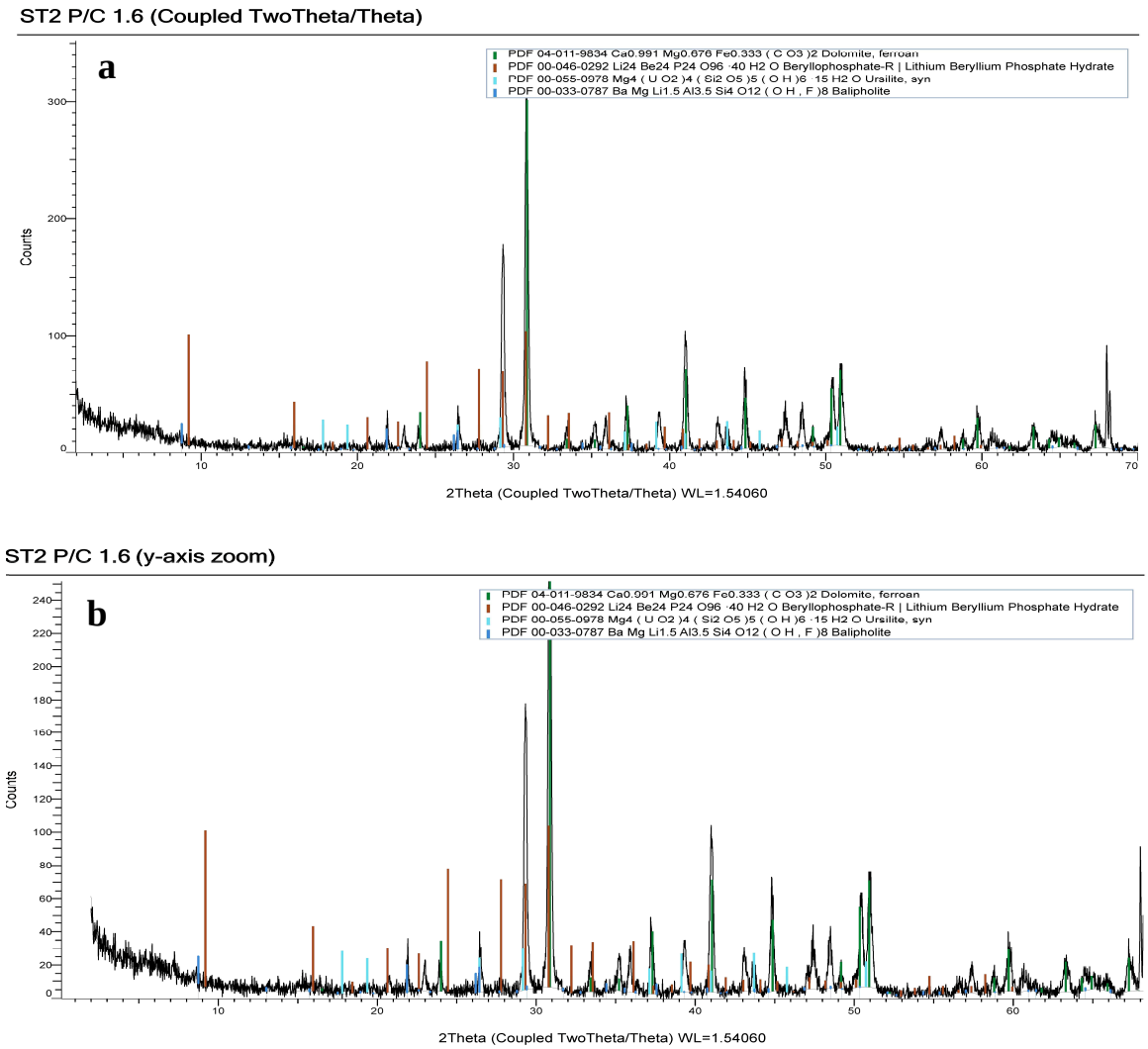

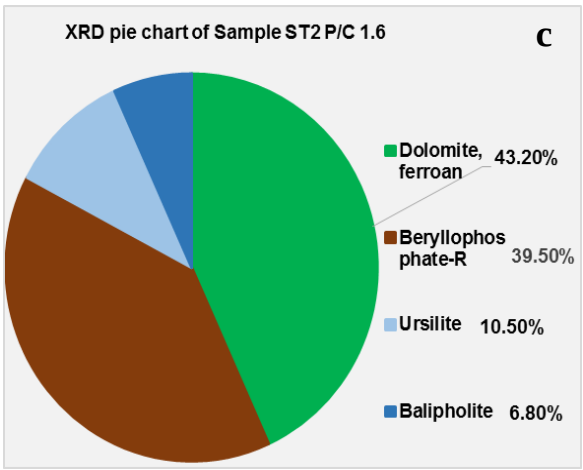

Figure 3-35: *XRD response of ST2-1.6. Diagrams are taken along the X and Y axes to show the dominant mineral tendency for carbonates, plus a circular representation of Dolomite in the sample (photographs a, b and c).*

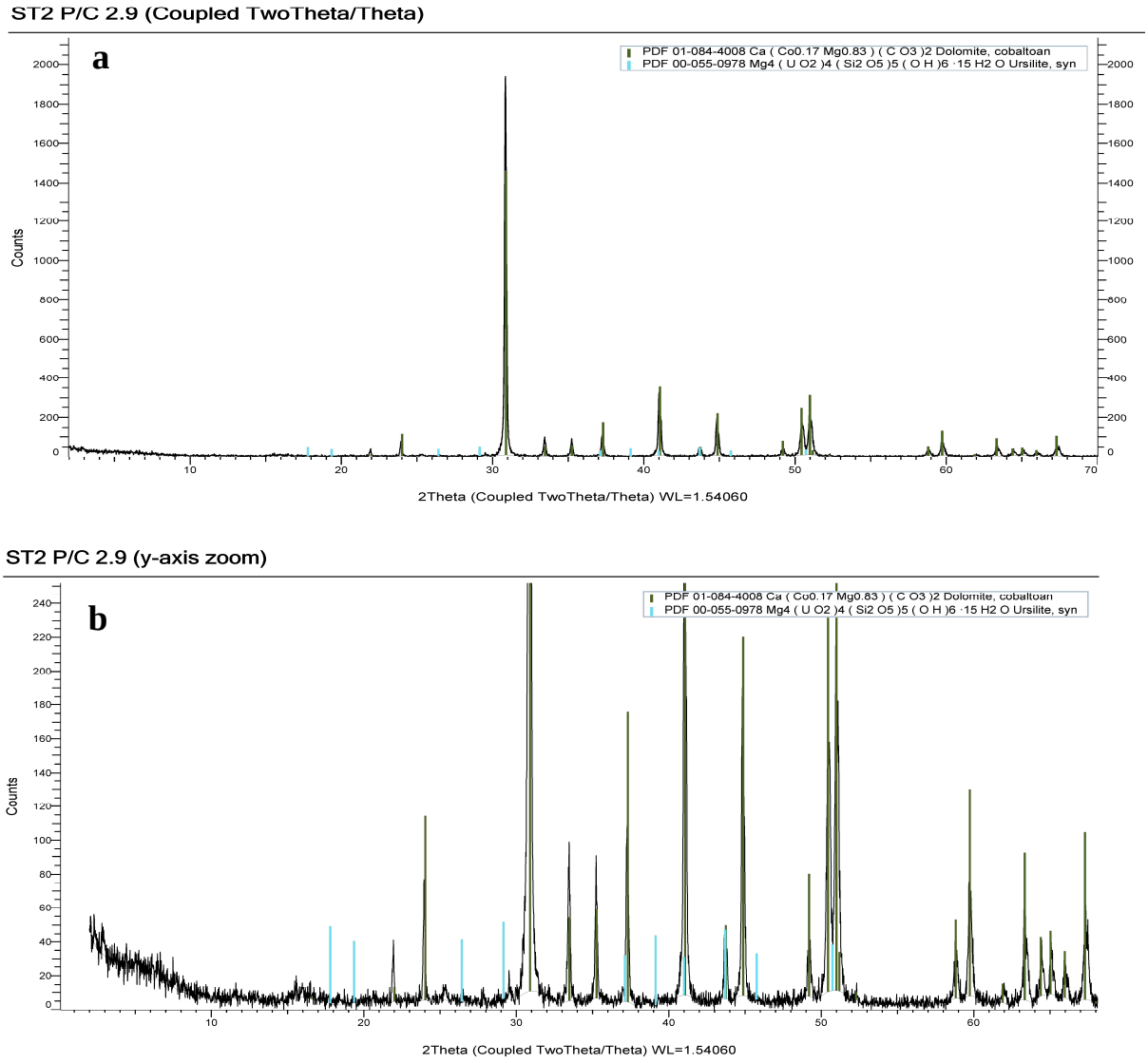

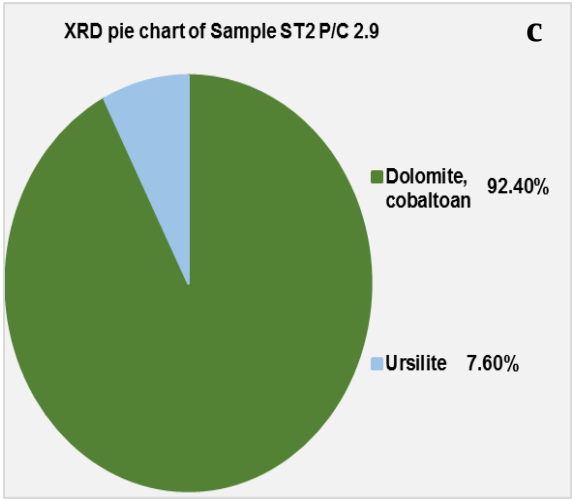

Figure 3-36: *XRD response of ST2-2.9. Diagrams are taken along the X and Y axes to show the dominant mineral tendency for carbonates, plus a circular representation of Dolomite in the sample (photographs a, b and c).*

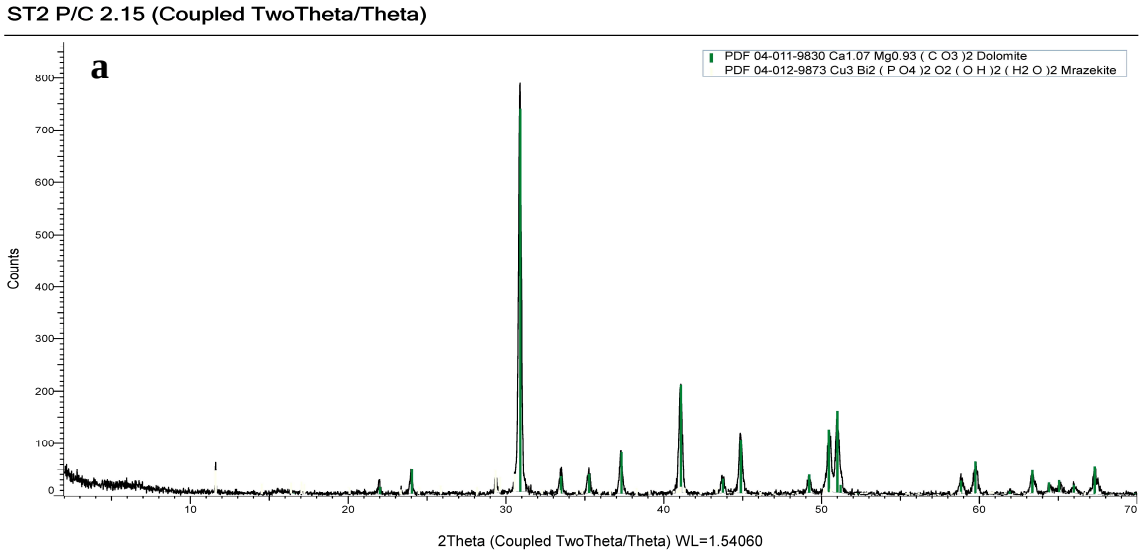

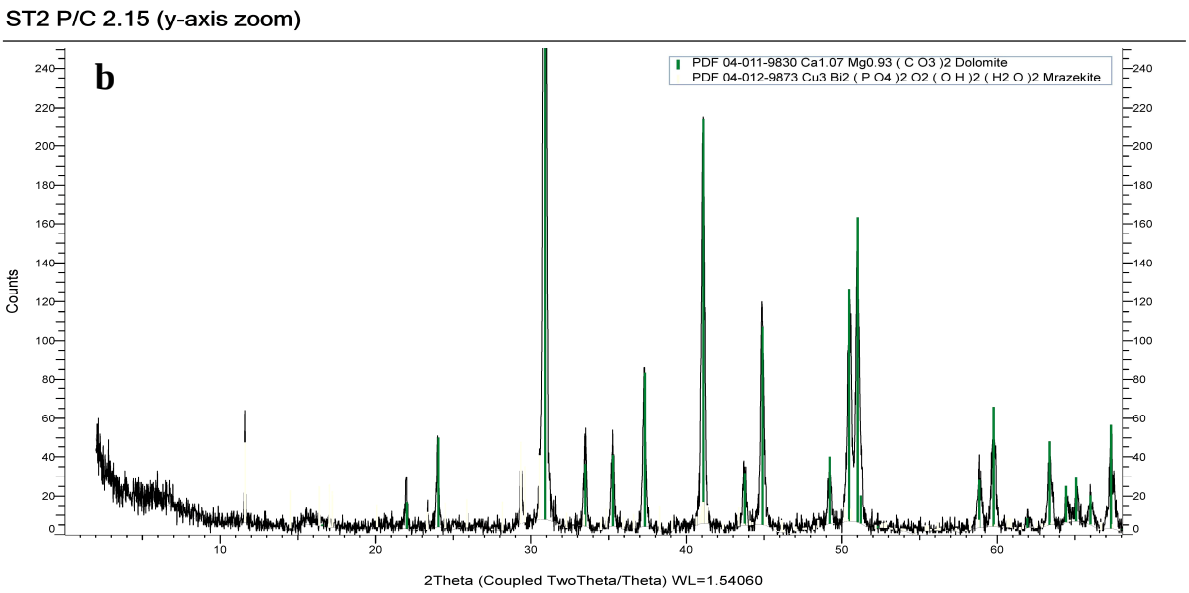

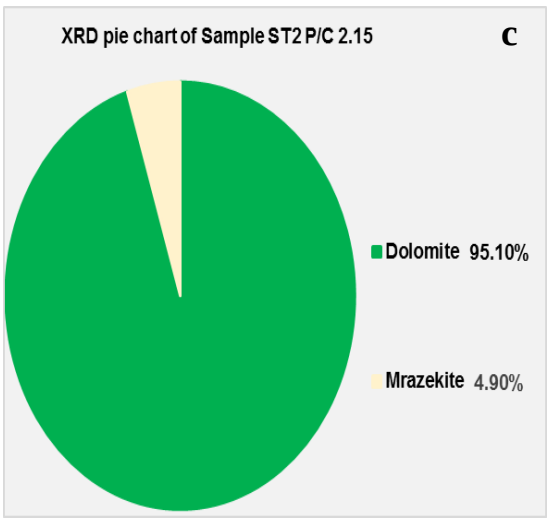

Figure 3-37: *XRD response of ST2- 2.15. Diagrams are taken along the X and Y axes to show the dominant mineral tendency for carbonates, plus a circular representation of Dolomite in the sample (photographs a, b and c).*

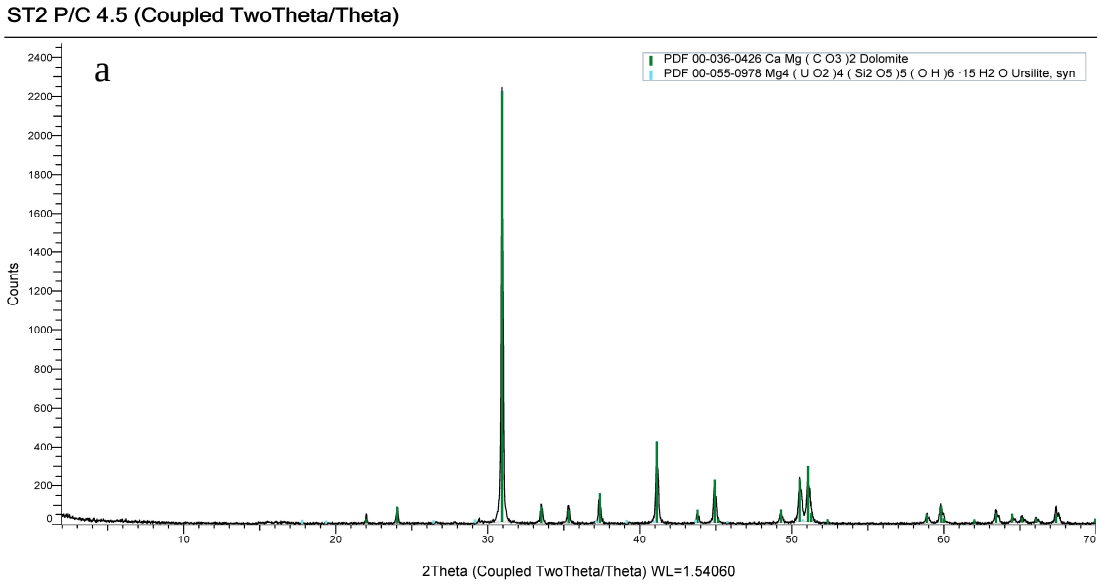

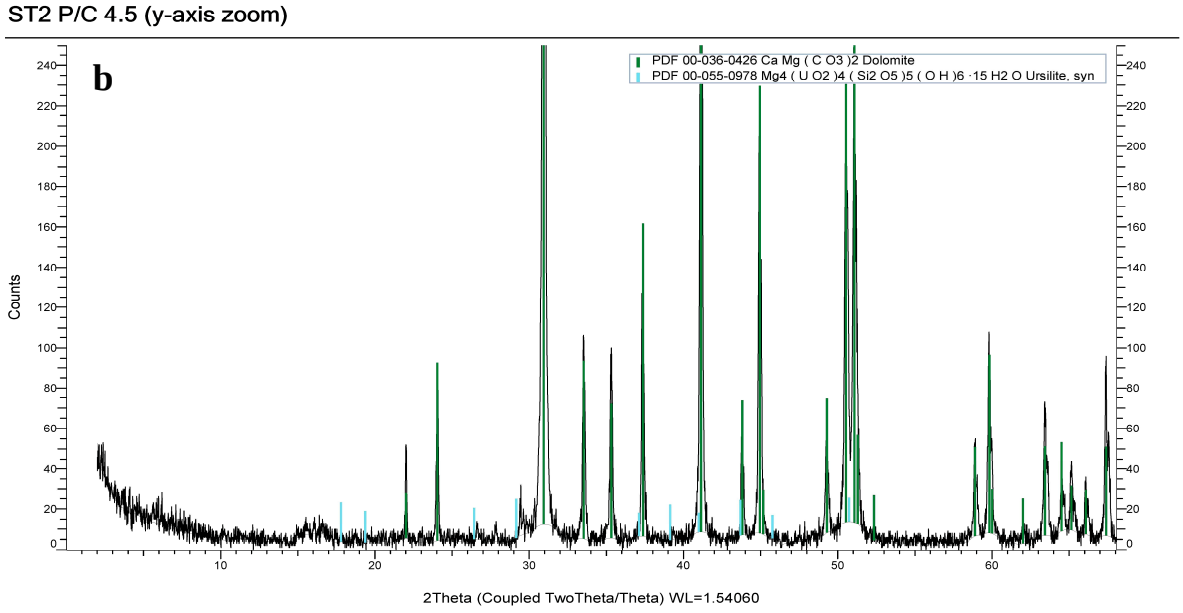

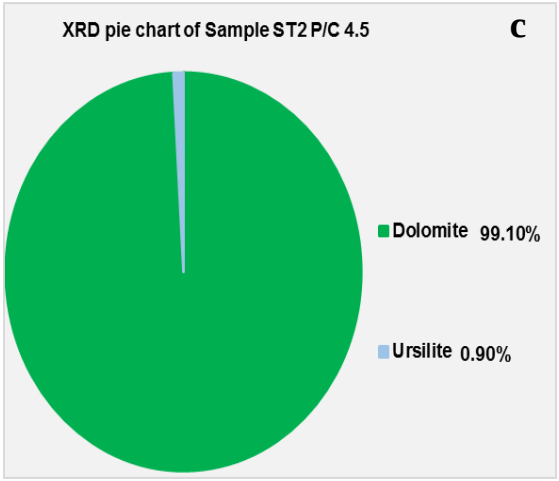

Figure 3-38: *XRD response of ST2- 4.5 Diagrams are taken along the X and Y axes to show the dominant mineral tendency for carbonates, plus a circular representation of Dolomite in the sample (photographs a, b and c).*

3.5 Summary of XRD study.

The typical section of the Sirab Formation: dolomite is predominant in the majority of the samples analyzed. Some samples have less than 50% dolomite (XRD responses) such as STF 185 and ST2 1.6 levels. However, the magnesium content can vary considerably from one horizon to another in the sample. Unfortunately, the bulk analysis method such as XRD can only give the general mineralogical trend of the sample. It differs from other methods such as the scanning electron microscope which makes it possible to describe the variations of the mineralogical composition in each horizon of the outcrop. In the XRD machine, the result of the diffractometer which analyzes the horizon of the outcrop strongly depends on the choice of the level of the outcrop which is introduced inside the machine. This means that the XRD result observed on a single sample reflects a general trend in rock mineralogy. The STF 185 and ST2 1.6 levels (less than 50% dolomite) can then also be more dolomitic in other horizons of these samples which would not have been analyzed by the DRX diffractometer? This hypothesis can be supported by the fact that the quartz, the evaporites as well as the calcite which accompany the dolomite in the carbonates of the Sirab Formation (figure 1-13 in Chapter 1) have not been relatively all identified by DRX, according to their similar proportions on the field descriptions (see sedimentology data in chapter 1).

The XRD results of the twenty five (25) samples from the type section of Sirab (Wadi Shital ST-1 & ST-2) confirm that dolomite predominates over calcite. In the continuation of the study of this chapter, the ratios CaO (%) on MgO (%) were exploited in order to verify for the upper Shital through the section of Wadi Shuram (WS9), in the Aswad Member (WA-1) and another small part of the upper Shital in the stratotype section of Aswad (WA-2), the persistence of the predominance of dolomite in these different sections of field all belonging to the Sirab Formation.

3.6 Summary table of microscopy, XRD and field data.

XRD and Microscopic data			Field work data
Dolomite and calcite (matrix/main minerals).			**Dolomite and calcite (matrix/main minerals).**
Minerals	**concentration**	**Frequency**	**occurrence**
Quartz, Silica and all (SiO_2).	Minor concentration.	Repeated 7 times in different XRD tests and on different samples.	Frequently encountered in sediments such as quartz vein, clastic or siliceous inputs and chert replacement.
Gypsum and other evaporites such anhydrite and halite.	Minor concentration.	Repeat 1 time by XRD test and observe at least 3 times in thin section.	Frequently encountered as precipitated evaporate, dissolved and withdrawn from beds.
Esperite.	Minor concentration.	Repeated 7 times in different XRD tests and on different samples.	?
Biotite and Muscovite.	Minor concentration.	Repeated 3 times in different XRD tests and on different samples.	More than once observed in sediment beds.
Ursilite.	Minor concentration.	Repeated 3 times in different XRD tests and on different samples.	?
Allacite.	Minor concentration.	Repeated 2 times in different XRD tests and on different samples.	?
Any type of iron.	Minor concentration.	Repeated at least 2 times in different XRD tests and on different samples	Encountered as an eroding surface during Angudan unconformity which eliminates and replaces certain thicknesses of the Shital Member or younger units, encountered as crusts of hematite characterizing paleo-caliche development in mudstones of the Ramayli Member.
Dolomite, Cobaltoan.	Minor concentration.	Repeated 2 times in different XRD tests and on different samples	?
Rarest minerals, detected at least once by XRD			
Isokite.	Very low concentration	Very low frequency, encountered only once per XRD response.	?
Mrazekite.			
Althousite.			
Balipholite.			
Bigcreekite.			
Danalite.	Very low concentration.	Very low frequency, encountered only once per XRD response.	
Plagioclases (Potassic).			
Graphite.			
Fairzievite.			
Wairouite.			
Chabourneite.			
Beryllophosphate.			
Albite.			
Radovanite.			

Table 3-1: *Main minerals found in sediments of the Sirab formation through the composite stratotype section of Wadi-Shital ST-1 and ST-2. Summary of XRD, microscopy and field data descriptions.*

3.7 Potential environmental origin of minerals detected.

Dolomite and calcite (matrix/main minerals).					
Mineral	**Detected or Estimated**		**Environmental occurrence**	**Biochemistry process**	
	by XRD	**Field data**		**Authigenic/ biogenic**	**None authigenic /biogenic**
Quartz, Silica and all (SiO_2).	✓	✓	**Mainly present in continental environment**. Present as the main mineralogical constituent in magmatic, metamorphic and sedimentary rocks. In carbonate, quartz and various forms of silica are associated with the continental alteration products of the constituent minerals of magmatic and metamorphic rocks as well as reworked sedimentary.	✓	+/-
Gypsum and other evaporites such anhydrite and halite.	✓	✓	**Continental environment (like sebkhas):** Found in lakes in arid, semi-arid regions, temporary lakes or partially or totally confined basins. **Under-air marine environments (like sebkhas):** Present near the sea, between low tide levels and flooded levels, in partially flooded coastal plains (occasional flooding al lowing the renewal of ions, as well as the contribution of rainwater, dew; mineral deposits inside sand and mud during shallow or dry marshes; Evaporites mixed with other detrital terrigenous elements of the continent, as well as sands). **Shallow basin Environments:** basins of variable size and depth (e.g. lagoons) or rift basins either closed (basin with an eye structure), or half isolated (threshold basin). **Deep basin Environments:** Present in areas with high subsidence (deposits of minerals in laminae, alternating with organic matter, carbonates).	+/-	*none*
Any type of iron.	✓	✓	**Mainly in continental environment.** Weathering product of silicates, aluminous silicates, severely weathered clay rocks, etc. Altered rocks of endogenous and effusive origin rich in ferro-magnesians such as peridots, gabbros and basalts are the main sources of continental iron enrichment.	✓	✓
Biotite and Muscovite.	✓	✓	**Mainly in continental environment.** Mineral of eruptive, metamorphic and sedimentary rocks resulting from the alteration of the silica network of eruptive, metamorphic and sedimentary rocks with partial replacement of Aluminum in the silica network.	none	✓
Esperite.	✓	None	**Mainly in environment of metamorphosed zinc deposits associated with larsenite (***first order in the continental environment***):** Calcium-larsenite, generally in relationship with (willemite, franklinite, calcite, hardystonite, zincite, clinohedrite and glaucochroite). www.rockandmineralshows.com	+/-	?
Ursilite.	✓	none	**Mainly found in environment of carbonate:** Usually due to uranium-coal oxidized along fractures in coal, in sediment buried about a few meters (~ 20 to 50 m). The mineral associates with the dominant forms of Ca and Mg. www.rockandmineralshows.com	+/-	+/-

Allacite.	✓	none	rare arsenate mineral that forms as a secondary in veins that pass through deposits of metamorphosed manganese minerals. May also be from weathered apatite or metamorphosed stratiform zinc. Mainly in association with other minerals such as: sinadelite, hematolite, hausmannite, pyrochroite, fluorite, pyroaurite, leukophenicitis, hodgkinsonite, adelite, franklinite, willemite, friedelite, caryopillite, sphalerite, barite, calcite, serpentine or chlorite **(environment of carbonates).**	+/-	?
Cobalt.	✓	none	Ores generally sulfur and / or arsenic in association with a whole range of other ores such as copper, nickel, silver, lead, manganese, zinc, etc., **Mainly in the environment of carbonates which is accompanied by hydrothermal fluids**.	?	✓

Table 3-2: *First order accessory minerals in Wadi-Shital ST-1 & ST-2 (Sirab Formation), their environmental occurrences and their possible authigenic or non-authigenic control.*

3.8 Mineralogy in Wadi Shuram and Wadi Aswad sections.

After having defined the mineralogical composition of carbonates which predominates in the type section of Sirab at Wadi Shital ST-1 & ST-2, here are the field outcrops belonging to the upper Shital in the section of Wadi Shuram (WS9: depocenter of the Shital Member with the facies at Conophyton Reefs) as well as outcrops belonging to the stratotype section of the Aswad Member (WA1 and WA2: Thrombolite - Oncolite facies). Their mineralogical evaluation is given below in order to affirm whether or not dolomite remains the main constituent of carbonates in the Sirab Formation.

The Major Elements and the Y/Ho ratios obtained from the inorganic geochemical analysis carried out by the ICP-MS/OES method on the powder samples of the rocks belonging respectively to the upper Shital stratigraphic level (section WS9) as well as for WA1 and WA2 (Aswad locality field sections) made it possible to determine the mineralogical trend of the carbonates.

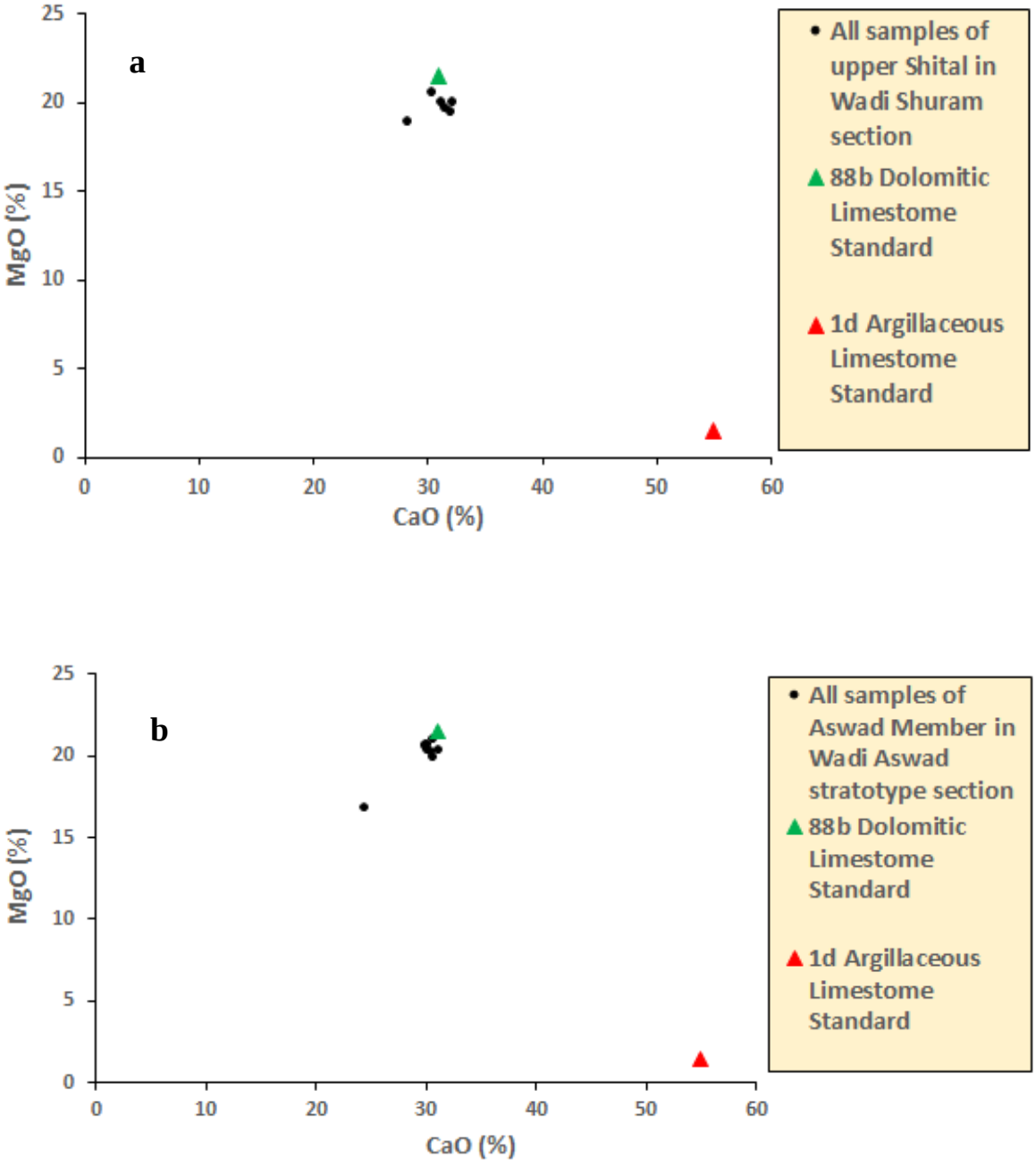

Figure 3-39: *a) upper Shital outcrop plots (samples) from the Wadi Shuram section (WS9), b) Outcrop plots (samples) covering the upper Shital and Aswad Member in the stratotype section of Wadi Aswad (WA1 and WA2). See figure 2-1 in chapter 2 where the sections analysed in this thesis appear. 88b Dolomitic Limestones and 1d Argillaceous Limestones (standards) are the Georem benchmarks (http://georem.mpch-mainz.gwdg.de) used for comparison.*

In usual practice, the MgO (%) versus CaO (%) ratio is used to differentiate calcite from dolomite in the carbonate. The upper Shital stratigraphic level in the section of Wadi Shuram (WS9) as well as the upper Shital and Aswad Member in the section WA1 and WA2 along the stratotype locality of Aswad are all rich in dolomite rather than calcite.

The implication or not of diagenesis in the process of enrichment in magnesium ions in the Sirab Formation is presented and discussed in the following chapter 4. However, although dolomite is abundantly enriched in the Sirab Formation at Haushi - Huqf, the mixed carbonate associated with dolomite, calcite, evaporite, quartz as well as clasts of all kinds can be subject to strong contamination or low caused by contributions of geological materials from different environments (terrigenous, marine, etc.,).

The composition of the REEs is very significant of the environment originating in the sediment. Indeed, the production of REEs in the sediment is closely linked to the mineralogical composition of the sources originating in the sediment, which confers a parental inheritance of REEs in relation to the mobilization environment at the start of the sediment. SiO_2, Al_2O_3, Fe_2O_3 can therefore serve as a benchmark to track the degree of contamination of carbonates (CaO, MgO) by terrigenous materials. Recording the Y/Ho ratio being sensitive to sea-water and freshwater variations (Nozaki, 1996;

Lawrence, 2006) may at first glance help to determine the proximity of the carbonate ramp to the sheltered environment in the vicinity of the peritidal zone or with the submerged environment off the tidal and subtidal zone.

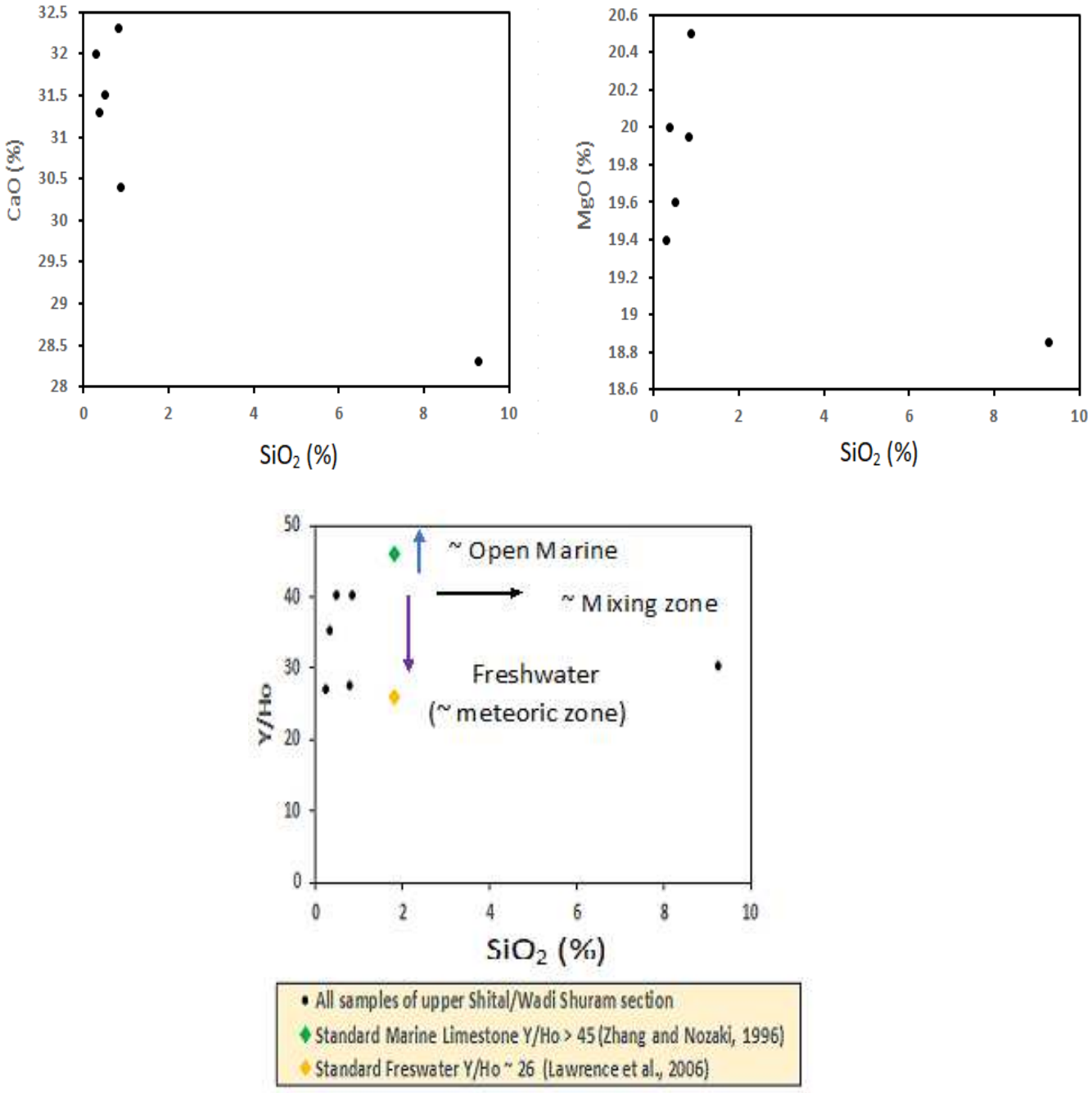

Figure 3-40: *CaO (%), MgO (%) and Y/Ho on SiO_2 (%) to determine the level of contamination of carbonates by silica as well as the approximation of the ramp of carbonates in a marine or terrigenous environment. Above here, captions are for samples of upper Shital in section of Wadi Shuram (WS9).*

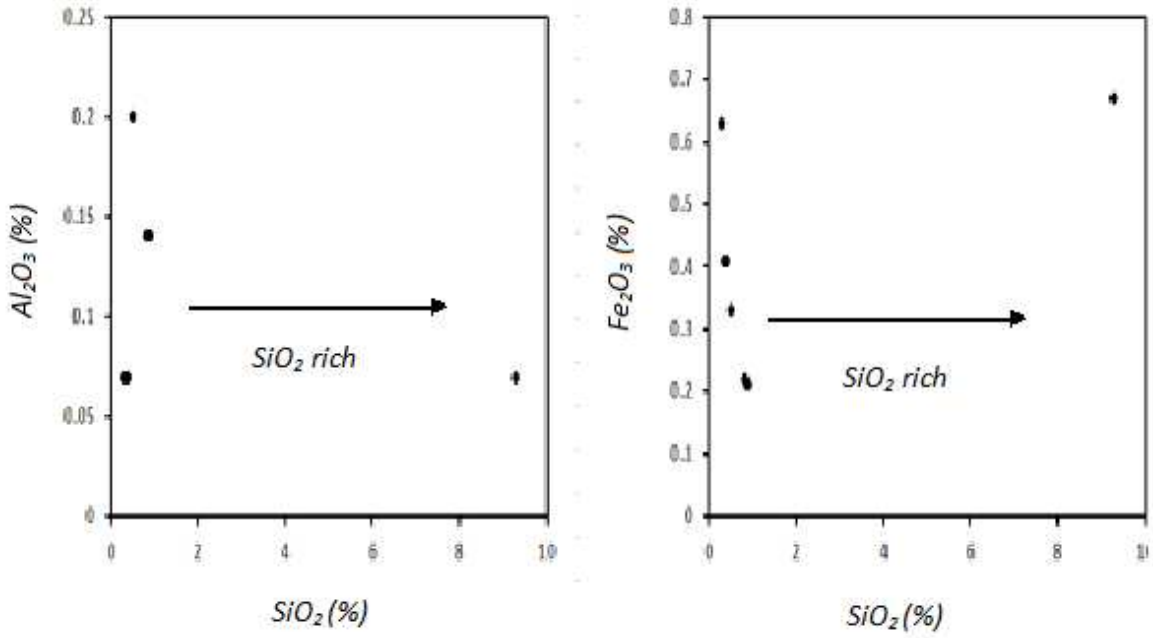

Figure 3-41: *Al_2O_3 (%) versus SiO_2 (%) ratios as well as Fe_2O_3 (%) versus SiO_2 (%) to determine the terrigenous components most present in mixed carbonates of the Sirab Formation. Here, captions are for samples of the upper Shital in section of Wadi Shuram (WS9).*

Like the Wadi Shital ST-1 & ST-2 composite stratotype section of Sirab Formation, dolomite predominates in the WS9 section of the upper Shital at Wadi Shuram locality. Dolostone and dolomite associated with calcite, evaporites and terrigenous materials (mixed carbonates) contain relatively quartz (SiO_2 less abundant than carbonate, figure 3-39). The signal of a persisting marine presence through the chemical composition of the analyzed samples was not satisfactorily detected. Figure 3-40 rather assumes that the section of Wadi Shuram (WS9) of the upper Shital would lie roughly in an intermediate zone between freswater and sea water (Y/Ho greater than 26 and less than 42). Thus, such a result (unsatisfactory for a clear marine implication) can be justified by the structure of the regional

relief (paleo-topographic) in the Haushi-Huqf region during the carbonate deposition and the filling of the basin, if the latter did not have been in direct contact with the open marine environment. This may infer that the development of Conophyton Reefs in the upper Shital is the beginning of modification of the chemical composition of the sediment at the water-sediment interface without claiming a direct passage between two distinct environments.

The SiO_2 (%) generally very abundant in the terrigenous sediments is less rich in proportion compared to the carbonates in the Sirab. However, the proportion of silica remains much greater than that of iron and aluminum after the highest proportions of carbonates. But this (silica) does not seem to indicate an exclusive presence of siliceous rocks among the samples analyzed in this thesis. Because the sandstone horizon (quartz Arenite Sandstone) which overhangs the entire Sirab region in Al-Huqf as mentioned in the chapter see figure 1-13, does not consist of a filling deposit of the Formation but rather a summit of an eroded palaeo-relief (Gold, 2010). As such, no samples of these Arenites Sandstones were analyzed in this study. As such, this unchanged data of the proportion of carbonate with silica, aluminum and iron as the main Major Elements implies that the grain size of the sediment probably played a very limited role from upstream to downstream on the final composition of the carbonates.

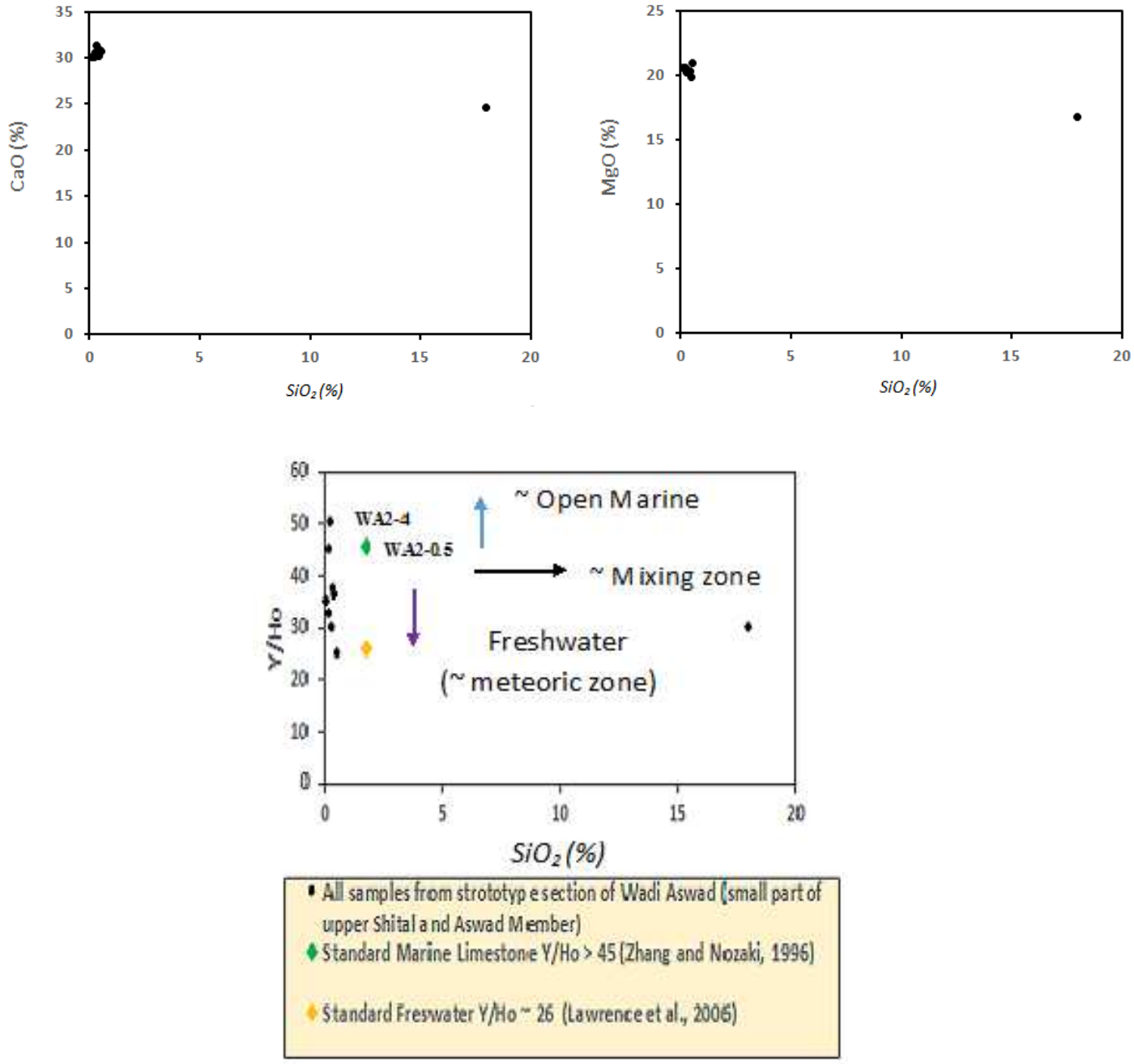

Figure 3-42: *CaO (%), MgO (%) and Y/Ho on SiO_2 (%) to determine the level of contamination of carbonates by silica as well as the approximation of the carbonate ramp in the marine or terrigenous environment. Here, captions are for samples of stratotype section of Wadi Aswad (upper Shital and Aswad Member).*

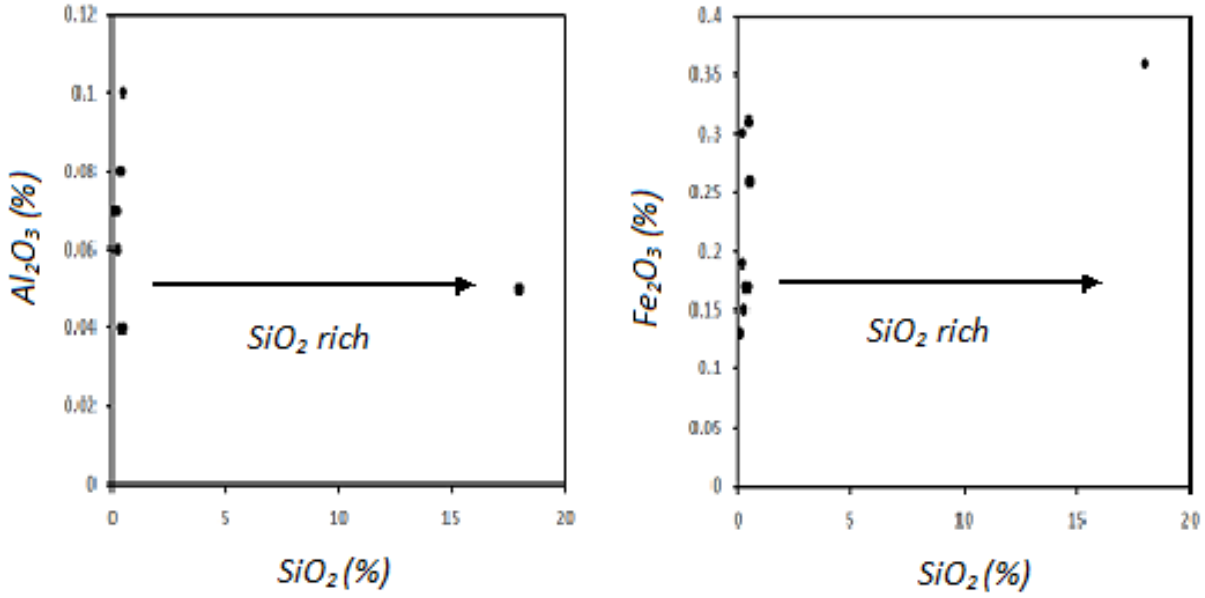

Figure 3-43: *Al_2O_3 versus SiO_2 ratios as well as Fe_2O_3 versus SiO_2 to determine the terrigenous components most present in mixed carbonates of the Sirab Formation. Here, captions are for samples of stratotype section of Wadi Aswad (upper Shital and Aswad Member).*

As in the previous section of Wadi Shuram (WS9), dolomite predominates in section WA1 and WA2 in the locality of Wadi Aswad. Dolomite associated with calcite, evaporites and terrigenous materials (mixed carbonates) contain relatively quartz (SiO_2, see figure 3-42). The presence of a marine signal was recorded on at most two samples belonging to the Aswad Member (WA2-0.4 and WA2-4, see sample annotation table as well as figure 2-1 of chapter 2 to better locate the levels outcrop). Unlike the section of Wadi Shuram WS9 and Wadi Shital ST-1 & ST-2 where no marine presence has been recorded so far, the locality of Wadi Aswad seems favorable to a temporary connection with the open marine environment. However, only two (2) samples out of a total of forty (40) analyzed in this study

have a Y/Ho ratio correlable to the marine presence. Chapter six (6) of this thesis on the Geochemistry of Trace Elements and REEs will help to deepen the discussion in relation to the marine connection. At this time, section WA2 is likely to include significant change in the deposit environment of the Sirab Formation specifically at the Aswad Member. It can also be postulated for a palaeo-geographic indication of the location of the sea through Oman in the region of Al-Huqf based on the geographical distribution of field sections (figure 1-3 of chapter 1).

On the other hand, the proportions of SiO_2 (%) remain relatively balanced with those of Al_2O_3 (%) as well as Fe_2O_3 (%), figure 3-43. This result is the same in the section of Wadi Shuram (WS9) for the figures 3-41. This unchanged data in the proportion of carbonate relative to silica, iron and aluminium tends to limit the importance of the granulometry of the sediment on the general mineralogical composition.

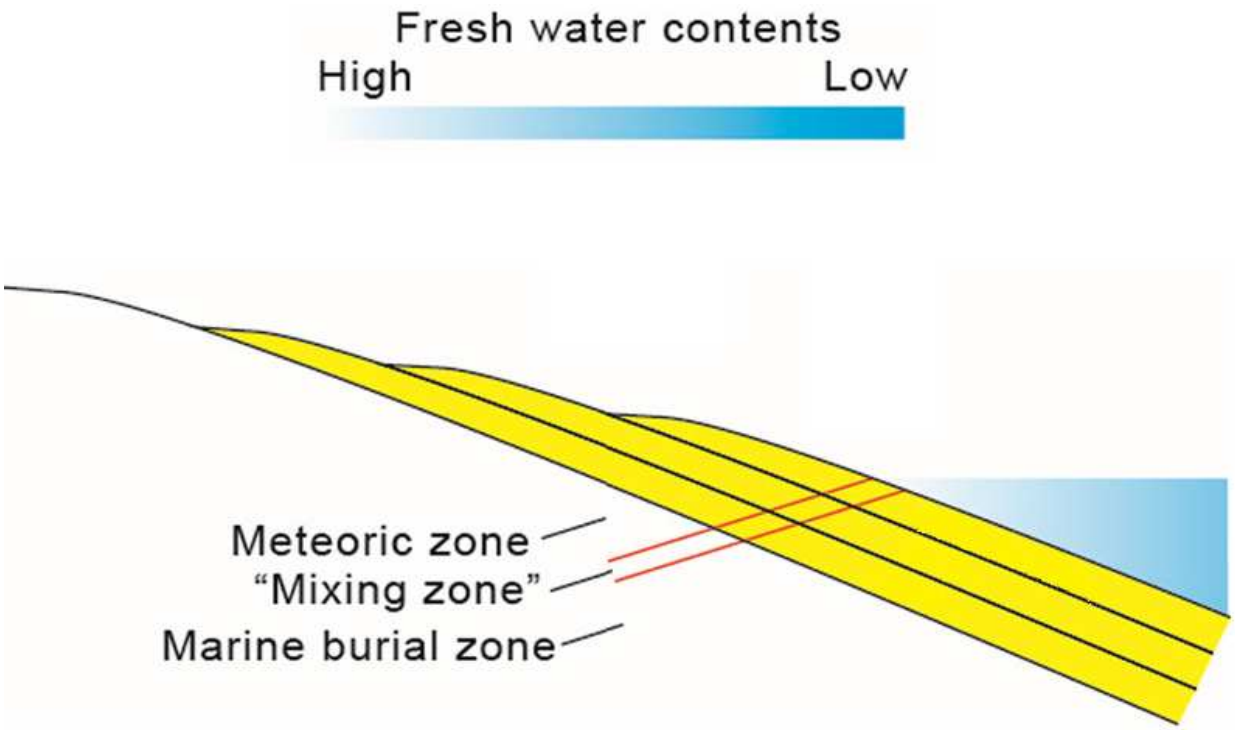

Figure 3-44: *Cartoon to illustrate a possible carbonate contamination by terrigenous materials as well as the position of the ramp according to the sea water, caption from Zhao and Zheng (2016), modified.*

4 Fourth Chapter: *Diagenetic study*

4.1 Introduction.

In the sediment and more particularly for dolomite carbonates, the hypothesis of the origin of magnesium enrichment can be explained by the phenomenon of diagenesis during deep burial. However, in certain environments where the concentration of magnesium ions is high (example of certain hypersaturated Mg lakes), primary dolomite can form by direct precipitation and independently of the diagenetic process. To differentiate magnesium-rich sediments generated by diagenetic dolomitization or by primary dolomite, the use of geochemical tracers capable of filtering the variations in the concentrations of Sr and Mg ions as a function of the depth of the sediment is essential. The recorded values of the curves of oxygen as well as carbon as a function of depth also make it possible to differentiate magnesium enrichment by diagenetic route or by primary precipitation. In chapter 2, it was briefly stated that a large positive $\delta^{13}C$ isotopic peak occurs at upper Shital. This indication is considered in this thesis as a signal indicating a possible change in the chemical composition of the environment of the depositional of the Sirab Formation. Apart from the positive $\delta^{13}C$ peak at the passage of the upper Shital through the set of field sections of the Sirab Formation (Gold, 2010), the remains of the $\delta^{13}C$ and $\delta^{18}O$ values for the Wadi Shital ST-1 field sections, Wadi Shuram (WS9) as well as Wadi Aswad (WA1), combined with chemotratigraphy data helped to diagnose the diagenetic index tracers of the Sirab Formation sediment.

Based on the $\delta^{13}C$, $\delta^{18}O$ isotope ratios, a strong evolutionary similarity in the chemostratigraphic composition of the sediments across the different Members of the Sirab Formation that are distributed in various field sections was observed. In the Aswad Member, the primary dolomite facies (*fd*) and dolomite zonation as elongated or banded filaments (*zd*; see figure 3-12) within the Thrombolite - Oncolite facies suggest that the deposition of these carbonates is located near an open marine environment and that the uppermost unit of the Formation could be submerged by seawater. As such, the Aswad Member may therefore be positioned slightly around the marine burial zone due to the Y/Ho ratios >45 in the case of samples WA2-0.4 and WA2-4. However, as the majority of the samples analyzed in this thesis have Y/Ho ratios < 45, it therefore seems coherent to locate approximately the major part of the Sirab carbonate ramp between the meteoric zone and the mixing zone (see figure 3 -43 in chapter 3) and to probably consider that the position of the marine palaeo-shoreline is located further north of the current Al-Huqf region in the locality of Aswad in Oman rather than towards the center at Wadi Shital ST-1 or at south to Wadi Shuram. Additionally, the marine signature trace on two samples from the Aswad Member can be correlated to the facies of the sediment versus the dolomite. If we can retain a certain marine implication for the top of the Formation, precisely towards the current north of the region and that at the same time is recognized the precipitation of the primary dolomite on the facies of the Member of Aswad, that limits the consideration of effective diagenesis for the whole Member and for the Formation in

general. The majority of the Y/Ho ratios < 45 counted on thirty-eight (38) of the samples in this study tend to confirm the slightest marine involvement and, correlatively, to support a deposit of the carbonate ramp located above the level of marine influence (peritidal zone).

A completely different analysis of dolomite abundance would be that, as all Members of the Sirab Formation harbor carbonate sediments with a high magnesium content (dolomite) and this almost generalized dolomitization is observed even in the Buah-Ramayli transition at the base of the Formation then, the hypothesis of an overall and general diagenetics controlled by burial would be plausible. Especially since in the majority of the thin sections, the calcite replacing the dolomite in the cement was defined in the compacted sediment. This results in the amplitude and degree of compaction of the sediment being variable depending on the levels in the stratigraphic column of the Formation. Microscopic analysis of thin sections indicates that dolomite constitutes the matrix of the sediment in the majority of cases (micritical for muds). For mud levels whose proportion of micrite dominates sparite, these rocks have been qualified as dolomicrite, whereas sediments with grain size proportions greater than micrite and of which dolomite remains the main constituent have been qualified as dolostones. For example, the grainstones of the Buah-Ramayli transition zone are dolostones while the STF 185 level (Conophyton Reef of section Wadi Shital ST-1) is dolomicrite.

Due to the abundance of dolomite and the presence of calcite as detected by XRD in the sedimentary units of the compacted sludge, the cement which develops there in these muddy parts of the sediment is therefore associated dolomite with calcite. As such, dolomite can therefore be hastily interpreted as diagenetic and more specifically, when defined in the first two members of Sirab (Ramayli and Shital). Usually in the context of ancient sediments around the Ediacaran - Cambrian age, such widespread dolomitization takes place by means of a relatively continuous diagenetic system to allow sufficient importation of Mg and exportation of excess Ca and Sr (Land, 1985). On the other hand, the Ca-rich zones in the dolomites of the Sirab Formation were dissolved and their fluid compositions slightly varied during stabilization of the dolomite (Land, 1985; Tucker, 1990).

Concerning the intercalary evaporite levels in the stratigraphy, anhydrite for example can form on different seawater levels (starting from shallower to deeper burial environments). This evaporite mineral commonly replaces carbonates and clogs porosities. In the Sirab Formation, the beginning of the appearance of anhydrite laths (the oldest anhydrite formed) is found in the dolomite matrix. These early anhydrite tissues consist of single slats (in a decussate arrangement), suggesting growth in poorly consolidated carbonates (initial anhydrite growth prior to compactions). But, the replacement of dolomite by anhydrite was not photographed in the thin sections of this work. However, the sedimentological descriptions of the field work clearly mention the presence of this evaporite. On the other hand, the

presence of silica in dolomitic sediments is relatively abundant in all field sections.

Calcite, dolomite and quartz are associated with each other in the dolomitic matrix. Individually, salt dolomite, or salt associated dolomite, was characterized by curved crystal faces and rapid extinction indicating a distorted crystal lattice (Radke, 1980). Despite its relatively common occurrence, the origin of salt dolomite is poorly understood. Radkhe suggest that the salt form reflects a preferential absorption of Ca towards the crystal corners, which causes an expansion of the lattice relative to the centers of the faces. Almost all saddle dolomite has been interpreted to have formed from brine with salinities 2-6 times that of seawater and at temperatures between 60 and 150°C. The few reliable homogenization temperatures of fluid inclusions of saddle dolomite range from 90 to 215°C, and homogenization temperatures of sphalerite, which sometimes accompanies precipitation of saddle dolomite, reach 220°C (Roedder, 1968; Beales, 1980; Morrow, 1986 and Lee, 1987).

Finally, the use of the concentrations of the Inorganic Geochemical Elements Mn, Sr, Mg and Fe can help to understand the relative degree of weathering associated with meteorics, burial diagenesis as well as dolomitization. Textural, mineralogical and chemical changes are associated with the stabilization of the original metastable

carbonate assemblages in a diagenetic environment. These changes involve the dissolution/re-precipitation reaction.

$$CaCO_3 + H_2O + CO_2 \longleftrightarrow Ca(HCO_3)_2$$

Substitution of Ca^{2+} by trace elements such as Sr^{2+}, Mn^{2+}, Fe^{2+}, Pb^{2+}, Zn^{2+} and Na^{+} in the $CaCO_3$ network can occur to varying degrees due to different partition coefficients and large differences in composition in marine water and meteoric (Brand, 1980). Open or partially closed diagenetic systems and/or single or multiple dissolution-reprecipitation events will generally lead to a decrease in the concentrations of Elements in which the partition coefficient (Kcalcite-water) <1 (Sr^{2+}, Na^{+}, Mg^{2+}), and an increase for those where K > 1 (Mn^{2+}, Fe^{2+}, Zn^{2+}). This allows that more the deviation of a particular coefficient from unity, the greater the depletion or enrichment for a given degree of diagenesis with meteoric water.

Many Elements, including iron and manganese, reach high concentration thresholds in the Sirab Formation such that one might think that a diagenetic alteration would have occurred while at the opposite of these threshold concentrations; the primary and preserved forms of dolomite such as those found in the Aswad Member, suggest that diagenesis would not have had a determining effect on the concomitant enrichment of manganese and iron.

For the Mn content to increase in sediment to the detriment of Sr, the sources of Sr production in the geological cycle are decisive. The seawater-sediment interface can be enriched in Sr from two different sources. Either Sr originates from the continental crust by subaerial weathering and fluvial transport or from the oceanic crust by hydrothermal activity at mid-ocean ridges and underwater weathering of basalts (Tucker, 1990). Previous Sr values recorded in different sections of the Sirab Formation ranged from 53 to 586 ppm. In the samples analysed in this thesis, no Sr value exceeds 500 ppm while the majority of them are between 50 and 120 ppm. Modern mixing zones display Sr values between 100-250 ppm as opposed to the Sr values of modern dolomites formed in modern hypersaline and evaporitic environments 600 - 900 ppm (Beherens, 1972). Approximate values of Sr (53-586 ppm) were found in other Neoproterozoic rocks and are not uncommon in the Precambrian (e.g. Leather, 2002; Tucker, 1983; McCarron 2000 and Gold, 2010). Generally low Sr concentrations are considered to be indicative of some degree of diagenetic alteration of the original calcite or aragonite (e.g. Brand, 1980 and Brand, 1983b).

Petrographically, it is observed that more dolomites than calcites and carbonates associated with evaporites in the Sirab Formation (see petrographic study in chapter 3). The carbonate beds associated with salts (dolomite in salts) are limited to a few evaporite units recognized in the field and presented in Chapter 1 on the sedimentology of the Sirab Formation. Tucker and Wright (1990) believe that unlike HMC,

the Mg/Ca ratio results in the formation of LMC which occurs during periods of sea level rise. But all the tests (thin sections made by the red technique alizarin), XRD tests as well as MgO (%) versus CaO (%) ratio, sufficiently demonstrates that dolomite predominates in all sections.

4.2 Reports of $\delta^{13}C$ and $\delta^{18}O$.

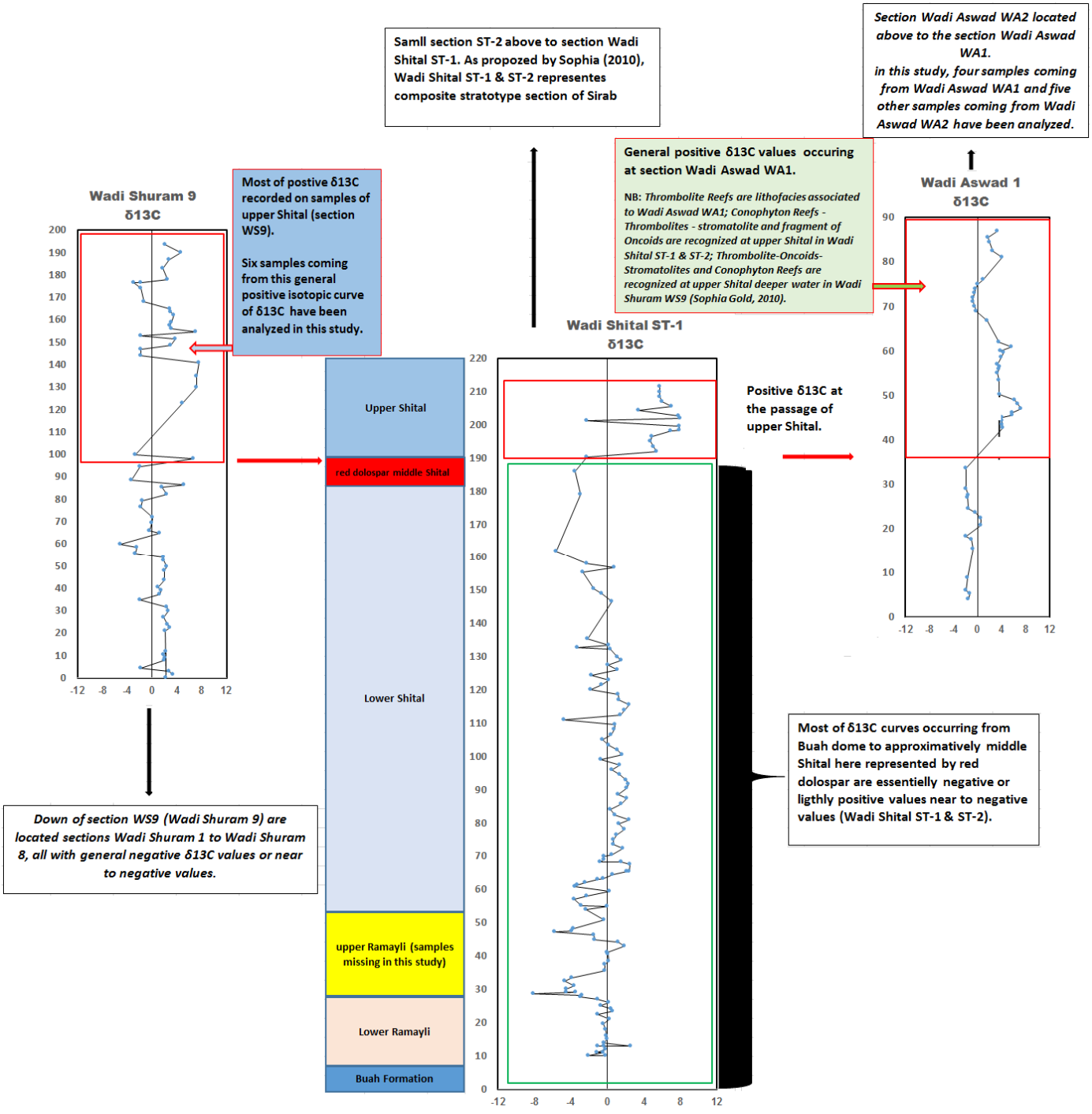

Figure 4-1: *$\delta^{13}C$ isotope curves of the field sections used in this study (Wadi Shuram WS9, Wadi Shital ST-1 and Wadi Aswad WA1). See the chart color of the Sirab Formation Member in Chapter 2 (figure 2-1).*

The type section of Sirab (Wadi Shital ST-1) without the addition section ST-2 (see chapter 1 at point 1.8) in the middle of figure 4-1, allows a better understanding of the $\delta^{13}C$ isotopic variations that occur. Although the common feature of all the Sirab sections is the positive $\delta^{13}C$ peak that manifests in the stratigraphy at the upper Shital level in the Wadi Shital ST-1 section, the outcrop levels before the upper Shital retain $\delta^{13}C$ isotopic values less divergent. Most of these values are negative from the Buah-Ramayli transition zone down to about the lithostratigraphic level 62 m above the base of Wadi Shital ST-1. All of this lithostratigraphic height includes the Buah Dome outcrops in the transition zone as well as the lower and upper Ramayli outcrops. Then, beyond 62 m from the lithostratigraphic level, the majority of the rhythmic carbonate cycle of the Shital Member in the lower unit (lower Shital) shows positive $\delta^{13}C$ isotopic values until about the 150 m lithostratigraphic level without however reaching a peak accentuated positive, as during the passage of the higher Shital. Between 150 m and 185 m, the isotopic values again become negative under the sandstone horizon indicated in figure 1-13 of chapter 1. A significant hiatus in the stratigraphic succession of outcrops occurs from 136.2 m and continues to level 184.8 m below the sandstone horizon (figure 1-13). In common, the outcrops from the Buah-Ramayli transition zone to the first 62 meters have $\delta^{13}C$ values between (-4.64‰ VPDB and -0.2‰ VPDB). The $\delta^{13}C$ values from level 132.2 m up to 186 m oscillate around (-5.63 ‰ VPDB and 0.77 ‰ VPDB), see tables of $\delta^{13}C$ and $\delta^{18}O$ values in appendix 4 to volume 2. When the upper Shital passes above 185 m of the lithostratigraphy,

the peak of the $\delta^{13}C$ isotopic values remains almost unchanged in the Wadi Shital ST-1 section (horizon of Conophyton Reefs), without addition of the section ST-2.

The section of Wadi Shuram WS9 in figure 4-1 begins with slightly positive $\delta^{13}C$ values. Indeed, these positive values in $\delta^{13}C$ strongly coincide with the pads of the lower Shital of the Wadi Shital ST-1 section. The transition to negative values $\delta^{13}C$ before reaching the positive peak in the central deposit of Conophyton Reefs from the upper Shital at WS9 also occurs and this can be assimilated to the level immediately preceding the sandstone horizon (middle Shital). Like the Wadi Shital ST-1 section, also in the Wadi Shuram section, the Thrombolite- oncolite facies of the Aswad Member does not appear either (figure 1-5). However, positive $\delta^{13}C$ values that occur in the upper Shital at this section of field revert to negative values in some outcrops before turning positive again. The lowest outcrop levels of the section such as Wadi Shuram 1 to 8 were not presented in this thesis including the level of Wadi Shital 10 (figure 4-1).

The section of Wadi Aswad WA1 located stratigraphically above the rhythmic carbonate cycle begins with negative $\delta^{13}C$ values that manifest at the middle Shital before moving to the positive peak of $\delta^{13}C$ values of the upper Shital. Here again in the section of Wadi Aswad WA1, the Thrombolite-Oncolite- facies does not appear (figure 2-1 in chapter 2) but the unity is characteristic of Thrombolite

Reefs of which some Thrombolitic levels have also been recognized below of the Sandstone horizon in the Wadi Shital ST-1 section. The change to positive values $\delta^{13}C$ therefore marks the correlation of the section of Wadi Aswad 1 to the unit of the upper Shital (Conophyton Reefs) in the sections of Wadi Shital ST-1 as well as Wadi Shuram WS9. On the other hand, in Wadi Shuram WS9 and in Wadi Aswad 1, the upper Shital characterized by the positive peak of the isotopic values $\delta^{13}C$, always reverts to negative values between approximately 220 m before becoming positive again.

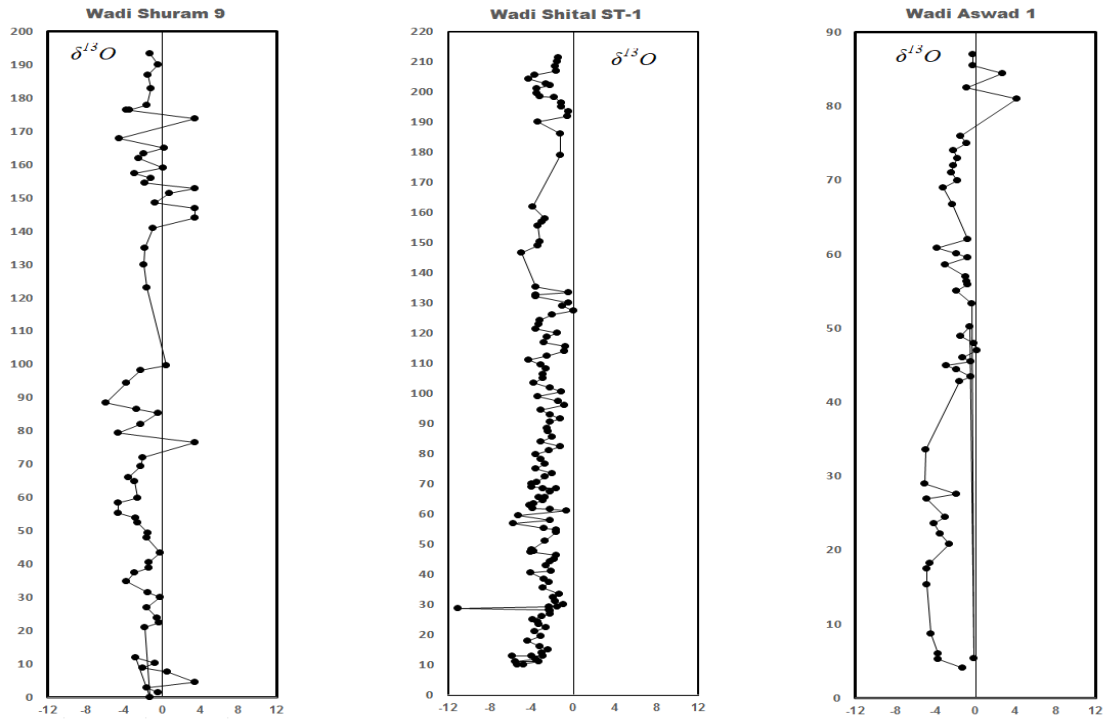

Figure 4-2: *$\delta^{13}O$ isotope curves of the field sections used in this study (Wadi Shuram WS9, Wadi Shital ST-1 & ST-2, Wadi Aswad WA1).*

Regardless of the stratigraphic correlation as presented in figure 4-1 for the $\delta^{13}C$ isotopic values, the $\delta^{18}O$ curves seem to preserve primary isotopic values. There are hardly any emblematic fluctuations in the $\delta^{18}O$ values unlike the $\delta^{13}C$ whose upper Shital shows a positive peak. Diagenetic analysis of sediments is interdependent on $\delta^{13}C$ and $\delta^{18}O$ isotopic values because whether or not bioherm productivity is preserved during sediment burial, records of temporal variations in $\delta^{13}C$ isotopic values should normally indicate this. Moreover, the presence of water (H_2O in general with oxygen as the main Geochemical Element) in the water-sediment interface during the evolution of the deposition of the sediment and its subsequent burial, leads to temporal variations of the isotopes $\delta^{18}O$ which can help replenish the environment (palaeo-redox) of the entire Formation.

4.3 Diagenesis of Wadi Shital ST-1 & ST-2 section.

4.3.1 *Sr excursions.*

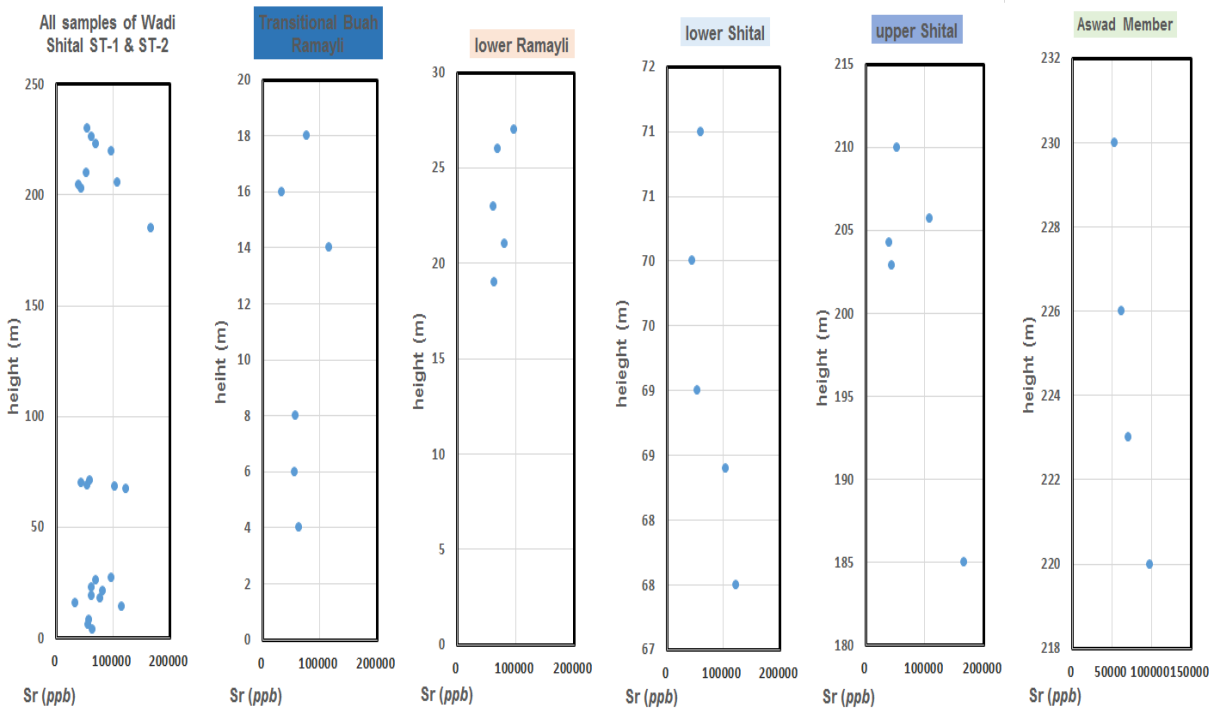

Figure 4-3: *Sr (ppb) curves plotted against depths for outcrop levels of the Sirab Formation in Wadi Shital ST- & ST-2 section. The colorings that accompany each level of lithology were discussed in chapter 2 (figure 2-1) of this thesis and are repeated here for the sake of clarity and logic in the flow of ideas.*

The strontium curve excursions that occur in the Wadi Shital section ST-1 & ST-2 give little information on diagenesis at this stage of the study. In the laboratory, the values obtained from the ICP-MS carried out at Trinity College Dublin for the outcrops in this section were all in ppb. Although strontium (Trace Element) has low concentrations

compared to manganese (Mn) which was measured in ppm and detected as a Major Element. The Sr excursions in the Sirab type zone for the different outcrop levels analyzed do not offer the possibility of making a correct diagenetic analysis of the sediment when comparing only the Sr values with respect to the depth of the sediment.

In sediments, the absolute concentrations of Mn, Fe and Sr depend on a number of factors including their availability, local redox conditions and the water/rock ratio (Tucker, 1986). Additionally, Kaufman (1993) or Kaufman (1995) had the most confidence in the stable isotope results of carbonates with Mn/Sr ratios < 3, but they suggested that carbonates with Mn/Sr < 10 also retained abundant $\delta^{13}C$ primary signatures.

4.3.2 Concentrations of Fe and Mn.

	ICP-MS Data	
Samples	**Fe (ppm)**	**Mn (ppm)**
STB 4	1054	972
STB 6	934	1109
STB 8	2110	2687
STB 14	3819	1619
STB 16	908	749
STB 18	1960	2620
STB 19	2869	2588
STB 21	1328	1219
STB 23	1967	1088
STB 26	699	751
STB 27	824	1426
STF 67.5	1846	839
STF 68.4	4186	581
STF 69	2911	729
STF 70	1086	549
STF 71	1555	677
STF 185	21550	1402
STF 202.9	1176	1041
STF 204.3.	485	861
STF 205.7	949	1180
STF 210	1716	917
ST2 1.6	902	1144
ST2 2.9	679	601
ST2 2.15	852	537
ST2 4.5	1518	1222

Table 4-1: *Fe and Mn concentration values analyzed by ICP-MS at the geochemistry laboratory of Trinity College Dublin on outcrops belonging to the Wadi Shital ST-1 and ST-2 section (composite stratotype section of Sirab). All Fe and Mn values are obtained in ppm.*

The use of Fe as well as Mn as a proxy to scrutinize diagenesis in sediments can be very beneficial. Evidence of diagenesis can be preserved as evidence of their existence over time in ancient sediments. For example, modern carbonates contain very little Fe and Mn (tens of ppm). These elements mainly have very low

concentrations in seawater while their high values are recognized in the pores of diagenetic fluids. Because, diagenetic fluids (by extension the fluids encountered in the pores of the sediments during burial) have a negative oxidation-reduction potential (Eh). And this is generally the case for most buried sediments (Tucker, 1986).

(Gold, 2010) finds that the Fe concentrations are high in the Sirab Formation and vary from 460 to 13,000 ppm while the majority of them exceed 2,000 ppm. Sophia's results were similar to the Fe concentrations reported by McCarron (2000) on the Shuram Formation and by Leather (2002) on the Hadash Formation. However the works of those authors were located either in the localities of Shuram or Hadash, or represent all the sections of the Sirab Formation known to date in the case of the values reported by Gold (2010) for the field sections scattered in Al-Huqf in Oman. The ICP-MS results from the geochemistry laboratory also indicate iron concentrations mainly greater than 1000 ppm for the part of the section of Wadi Shital ST-1 & ST-2.

4.3.3 Mn/Sr ratios.

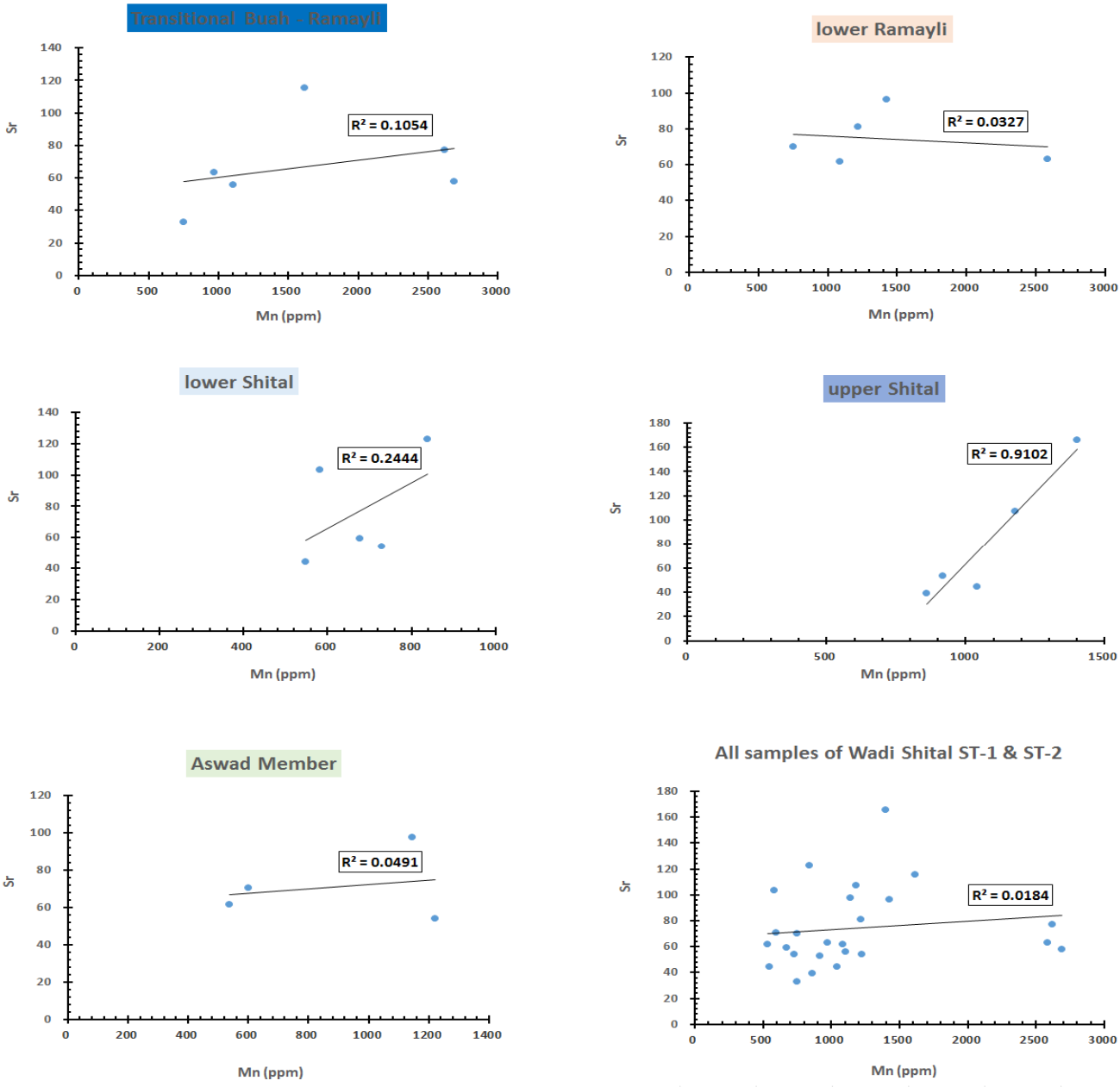

Figure 4-4: *Mn/Sr plots for outcrops belonging to the section of Wadi Shital ST-1 and ST-2 (composite stratotype section of the Sirab Formation).*

Mn and Sr show distinctly different partition coefficients in calcite. Mn is preferred over Sr as a replacement for Ca in the calcite lattice during dissolution/recrystallization events (Tucker, 1986). This leads to the incorporation of Mn into the carbonates and the expulsion of Sr during diagenesis. The Mn/Sr ratio can therefore serve as an indicator for screening samples (e.g. Kaufman, 1995, Veizer, 1983b). Additionally, Marshall (1992) showed that the correlation with isotope ratios suggests that diagenetic recrystallization of carbonates results in a predictable exchange of Trace Elements in an open system.

The result of the Mn/Sr plot excursions for Wadi Shital ST-1 and ST-2 in Figures 4-4 is inconclusive in terms of actual diagenesis. These results are similar to published data on other Precambrian carbonates (e.g. Veizer, 1992). Progressive diagenesis would therefore favor the increase in Mn to the detriment of Sr. However, the shape of the excursions in figure 4-4 (f), which reproduces the outcrop levels analyzed, suggests an early onset of post-burial diagenesis. But the amplitude and the degree of compaction of this burial remain enigmatic at this stage of the study.

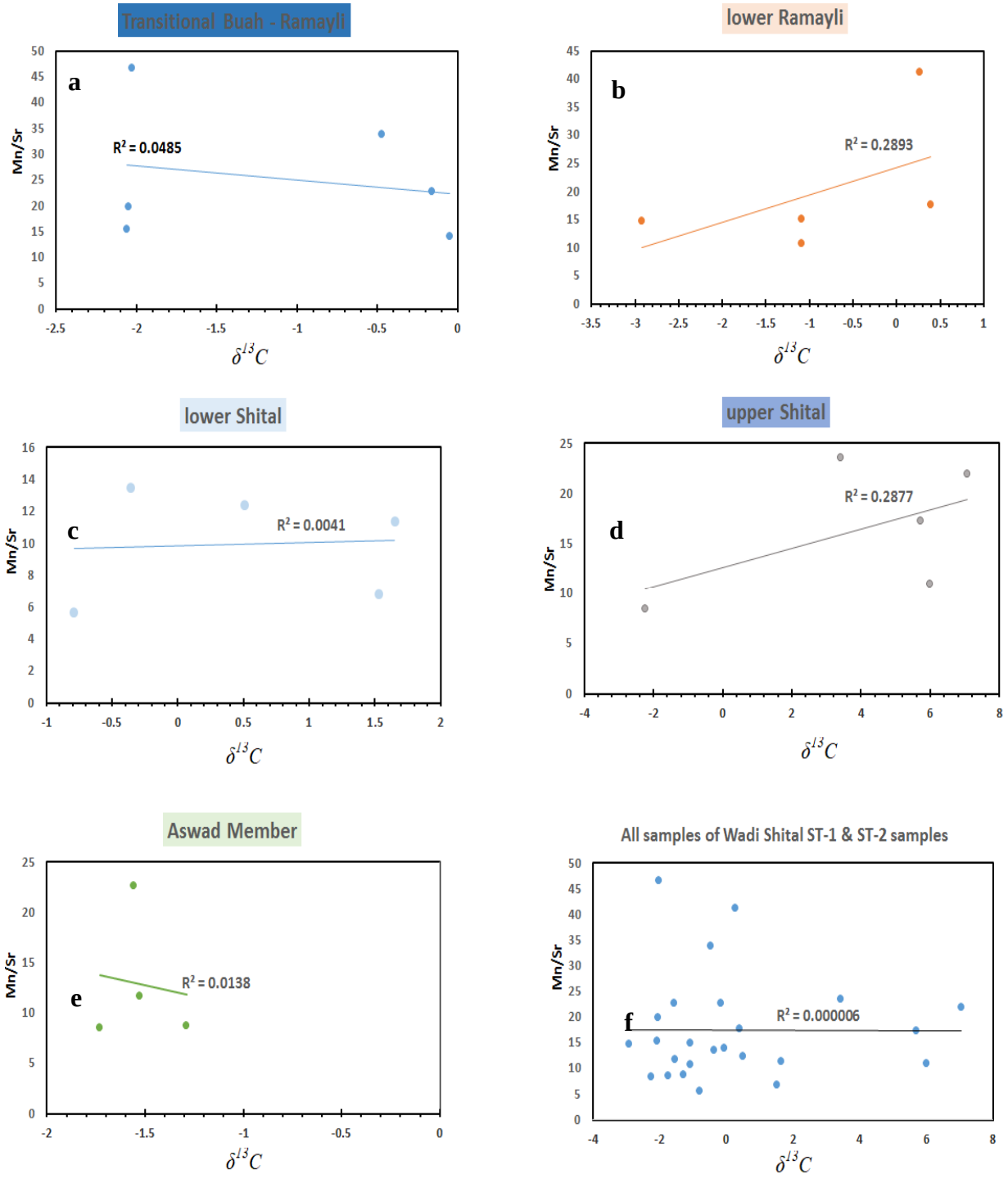

Figure 4-5: *Graphs of Mn/Sr ratios as a function of $\delta^{13}C$ for outcrops belonging to the section of Wadi Shital ST-1 and ST-2 (composite stratotype section of the Sirab Formation).*

The Mn/Sr correlation values with respect to $\delta^{13}C$ demonstrate that there is no diagenetic relationship of Mn enrichment in the Wadi Shital section ST-1 & ST-2. The correlation values being all (R^2 <0.3), are sufficient to imagine that in the event of a generalized burial, the Mn/Sr corrections against $\delta^{13}C$ should have been higher than the current values in Figures 4-5. However, certain values (R2) to one decimal place obtained in figures 4-5 (b) and 4-5 (d) respectively for the lower Ramayli and upper Shital samples, claim a diagenetic implication which is not general (early diagenesis). This early diagenesis is likely at this stage of the study to be discreetly disseminated in certain levels of the Sirab Formation stratigraphy. But with regard to figure 4-5 (f), no strong argument can unequivocally prove the existence of a systematic diagenesis on the whole of the composite stratotype section of Sirab (type section of Sirab).

4.3.4 Mn/δ^{13}C and Fe/δ^{13}C ratios.

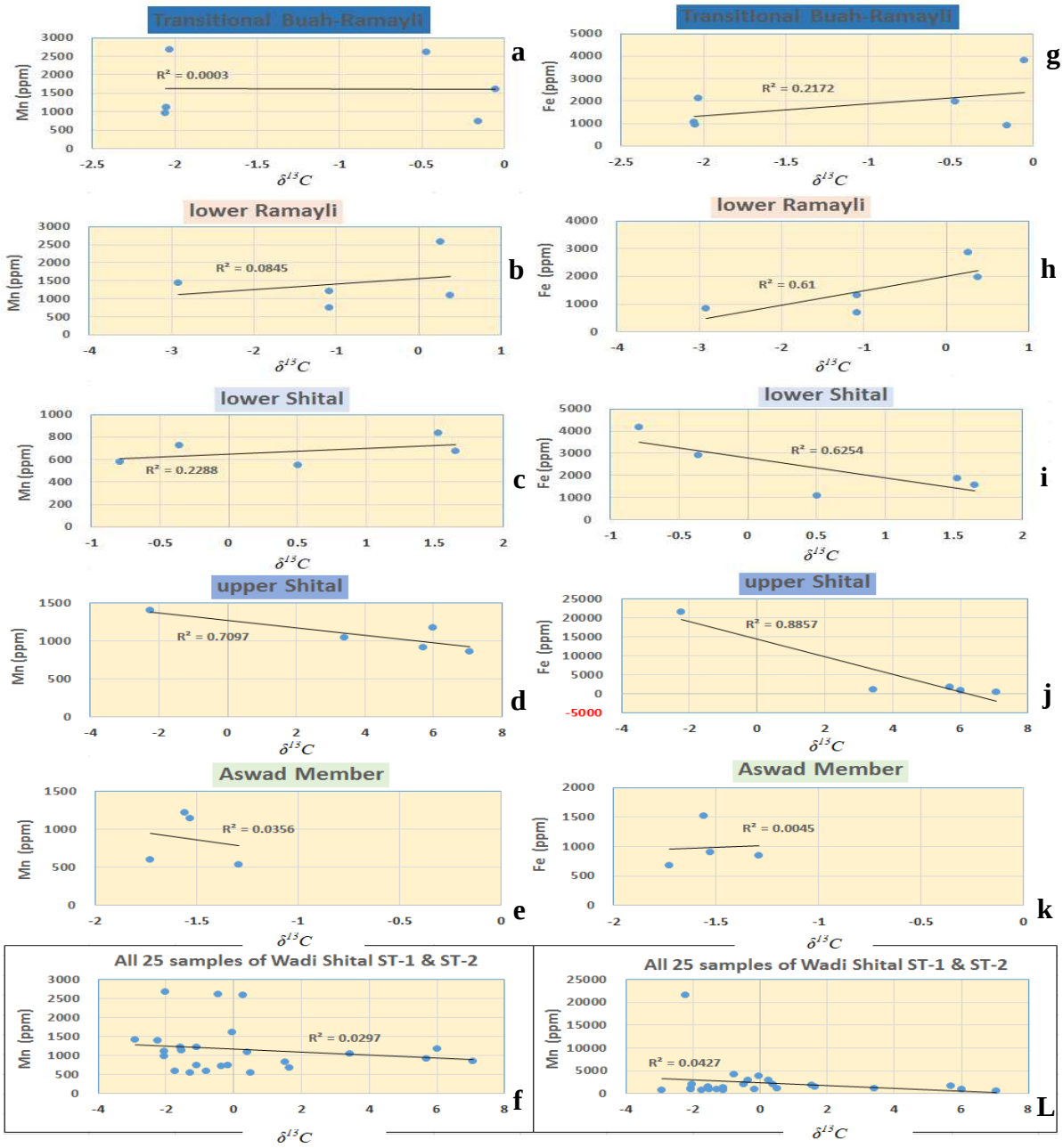

Figure 4-6: *Cross-plots of Mn and Fe concentrations versus $\delta^{13}C$.*

Mn and Fe are preferably incorporated into the calcite network under reducing conditions. Such conditions rarely occur in a Phanerozoic deposition environment, but are common in a diagenetic environment (Brasier, 1992.). As such, the correlation of either of these elements with $\delta^{13}C$ or $\delta^{18}O$ should indicate an alteration of the isotopic signal by diagenesis. When such a correlation occurs, it can be used to extrapolate to the primary marine value (Marshall, 1992). Where there is a high enrichment in Fe, this could be related to the accumulation of siliciclastic detritus carried by the wind on the mudflats, but some could also be related to the enrichment by microbial processes in the thin interval of the facies of mudflats.

Overall, the correlations between Mn and Fe against $\delta^{13}C$ indicate that there was no diagenetic effect linked to a general burying phenomenon of the sediment. Regardless of the stratigraphic order of the sedimentary units from bottom to top, some outcrop horizons, such as upper Shital, show a positive correlation (R^2) for Mn enrichment (figure 4-6 d). Iron is positively correlated (R^2) with $\delta^{13}C$ in the lower Ramayli, the lower Shital as well as the upper Shital (figures 4-6: h, i and j). In contrast to the horizons positively correlated for Mn and Fe with respect to $\delta^{13}C$, figure 4-6 (f) as well as figure 4-6 (L) prove that there is no stratigraphic correlation link ($R^2 < 0.05$) for the enrichment in Mn and Fe compared to $\delta^{13}C$, in the whole Formation. As such, the diagenesis in this composite stratotype section of Sirab would not have been generalized. It seems to be limited to the early sediment burial effect that occurs after deposition and would probably not

involve a large mass burial of the overlying sediments which would cause the rocks to compact in the basin. This would also indicate possible times of interruption of the sediment burial depending on the supply of the Basin.

4.3.5 $\delta^{18}O$ / $\delta^{13}C$ ratios.

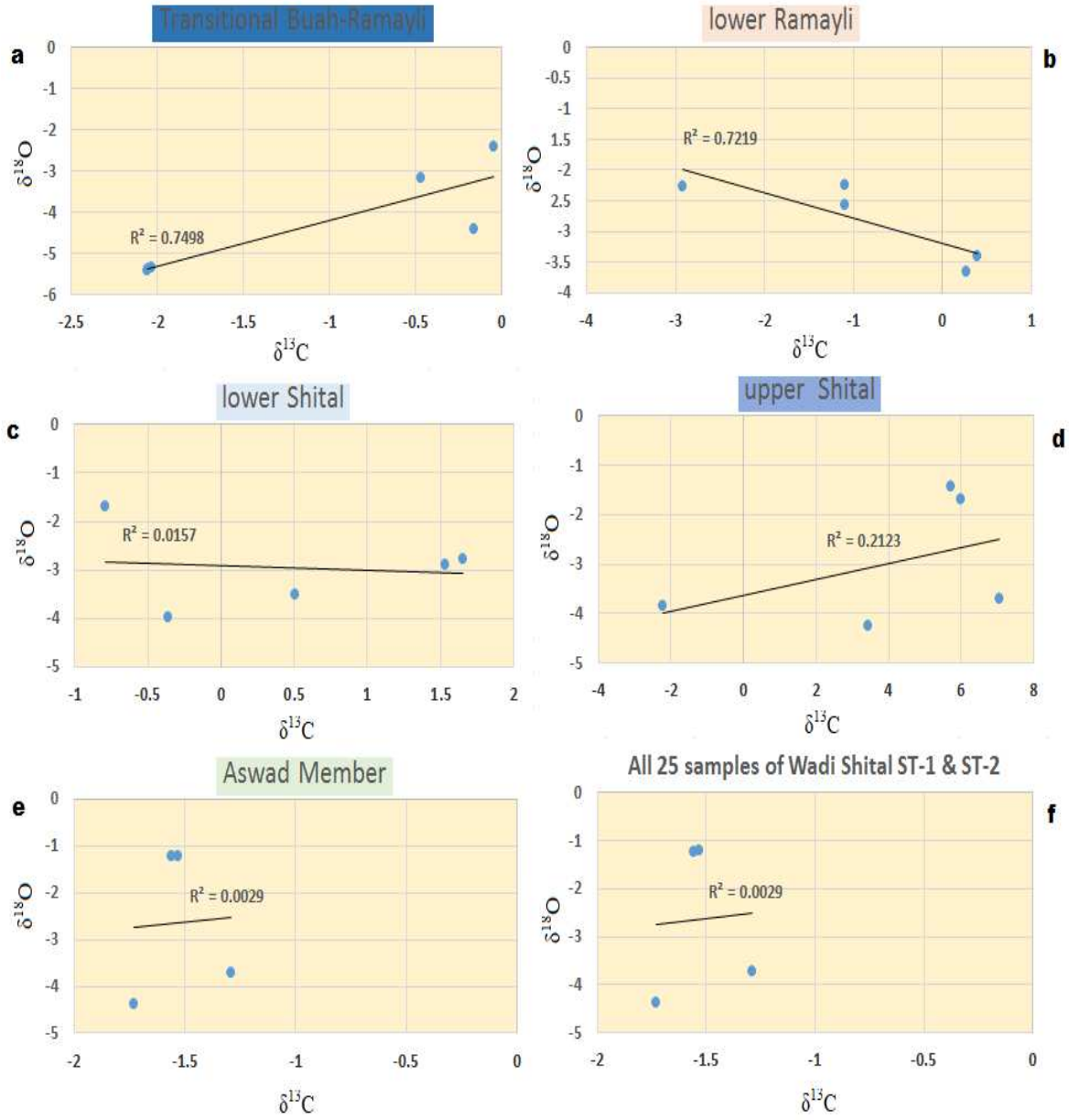

Figure 4-7: *Correlation of carbon and oxygen for the section of Wadi Shital ST-1 and ST-2 (composite stratotype section of the Sirab Formation).*

When the plots of $\delta^{13}C$ and $\delta^{18}O$ produce a straight line with a positive slope, a covariation is said to occur. The covariation of $\delta^{13}C$ and $\delta^{18}O$ may suggest a diagenetic alteration of carbon and oxygen isotope (Kaufman and al., 1995). In such a case, only the samples with the richest $\delta^{18}O$ values are considered as potentially no weathered (Fairchild and al., 1990). The correlation values (R^2) of $\delta^{13}C$ and $\delta^{18}O$ of the outcrops of Wadi Shital ST-1 & ST-2 (composite stratotype section of Sirab) are presented in figures 4-7 for each Member and unit of distinct outcrops while, figure 4-7 (f) summarizes the correlation R^2 for the whole section.

It appears in figure 4-7 (a) as well as 4-7 (b), that in the Buah-Ramayli transition zone and in the lower Ramayli, the $\delta^{18}O/\delta^{13}C$ isotopic signals are altered. Their correlation ratios ($R^2 > 0.70$) are favorable to the effect of diagenesis. But here again, figure 4-7 (f) shows that in the whole of the section, there is no logical correlation link (R^2) between the different levels of the outcrop stratigraphy so as to conclude of a general alteration of the $\delta^{13}C$ and $\delta^{18}O$ isotopes which may lead to an open system of diagenesis in the sediments for the section of Wadi Shital ST-1 & ST-2.

4.4 Diagenesis in sections of Wadi Shuram and Wadi Aswad.

4.4.1 Wadi Shuram WS9 (Depotcenter of Conophyton Reefs).

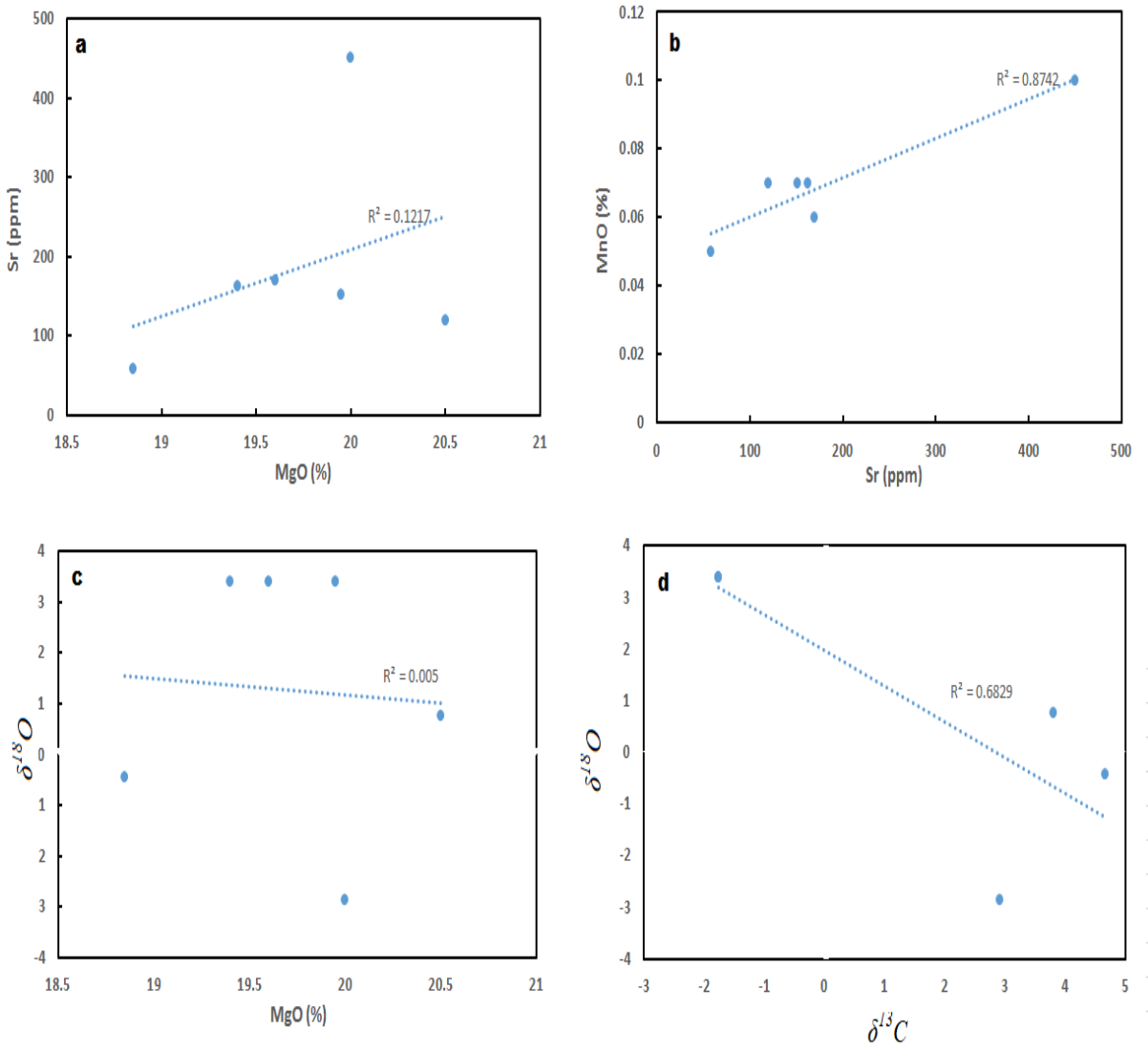

Figure 4-8: *Sr/Mg diagrams; Mn/Sr; $\delta^{18}O$/MgO as well as $\delta^{18}O$ /$\delta^{13}C$ to analyze sediment diagenesis in the Wadi Shuram (WS9) section for the upper Shital outcrops (the depotcenter showing facies of Conophyton Reefs).*

The MgO (%)/CaO (%) ratios presented in chapter 3 mainly concluded that dolomite is the dominant mineralogical form of mixed carbonates in the Sirab Formation. Thus, heavily dolomitized coarse-grained sediments (grainstone or packstone) have been designated dolostones, and the samples of the Buah-Ramayli transition zone are an example of such rocks. For fine-grained sediments in which micrite is more abundant than sparite, the latter were qualified as dolomicrite such as the finely stratified sediment beds from the β facies to the lower Shital (figure 1-11) or the red dolospar at the middle part of Shital (figure 2-1, sample STF 185 of Wadi Shital section ST-1 & ST-2) or again the sediments of the Aswad Member (Thrombolite-Oncolite). Diagenetic analysis in the type section of Sirab was inconclusive in supporting that surficial fluids exerted a positive diagenetic influence on sediment pores to enrich Mn at the expense of Sr. figure 4-8 (a) shows that for the enrichment in Mg which can occur by diagenetic pathway, there is no possible correlation with Sr.

In contrast to the non-diagenetic Mg, figure 4-8 (b) shows that the percentage of Mn in the upper Shital for the depotcenter part (deeper water) for the facies of Conophyton Reefs in the section Wadi Shuram (WS9) has a positive correlation with Sr ($R^2 = 0.8742$). Figure 3-43 in Chapter 3 assumes that due to the majority Y/Ho ratios, the deposition of carbonates of the Sirab Formation can be placed in the mixing zone above the marine burial zone. However, in the sedimentological field analysis, the deeper water in the lithostratigraphy Formation occurs within section of Wadi Shuram (WS9), see figure 1-5. Consequently,

it seems that the positive correlation of Mn with Sr as a link of diagenetic enrichment of Mn to the detriment of Sr will be justified in this section by the depth of the water which should have exerted a certain influence on the pores of sediment drowned in the water slice to enrich the Mn. This hypothesis can be justified by the effect that in the type section of Sirab at Wadi Shital ST-1 & ST-2, the effect of diagenesis is considered as an early diagenesis post-deposition phenomenon and not a generalized diagenesis. If this is the case, then the moment of early diagenesis could have been multiple depending on each moment of deposition and in function of field section where it occurred. However, the Shital Member is deeper in the section of Wadi Shuram (WS9) and this seems to be the cause of the apparent diagenesis.

Figure 4-8 (c) does not record a correlation between the isotopic signal $\delta^{18}O$ and MgO (%). The true origin of the Mn enrichment continues to elude any diagenetic link at first sight and this will be analysed in the following chapter 5. The figure 4-8 (d) shows that the isotopic signals of $\delta^{18}O$ and $\delta^{13}C$ tend to be positively correlated (R^2 = 0.6869). The $\delta^{18}O$ values for carbonates precipitated in seawater should be primarily controlled by mineral species ($\delta^{13}C$), seawater temperature and salinity as well as pH (Jasmine, 2007; Zhum, 2004; Zhum, 2006; Zhang, 1997). As a result, the $\delta^{18}O$ and $\delta^{13}C$ ratios are correlable probably due to the palaeo-redox conditions of the deposition environment at the Wadi Shuram section (WS9).

4.4.2 Wadi Aswad.

4.4.2.1 Wadi Aswad (WA1).

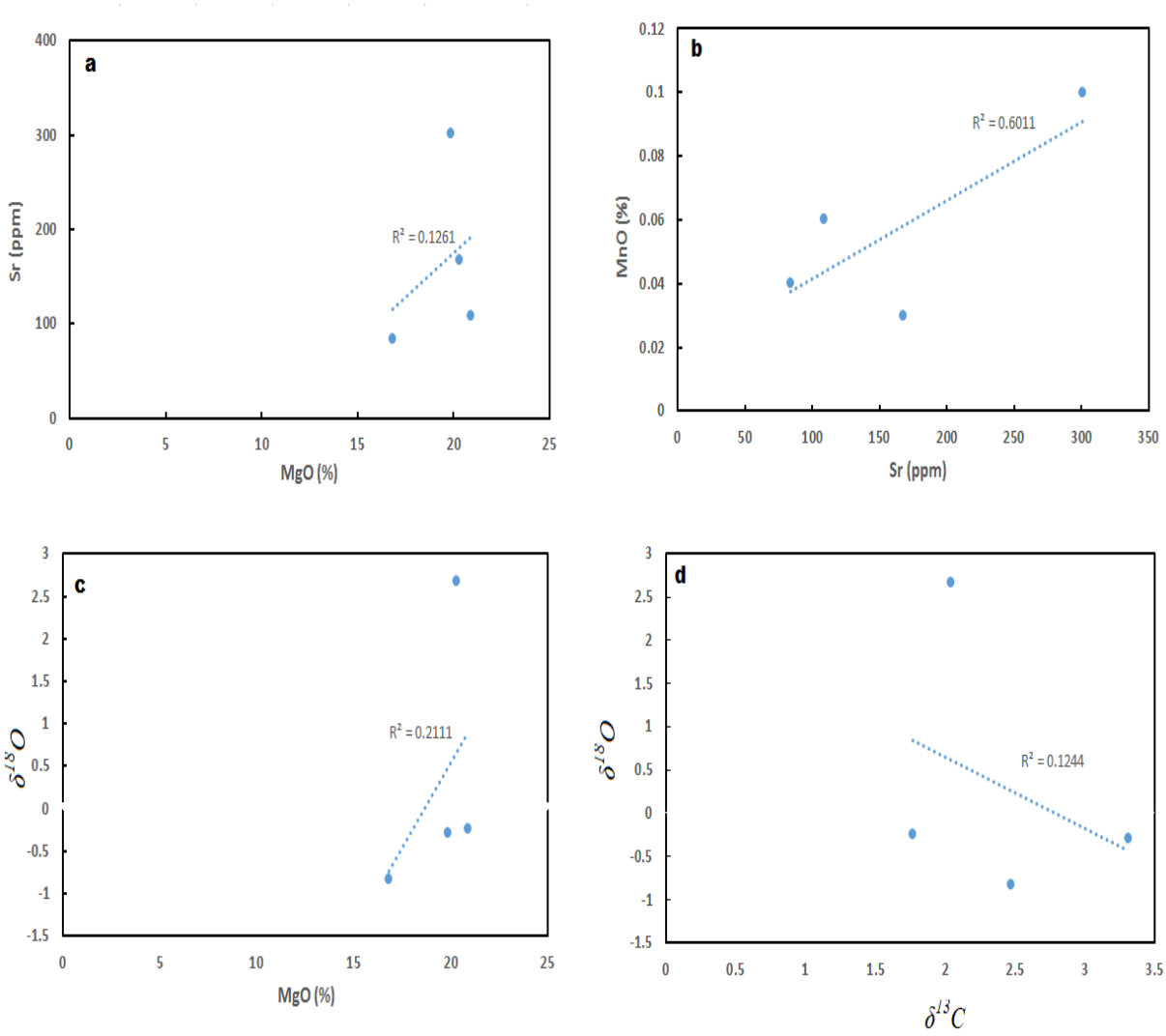

Figure 4-9: *Sr/Mg, Mn/Sr, $\delta^{18}O$/MgO as well as $\delta^{18}O/\delta^{13}C$ diagrams to analyze the diagenesis in the sediments of the Wadi Aswad section for the outcrops belonging to Wadi Aswad (WA1).*

Figure 4-9 (a, c and d) do not have possible correlations. Indeed, the enrichment in Mg in the figure (a) does not depend on the detriment nor conversely on the enrichment of the Sr. Isotopes $\delta^{18}O$ in the figure (c) do not also determine the accumulation of the Mg in percentage in the sediment. And the last list of these no correlable ratios for figures 4-9 is $\delta^{18}O$ / $\delta^{13}C$.

The only correlable ratio here for the outcrops belonging to the stratotype section of Wadi Aswad (WA1) is the ratio of Mn to Sr. Like the section of Wadi Shital ST-1 & ST-2 as well as Wadi Shuram WS9, it seems obvious that the Mn enriched at the expense of Sr would not be the effect of a deep diagenesis of the entire Sirab Formation. However, it is likely that early and localized moments of diagenesis across different levels of the Formation lithostratigraphy may have contributed on the one hand to the Mn accumulation. But, the Mg present in the dolomite seems rather to be of primary origin and very little diagenetic.

4.4.2.2 Wadi Aswad (WA2).

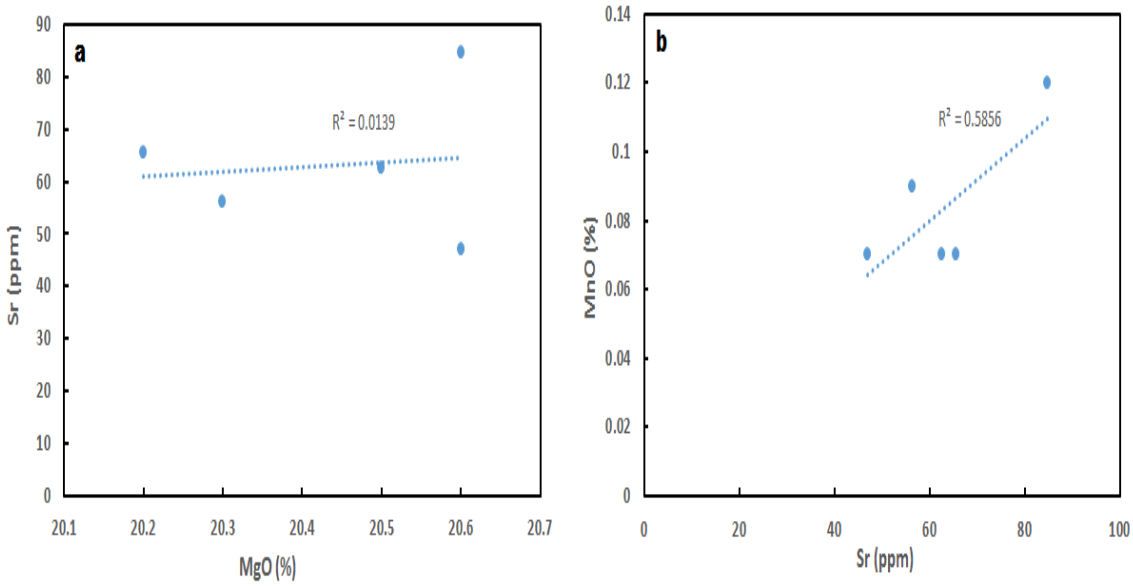

Figure 4-10: *Sr Sr/Mg and Mn/Sr diagrams to analyze sediment diagenesis in Wadi Aswad for outcrops belonging to Wadi Aswad section (WA2).*

Figure 4-10 (a) asserts once again that Mg enrichment within the carbonate does not correlate with Sr while diagenesis so far assumed to be early (post-deposition) is recognized with for (R^2 = 0.5856) in figure 4-10 (b).

So far, the only demonstrable evidence of diagenesis appears to be recorded randomly across the stratigraphy of the Sirab Formation, but no general indication of overall diagenesis has been conclusive. Although Mn has benefited to varying degrees from an early (+/-) burial effect encouraging to its enrichment in certain horizons of the

lithostratigraphy, it follows that the enrichment in Mg in the carbonate is not digenetic. Because, nowhere here and according to diagenetic analyzes, there is evidence of general diagenesis route for the entire Formation. On the other hand, some horizons within the stratigraphy would have been. The table 4-2 below shows that for the MgO (%) obtained by ICP-MS/OES, their MnO (%) counterparts are far lower. Such a large difference in concentration in (%) between Mg and Mn is allegedly not due to the same phenomenon of diagenetic enrichment of Mg and Mn in the sediments during burial. Probably the Mg content would always have been higher in the palaeo-environmental context of the Sirab Formation whereas the early diagenesis effects that are generated as a result of the series of sediment depositions in the basin, led to some non-generalized enrichments of Mn through certain horizons of the stratigraphy.

	SAMPLE	MgO (%)	MnO (%)
Wadi Shuram (WS9)	WS9-144	19.95	0.07
	WS9-151.5	20.5	0.07
	WS9-157.5	20	0.1
	WS9-171	19.4	0.07
	WS9-177.3	19.6	0.06
	WS9-190	18.85	0.05
Wadi Aswad (WA1)	WA1-82.5	16.8	0.04
	WA1-84.5	20.3	0.03
	WA1-85.5	20.9	0.06
	WA1-87	19.85	0.1
Wadi Aswad (WA1)	WA2-0.5	20.5	0.07
	WA2-4	20.2	0.07
	WA2-9	20.6	0.07
	WA2-15.5	20.3	0.09
	WA2-21.75	20.6	0.12

Table 4-2: *The MgO (%) and MnO (%) values obtained from the ICP-MS/OES analysis for the samples from the sections of Wadi Shuram (WS9) as well as Wadi Aswad (WA1 & WA2) of the Formation of Sirab.*

4.5 Summary of chapter four.

Finding compelling evidence for active and generalized diagenesis throughout the Sirab Formation remains a difficult task. However, with the exception of hard evidence (Mn/Sr, Mn/Sr versus $\delta^{13}C$, $\delta^{18}O/\delta^{13}C$, $Mn/\delta^{13}C$ ratios) which do not have significant correlations of diagenesis by burial of sediments for all of The Sirab Formation, the same reports nevertheless allow us to show the existence of some moments of early diagenesis which occur in certain levels or Members of the lithostratigraphy.

The stratotype section of the Sirab is sufficient to detail the entire Formation since it contains all the Members of the Sirab with the exception of the variation of the lateral level at the base of the Formation which is found in the so-called the shoal depression of ancient palaeo-topographic relief as in Wadi Shuram and Wadi Saluttiyat (Nicholas and Gold, 2012). In these areas with high paleotopographic background, the base of the Formation (Ramayli Member) unconformably overlies the Buah Formation or the Shuram Formation and this irregularity of the Sirab lithostratigraphy through the Al-Huqf Supergroup in the localities of Wadi Shuram and Wadi Saluttiyat, led to the appointment of a fourth (4) Member to Sirab known as Salutiyyat (Gold, 2010). Strictly speaking, the distinction of being the Salutiyyat and Ramayli Member at the base of the Formation is structural and not from a sedimentary facies or petrographic point of view. Thus, the Salutiyyat is in a way the lateral

equivalent of the Ramayli Member found in the Buah -Ramayli transition zone through the type section of Sirab (Wadi Shital ST-1 & ST-2).

Lawrence (2006) find that seawater generally contains Y/Ho ratios greater than 45 and relatively lower concentrations of LREEs compared to their HREEs counterparts which are more concentrated in the same sediment and in the marine environment . In addition, the burial of sediment under the marine zone (infratidal and tidal) implies that the hydrothermal fluids including seawater exert a certain influence at the surface of the sediment on the water-sediment interface so that the pores of sediments show positive Eu* anomalies during burial.

In total, twenty five (25) samples were analyzed for the Wadi Shital ST-1 & ST-2 section, six (6) samples for the Wadi Shuram section (WS9) also qualified as a depotcenter in which we find the facies of Conophyton Reefs, four (4) samples for the stratotype section of the Aswad Member at (WA1) and finally five (5) samples for the section of Wadi Aswad at (WA2). The possible Y/Ho results for the presence of marine water correspond to only two (2) samples out of a total of forty (40) samples. The two (2) samples (Y/Ho = 45 for WA2-0.5 and Y/Ho = 50 for WA2-4) are all in the second part of the stratotype section of the Aswad Member at Wadi Aswad (WA2). Thus, the vast

majority of the Formation therefore presents a Y/Ho ratio that is unfavorable to the presence of marine water.

However, in dolostones and dolomicrite of the Sirab Formation, the accumulation of Mg in carbonate does not appear to be directly related to the effect of diagenesis. In apparent contrast, certain levels of the Formation stratigraphy are favorable to the effect of early diagenesis (figure 4-10b, figure 4-9b, figures 4-8 b and d, figure 4-7, figure 4-6, etc.,), see full diagenetic analysis of this chapter. Seen from this angle, the Eu/Eu* and Ce/Ce* anomaly inherited from the REEs Geochemical heritage can help determine the role of hydrothermal fluids during early diagenesis.

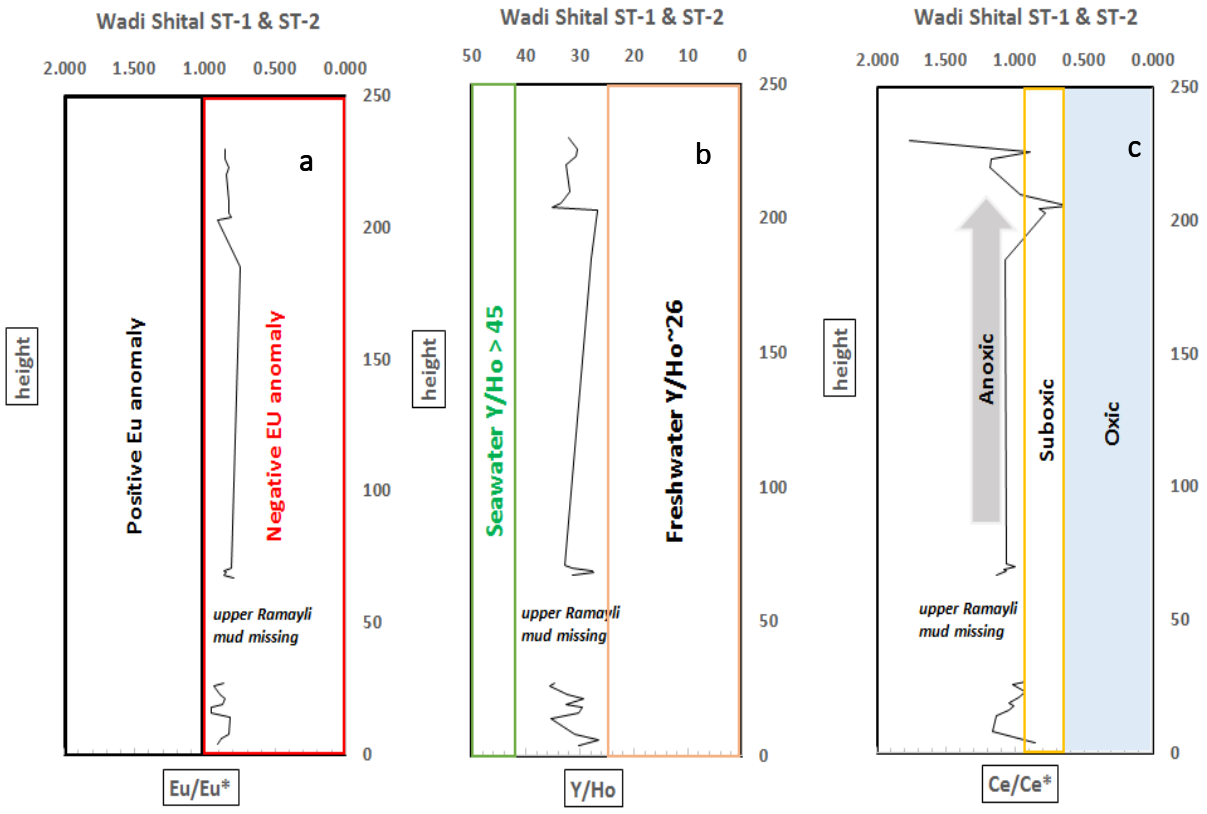

Figure 4-11: *Eu/Eu*, Y/Ho, Ce/Ce* diagrams plotted against the stratigraphic height for the different outcrop levels of the Sirab type section (Wadi Shital ST-1 and ST-2).*

Eu/Eu* and Ce/Ce* anomalies in ancient and modern seawater have been documented by numerous authors (e.g. McLennan, 1989; Tostevin, 2016). For zero intensity, the Ce/Ce* ratio is equal to (1) and as the scale of the anomaly is reduced, the new values of the Ce/Ce* ratio correspond to increasing intensity of the anomaly. Further, it has been suggested that a pronounced negative Ce* anomaly can be divided into three: (a) less than <0.5; (b) ~ 0.6–0.9 and (c) ~ 0.9–1.0 which represent oxic, suboxic and anoxic marine waters, respectively (Chen et al., 2015). The Y/Ho ~ 26 ratio is

characteristic of freshwater while Y/Ho > 45 indicates the report of seawater.

Figure 4-11 (c) indicates that the samples analysed in the type section of the Sirab Formation exhibit anomalies in the (Ce*) characteristics of anoxic marine waters. But in contrast to the seawater report (Y/Ho values), the majority of samples from the type section of the Sirab Formation at Wadi Shital ST-1 & ST-2 have Y/Ho ratios below of 40. This majority value of Y/Ho stipules almost the absence of a marine signature. Only two (2) samples located in the stratotype section of the Aswad Member in the locality of Wadi Aswad, had Y/Ho values between (45) and (50), respectively for samples WA2-0.5 and WA2-4. These two samples detected out of a total number of (40) samples, statistically represent a low value of the significant presence of seawater. Especially since the two values Y/Ho = 45 and greater than 45, are specifically encountered in section WA2 at Aswad Member while, even the deeper Water level of the facies of Conophyton Reefs at section Wadi Shuram (WS9), does not contain Y/Ho > 45 (figures 3-39). However, anoxic conditions can weaken Ce depletion as a result of redox reactions leading to the oxidation of Ce^{3+} to insoluble Ce^{4+} because dissolved Ce^{3+} is partially recovered from seawater in the anoxic marine system and by elsewhere, the analytical method of the laboratory can lead to a loss of the intrinsic signalling of the anomaly in (Ce*) during the dissolution of the carbonate by the acid. However, if this last would be the case, the geochemical values recorded from Blanks (Quality Control) dissolved by acidification in

the same process as the carbonate samples and, typical of well-defined marine and terrestrial environments, would also have to be altered. This was not the case for the geochemical analysis of this thesis. On the other hand, the absence of significant negative (Ce*) anomalies in many marine types of sediment was considered evidence of anoxic seawater.

Regarding Eu* anomalies, when they are positive and more important, they can be linked to the presence of seawater with a mixture of hydrothermal fluids (Meyer, 2012). Apparent anomalies in Eu* can also result from interference with barium oxides formed during the analysis, and this can be assessed by measuring Ba concentrations (Jarvis, 1989). Figure 4-11(a) indicates that the excursions of Eu/Eu* with respect to sediment depth that occur in the typical section of the Sirab Formation, are negative. Therefore, they are not related to the hydrothermal fluids that occur under circumstances of diagenesis by burial of sediments, would enrich Mn to the detriment of Sr (Land, 1985). In addition, barium has poorly weight in the ICP-MS analysis compared to the Major Elements that appear in the Sirab Formation. This does not allow to consider a significant influence of the laboratory process in respect to barium for having a considerable error of Eu/Eu* values reported.

	STB 4	STB 6	STB 8	STB 14	STB 16	STB 18	STB 19	STB 21	STB 23
Eu/Eu*	**0.911**	**0.886**	**0.830**	**0.822**	**0.958**	**0.958**	**0.875**	**0.853**	**0.892**
Ce/Ce*	**0.855**	**1.009**	**1.165**	**1.131**	**1.043**	**1.005**	**1.046**	**0.970**	**0.927**
Sample	**STB 26**	**STB 27**	**STF 67.5**	**STF 68.4**	**STF 69**	**STF 70**	**STF 71**	**STF 185**	**STF 202.9**
Eu/Eu*	**0.936**	**0.865**	**0.794**	**0.867**	**0.847**	**0.863**	**0.810**	**0.784**	**0.908**
Ce/Ce*	**1.015**	**0.924**	**1.133**	**1.063**	**1.084**	**1.002**	**1.064**	**1.074**	**0.776**
Sample	**STF 204.3**	**STF 205.7**	**STF 210**	**ST2 1.6**	**ST2 2.9**	**ST2 2.15**	**ST2 4.15**		
Eu/Eu*	**0.810**	**0.827**	**0.827**	**0.846**	**0.830**	**0.852**	**0.861**		
Ce/Ce*	**0.824**	**0.614**	**0.958**	**1.179**	**1.169**	**0.888**	**1.767**		

Table 4-3: *Values of Eu/Eu* and Ce/Ce* anomalies analyzed in the type section of Sirab (Wadi-Shital ST-1 & ST-2).*

5 ***Fifth Chapter:*** *Major Elements chemostratigraphy*

5.1 Introduction.

The series of Inorganic Geochemical analyzes by ICP-MS carried out at the Trinity College laboratory as well as by ICP-MS/OES carried out at the ALs laboratory (OMAC Laboratories in Ireland), respectively on 25 samples of the composite stratotype section of Sirab at Wadi Shital ST-1 & ST-2 as well as on 15 samples of upper Shital samples in the section of Wadi Shuram (WS9) and Wadi Aswad (WA1 and WA2), have identified a number of Elements Major Inorganic Geochemicals that feature in the composition of the dolostone and dolomicrite of the Sirab Formation. In the first laboratory process at Trinity College, for the type section of Sirab, Elements such as SiO_2, Na_2O, K_2O and Cr_2O_3 were not measured. The laboratory grid presented in appendix 2 to volume 2 details that: for the section of Wadi Shital ST-1 & ST-2 (typical section of Sirab), the Major Elements which accompany the geochemical composition of the carbonates are Fe, Mn, Al and P; after Ca and Mg which are more abundant by weight and are considered the main geochemical constituents of dolomitic carbonates. The ALs (OMAC) laboratory grid in appendix 3 to volume 2 shows that: for outcrop samples from the Wadi Shuram section (WS9) of the upper Shital level as well as samples from Wadi Aswad (WA1 and WA2) in the stratotype section of Aswad Member, the Major Elements obtained are almost identical to the previous data from the TCD laboratory. Moreover, contrary to the TCD laboratory, the data from the ALs Lab (OMAC) laboratory were calculated as a percentage of the total weight of the Major

Elements and the SiO_2, K_2O, Na_2O not measured at the TCD laboratory were evaluated in percentage at the analysis laboratory of ALs (OMAC). Here, apart from CaO (%) and MgO (%), the weight of SIO_2 (%) is greater compared to the Major Elements previously measured at TCD and, K_2O (%), Na_2O (%) as well as Cr_2O_3 (%) have concentrations similar to P_2O_5 in the sediment, the majority of which do not exceed 0.08 (%). The range of values measured as a percentage for the concentration of SiO_2 in the sediment is around 0.11 to 18 (%). For Fe_2O_3, 0.3 to 0.67 (%). For Al_2O_3, 0.06 to 0.14 (%). For MnO, 0.03 to 0.12 (%).

As such, SiO_2 therefore represents, after carbonate ($CaCO_3$), the most abundant proportion of Major Element in the sediment of the Sirab Formation. However, SiO_2 can be identified in the sediment as quartz or a siliceous (chert) component. Several chert horizons have been recognized in the Sirab Formation. It is possible that the siliceous components belong to a continental origin because the continental slope is rich in silica. Either it comes from primary silica (e.g. opal) by precipitation on the bottom of the marine sediments, as this can be remobilized by tidal movements near the shoreline and finds itself trapped in the sediment of the supratidal zone later. Fe_2O_3 and MnO were mentioned in chapter 4 above for their participation during "diagenesis". And finally, Al_2O_3 is more explicit in the continental environment than in the sea. Phosphate (P_2O_5), which is a major component of plants and the teeth of marine organisms such as fish, is by far the least abundant Major Element compared to Fe, Al and Mn

in the Sirab Formation. Thus, the (P) concentration in the sediment can therefore relate to any environmental context of basin filling in the case of the Sirab Formation. There is little chance with regard to the weight of the (P) analyzed in the TCD laboratory (appendix 2) and of the P_2O_5 (%) analyzed in the ALs laboratory (OMAC) that the (P) has a determining environmental origin on its enrichment within sediment. SiO_2, Fe_2O_3 and Al_2O_3 which are the major constituents after CaO and MgO (dolomitic carbonates) can therefore be exploited as an analysis of the environmental conditions for the Sirab.

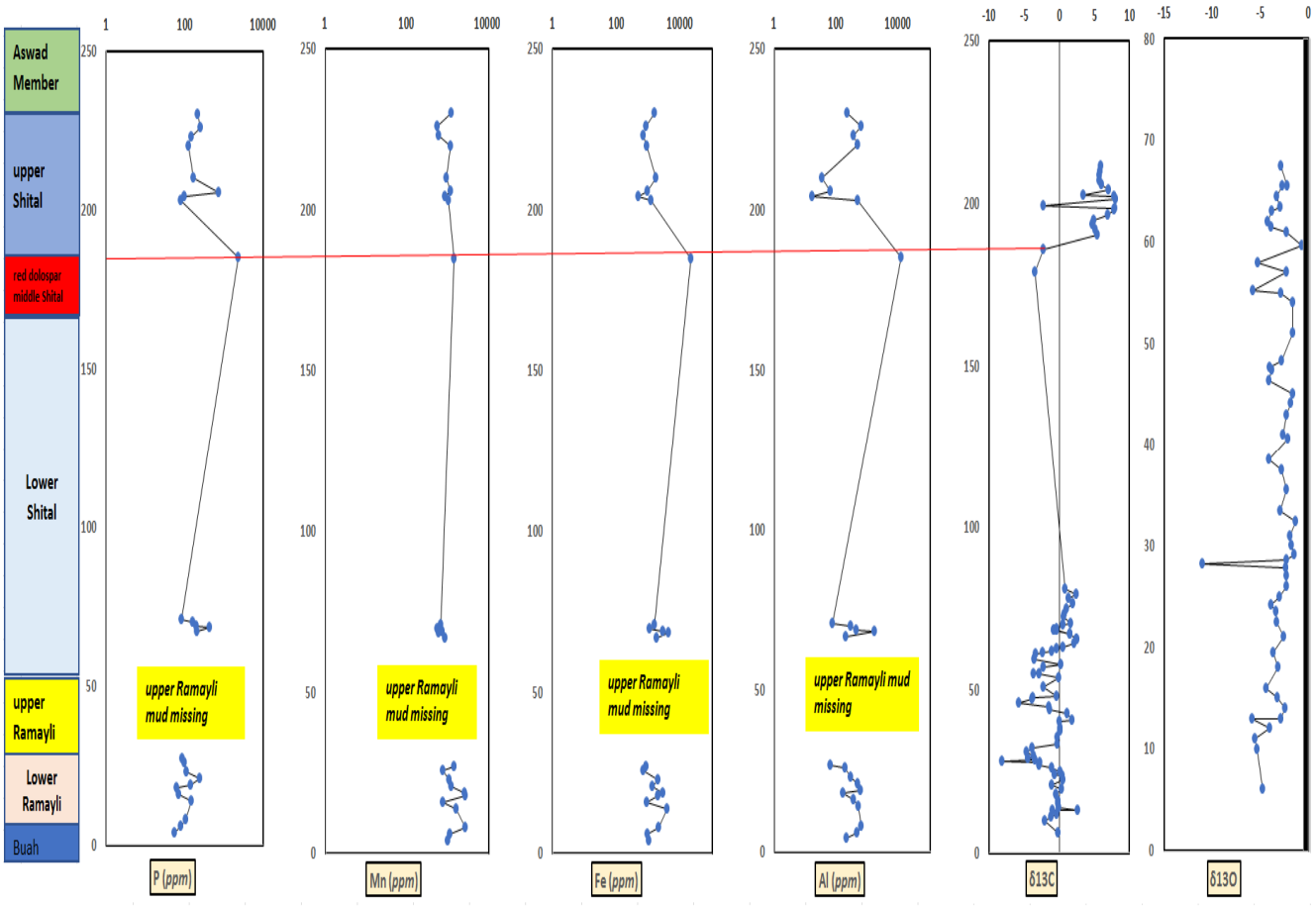

Legend:

$\delta^{13}C$: ——— *Generally speaking, when the Upper Shital passes through the Sirab Formation, the isotopic curve $\delta^{13}C$ marks a postive peak of VPDB (‰) values. For the samples analyzed in the Wadi Shital ST-1 & ST-2 section, the values of $\delta^{13}C$ VPDB (‰) were only matched to the samples in the Wadi Shital ST-1 section. the repercussion of the characteristic positive peak of $\delta^{13}C$ at the passage of the Upper Shital appears to have more affected the curves of the major elements Fe, Al and P. Mn is less affected. the sample of red dolospar (STF 185) before passage through the Upper Shital records in the chemistratigraphy of Major elements a very important shift except for the Mn concentrations. Petrographic, STF 185 is a compacted mud sample (more dolomicrite than dolostone).*

$\delta^{18}O$: ——— *Unlike the carbon istopes ($\delta^{13}C$), the oxygen istopes in the section of Wadi Shital ST-1 & ST-2 all retain negative VPDB (‰) values. As such, the composition of the oxygen isotopes retained their primary signatures, thus showing that, the flow of oxygen through the water-sediment interface during the Ediacarian-Cambrian had not been disturbed by temporal environmental events.*

Figure 5-1: *Graph of Major Elements P, Mn, Fe and Al compared to $\delta^{13}C$ and $\delta^{18}O$, for samples from the type section of Sirab at Wadi Shital ST-1 and ST-2.*

Figure 5-1 shows the evolutionary relationship of the isotopes $\delta^{13}C$ and $\delta^{18}O$ with respect to the enrichments of the Major Elements in the type section of Sirab. The $\delta^{18}O$ isotope values appear to have retained signatures close to the primary when analyzed from the base of the section to the top of the Wadi Shital ST-1 section. The ST-2 addition section of the composite stratotype section of Sirab lacks $\delta^{13}C$ and $\delta^{18}O$ values. However, the general pace of the excursions that occur in the Wadi Shital ST-1 section remains a good indication of the carbon and oxygen isotope profiles for the Sirab Formation.

As mentioned in the previous paragraph, the isotopes of oxygen ($\delta^{18}O$) all have negative VPDB (‰) values for section of Wadi Shital ST-1, negative or very near to negative values for sections Wadi Shuram (WS9), Wadi Aswad (WA1 & WA2); and as such appear to retain isotopic signatures close to their primary values. In particular, the alteration of oxygen isotopes in the typical section of Sirab at Wadi Shital ST-1 does not appear to have existed. This hypothesis leads one to probably imagine that, in Sirab, the water level at the water - sediment interface had been more or less constant (Y/Ho) while the current observations of the evolution of the continental slope (Y/Ho ~ 26) at the oceanic basins of the marine environment (Y/Ho > 45) show that, the depth of the water at the water - sediment interface does not remain constant. The current lake environments and perhaps the mixing zones can present constant levels (Y/Ho) and stagnant waters are also admitted.

The REEs content of carbonates is sensitive like $\delta^{18}O$ to the slightest alteration such as diagenesis so, the analysis of REEs and $\delta^{18}O$ can be a powerful tool to recognize the degree of alteration of carbonates (e.g. Azmy et al., 2011 and Azmy et al., 2012). Therefore, examination of the Major Element production profile against $\delta^{13}C$ and $\delta^{18}O$ values that reflect carbon and oxygen isotope weathering within the stratigraphic column proves to be a powerful screening tool to determine the reasons for enrichments in Geochemical Elements in the stratigraphic column. On the other hand, variations in sea level, in particular those related to temporal events, are generally associated with changes in the concentrations of Trace Elements and Rare Earth in the sediments due to inputs of terrestrial matter and changes in redox conditions (e.g. Wignall and Twitchett, 1996; Murphy et al., 2000; Arnaboldi and Meyers, 2007; Wignall et al., 2007; Piper and Calvert, 2009; liwiński et al., 2010).

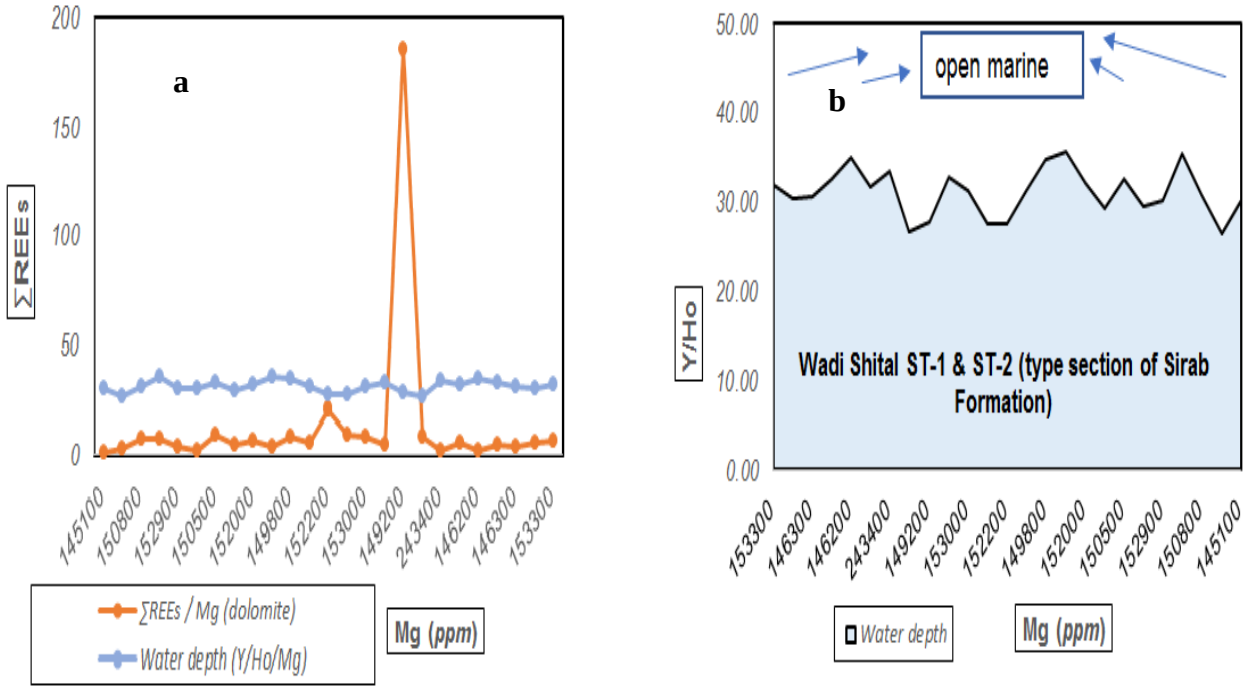

Figure 5-2: *Graph showing the distribution relationship of ∑REEs with respect to the concentration of Mg contents in the sediments as well as the chemostratigraphic relationship of the concentrations of Mg contents in the sediments with respect to the water-sediment interface (Y/Ho). Type section of Sirab in Wadi Shital ST-1 and ST-2.*

REEs distribution curve in the sediments is closely related to that of the concentration of Mg contents (figure 5-2 a) and the Y/Ho curve shows that the REEs and Mg concentration contents in the sediments remain aligned with the water-sediment interface with the exception of the STF 185 outcrop level (figure 5-2 b) whose REEs/Mg ratio is above the Y/Ho line. STF 185 (compacted reddish mud; see petrographic description) may therefore be a deposit of chemotratigraphic composition different from the rest of the outcrops of the section of Wadi Shital ST-1 & ST-2 and this the one sample in

the batch of samples from the analysis of this thesis which diverge (petrographically and chemo-stratigraphically) from the rest of the sediments of the type section of the Sirab. Apart from STF 185 shown in figure 5-2 a, it appears as such that the ∑REEs can therefore constitute a good screening tool to analyse the chemostratigraphic description of the Major Elements in the Sirab Formation.

The Mg contents in the typical section of Sirab at Wadi Shital ST-1 & ST-2 being closely ordered with respect to the ∑REE distributions, they were subsequently measured with respect to the concentrations in the sediments with the remains of the other Major Elements detected by ICP-MS in order to find the logical link that would justify the appearance at the same time in the sediments of concentrations of Mg and other Major Elements.

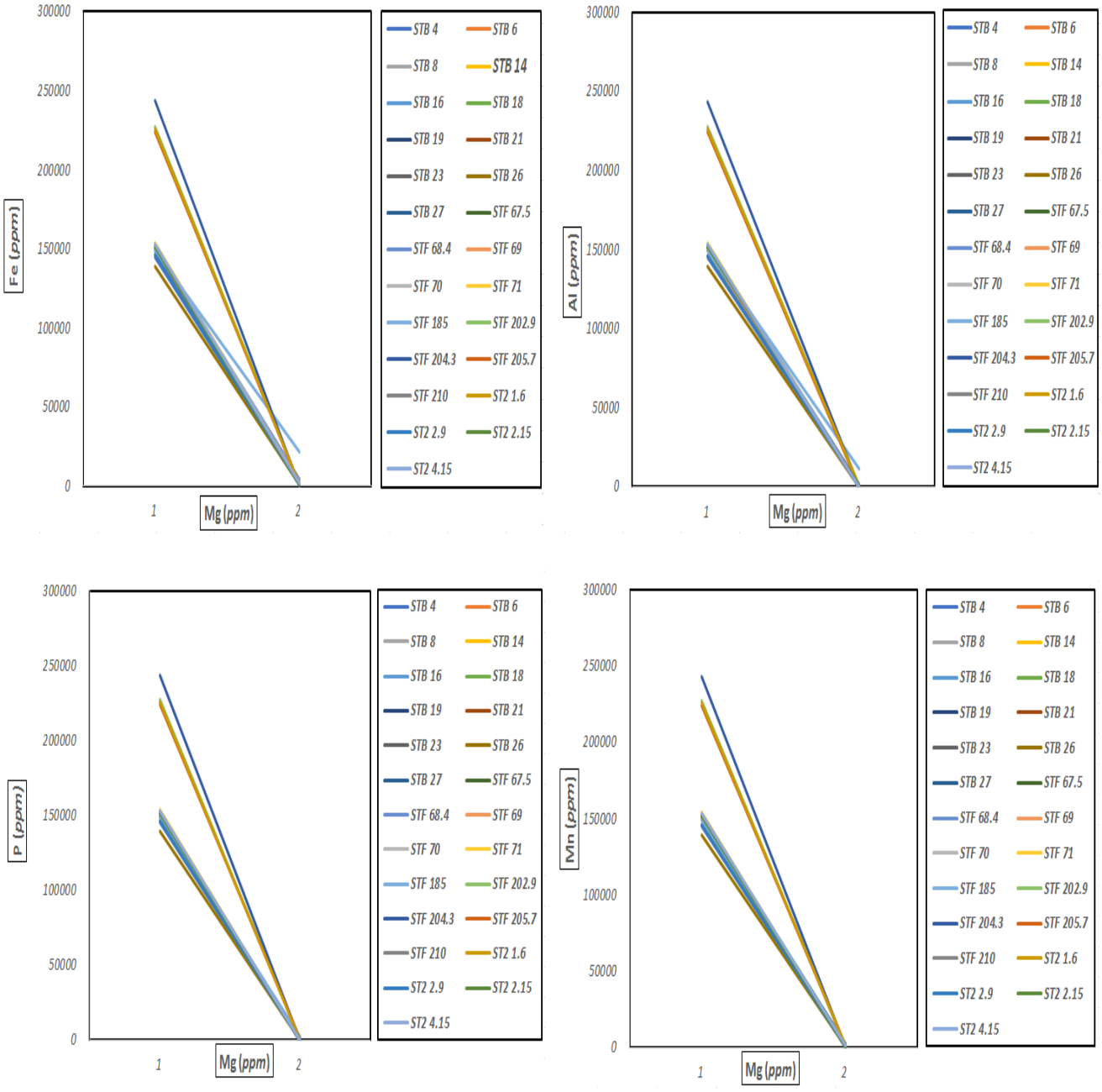

Figure 5-3: *Graph of the concentrations of the Major Elements compared to their homologous concentrations in Mg in the type section of Sirab (Wadi Shital ST-1 and ST-2).*

In section Wadi Shital ST-1 & ST-2, the Mg concentrations follow the distribution of ∑REEs (figure 5-2 a). As such, concentrations of Mg located at different horizons of the stratigraphy on the Sirab Formation displays precise environmental events according to the fractionation of ∑REEs. Seen in this sense, the Major Elements other than Ca and Mg which essentially constitute the mineral framework of dolostones and dolomicrite should also depend on the approximate environmental conditions of the ∑REEs distributions.

The set of graphs in figure 5-3 summarize that, with respect to the Mg concentrations, the Major Elements which are homologous to them at the same levels of the Formation stratigraphy, all have similar concentration profiles in the sediments as those of Mg. Recall that, the ∑REEs fractionation conditions that prevailed during the accumulation of Mg approximately recorded the variations in the content of Major Elements other than Ca and Mg in the same sediments. This therefore makes it possible to translate temporal or permanent environmental events during the filling of the Sirab Formation. As such, the paleoredox condition of the deposition was the same for the recorded REEs contents as those of the Major Element concentrations (Fe, Al, Mn and P) as shown by the bar graphs in the figure 5-3.

However, in figure 5-2 a, an outcrop level (STF 185) appears to exhibit a large offset which may express a brief temporal event differing from the distribution of ∑REEs. Petrographically speaking, the STF 185 level lies on the sandstone horizon (figure 1-13) while the microscopic study of the sediment in chapter 3 defines it as a compacted dolomite mudstone with a red coloration (figure 3-10). In the field, the red mudstones outcrop in the stratigraphy of the composite stratotype section of Sirab above the STF 178 level in the section Wadi Shital ST1 and their occurrences continue intermittently until shortly before the passage to the addition section ST-2.

As such, the STF 185 level with a peak distribution of ∑REEs therefore represents a granulometric change in the texture of the sediment (mudstone) rather than a change in the sediment deposition environment as shown in figures 5-2 a and b.

5.2 Major Elements in section Wadi Shital ST-1 & ST-2.

5.2.1 Contribution of the Eu/Eu* and Ce/Ce* ratios.

Indeed, Rare Earth Elements are a group of 15 lanthanide elements (La, Ce, Pr, Nd, Pm, Sm, Eu, Gd, Tb, Dy, Ho, Er, Tm, Yb, Lu), as well as Sc and Y (Mclennan, 1989 and Walters & Lusty, 2011). Lanthanide Elements are often separated into groups by atomic weight (Mclennan, 1989; Laveuf & Cornu, 2009; Walters & Lusty, 2011). Commonly abbreviated REEs, the composition of lanthanides within the sediment can be split into three large groups: LREEs or light Rare Earth starting from La - Sm; MREEs or medium Rare Earth start from Eu - Dy; as well as HREEs or heavy Rare Earth starting from Ho - Lu, (McCabe, 2020). Due to geochemical similarities, Y is often included in HREEs, while Sc behaves geochemically differently from all other REEs, but similar to elements such as Ni, Cr, V and Co (Mclennan, 1989).

Sc is a compatible element in igneous systems which exhibits dispersed lithophilic behavior and therefore rarely forms minerals in which it is a major component (Mclennan, 1989; McLennan et al., 1993; Salminen et al., 2005). Most of the Sc in the lithosphere is contained in ferromagnesian minerals, particularly pyroxene, and, as these minerals are sensitive to chemical weathering under surface

conditions, Sc is often released in sedimentary rocks where, as Cr and Ni, it is absorbed by clay minerals.

In their review, Laveuf and Cornu (2009) noted that there are essentially two types of minerals that host REEs in great abundance: heavy minerals and phosphates. Heavy minerals, especially zircon, heavy Ti minerals, and garnet tend to contain a higher abundance of HREEs compared to LREEs, while phosphate minerals, such as apatite, monazite and xenotime and silicate minerals such as allanite and titanite contain higher abundances of LREEs compared to HREEs (McCabe, 2020). While many heavy minerals rich in HREEs are considered to be chemically stable and therefore resistant to weathering, such as the marine environment (e.g. see Laveuf & Cornu, 2009), the same is not true of most primary minerals REEs-phosphates (Sawka et al., 1986; Banfield & Eggleton, 1989; Milodowski & Zalasiewicz, 1991; Berger et al., 2008; Berger et al., 2014; Laveuf & Cornu, 2009), which under certain conditions such as climatic, environmental or diagenetic, decompose to form secondary minerals such as florencite, rhabdophane, thorite, monazite, or adsorb squarely on the surface of clay minerals, as is the case in the continental environment.

As such, the tendency of REEs to split into LREEs, MREEs or HREEs can help determine in addition to other geochemical relationships previously exploited in this thesis such as Y/Ho, the level of carbonate

ramp establishment relative to the marine or continental environment. Moreover, the mixing zone in figure 3-43 (chapter 3) would correspond to the exchanges in the LREEs and HREES fractionations, with a more or less beneficial ratio to the LREEs as a function of the Y/Ho ratios obtained on the levels of samples analysed.

Tables 3-1 and 3-2 in chapter 3 of this thesis, tend to correlate the occurrences of minerals detected by XRD as well as macroscopically on land at Wadi Shital ST-1 & ST-2, with types of environments where these minerals appear. So far, looking at tables 3-1 and 3-2, the carbonates of the Sirab Formation along the typical field section harbor a relative abundance of both easily weatherable and difficult to weather primary minerals. However it seems more obvious that SiO_2 and Al_2O_3 are more abundant in the carbonates of Sirab. This facilitates a greater tendency for the fractionation of REEs into LREEs within carbonates. In addition, the frequencies of occurrences of accessory minerals constituting carbonates and fractionation of REEs can be simulated from the tables above in the text of this paragraph.

The Major Elements (Fe, Mn, Al and P) detected by ICP-MS apart from Ca and Mg which are the main mineralogical constituents of dolomites in the section of Wadi Shital ST-1 & ST-2 are naturally linked to the origin of the overall mineralogy of carbonates in relation to the environment of Formation or establishment of the carbonate ramp. (Tucker, 1986) found that Fe and Mn are preferentially enriched

in the sediment during diagenesis and Mn more particularly replaces Sr in the calcite network during sediment burial. However, the analysis of diagenesis in the Sirab Formation presented in chapter 4 limits the effects of diagenesis to post-deposition events (early diagenesis) so that no argument currently seems to assert a generalized and favorable diagenesis for enrichment of Fe and Mn in the entire Sirab Formation. P may not be emblematic of the deposition environment, since in a marine or continental environment, fish teeth or even terrestrial plants trapped in the sediment can transfer their P content into the composition of the sediment in which they figure. On the other hand, Al is more significant of the continental environment because of its clayey potential.

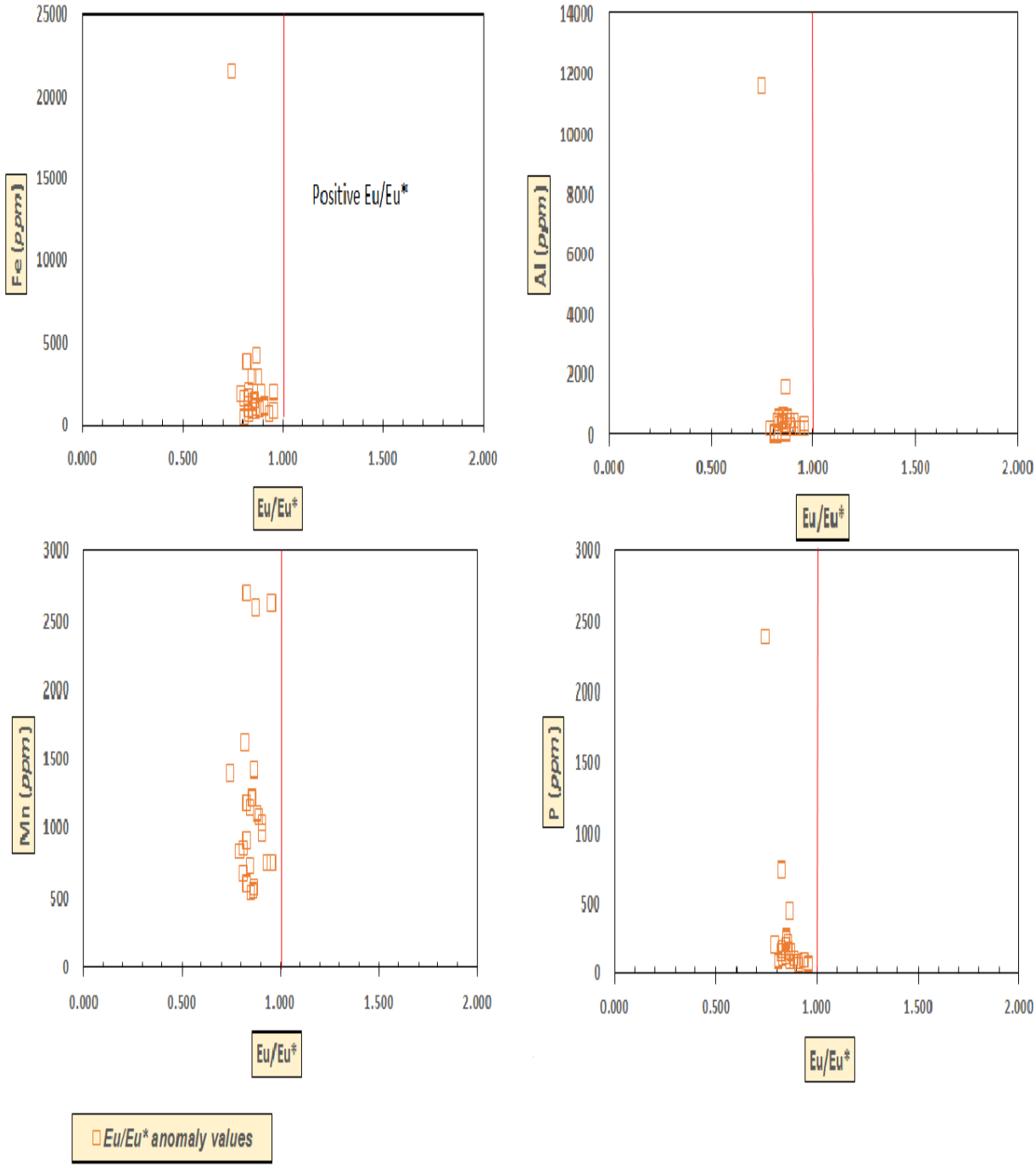

Figure 5-4: *Graphs of major elements (Fe, Al, Mn and P) on Eu/Eu* for the determination of Eu anomalies with respect to major elements in the stratotype composite section of Sirab (Wadi Shital ST-1 and ST-2).*

The graph of figure 5-4 shows that the Major Geochemical Elements found in the mineralogical composition of the carbonates of the type section of Sirab at Wadi Shital ST-1 & ST-2, after the analysis of the samples of outcrops by ICP-MS; all have negative Eu anomalies. (Meyer et al., 2012) considers that larger positive Eu anomalies may be present where seawater is mixed with hydrothermal fluids while (Jarvis et al., 1989) believe that apparent Eu anomalies may result from interference with barium oxides formed during analysis, and this can be assessed by measuring Ba concentration.

Barium oxides are unlikely to have significantly interfered with the laboratory process during ICP-MS analysis, considering the general appearance of Eu* anomalies in figure 4-11 (chapter 4). As such, neither the hydrothermal fluids can be associated with the palaeo-ecological environment where the concentrations of Major Elements Fe, Al, Mn and P were enriched in the type section of Sirab, and even less the interference with the barium during sample handling in the laboratory during geochemical analysis of rock samples can be taken as an argument for apparent Eu* anomaly.

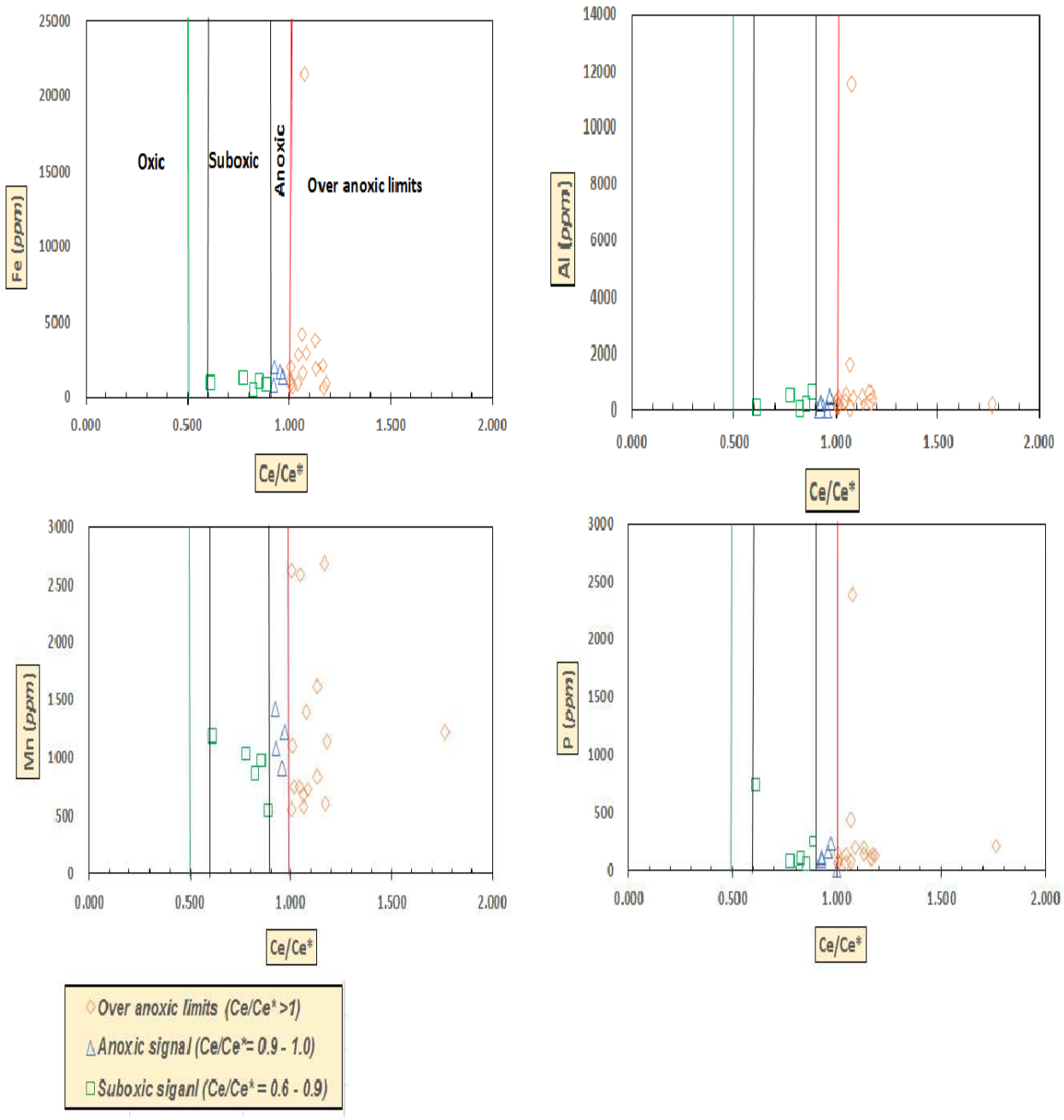

Figure 5-5: *Plots of major elements (Fe, Al, Mn and P) on Ce/Ce* for the determination of anomalies of Ce versus Major Elements in the composite stratotype section of Sirab (Wadi Shital ST-1 & ST-2).*

It seems from figure 5-5 that, the majority of the carbonate samples of the type section of Sirab were deposited in an anoxic environment in apparent contradiction with the diagenetic analysis in the previous chapter 4, which has At first sight, excluded any form of implication of a general diagenesis for the whole of the type section of Sirab as well as, in apparent contradiction with the majority Y/Ho ratios, which fix the paleo-marine level of the carbonate ramp of Wadi Shital ST-1 & ST-2 at the water - sediment interface, necessary to estimate the immersion or not of the ramp under the paleo-marine level of the water, depending on a possible general burial or not of the sediment (figure 5-2b).

When the negative Ce* anomaly (with Ce/Ce* values <1) coincides with a positive Y anomaly report, both (anomalies) become characteristic of the marine environment. This rule Ce negative and Y positive has been observed in several analyses of marine carbonates (e.g. Lawrence et al., 2006). The fractionation of HREEs in marine limestones is particularly at the base of the positive peak of Y which counts among the heavy Rare Earth. While Ce, a light Rare Earth, is not found in abundance in the heavy minerals that are generally found in the marine environment and that resist weathering. (McCab, 2020) finds that minerals such as Zircon, Ti in heavy minerals as well as garnets, have a high potential in HREEs against low fractionations in LREEs and resist the effects of weathering while, minerals phosphatic such as apatite, monazite and Xenotime with silicate minerals such as allanite and titanite, contain LREEs more abundantly relative to

HREEs. In the typical section of Sirab, Al (aluminosilicate or silicate minerals) and P (phosphate minerals) are listed as Major Elements detected by ICP-MS. Quartz is another silicate found in abundance in the sedimentology of the Sirab Formation through the Wadi Shital ST-1 & ST-2 (see chapter 1 on sedimentological description). As for Fe and Mn, these two Geochemical Elements are enriched in the sediment during diagenesis while in the section of Wadi Shital ST-1 & ST-2, there is no clear evidence of enrichment in Fe and Mn within sediments by diagenesis.

Figure 5-5 indicates that for the typical section of Sirab, the Ce* anomaly correspond to the negative values of the Ce/Ce* ratio which are found in general at marine environment in contrast to Y/Ho ratios of the majority of samples where these Ce* anomalies were measured. The enrichments in Major Geochemical Elements are distributed between the suboxic and anoxic classes and beyond the limits of the Ce/Ce* error for the anoxic class. As such, since the majority of samples point beyond the limits of the anoxic class, it appears that the Major Elements detected by ICP-MS would have been concentrated in the carbonate sediment ramp, in an environment not submerged by sea water and also not supplied with oxygen. The analysis of the oxygen isotopes $\delta^{18}O$ (figure 5-1) shows that the VPDB (‰) values of the oxygen isotopes generally retain their primary signatures since they are all almost negative or near to negative unlike the carbon isotopes whose VPDB (‰) values were altered with remarkable positive signatures especially in the upper Shital and this is seen over all

sections of the Formation. In fact, signatures close to the primary oxygen isotopes may correlate with the absence of effective diagenesis for the entire Formation and the contrary case may indicate an alteration of the isotopic signal. However, this argument does not at this stage allow us to understand why the majority of samples examined were enriched in Major Elements in anoxic rather than oxic zone? Moreover, the analysis of the reduction of S within the stratigraphic column of Sirab was not undertaken in this thesis and only the Ce/Ce* ratio is used here to signify that the majority of the samples have a high anoxic potential. In the absence of sufficient evidence of widespread submersion of the carbonate sediments ramp below sea level through its type section of Wadi Shital ST-1 & ST-2, oxygen degradation within the stratigraphic column sediment may attempt to be justified under more than one assumption. Either by the rotting of the organic matter on the surface of the sediments which would have by effect of the reduction of the sulphate, stifle the oxygen supply on the ramp, in an anoxic environment which consumes the sulphate, or by the oxygen content of the deposition environment which was insufficient from the start as in general for the case of the Ediacaran - Cambrian limit before that the atmospheric oxygen content begins to climb during the Carboniferous. Other environmental influences unsuspected until now can have also led to anoxic conditions in which the Major Elements were enriched in the sediments?

On the other hand, current observations show that, during the alteration of sediments in a mixed continental environment, Fe gradually replaces Al during the formation of laterite. However, in nature, sedimentary rocks contain a minor proportion of iron and this ore usually has a content of less than 15% of the total weight of the rock in which it is measured. As Fe exists under two degrees of oxidation, Fe^{2+} (the ferrous ion) and Fe^{3+} (the ferric ion), its behaviour is controlled by the geochemistry of the sedimentary and diagenetic environment. The main source of Fe for the ocean basin is currently considered to be the continental weathering of basic rocks and lateritic soils. Under the Eh and pH conditions of most surface waters, Fe is in the Fe^{3+} state, which is largely insoluble. Its concentration in solution is therefore very low, of the order of 1 ppm for river water and of the order of 0.003 ppm for sea water. Three routes of iron transport mechanisms are possible:

- In the form of oxide films on detrital particles;
- In association with organic matter;
- In the form of colloidal suspensions of hydroxides which precipitate by flocculation during the mixing of river and seawater.

Once deposited, Fe can be redissolved in sediments if Eh-pH conditions are required, then reprecipitated as Fe minerals. Figure 5-6 gives the stability conditions of these minerals as a function of Eh, pH, the activity of S = (pS^{2-} = -log [S^{2-}]) and the partial pressure of CO_2. (One of the main factors affecting the Eh of water is the organic matter content: its bacterial decomposition consumes oxygen and deploys reducing conditions). From these diagrams below, it can be seen that hematite is the stable form under moderately to strongly oxidizing conditions, i.e. in a sediment poor in organic matter. For minerals comprising ferrous Fe, the stability fields strongly depend on the PCO_2 and the pS^{2-} within of the solution. In marine sediments, sulfur is available by bacterial reduction of sulphates and pyrite or marcasite is formed; iron carbonates are rare.

$$4\ FeOOH + 4\ SO_4^{=} + 9\ CH_2O \rightarrow 9\ HCO_3^{-} + H^{+} + 6\ H_2O + 4\ FeS.$$

In meteoric environments (fresh water), this is not the case and iron carbonates are more frequent. However, even in the marine environment, if all the sulphur is consumed, sideritis can also form. A good example is the crystallization of siderite in some present-day intertidal marshes. The development of iron silicates (glauconite) is still the subject of hypothesis.

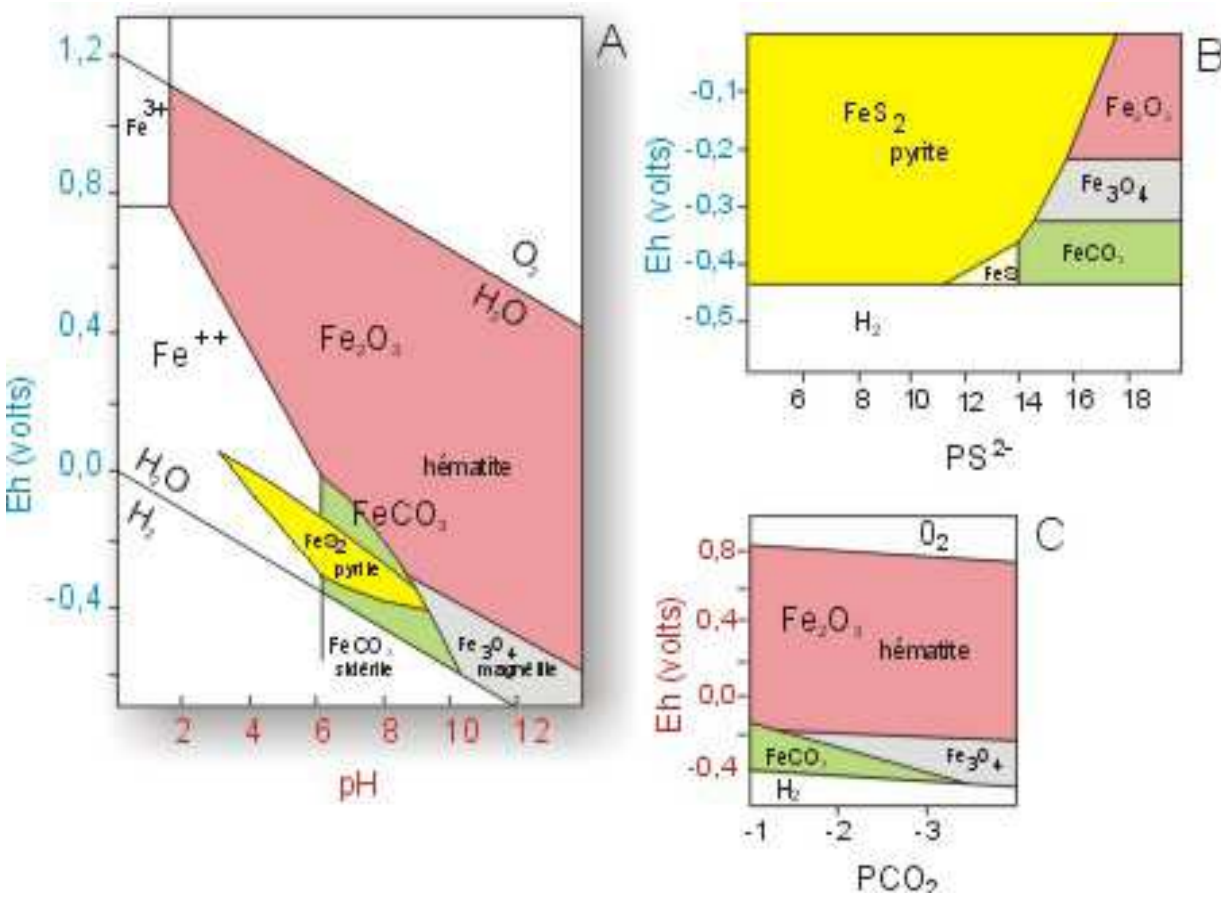

Figure 5-6: *Eh-pH stability diagram of ferric iron, ferrous iron, hematite, siderite, pyrite and magnetite. This diagram shows that hematite is the stable mineral in moderately to strong oxidizing environments. For minerals such as pyrite, siderite and magnetite, which are stable in a reducing medium, the stability fields strongly depend on the pH, but also on the concentrations of CO_3^{2-} and S^{2-}, from Krauskopf (1979), Berner (1971) and Tucker (1991).*

The case illustrated by the diagram is that of a solution rich in CO_3^{2-} and poor in S^{2-}. Otherwise, the stability field of pyrite widens to occupy almost the entire lower part of the diagram. If CO_3^{2-} and S^{2-} are in low concentration, the magnetite field increases. C: The stability fields of iron minerals as a function (B) of Eh and pS^{2-} (-log of the activity of S^{2-}) and as a function of (C) of Eh and PCO_2. The

Examples are from Krauskopf (1979), Berner (1971) and Tucker (1991).

However, the current equilibrium conditions during Fe formation are not the same as those which would have been present during the Cambrian Ediacaran. It could also be that, the substitution of Al by Fe although can be envisaged as lateritic development at the end of the neoproterozoic, could show divergences from figures 5-4 and 5-5.

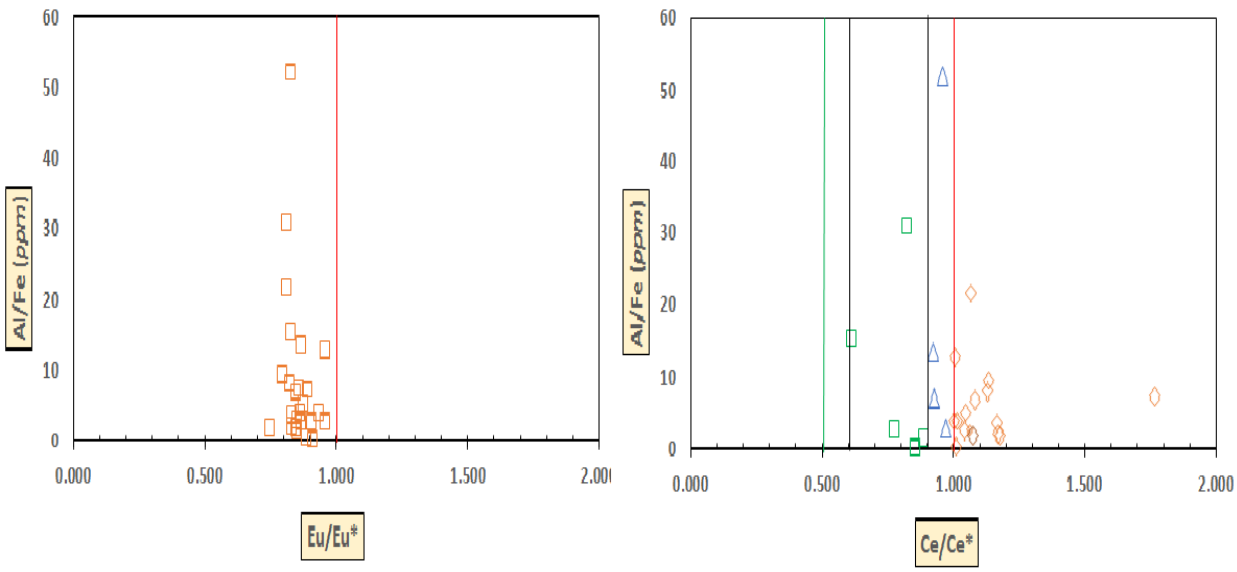

Figure 5-7: *Major Elements graphs (Al/Fe) on Eu/Eu* as well as Ce/Ce* for the determination of Ce anomalies with respect to Major elements in the composite stratotype section of Sirab (Wadi Shital ST-1 and ST-2).*

Figure 5-7 shows that, if the environmental conditions within the Ediacaran - Cambrian time limit would have been favorable to the development of lateritic soils by the surface weathering of rocks, the

Eu* anomaly would not have changed in the type section of the Sirab. And this will be the same for the reports of anomalies in Ce* in the samples of the type section of the Sirab. The Ce/Ce* would always have displayed a greater abundance of substitution of Al by Fe in an anoxic medium, followed by the suboxic environment (respectively Ce/Ce*>1 and 0.9 -1 then 0.6 - 0.9; see the legend in the figure 5-5). As such, the Fe and Al concentrations are intrinsically linked to a close source to each other without this being an environmental change that would enrich for example iron (Fe^{2+}) in a marine environment, to the detriment of iron (Fe^{3+}) and Al in continental environment or diagenetic environment, or again in superficial weathering zones.

5.2.2 Trend of REEs within the composition of carbonates.

Lanthanides (Rare Earth) represent an essential source of chemotratigraphic analysis due to their grouping in LREEs, MREEs and HREEs. During the evolution of the sediment, the REEs signature trapped in the sediment preserves the original heritage of the start environment. Because the fractionation of weathering resistant minerals (HREEs) occurs more in the marine environment due to their weathering preservation conditions within marine environment in general, HREEs are more favorable in relatively marine carbonates than LREEs which are more abundant in weathering zones. A better way to compare the fractionation trend of REEs into HREEs as well as LREEs is to plot in comparison the excursions of the values of carbonate concentrations (Mg/Ca) with respect to the lithostratigraphy (depth), and against the values corresponding to the same samples of HREEs and LREEs. Next, analyze the resemblance of the profiles between the carbonate values and the REEs trend values.

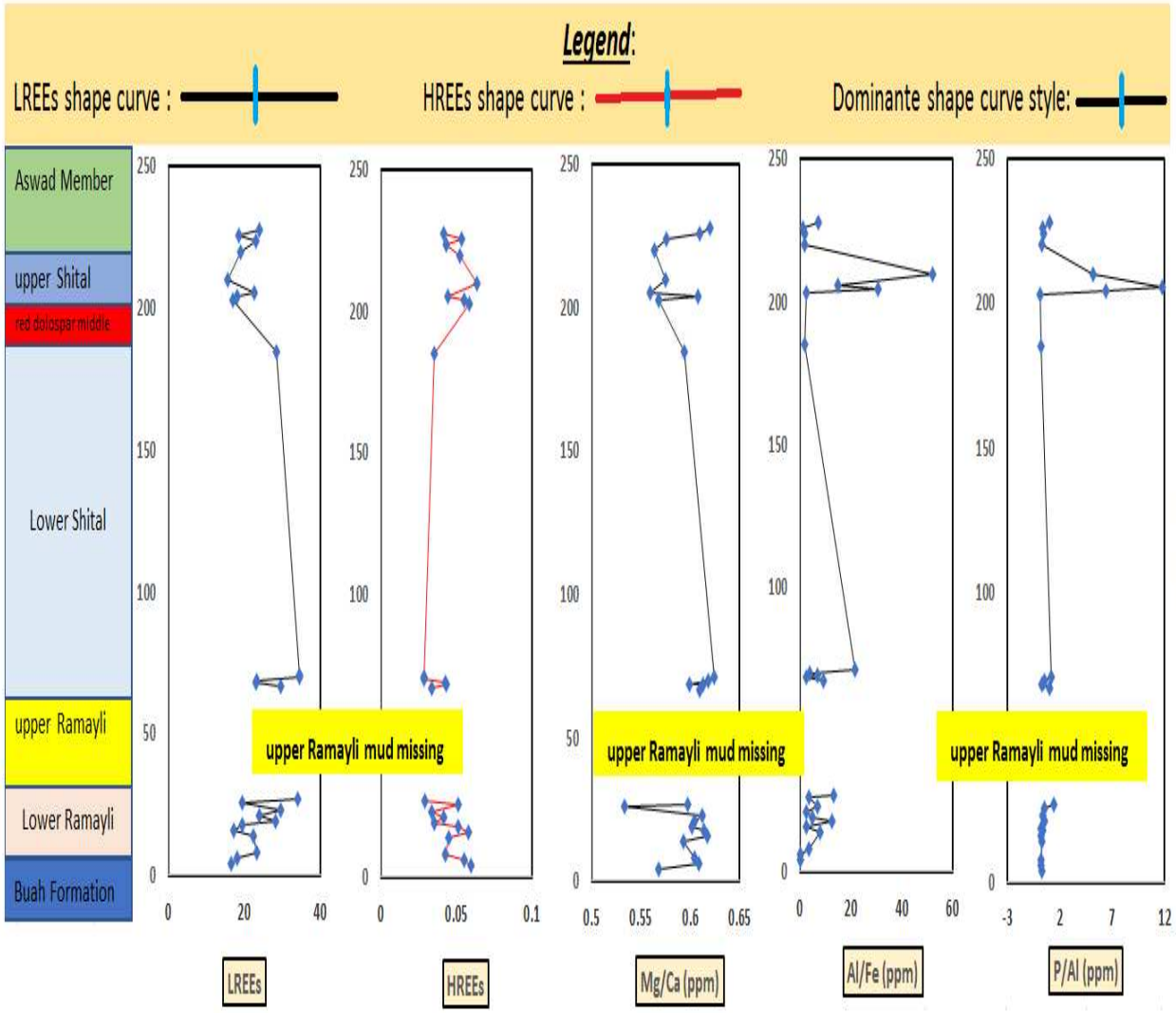

Figure 5-8: *Graph of LREEs, HREEs, Mg/Ca, Al /Fe and P/Al profiles for the type section of Sirab (also called composite stratotype section of Sirab at Wadi Shital ST-1 and ST-2).*

Figure 5-8 shows that, in carbonates, the general tendency of the excursions which occur is close to that of the LREEs curve. As such, the fractionation of REEs into LREEs appears to be the closest tendency of carbonates within type section of Sirab.

Webb and Kamber (2000), Northdurft et al., (2004), Madhavaraju & León (2012), have reported that there are many potential sources of REEs enrichment in carbonate rocks. Sources include the incorporation of REEs directly from old seawater, the intercalation of detrital materials rich in REEs (especially phosphate minerals, Fe and Mn hydroxides) and the enrichment of REEs during diagenesis process. Based on chemical data alone, it is difficult to decide which variable (or combination of variables) controls the abundance of Rare Earth although it is already known that, the fractionation of REEs in the continental environment is rich in LREEs relatively to HREEs.

Based on the potential sources of Rare Earth in the carbonate rocks mentioned above, figure 5-9 shows binary diagrams comparing the abundance of carbonate Rare Earth in the section of Wadi Shital ST-1 & ST-2 with the Major Elements Fe, Al, Mn and P. In general, there is a positive linear relationship between the abundance of Rare Earth and these Elements for all carbonate samples analysed in the section of Wadi Shital ST-1 & ST-2. This suggests that apart from Mn considered in isolation, clay minerals, phosphate minerals as well as iron minerals such as iron carbonates can all be linked and analysed closely with fractionation results of REEs. As for Fe-Mn hydroxides, this remains undetermined depending on the covariance ratio of Mn with respect to REEs.

In the Wadi Shital ST-1 & ST-2, the ranges of the limit values of the REEs are very lower and are pushed back to the ppb values. Thus properly speaking, there is not abundance of REEs fractionation within Sirab sediments as analysed in Wadi Shital ST-1 & ST-2. But, the term abundance of REEs is relatively used to explain the general tendency and dominant trend of REEs according to their very low results fractionation within Sirab Formation which can be divided as LREEs MREEs and HREEs. On this angle, the general trend of outcrop samples from the typical section of Sirab at Wadi Shital ST-1 & ST-2 shows a similar trend to LREEs fractionation. However, the observation also suggests that Mn dissociates from enrichment in clay minerals, phosphate minerals and iron carbonates. But taken in isolation, Mn enrichment without the action of diagenesis (Fe-Mn) in the LREEs-prone environment cannot be understood at this stage of the study. Furthermore, the ICP-MS/OES analysis of the Wadi Shuram WS9 as well as Wadi Aswad WA1 and WA2 sections (see appendix 3) in volume 2 shows that the MnO weights (%) do not exceed 0.12%. Therefore, the Mn can therefore be extrapolated as a relative enrichment in the different sections of the Sirab Formation and the limited early diagenesis considerations suspected on some horizons of the lithostratigraphy of the Sirab would probably be at the origin of the low concentration of this Element?

Therefore, it appears from the Inorganic Geochemical data available from the Wadi Shital ST-1 & ST-2 section that the carbonate samples can be considered as sediments deposited under environmental

conditions sufficiently similar not to significantly modify their REEs trend profile.

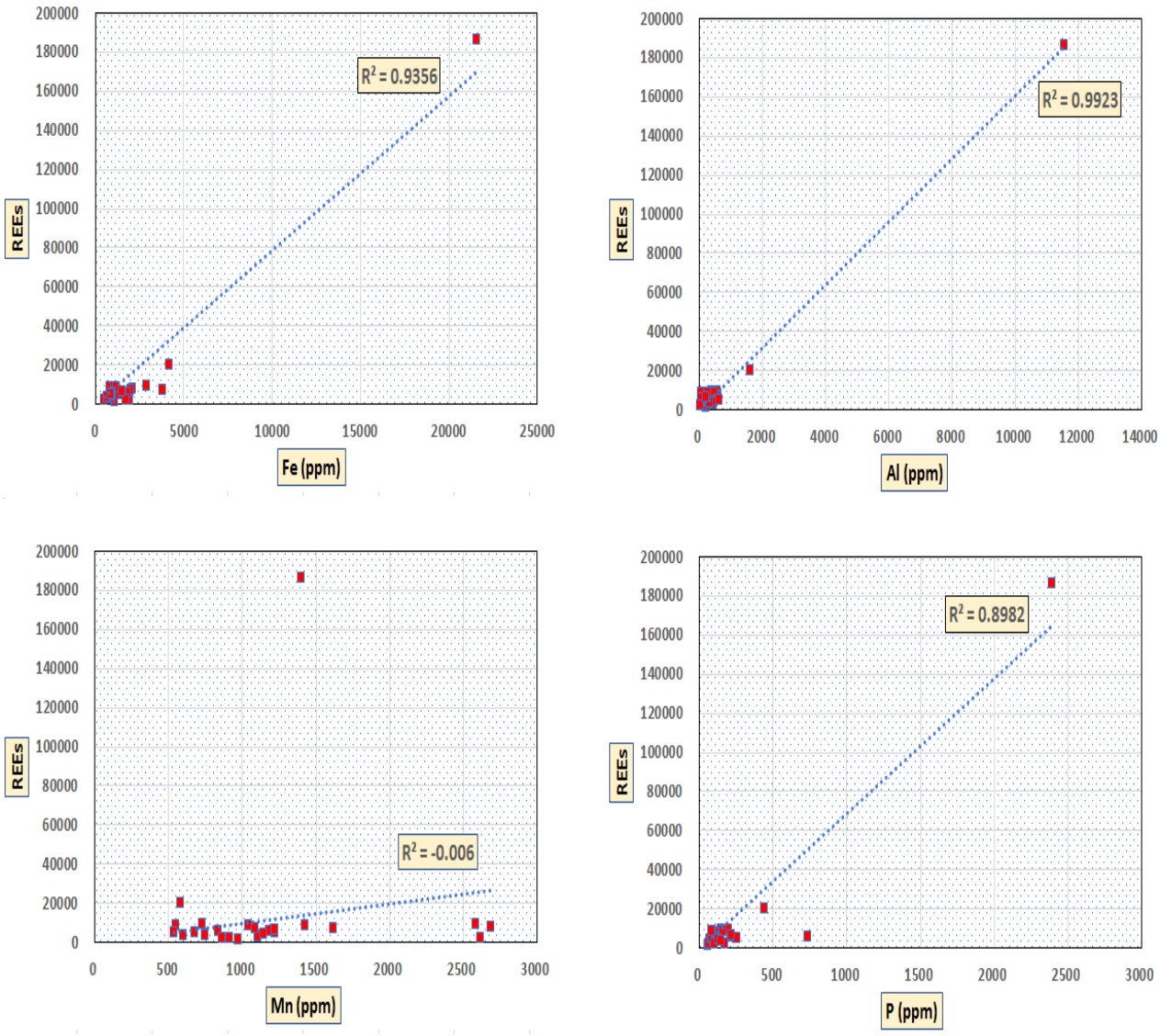

Figure 5-9: *Binary diagrams comparing fractionation of REEs within carbonates with Major elements Fe, Al, Mn and P for the section of Wadi Shital ST-1 and ST-2.*

5.2.3 Contamination of carbonates.

Aluminum is generally of detrital origin and is generally immobile during diagenesis. To determine the redox state of his study environment, McCabe (2020) plotted Al against Cr, Mo, U, V, Ni and Cu. Tribovillard et al., (2006) believe that if the control of authigenic hydrogen over key elements can be distinguished from detrital controls, then it would be possible to determine the redox state of the environment. To achieve the authigenic hydrogen control desired by the authors, the use of Al plots against key Elements such as Mo, U, V, Ni, and Cu, can aid. In addition, sediments rich in OM or having been enriched in OM can also be determined by this method.

In the typical section of Sirab a Wadi Shital ST-1 & ST-2 as well as in sections Wadi Shuram WS9 and Wadi Aswad WA1 & WA2, the Al is one of the most abundant Major Elements after CaO, MgO, SiO_2 and Fe_2O_3. The Al graph used in this thesis is plotted against the five key Elements proposed by Tribovillard et al., (2006). Cr was also plotted against Al as McCabe (2020) had also experimented with during its study to determine the redox state of clay zones. Geochemical Elements such as Si, K, Na, were unfortunately not measured by ICP-MS analysis performed at Trinity College on outcrop samples from the Wadi Shital ST-1 & ST-2 section. In the absence of the quantification of the weights of the Elements (Si, K and Na), the use of the method proposed by Tribovillard et al., (2006), can help to

verify the influence of LREEs fraction carried by clays on carbonates of Wadi Shital ST-1 & ST-2.

Furthermore, the Al is generally of detrital origin and this Element remains more particularly immobile during diagenesis. It has been argued in chapter 3, 4 and in this chapter 5 that the diagenesis particularly for the section of Wadi Shital ST-1 & ST-2 under study as well as in general for the Sirab Formation, is inconclusive. Most of the Al concentration in carbonates is therefore assumed to be related to terrigenous sediments which are concentrated through weathering in the emerging environment.

- Concentration of Al and six others Minor Elements in type section Wadi-Shital ST-1 & ST-2.

Sample/test ICP-MS	Al (ppm), ICP-MS values	Cr (ppb)	Mo (ppb)	U (ppb)	V (ppb)	Ni (ppb)	Cu (ppb)
STB 4	205	725	1000	419	2031	15880	1948
STB 6	444	1421	1000	734	1294	11030	5895
STB 8	586	2528	12	958	2375	14790	17100
STB 14	476	1764	272	1055	3316	1016	23570
STB 16	335	1717	8	241	2455	51390	2705
STB 18	154	836	11	133	1402	27160	886
STB 19	564	2055	17	483	2902	20740	10190
STB 21	472	1453	15	699	2258	28350	4134
STB 23	281	1114	27	126	4503	18940	2471
STB 26	185	3700	36	141	4811	60420	6524
STB 27	61	478	13	132	2382	74210	4492
STF 67.5	196	2638	38	656	9031	48080	9021
STF 68.4	1598	5714	272	2256	6723	63420	6829
STF 69	421	2962	116	674	11990	4258	5425
STF 70	275	1177	22	304	3110	1344	3843
STF 71	72	732	23	805	6093	31350	9780
STF 185	11570	24290	334	2149	41910	58900	1500
STF 202.9	465	887	17	405	11750	27090	1085
STF 204.3.	16	1308	29	182	8023	20900	1629
STF 205.7	63	1669	45	555	12710	16900	2905
STF 210	33	1727	55	481	3858	16090	1978
ST2 1.6	462	4825	24	216	3536	14490	1528
ST2 2.9	332	2913	8	398	2947	29570	1256
ST2 2.15	610	4047	21	352	3164	0.016	1848
ST2 4.5	207	2822	42	171	7275	64970	2453

Table 5-1: C*oncentration of Al in ppm, Al (ppm) and Cr, Mo, U, V, Ni, Cu (ppb) as obtained for type section of Sirab in Wadi-Shital ST-1 & ST-* 2.

Using the procedure proposed by Tribovillard et al., (2006) as well as McCabe (2020), the values of Cr, Mo, U, V, Ni and Cu were crossed with the percentage of Al of each sample case (figure 5-10 below). As predicted by McCabe (2020), if a positive linear relationship is observed on the different diagrams in Figure 5-10, then it is likely that the inspected Element has a strong detrital origin. Conversely, if there

are enrichments of the Elements mentioned above without there being a concomitant enrichment in Al, or even a decrease in Al, then it is probable that the element under control has an essentially authigenic.

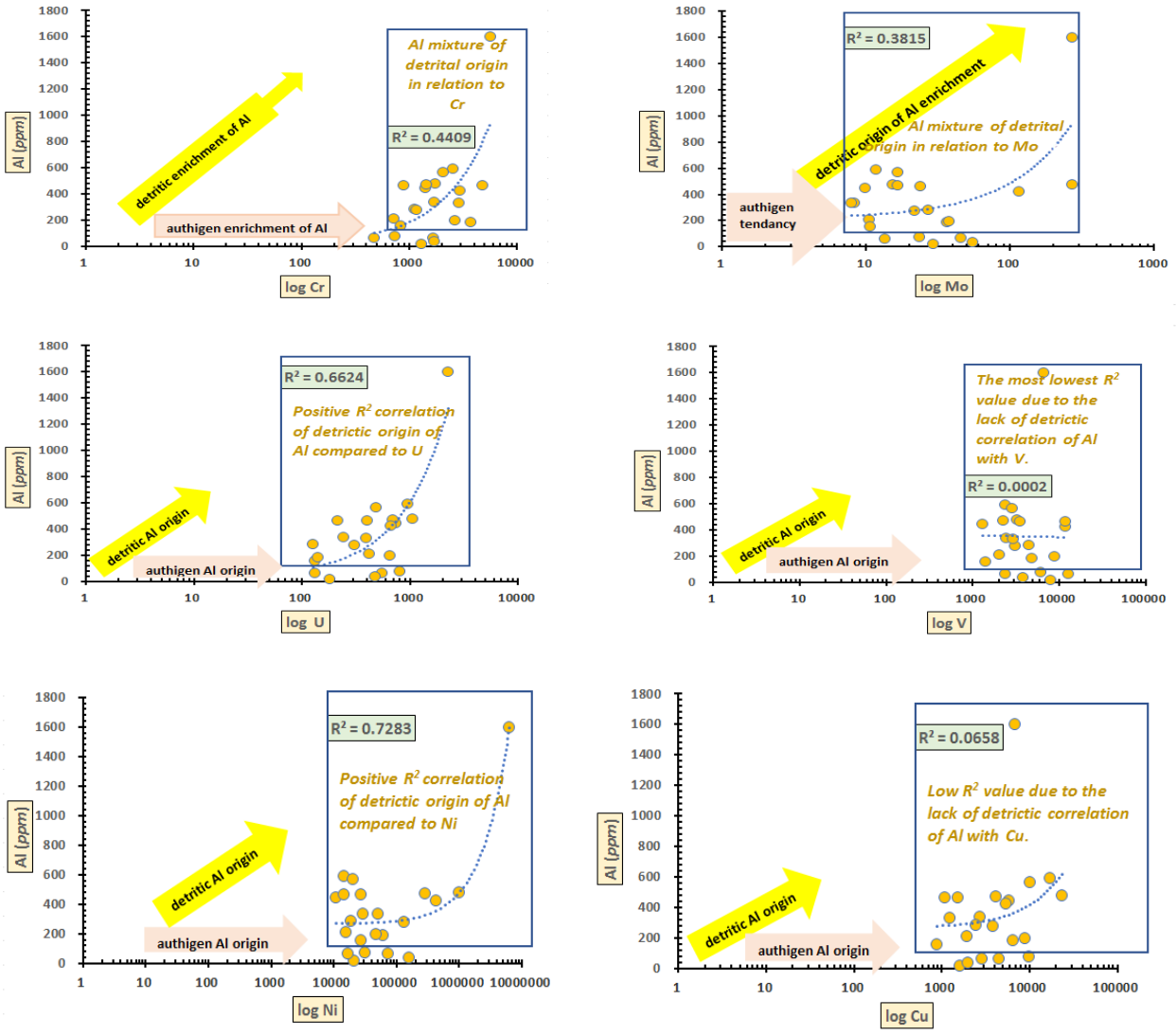

Figure 5-10: *Group of diagrams symbolizing the relation Al (ppm) against Cr, Mo, U, V, Ni and Cu for the Sirab Formation, through its composite stratotype section of Wadi-Shital ST-1 & ST-2.*

The excursions that occur in the different graphs in figure 5-10 do not all offer linear relationships with respect to Al against Cr, Mo, U, V, Ni as well as Cu. U and Ni have satisfactory covariance ratios (R^2>0.6) but remain statistically inferior compared to tests carried out on four other Elements (Cr, Mo, V and Cu) whose ratios are R^2 <0.45. The lack of a linear relationship on these four Elements inspected cannot lead to a conclusion that Al was authigenically enriched. Indeed, in the carbonates at Wadi-Shital ST-1 & ST-2 section, the values of concentration ranges for Cr, Mo, U, V, Ni and Cu are significantly pushed to very low limits (*ppb*). As such, the carbonates in type section of Sirab can therefore be considered to be relatively contaminated with detrital clays. By way of illustration, the concentration ranges (*ppm*) of the Elements such Cr, Mo, U, V, Ni and Cu used by McCabe were of the order of (Cr 0-250; Mo 0-20; U 0-8; V 0- 250; Ni 0-150; Cu 0-500 as well as Cu 0-150) with Al (%) = 25. The approximate verification of the weight of Al_2O_3 (%) obtained by ICP-MS/OES on the other sections of the Sirab Formation at Wadi Shuram WS9 as well as Wadi Aswad WA1 & WA2 indicates this does not exceed 0.14 (%) while U and V in (*ppm*) are respectively less than 2 (*ppm*) and 20 (*ppm*). In the typical section of Sirab, the maximum value of the Al concentration is 11,570 (*ppm*) for the STF 185 (red dolospar) sample while the majority of the values of the concentrations of this Element in the other samples varied by turn of 200 (*ppm*) and 400 (*ppm*); see table 5-1. As for Cr, Mo, U, V, Ni and Cu in the type section of Sirab, they all had ppb concentrations (see appendix 2 in volume 2).

Moreover, the concentrations of Trace Elements that are Cr, Mo, U, V, Ni and Cu in the section type Wadi-Shital ST-1 & ST-2, are relatively low so that only a few of these Elements can be considered as likely to clump together to form some rare minerals such as * *Radovanite*, *Mrazekite*, etc. (see table 3-1 for accessory minerals detected by XRD) *.

5.2.4 Origin of the relative enrichment in Phosphorus.

As a Major component of bones and teeth (hydroxyapatite and fluorapatite respectively) and of all plants, phosphorus is a major component of the range of phosphate minerals. In a reworked environment such as in the hinterland where the sediments are constantly transported and deposited on the bottom of the continental slope, the detrital phosphate is generally mixed in the sediment under the influence of continental weathering, largely the fractionation of which of LREEs is more abundant compared to HREEs. Moreover, unlike P from weathering surface environments, authigenitic phosphate is almost free from any terrestrial reorganization process. Distinguishing then one from the other (P from detrital minerals LREEs or P from heavy-authigenic minerals HREEs), can help position the carbonate ramp deposit relative to currently known environmental zones.

- Concentration of P and Th in *ppm* for Wadi-Shital ST-1 & ST-2.

Sample / test ICP-MS	P (ppm)	LREEs	HREEs	Th (ppb)
STB 4	55	1150	69	53.86
STB 6	79	*2670*	*147*	254.8
STB 8	107	6849	293	509.4
STB 14	146	6703	300	208.7
STB 16	72	3669	212	143.6
STB 18	63	1676	86	61.72
STB 19	144	8660	306	355.6
STB 21	245	4756	198	313.2
STB 23	112	6329	214	182.1
STB 26	97	3139	161	69.72
STB 27	88	7553	221	75.38
STF 67.5	210	5471	184	91.52
STF 68.4	439	17888	779	1539
STF 69	200	8347	359	453.7
STF 70	159	8146	236	158.6
STF 71	83	4401	127	045.14
STF 185	2391	167266	5894	16570
STF 202.9	80	7086	415	117.5
STF 204.3.	100	1712	95	5.826
STF 205.7	734	5224	231	44.57
STF 210	170	1870	118	18.9
ST2 1.6	126	3909	205	180.7
ST2 2.9	147	3347	145	180.1
ST2 2.15	254	4592	246	261.9
ST2 4.5	217	5941	247	120.7

Table 5-2: *concentration of P in ppm, LREEs, HREEs and Th for Wadi Shital ST-1 & ST-2.*

McCabe (2020), tried to correlate P (%) against Th (ppm) in a binary diagram then, had drawn another diagram Th (ppm) against ∑LREEs (ppm) to finally seek a logical explanation of the origin of the enrichment of (P). Whether or not related to an authigenic source, Th is present as a Minor Element in a range of heavy detrital minerals such as zircon, allanite, titanite, and apatite and is typically present most abundantly in monazite (a rich mineral phosphate). But monazite does not need to be present in abundance in sedimentary rocks to have

a measurable effect on the composition of trace elements in the rock (McLennan et al., 1993).

On the other hand, Th can also be present in a range of secondary minerals such as thorite, huttonite, thorogummite, brockite and grayite (hydrated phosphate minerals of the Thrhabdophane group). These minerals are found in the chemical weathering of less stable primary minerals such as apatite and allanite. During early diagenesis, authigen monazite can form by dehydration of rhabdophane and often the authentic minerals are associated with it.

In order to estimate the probable origin of (P), this Element was compared to Th and then, other comparative diagrams Th/LREEs as well as Th/HREEs were exploited in the hope of finding an explanation as to the environmental source of phosphate enrichment.

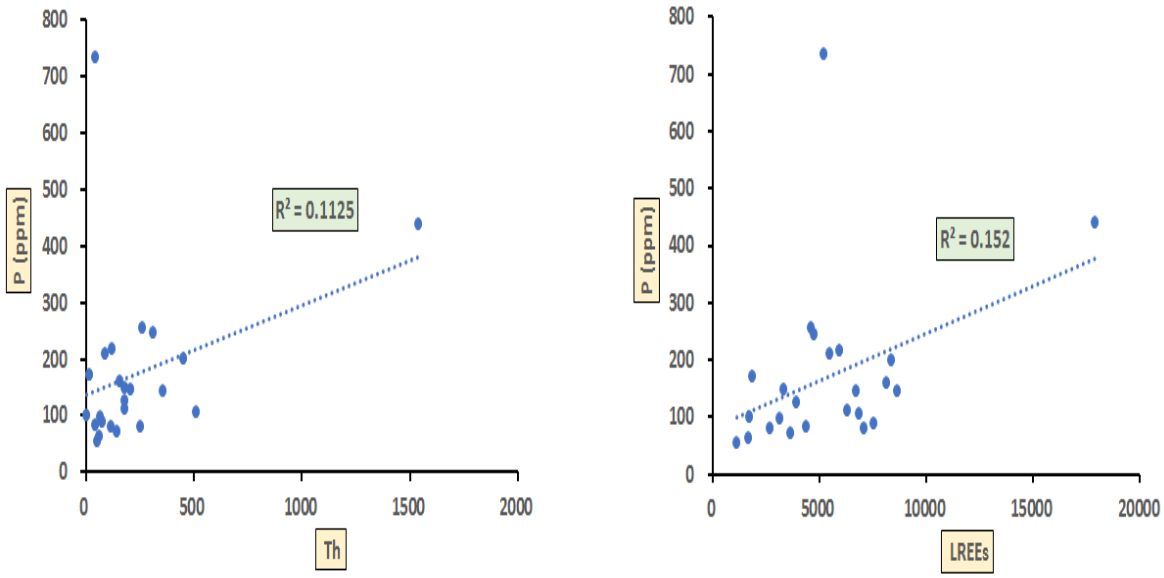

Figure 5-11: *ICP-MS P/Th and P/LREEs concentration to determine the detrital relationship of P enrichment in the typical section of Sirab at Wadi Shital ST-1 & ST-2.*

The diagram (P/Th) of figure 5-11, measures the influence of Th present in certain phosphate minerals which are accessory to the main mineralogy of dolomitic carbonates of the section of Wadi-Shital ST-1 & ST-2 while, the diagrams (Th/LREEs) tend to exploit the rational relation which will justify the dependence of Th in the accessory phosphatic minerals compared to the phenomenon of surface weathering of rocks from which, the fractionation of REEs into LREEs is more abundant and takes place most in a continental environment.

Geochemically speaking, Th is present in the range of heavy detrital minerals such as zircon, allanite, titanite and apatite, and can also be found in phosphate minerals such as monazite, without the latter mineral being abundantly present in sedimentary rocks to have a measurable effect on the composition of Trace Elements in the rock (McLennan et al., 1993). As the relatively enriched concentrations of P in the typical section of Sirab at Wadi Shital ST-1 & ST-2 allow P to be classified as one of the six Major Elements analysed by ICP-MS at the laboratory of Trinity College, if its concentrations are linked to environmental sources of detrital origin, then the P in the section of Wadi Shital ST-1 & ST-2 would logically depend on the zones of continental alterations with a favorable relation to the LREEs whereas if the P would have had an authigenic source, the measurable Th in abundance in heavy minerals would indicate a favorable relationship to the authigenic P.

The covariance ratios of Th with respect to P as well as of LREEs (alterations of rocks to phosphatics) with respect to P show ratios R^2 <2 (figure 5-11). As, to bind P phosphorus to the alteration of phosphate rocks in continental environment seems unlikely for the type section of Sirab at Wadi Shital ST-1 & ST-2. However, figure 5-12 with the covariance ratio HREEs against P for heavy minerals that may contain P in marine environment, also shows an R^2 value <2 and therefore, not significant to conclude from an authigenic origin enrichment of P in sediments found at Wadi Shital ST-1 & ST-2.

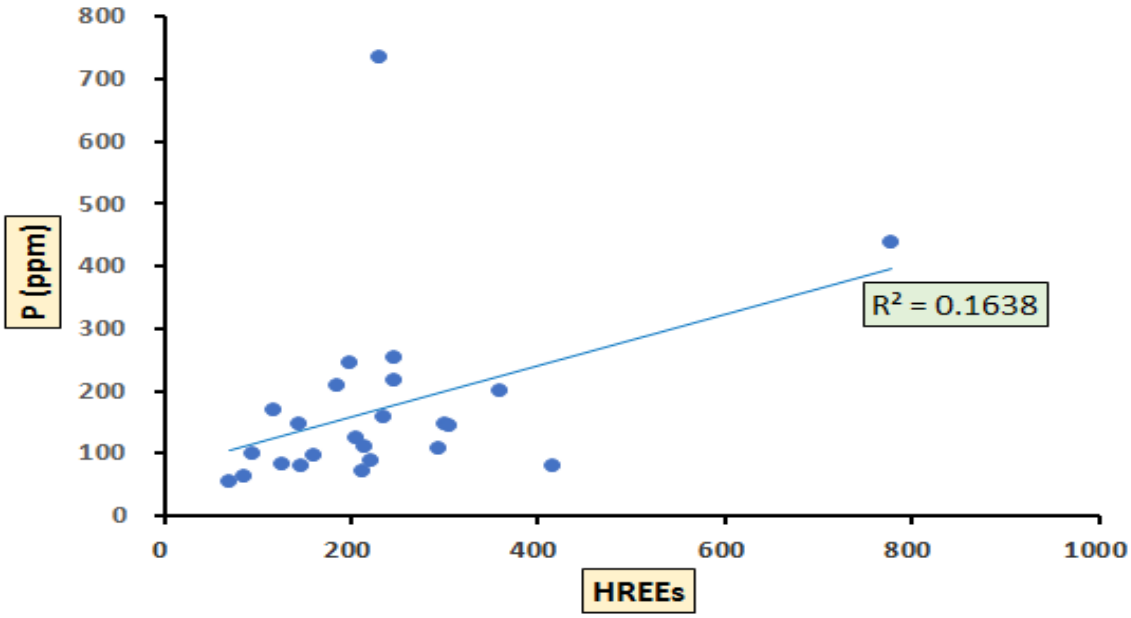

Figure 5-12: *ICP-MS P/HREEs concentration to analyze the authigenic link of P enrichment in the typical section of Sirab at Wadi Shital ST-1 & ST-2.*

5.2.5 Mineralogical type of iron in SIrab carbonates.

It was briefly suggested in point 5.2.1., from paragraph 12 that the Fe concentrations in the sediment of Sirab Formation could help in the analysis of palaeo-anoxic conditions along the type section Wadi Shital ST- 1 & ST-2. In fact, current observations show that, during the alteration of sediment in a continental or mixed environment, Fe gradually replaces Al during the formation of laterite. However, in nature, sedimentary rocks contain a minor proportion of Iron in present-day sediments and this ore generally has a content of less than 15% of the total weight of the rock in which it is contained. As iron exists under two degrees of oxidation, Fe^{2+} (the ferrous ion) and Fe^{3+} (the ferric ion), its behaviour is controlled by the geochemistry of the sedimentary and diagenetic media. The main source of iron for the ocean basin is currently considered to be the continental weathering of basic rocks and lateritic soils. During the alteration of continental rocks for iron enrichment in the ocean basin, the fractionation of LREEs is more pronounced and this terrigenous tendency of REEs can be transmitted in the chemostratigraphic composition of the carbonates of the ramp which would be localized close to a continental rock weathering.

Iron is generally found in the Fe^{3+} state in most surface water and remains almost insoluble. So that, (Fe_2O_3) has very low concentrations in solution, of the order of 1 ppm for river water and of the order of 0.003 ppm for sea water. However, the conditions of iron

accumulation in the Ediacaran - Cambrian time limit diverge from those of current observations in sediments or in laboratories. Theoretically, the continental environment mobilizes high concentrations of iron and a negative (Eh) due to the fact that the clays which it mainly contains exhibit high potentials for fractionation into LREEs as observed in actual days. Seen from this angle, it is evident that the drift of the continental rocks weathering process precedes its subsequent accumulation on various levels of the continental slope, down to the foot of the marine sediments. The binary diagram "REEs crossed with the values of iron concentrations was $R^2 = 0.9356$ (figure 5-9), that is to say close to the value 1. This strongly positive correlation of Fe compared to the REEs means that the two concentrations (Fe and fractionation of REEs) in the section of Wadi Shital ST-1 & ST-2, agree in the sediments. The oxidation of iron (Fe_2O_3) in any type of terrestrial environment occurs depending on: the abundance of iron (Fe), Eh, the nature of the solvent such as the pH of the water, before being transported and deposited in sediment as concentrated iron. Under the majority of Eh and pH conditions in surface water, iron is in the Fe^{3+} (Fe_2O_3) state, while FeO is deficient in oxygen. The field coexistence of pyrite (FeS_2) and ferrous iron (FeO) with respect to Eh and PS^{2-} shows that the field of FeO is rapidly depleted when pyrite is formed. Thus, in the anoxic sediment with weak aeration, pyrite would tend to form to the detriment of the depletion of ferrous iron (FeO) while the field of ferric iron (Fe_2O_3) would still be protected from the absence of oxygenation. As the pyrite domain continues (figure 5-6). A high concentration of PS^{2-} and

Eh negative would then develop. Moreover, one can also imagine that in a hydride environment (mixed) where the parameters Fe, Eh, pH are subjected to permanent fluctuations, that the Fe/HREEs or Fe/LREEs also display fluctuations due to the exchange solutions between marine and continental environment.

Knowing that ferrous iron (FeO) contains less oxide than ferric iron and that it disappears in the presence of pyrite formation, FeO is therefore assigned a higher reducing potential than Fe_2O_3. In this way, depending on the REEs, there emerges a Fe_2O_3/LREEs tendency favorable to the environment where the rocks are weathered (oxygenated zone) and FeO/HREEs favorable to the reducing environment (anoxic). The method for estimating the FeO and Fe_2O_3 concentration values from the weight (ppm) of Fe obtained by ICP-MS is as follows:

- Fe_2O_3+FeO = Fe_{total} in (ppm) whereas the approximate amount of the total Fe concentration in relation to the ICP-MS analysis is almost equal to the 100% of the Fe contained in the analysis of the sample.

- Replacing the values of atomic masses of iron and oxygen in the formula gives:

($\underline{\boldsymbol{56*2+16*3}}$) g + ($\underline{\boldsymbol{56+16}}$) g= 232g.

160 72 =232 g.

On the other hand, 232g = 100% Fe (Fe_2O_3 + FeO) assumed to be the measurable value of Fe by ICP-MS.

Thus, 160+72=100 (%) ⟺ Fe_2O_3+FeO = Fe (100%)

Fe_2O_3 = 160*100/232 ~ 69(%): or Fe_2O_3 represents 69% of the weight of the Fe_{total} (ICP-MS) measured on the outcrop.

FeO = 72*100/232 ~ 31(%); or FeO represents 31% of the weight of the Fe_{total} (ICP-MS) measured on the sample.

- Calculation of estimation of the weight of Fe_2O_3 and FeO molecules.

ICP-MS samples	ICP-MS Fe (ppm)	Fe_2O_3 (ppm)	LREEs	FeO (ppm)	HREEs
STB 4	1054	727.26	1150	326.74	69
STB 6	934	644.46	*2670*	289.54	*147*
STB 8	2110	1455.9	6849	654.1	293
STB 14	3819	2635.11	6703	1183.89	300
STB 16	908	626.52	3669	281.48	212
STB 18	1960	1352.4	1676	607.6	86
STB 19	2869	1979.61	8660	889.39	306
STB 21	1328	916.32	4756	411.68	198
STB 23	1967	1357.23	6329	609.77	214
STB 26	699	482.31	3139	216.69	161
STB 27	824	568.56	7553	255.44	221
STF 67.5	1846	1273.74	5471	572.26	184
STF 68.4	4186	2888.34	17888	1297.66	779
STF 69	2911	2008.59	8347	902.41	359
STF 70	1086	749.34	8146	336.66	236
STF 71	1555	1072.95	4401	482.05	127
STF 185	21550	14869.5	167266	6680.5	5894
STF 202.9	1176	811.44	7086	364.56	415
STF 204.3.	485	334.65	1712	150.35	95
STF 205.7	949	654.81	5224	294.19	231
STF 210	1716	1184.04	1870	531.96	118
ST2 1.6	902	622.38	3909	279.62	205
ST2 2.9	679	468.51	3347	210.49	145
ST2 2.15	852	587.88	4592	264.12	246
ST2 4.5	1518	1047.42	5941	470.58	247

Table 5-3: *Theoretically calculated values of the molecular weights of Fe_2O_3 and FeO from ICP-MS measurements of Fe for carbonate samples of the typical section of Sirab (Wadi Shital ST-1 & ST-2).*

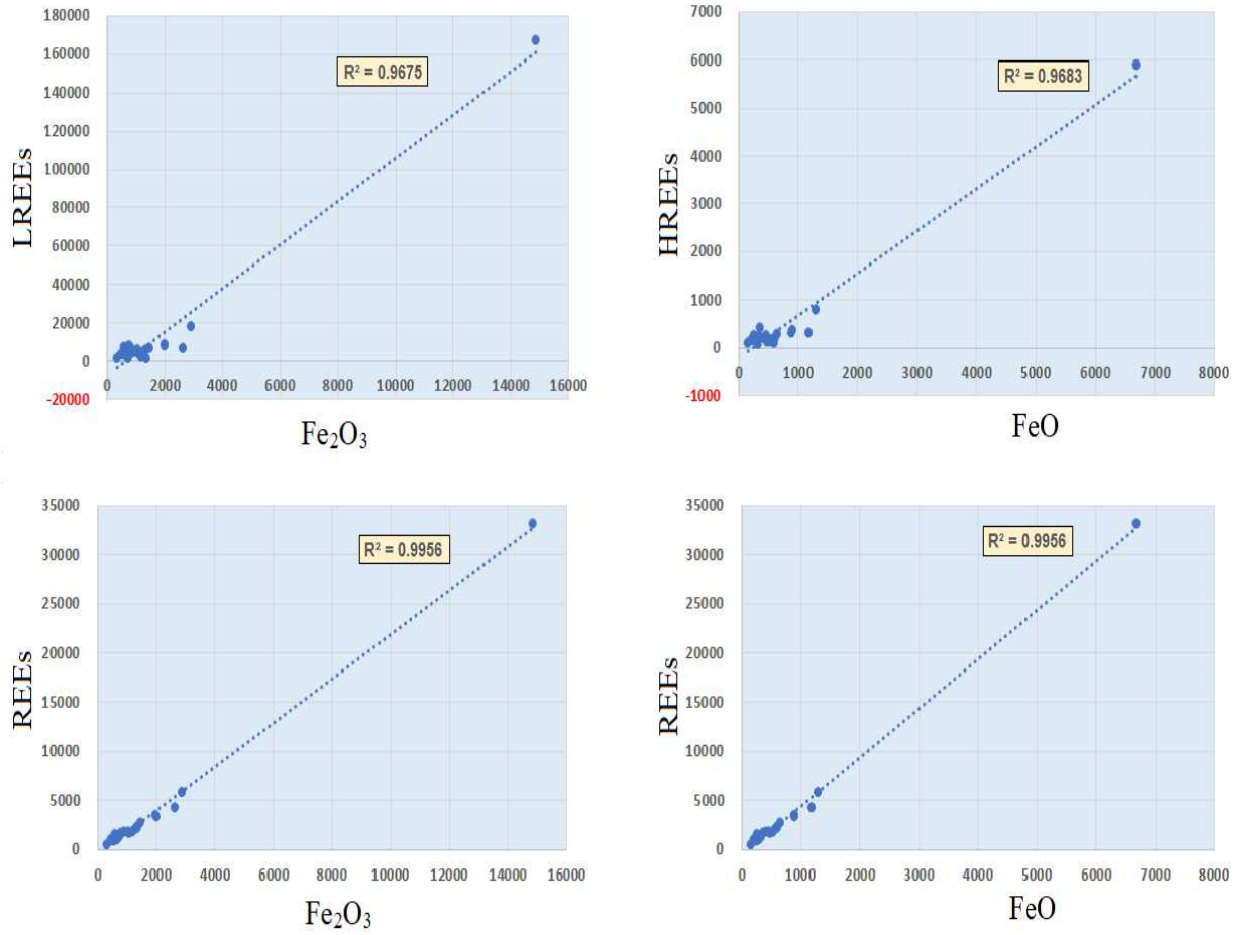

Figure 5-13: *Graphs of the theoretical estimate of the mineralogy of Fe type Fe_2O_3 or FeO, preferentially abundant in the type section of Sirab at Wadi Shital ST-1 and ST-2.*

The R^2 on all graphs in figure 5-13 (Fe_2O_3/LREEs; FeO/HREEs as well as Fe_2O_3/REEs and FeO/REEs), shows that in the Formation of Sirab along Wadi Shital ST-1 & ST-2, there is no one dominant Fe type than the other which would have accumulated exclusively in the sediment. The proportion of Fe_2O_3-type iron should normally be more representative than FeO. However, the results of the graphs prove that even FeO can also be proportioned to the same extent as Fe_2O_3 while

the Ce/Ce* ratios of all samples examined in Wadi Shital ST-1 & ST-2 section place them as sediment deposits under anoxic conditions. Under the sole argument of the anoxic conditions of the sediment in relation to the PS^{2-}, the Formation of pyrite should normally be abundantly recognized in the microscopy of samples of the type section of Sirab or even, detected several times during the analysis by XRD. But instead of pyrite was rather iron carbonate that was detected (see table 3-1 in chapter 3).

Regarding to anoxic conditions, the majority of the Y/Ho ratios of the samples should have reflected the sea level (Y/Ho>45), values of seawater. However, having R^2 values (Fe_2O_3/REEs as well as FeO/REEs) similar indicates not only that there are no significant differences in the mineralogical compsition of Fe within sediments of the Sirab Formation but also, unlike the conditions of stability of Fe_2O_3 and FeO, that he would have had at one time in the sediment deposits, a mixture (input) of Geochemical Elements of continental and marine origin. It is possible that in Oman during the Ediacaran - Cambrian that the accumulation of Fe in the Sirab Formation probably did not depend on the circulation of oxygen but rather on inputs of Fe-rich material from either the continental environment or marine given that, the iron-like mineralogical compositions Fe_2O_3 and FeO are similar. Therefore, the absence of oxygenation of the sediment may not have influenced the process of accumulation of Fe, or less of Mn, as is generally the case during burial and the development of diagenesis.

In general, low atmospheric oxygen may be a general and prevalent condition throughout the Infracambrian temporal boundary before this increase towards the Carboniferous. Current observations of Fe concentrations in sediments prove that this Geochemical Element hardly exceeds 15 ppm and that the source of its concentration in ocean basins is mainly due to the weathering of continental rocks. On the other hand, several sediments dating from the Precambrian have accumulation values of the same Element (Fe) well above 500 ppm whether they are sediments with Y/Ho ratios favorable to the presence of marine water or not. Thus, the accumulation of ferrous or ferric-like Fe as a function of oxygen availability in sediments dating from the Precambrian and Infracambrian as the case of the studied Sirab Formation is probably not adapted to a similar phenomenon of trapping of OM under an anoxic column. In generally, anoxic waters after the Precambrian host Y/Ho >45. Thus, perhaps the low level of atmospheric oxygen during the filling of the Sirab Formation is the reason for the Ce/Ce* anoxia while the $\delta^{18}O$ of the oxygen isotopes in the type section of Sirab have values close to their primary signatures which ultimately indicate that the Sirab carbonate ramp (Wadi Shital ST-1 & ST-2) deposition environment had not been affected by significant fluctuations in oxygen variations which was still anoxic in the Ediacaran era?

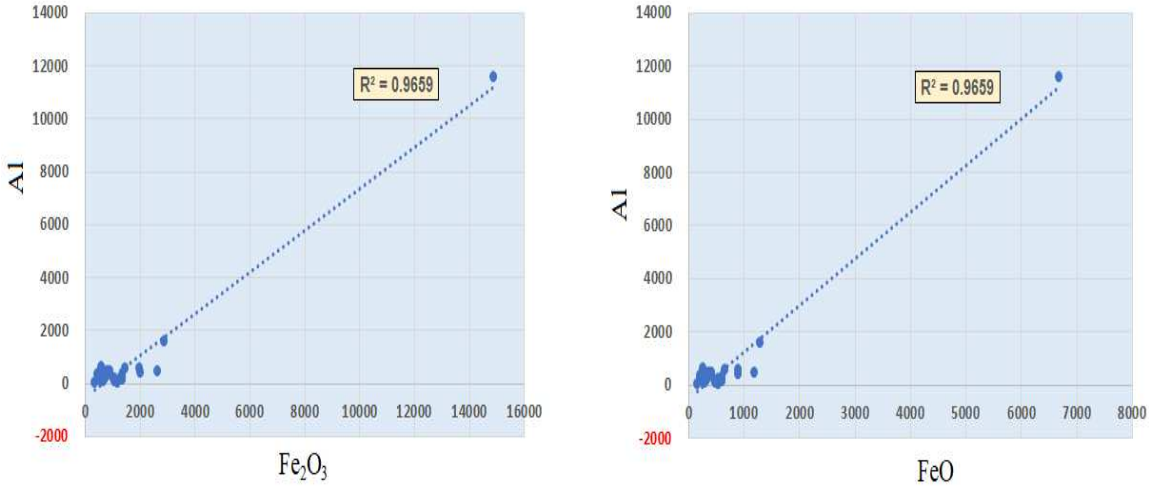

Figure 5-14: *Graph of estimation of environmental weathering rate of rocks in Wadi Shital ST-1 & ST-2 section based on Fe preference (Fe_2O_3 or FeO), Wadi Shital ST-1 & ST-2.*

The Al analyzed in point 5.2.3 of this chapter is a good indicator for screening the rate of sediment alteration. The Geochemical Element (Al) does not interfere with the geochemical parameters which are modified during diagenesis of the sediment to enrich Fe and Mn to the detriment of Sr. It (Al) remains intact during diagenesis and can therefore help to determine the tendency for the formation of Fe of the Fe_2O_3 or FeO type in the sediments by considering the Geochemical Element (Al) itself as preferentially present in continental environments with a high rate of alteration (LREEs more important than the HREEs in the formation of continental clays in general).

The values of R^2 as probable values of the substitution of Al by Fe remain favorable to the formation of Fe_2O_3 as well as FeO. And the ratios REEs/Fe_2O_3 as well as REEs/FeO are similar. Strictly speaking, the anoxic signal (Ce/Ce*) detected in the type section of Sirab, may be a factor due to the low oxygenation rate of the Precambrian atmosphere.

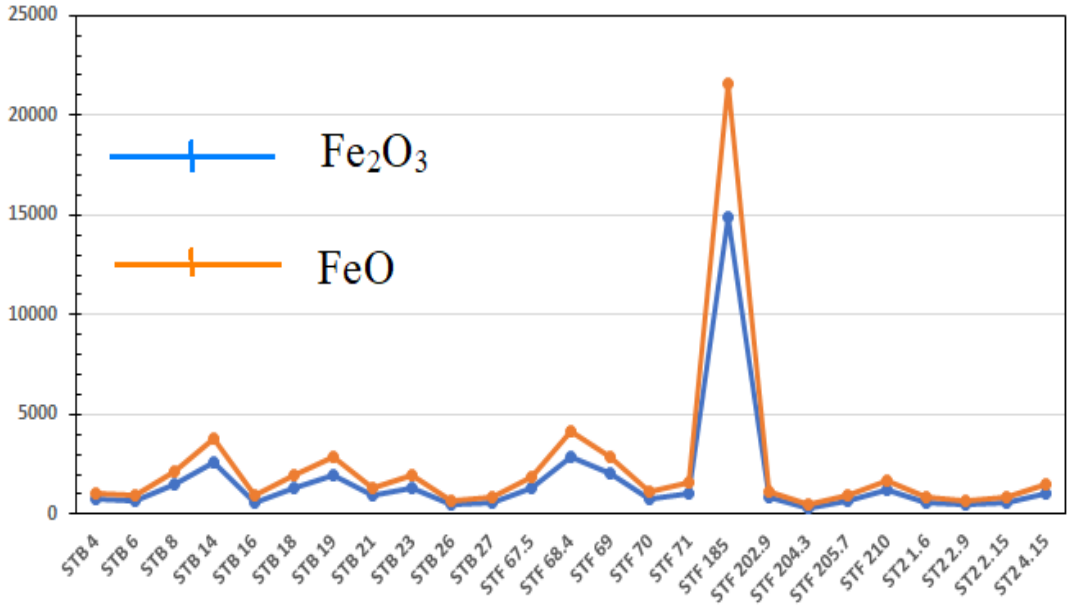

Figure 5-15: *Fe (Fe_2O_3 and FeO) composition curve in the typical section of Sirab in Wadi Shital ST-1 & ST-2.*

The curves in Figure 5-15 which illustrate the fluctuations of Fe (Fe_2O_3 and FeO) in the sediments of the Sirab Formation at Wadi Shital ST-1 & ST-2. The composition of the Fe accumulated in the sediments is not very variable. Fe_2O_3 and FeO are present in the composition of Fe_{total} without any influence from anoxic conditions.

5.2.6 Probable source of mobilization of Mn.

Rare Earth Elements have no redox chemistry, except for Ce and Eu (McLennan, 1989). However, siliciclastic detritus (LREEs) is the main source of sedimentary REEs enrichment, and profiles of REEs in continental rocks reflect the content of REE in (PAAS) which represents the average composition of rock crust (Taylor & McLennan, 1985). In contrast, authigenic sediments with negligible detrital influence can potentially preserve seawater REEs composition with depleted LREEs (McLennan, 1989).

The correlations of REEs in the type section of Sirab (Wadi Shital ST-1 & ST-2) against the Major Elements Fe, Al, Mn and P are positive for Fe, Al and P with the sole exception of Mn (figure 5 -9). Evidence for general diagenesis in the type section of Sirab is inconclusive ($\delta^{18}O$ isotope ratio in figure 4-2, Figure 4-4, figure 4-5, figure 4-6 as well as figure 4 -7, see chapter 4).

In addition, the redox parameter which during the Ediacaran-Cambrian in Oman during the infilling of the Formation seems to be favorable for anoxic conditions (figure 5-4). Anoxia refers to conditions in which oxygen is likely to be minimal to virtually absent. Anoxic-euxinia develops in the presence of HS- (sulphate-reduction in marine sediments) while the term "dysoxic" refers to conditions varying between anoxic and oxic, or when oxygen levels are relatively

low but constant (Wignall & Myers, 1988). The constancy of the oxygen level in the sediment may also reflect a stable record of the isotopic values of oxygen ($\delta^{18}O$) in the sediment.

Relative to oxygen levels, manganese is enriched in Mn oxides under oxic conditions. Diagenesis reduction produces soluble Mn^{2+} which diffuses away from the site of reduction (Morford et al., 2001). Reduced Mn can be reprecipitated in the presence of O_2, where it forms Mn carbonate when alkalinity is high. Although Mn is generally depleted in sediments undergoing anoxic diagenesis, there is also evidence that recycling of this Element beyond redox limits can be important (Calvert and Pedersen, 1996; Morford et al., 2001).

In the Ara Group in Oman, manganese (Mn) concentrations in Platform samples appear to be the result of diagenetic processes rather than depositional conditions because Mn is strongly involved in carbonate diagenesis (Veizer, 1983b; Banner and Hanson, 1990). This includes redox variation and water-rock interaction while the results of the two processes generally remain difficult to separate (Banner and Hanson, 1990). As for manganese (Mn) concentrations in the basin (U) of the Ara Group, this Element is globally depleted compared to its homologous concentrations in the Platform (A4). Depletion of Mn relative to PAAS in Basin samples suggests removal of reduced Mn in sediments; this can occur in a range of conditions from dysoxic to deuxinic (Froelich et al., 1979). Reduced soluble Mn^{2+} can form solid

Mn carbonate (e.g. Pratt et al., 1991), undergo oxidation in the presence of an oxic background (Calvert and Pedersen, 1996) or diffuse away from the site of reduction. This latter process leaves the sediments permanently depleted of Mn, and the Mn concentrations in the sediments are a function of the Mn content of the detrital fraction delivered to the Basin (Calvert and Pedersen, 1996). On the other hand, the extent of Mn depletion is also a function of the duration of oxygen starvation (Calvert and Pedersen, 1996), and Mn loss may have been less efficient during deposition of the U and Thuleilat shales. For example, the environmental condition of the repository may have been permanently or temporarily dysoxic in these units. As such, it seems essential to try to understand whether in the Sirab Formation, relatively high concentrations of Mn are linked yes or no to the development phases of carbonates?

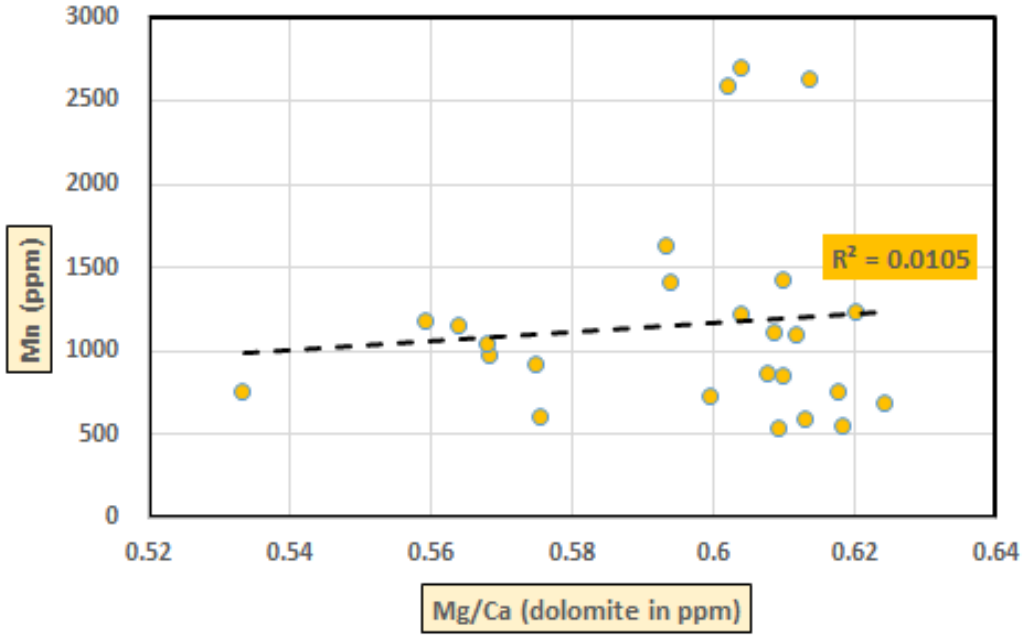

Figure 5-16: *Mn and dolomite (Mg/Ca) correlation to determine if the manganese (Major Element Mn) concentrations are due to the carbonate composition in the typical Sirab section (Wadi Shital ST-1 & ST-2).*

The Mn/dolomite correlation ratio in figure 5-16 does not suggest that Mn concentrations as a Major Element in the typical section of Sirab are related to carbonate development phases. The Mn concentrations seem to be independent of the process that led to the formation of dolomites during the filling of the carbonate ramp. Normally, the absence of oxygen should lead to the loss of Mn concentration in the sediments. On the other hand, the Mn concentration is a relative term to express that apart from the dolomites whose main composition is (Ca and Mg) as well as other Major Elements detected in carbonates such as Fe, Al, P, (Na%) and (K%), the Mn is also a Major Element in the Sirab carbonates. Therefore, to try to understand the relative

enrichment in Mn in the Sirab through its section Wadi Shital ST-1 & ST-2 requires certain precautions. As the relative concentrations of Mn are not related to the development of carbonates in the dolomites, it is possible that the Mn was transferred to the sediments (Sirab Formation) by contributions of detrital fractions. Indeed, the loss of oxygenation is a redox characteristic of the Sirab and the Ara Group which today appear to be lithostratigraphic equivalents in Oman. However, anoxia should normally result in a lower concentration of Mn within the sediment, while a reducing environment, such as during diagenesis, is likely to mobilize Mn^{2+} ions which may subsequently form manganese carbonate during the process of sediment oxygenation. At the present stage of the study, the oxygenation of the sediment at Wadi Shital ST-1 & ST-2 is not proven, just as diagenesis does not appear to be involved as an environmental redox in relation to Mn. The absence of oxygenation and diagenesis in the Sirab Formation leads one to suspect that the Mn content is a detrital heritage.

5.2.7 verage composition of carbonates compared to MUQ.

The concentrations of Major and Minor Elements as well as REEs in the typical section of the Sirab Formation at Wadi Shital ST-1 & ST-2 were normalized to the MUQ. Figure 5-16 shows that compared to Andesite AGV-2 and marine dolomite, the concentration curves for Major Elements P, Mn and Al diverge in the distribution profile of the section of Wadi Shital ST-1 & ST-2 with respect to the profile of Andesite which also diverges from the profile of marine dolomite. Fe and Ca appear to have similar profiles in Andesite, marine dolomite and in Wadi Shital ST-1 & ST-2 while Mg is similar in marine dolomite and Wadi Shital ST-1 & ST-2 while it diverges in the Andesite. U is similar in marine dolomite and Wadi Shital while it diverges in Andesite. Ni, Sm and Lu are similar in Andesite and Wadi Shital ST-1 & ST-2 but diverge in marine dolomite. Dy and Y are similar in marine dolomite and Wadi Shital ST-1 & ST-2 but diverge in Andesite.

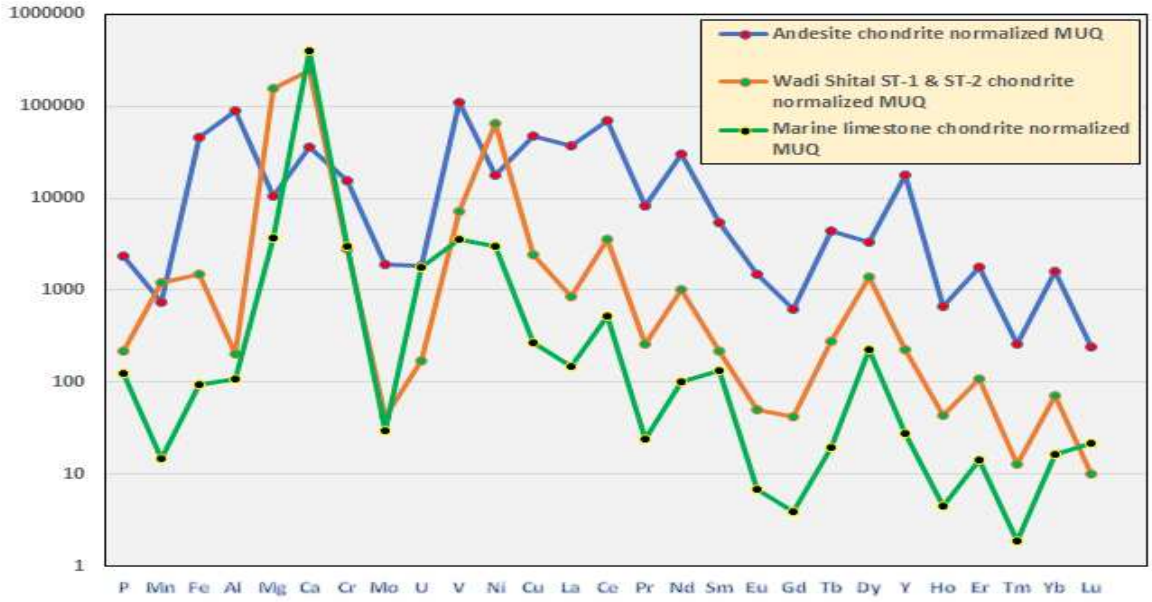

Figure 5-17: *Spider diagram showing the distribution pattern of MUQ-normalized chondrite major and minor geochemical element concentrations for Infracambrian sediments of the Sirab Formation as well as in AGV-2 andesite and marine dolomite of Devonian age.*

5.3 Wadi Shuram WS9 and Wadi Aswad (WA1 & WA2).

The analysis of Major Geochemical Elements from the Wadi Shuram WS9 as well as Wadi Aswad WA1 and WA2 field sections was carried out using analytical results from the ALs Laboratory (OMAC Laboratories in Ireland) obtained on the samples of these sections. The method of calculating REEs used by the ALs laboratory is based on the average of the concentrations of REEs in the chondrites normalized to PAAS. Calculation detection limits as well as additional laboratory Elements are presented in appendix 3.

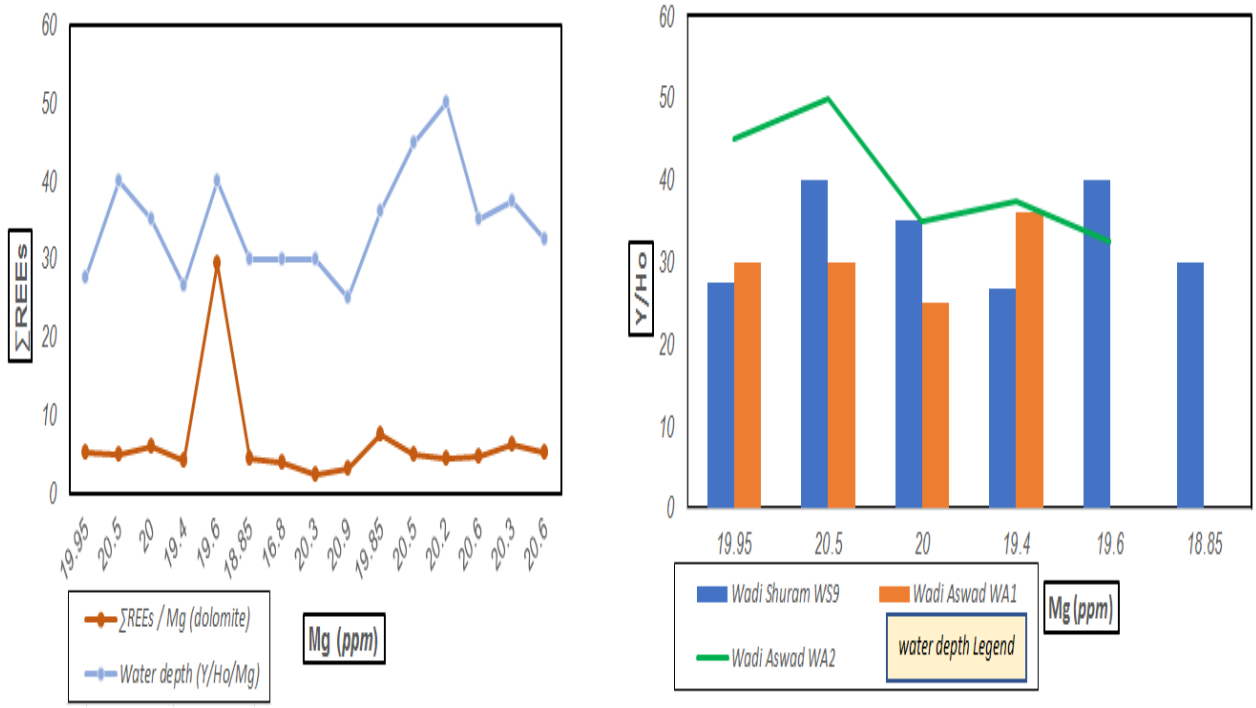

Figure 5-18: *Graph showing the distribution relation of ∑REEs compared to the concentration of Mg contents in the sediments as well as, the chemonstratigraphic relation of the concentrations of Mg contents in the sediments compared to the water-sediment interface (Y/Ho). Sections Wadi Shuram WS9; Wadi Aswad WA1 as well as Wadi Aswad WA2.*

The REEs distribution curve is closely linked to that of the Mg concentration concentration (figure 5-18 a). With the exception of the STF 185 level in the Wadi Shital section ST-1 & ST-2, the profile of the REEs and Y/Ho are identical in the paleo-marine description of the three (3) sections of the Sirab Formation which are analyzed in this thesis. Indeed, the Y/Ho curve shows that the REEs and Mg contents in the sediments of the Wadi Shuram WS9, Wadi Aswad WA1 and Wadi Aswad WA2 sections remain below the water-sediment interface line. As such, REEs can therefore constitute a good

screening tool for analyzing the chemostratigraphic description of the Major Elements.

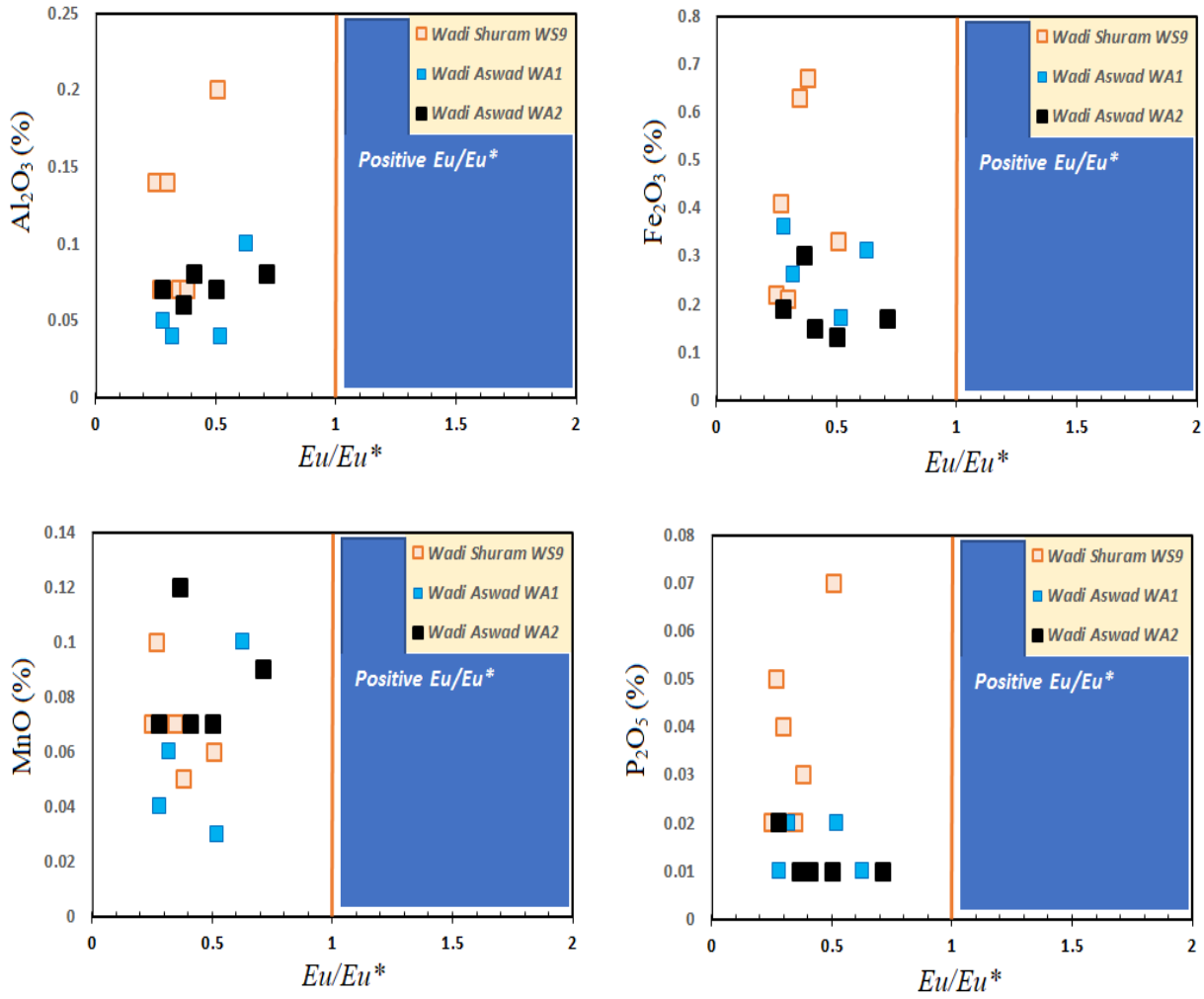

Figure 5-19: *Major Element plots (Fe, Al, Mn and P) on Eu/Eu* for the determination of Eu anomalies compared to concentrations in percentage of Major Elements (section Wadi Shuram WS9, Wadi Aswad WA1 and Wadi Aswad WA2).*

All samples from the Wadi Shuram WS9 sections as well as Wadi Aswad WA1 and WA2 have negative Eu anomalies. Meyer et al., (2012) consider that larger positive Eu* anomalies may be present where seawater is mixed with hydrothermal fluids. In view of the results of Eu anomalies in the three (3) sections of the Sirab Formation analysed in this thesis in relation to the absence of effective diagenesis, it is not possible to imagine any role for fluids hydrothermal, active when filling the Sirab Formation. On the other hand, Jarvis et al., (1989) estimate that apparent Eu* anomalies may result from interference with barium oxides formed during analysis. This can be assessed by measuring the concentrations of Ba. However, for all of our samples belonging to different sections of Sirab Formation analysed in this study, Eu anomalies are negative and there less evidence that the final results of Eu/Eu* found are caused by oxide barium interference.

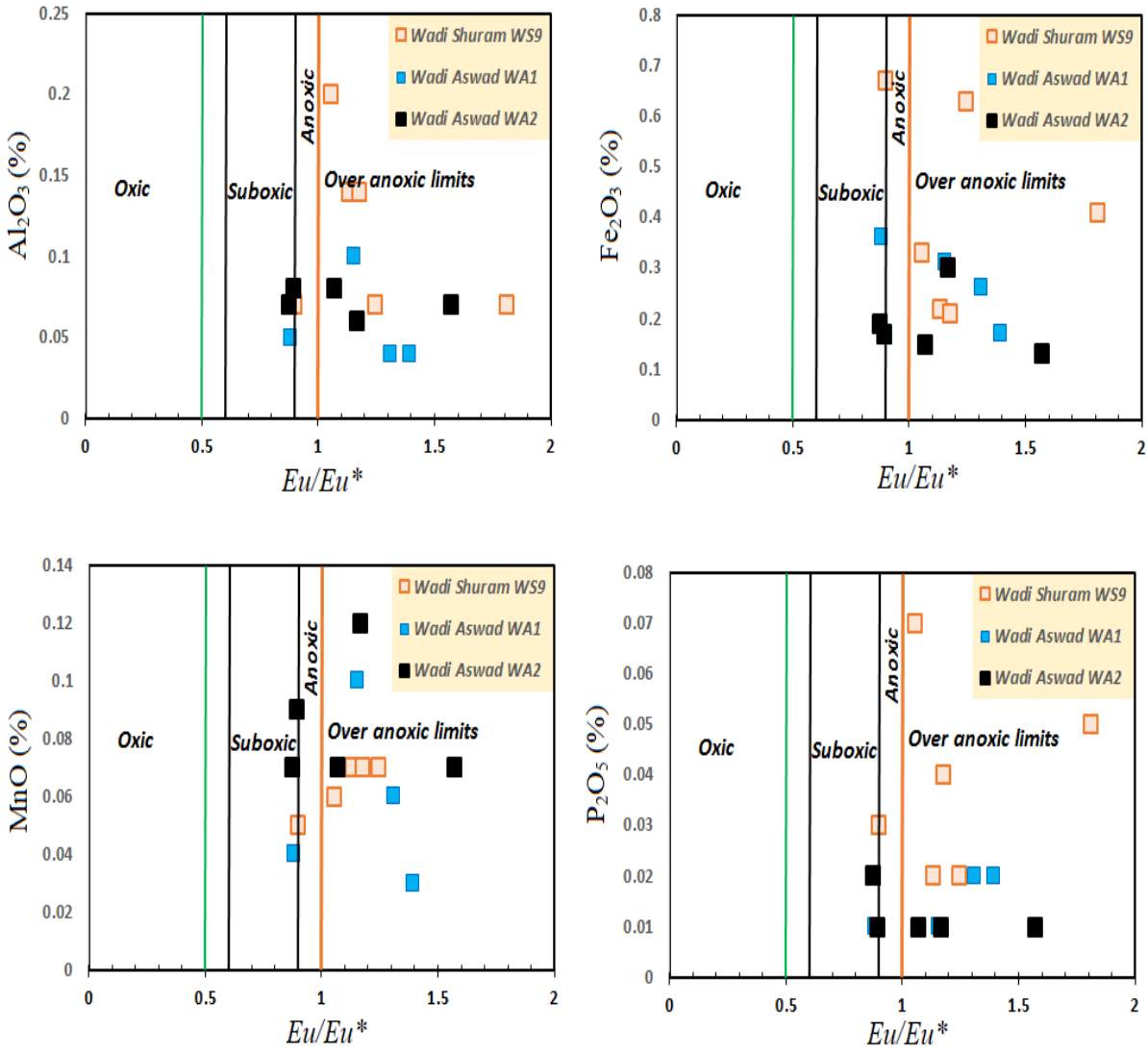

Figure 5-20: *Major Element plots (Fe, Al, Mn and P) on Ce/Ce* for the determination of Ce anomalies compared to concentrations in percentage of Major Elements (section Wadi Shuram WS9, Wadi Aswad WA1 and Wadi Aswad WA2).*

Like the typical section of Sirab (figure 5-5), the Wadi Shuram WS9 as well as Wadi Aswad WA1 and WA2 sections also exhibit a high anoxic potential (figure 5-20). Except by default for abnormal La/Nd ratios which can lead to an erroneous calculation of the anomalies which are not related to the geochemistry of this Element, we can admit at this point that there is a redox convergence of anoxic conditions for the Formation of Sirab through its different field sections.

5.3.1 REEs and correlation of Major Elements.

A) Section Wadi Shuram WS9.

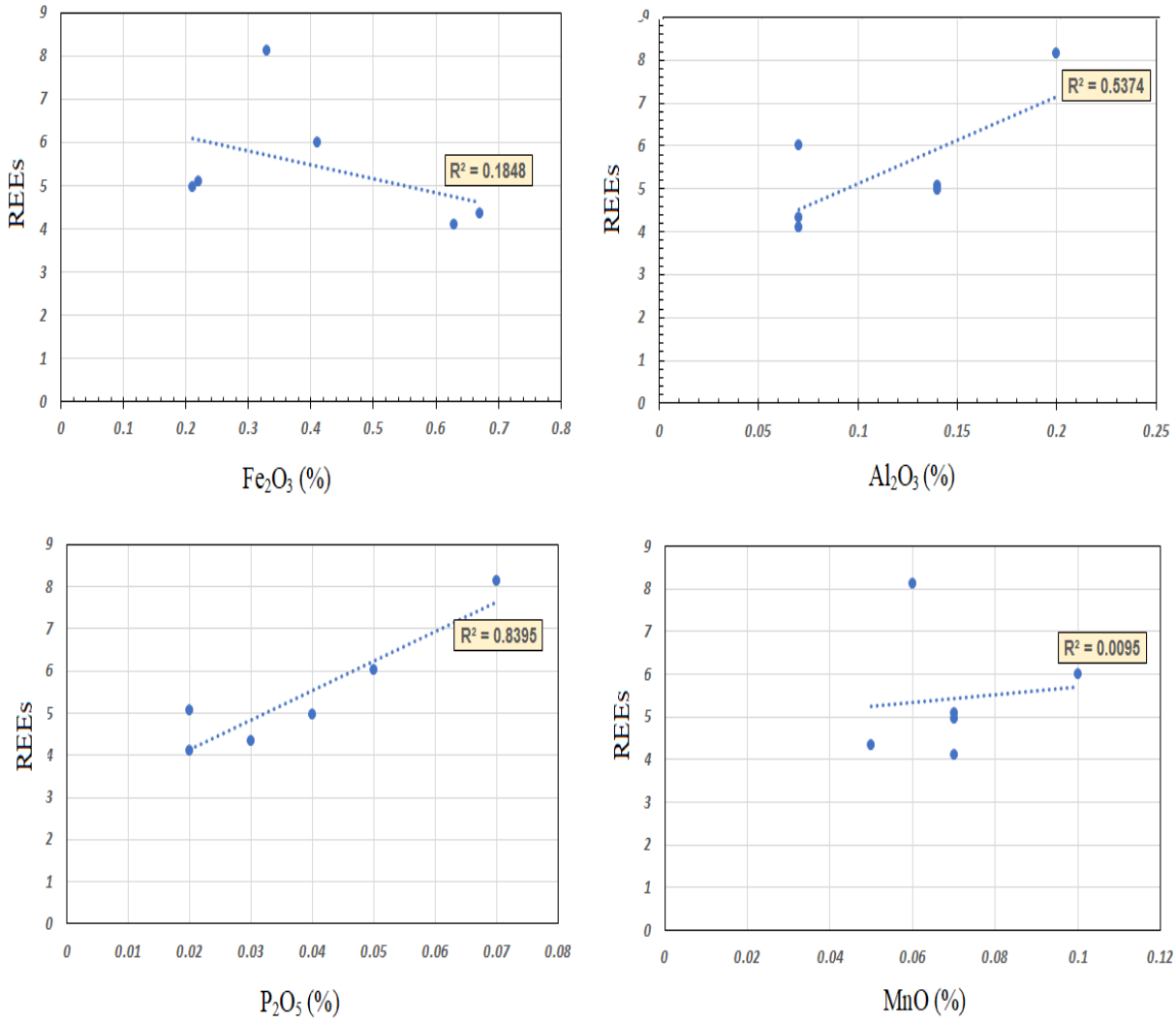

Figure 5-21: *Binary diagrams comparing the fractionation of Rare Earth in carbonates with the Major Elements Fe (%), Al (%), Mn (%) and P (%). Section Wadi Shuram WS9.*

The deciphering of the six samples of the Wadi Shuram WS9 section undertaken in this thesis (figure 5-21) shows that the Aluminum Al_2O_3 (%) and phosphate P_2O_5 (%) contents are the only ones to have R^2 correlation ratios favorable to the REEs. The samples used here in this section were carefully selected from the upper Shital horizon (depotcenter, facies of Conophyton Reefs). The Major Elements correlations in this section can be compared to those of Wadi Shital ST-1 and ST-2 to find similarities between REEs distribution and Major Element concentrations. However, in Wadi Shital ST-1 & ST-2 (figure 5-9), Fe concentrations were calculated in ppm and not in percentage. Fe (ppm) concentrations in the type section of Sirab are correlated to REE while Fe (%) in ppm is not in Wadi Shuram WS9. Statistically, the six carbonates selected as analytical samples in the Wadi Shuram WS9 section represent a very small number of the total volume of the section which extends beyond 190 m. The aluminum which remains stable during or in the absence of general diagenesis in the sediments is however enriched in all field sections of the Sirab Formation. Thus, aluminum levels may indicate contamination of carbonates by chemotratigraphic solutions of terrigenous rather than marine nature. As for phosphate, these low concentrations in the section of Wadi Shuram WS9 can be considered as a result in the mixing zone.

B) Section Wadi Aswad WA1.

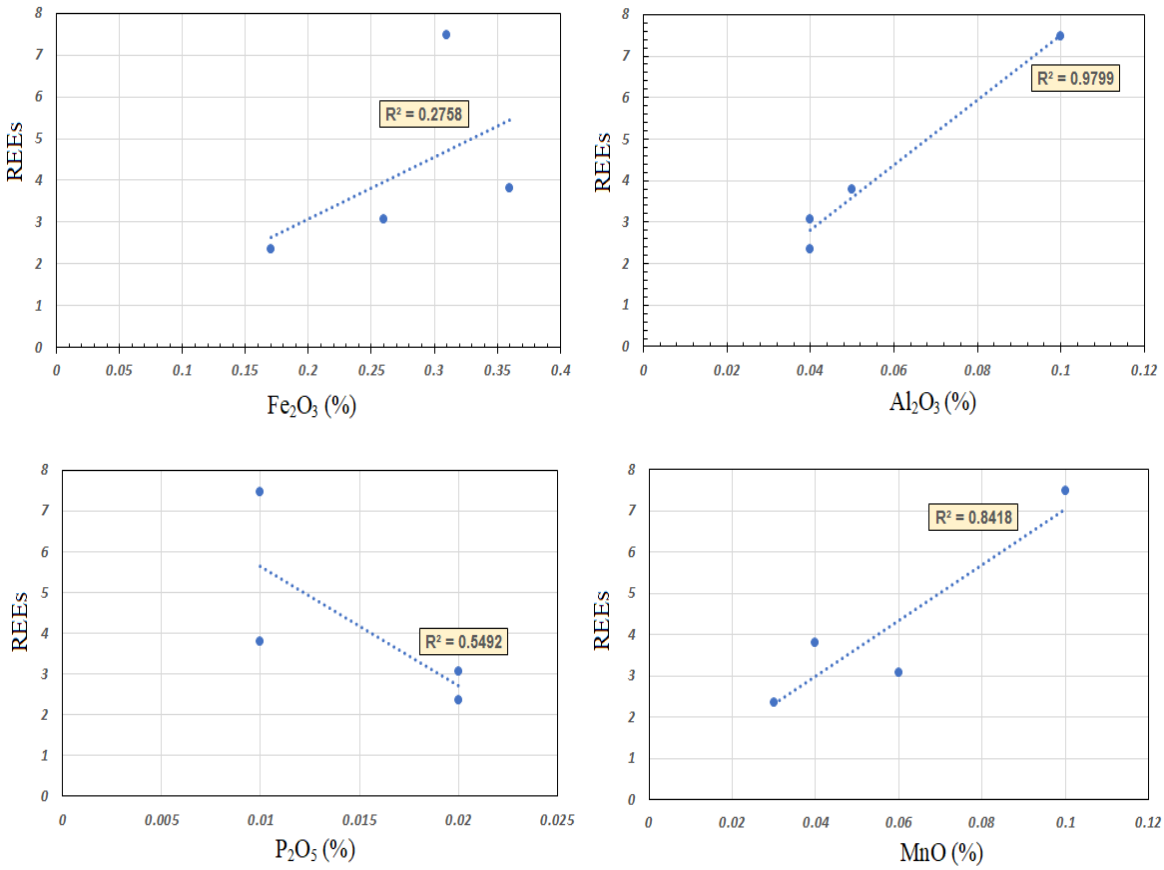

Figure 5-22: *Binary diagrams comparing the fractionation of rare earths in carbonates with the major elements Fe (%), Al (%), Mn (%) and P (%). Section of Wadi Aswad WA1.*

Almost the same as for figure 5-21, The decryption of the four samples of the section of Wadi Aswad WA1 undertaken in this thesis (figure 5-22) shows that, the concentration contents of Aluminum Al_2O_3 (%) and phosphate P_2O_5 (%), plus manganese MnO (%) have favorable R^2 correlation ratios for REEs. Statistically, these four carbonates selected as analytical samples in the section of Wadi

Aswad WA1 represent a limiting number of the total thickness of the section which extends beyond 80 m but can represent for the only facies of Thrombolite reefs of the section Wadi Aswad (figure 2-1) an excellent indicator of the contamination of carbonates by Geochemical Elements whose chemostratigraphic compositions are of terrigenous origin such as Aluminum.

C) Section Wadi Aswad WA2.

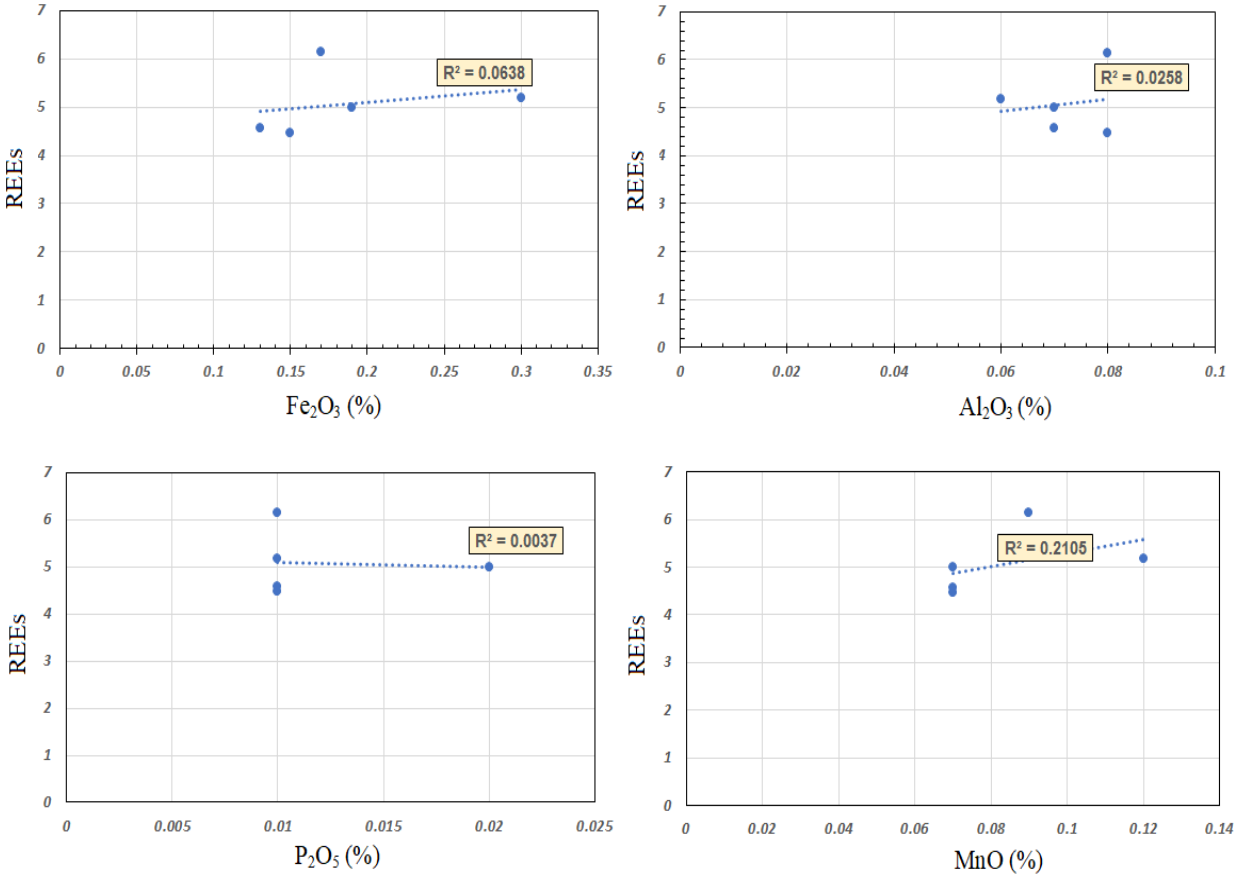

Figure 5-23: *Binary diagrams comparing the fractionation of rare earths in carbonates with the major elements Fe (%), Al (%), Mn (%) and P (%). Section Wadi Aswad W2.*

Unlike the Wadi Shuram WS9 and Wadi Aswad WA1 sections, the Wadi Aswad WA2 section does not indicate any possible correlation between the REEs and the Major Elements Fe_2O_3, Al_2O_3, P_2O_5, MnO. Wadi Aswad WA2 is the only field section analysed in this study that significantly differs from the point of view REEs/Major Elements compared to the other three sections including Wadi Shital ST-1 &

ST-2 (typical section of Sirab), Wadi Shuram WS9 (Conophyton Reefs depotcenter in upper Shital), as well as Wadi Aswad (Thrombolytic facies WA1 and Thrombolite-Oncolite facies WA2).

5.3.2 Contamination compared to average PAAS values.

In sediments, siliciclastic detritus is the main source of REEs. The REE profiles in the shales will reflect the REE contents in the post-Archean Middle Shales (PAAS), which represent the mean composition of the crust (Taylor and McLennan, 1985). In contrast, authigenic sediments with negligible detrital influence can potentially preserve the Rare Earth composition of seawater (Mclennan, 1989). Monitoring of the detrital fraction is necessary to assess the enrichment of Elements sensitive to oxidation-reduction compared to their detrital component (crustal). Elements incompatible with short residence times in seawater are ideally suited for this, as they will be transferred almost quantitatively to sediments, and therefore should closely reflect the composition of the continental crust (Taylor and McLennan, 1985; Webb and Kamber, 2000). However, some of these Elements are highly dependent on the source area and the grain size (Taylor and McLennan, 1985; Johnson and Grimm, 2001).

The correlations of REEs with detrital sources (enriched LREEs) in the three study sections of the Sirab Formation that are exploited in this thesis diverge between Wadi Shital ST-1 & ST-2 (figure 5-9), Wadi Shuram WS9 (figure 5-21), Wadi Aswad WA1 (figure 5-22) as well as Wadi Aswad WA2 (figure 5-23). These deviations may be related to the sources of origin of the sediment or also to the constituent size of the grains. Thus, if (REEs) which host detrital

components of the sediment are analyzed on the sole aspect of the Al_2O_3 content, this amounts to restricting the grain size of the sediment to clays. However, in Sirab, carbonates are petrographically described as grainstone, packstone, wackstone (dolostones) and mudstone (dolomicrite); see Gold (2010) or Nicholas and Gold (2012). In this way, the analysis of detrital fractions REEs which tend to LREEs was completed by the analysis of Th and Zr by comparing their average in the crust (PAAS). Knowing that Th is largely independent of factors such as grain size while diagenetic modification of Zr concentrations is unlikely in carbonate rocks, as this Element is mostly associated with non-carbonate components (Veizer, 1983a).

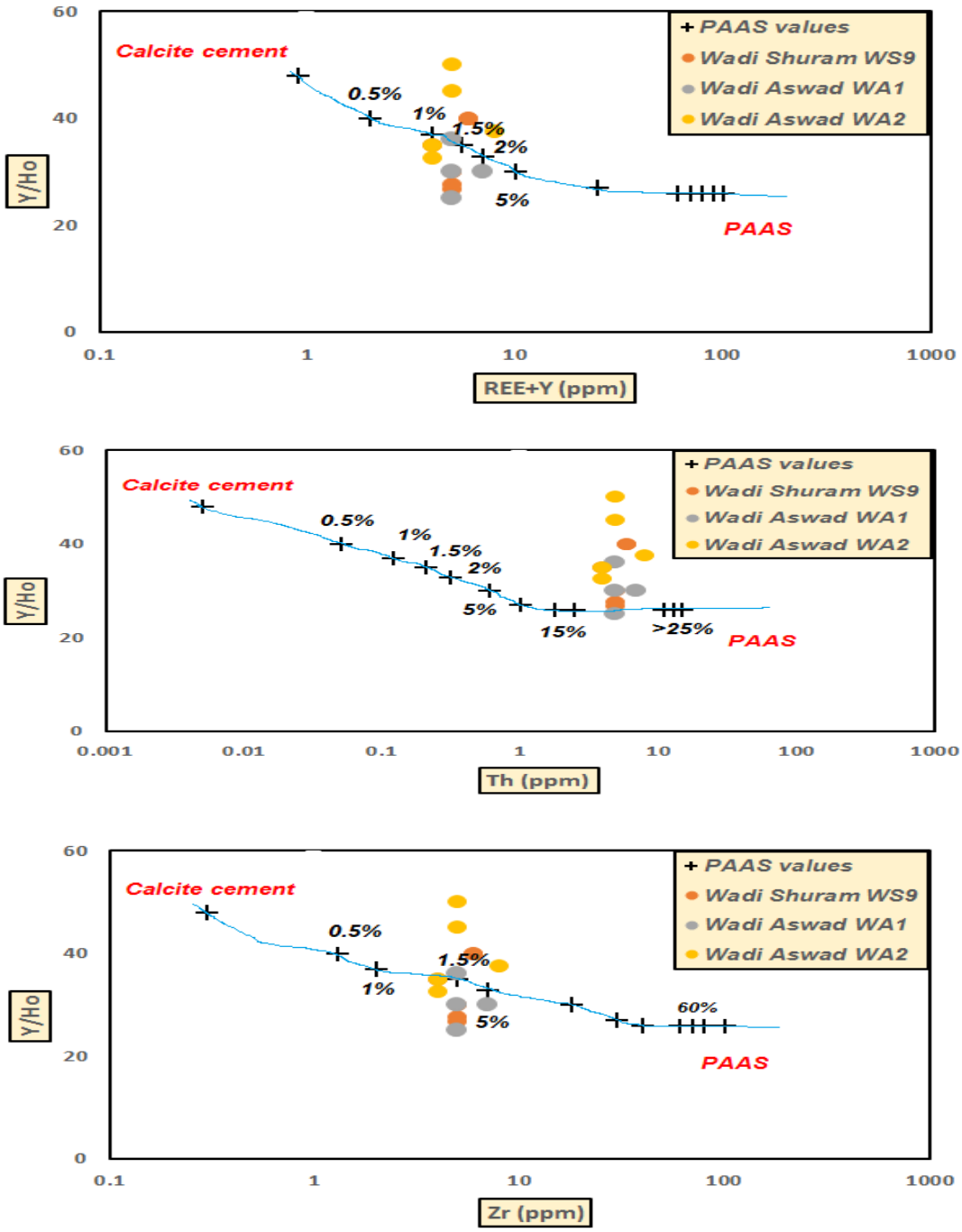

Figure 5-24: *Conservative mixing lines between sections Wadi Shuram WS9, Wadi Aswad WA1 as well as Wadi Aswad WA2 on Y/Ho versus. Zr, Th, and ΣREE+Y data. Calcite cement value it is what used by Nothdurft et al., (2004) and PAAS value it is what used by Taylor and McLennan (1985).*

It can be seen from figure 5-24 that the REEs, Th as well as Zr in the Sirab Formation through the Wadi Shuram WS9, Wadi Aswad WA1 and Wadi Aswad WA2 sections are depleted compared to their mean concentrations in the crust (PAAS). Th is depleted at less than 25% while Zr is less than 6%.

5.3.3 Discussion of chapter five.

The Al-Huqf Supergroup in theAl-Huqf region of Oman contains several field sections of the Sirab Formation. This situation leads to the placement side by side of more than one stratigraphic series of field which can then be classified step by step to geographically reconstruct the entire Formation (figure 1-5). The sedimentary facies encountered in the field in each of the stratigraphies within the sections constitute the main part of the Sirab sedimentology. The sections present common characteristics whose facies content is more developed or well preserved in certain geographical locations than in others. The composition of the sediment from the chemotratigraphic point of view (Major Elements) reflects local or temporary variations according to the field sections. For example, field observations in the locality of Wadi Shuram show that, the WS9 section combined with the WS1 to WS10 sections, offers a greater thickness of the Shital Member. In particular, the Thrombolite facies with the Conophyton Reefs and the stromatolites of the upper Shital bioherm are defined in WS9. This field section constitutes the depotcentrer of the Shital Member. On the other hand, in the typical Sirab section at Wadi Shital ST-1 & ST-2 and in the WA1 section, the facies defined in upper Shital also occurs in the same lithostratigraphic order of the Sirab Formation without however reaching a maximal flooding surface as in WS9.

In the absence of a chemotratigraphic comparison of the Major Elements between these three field sections, it would have been possible to imagine any sort of temporary variation in the order of Sirab deposition across the different field sections. This would then have affected the chemotratigraphic content of the sediment bed levels of the Formation.

Here, in the analysis of the Major Elements presented in this chapter 5, the $\delta^{18}O$ oxygen isotopes keep values close to the primary in all the Sirab sections and particularly in the typical Sirab section at Wadi Shital ST-1 & ST -2, all VPDB values (‰) of $\delta^{18}O$ are negative (figure 4-2). Ce/Ce* anomalies across Wadi Shital ST-1 & ST-2, Wadi Shuram WS9, Wadi Aswad WA1 as well as Wadi Aswad WA2 seem to confirm that the redox condition in all sections of Sirab was the same (anoxic). Anoxic deposits crossing the Ediacaran-Cambrian are a feature of the Ara Group in Oman (Schroder and Grotzinger, 2007) as well as in Lower Cambrian microbialites of the Jaíba Member in the Bambuí Basin in Brazil (Uhlein, Fabrício, Caxito et al., 2020).

The set up of the upper Shital unit throughout the Formation records a positive $\delta^{13}C$ peak (figure 4-1). Field observations indicate that, during the transition from the Ramayli Member to the Shital Member, the lower Shital unit is made up of a deposit of cyclic carbonates composed of α and β facies beds. The first α facies seems to be

developed under a larger volume of water, while the second β facies alternates under a thin layer of water (figure 1-11). In the lower Shital, the bioherm seems not to be well developed during the cyclic filling. However, throughout the Al-Huqf region where the Sirab outcrops, the presence of a sandstone horizon is inserted between the lower Shital and the upper Shital (Gold, 2010). This sandstone horizon discretely represents a subtle subdivision of the Shital Member as (Middle Shital). This sandstone is thin and is found in all the field sections mentioned by Nicholas and Gold (2012) at the passage of the upper Shital. The Conophyton Reefs bioherm appears to have emerged across the Formation from deposits above the sandstone unit with positive $\delta^{13}C$ values while $\delta^{13}C$ carbon isotopic values, VPDB (‰) located immediately below the sandstone horizon oscillate slightly between negative and positive values.

Comparing the development of the bioherm to the passage of the upper Shital with the positive peak in $\delta^{13}C$, it is deducible that this moment of deposition (upper Shital) introduces a temporary change in the geochemical carbon composition of the Formation through the Ediacaran-Cambrian. The change in the primary isotopic signature is proof of this. However, based on evidence of persistent anoxia, the environmental redox parameter in the Sirab Formation and the Ara group appears similar for these two Formations of relatively equivalent age. But data on $\delta^{13}C$ carbon istopes in the Ara group through the Ediacaran-Cambrian show that $\delta^{13}C$ is marked by a characteristic negative curve (Schroder and Grotzinger, 2007). The

age of the Ara group varies between 550 and 540 Ma (Loosveld et al., 1996; Amthor et al., 2003).

Besides the Ara Group, the thrombolite, grainstone, and microbial facies of the Jaíba Member in the Bambuí Basin in Brazil, lie stratigraphically in the lower Cambrian, slightly above 520 Ma, and the Jaiba Member records positive $\delta^{13}C$ isotope values (VPDB ‰ around 0 - 4 ‰, which can be close to the VPDB ‰ values in the upper Shital for the Sirab Formation which oscillate around 0 - 7 ‰). The same is true for the parts below the Jaiba Member that lie between the Ediacaran-Cambrian (Serra de Santa Helena Formation and Lagoa do Jacaré Formation), which also have positive $\delta^{13}C$ isotopes. See the work of Gabriel Uhlein, Fabrício, Caxito et al., (2020). As such, positive $\delta^{13}C$ in the bioherm spanning Ediacaran-Cambrian time is a recognized geochemical feature in other basins around the world.

In all the sections of Sirab studied in this thesis, the majority of the Y/Ho ratios measured on the samples record Y/Ho >26 and Y/Ho <45 values. Lawrence et al. (2006) find that the ratio Y/Ho = 26 is favorable to the presence of fresh water while Y/Ho > 45 is favorable to sea water. It seems that a strong dilution of the ratio Y/Ho > 45 of the sea water is the main source of the loss of the marine signal of the Sirab Formation and as estimated in chapter 3 (figure 3-43), a mixture may have been introduced on the original composition of the

chemistry of the seawater, at the water-sediment interface across the Formation.

The terrigenic fractions are enriched in REEs because the weathering of rocks is more of a phenomenon that takes place in a continental environment than in a marine environment. As such, the instability of minerals caused by weathering of rocks exposed to environmental conditions in the continent accelerates the fractionation of REEs with more abundant LREEs. The HREEs are well preserved in the marine environment and as the alteration is rather rare, the profile of the HREEs hardly registers any variation within the marine rocks which contain them while, the LREEs which cannot be fractionated in the medium marine due to the absence of weathering of the rocks that contain them, are generally lacking within marine sediments. Ideally, analysing the Major Elements in relation to their paleoenvironment requires examining the redox reasons that caused their concentrations in the sediments. Current observations provide a better understanding of the accumulation of certain geochemicals in sediments. For example, Al and Fe, accumulate in current continental environments due to the alteration of continental rocks and the dehydration of phyllitous minerals from which Al is substituted by Fe. The marine environment contains about 15 ppm of Fe and the deposition of both Fe and Al in the marine environment is most often the product of the transfer of terrigenous fractions to the ocean basin. Mn is often enriched in the presence of Fe as a result of post-burial redox that occurs during diagenesis. This slow and in-depth transformation of the

sediment (diagenesis) eliminates the Sr in the calcite network and replaces Mn. As for P, it is found in the composition of plants (terrestrial and aquatic plants as well as in the composition of the teeth of terrestrial organisms and fish).

Given that the REEs are dependent on the mineralogical composition of the sediment subject or not to the weathering process of rocks, the most abundant elements in dolostones and dolomicrite after Ca and Mg were measured against the REEs. In the typical section of Sirab at Wadi Shital ST-1 & ST-2, the REEs are compatible with Fe, Al, and P but not with Mn (figure 5-9) while the distribution profile of REEs split into LREEs and HREEs show a clear tendency for Fe, Al, Mn as well as P to exhibit similar profiles to LREEs (figure 5-8). Under the sole condition of a continental environment in the absence of all forms of mixtures with the marine environment, Al would be an excellent indicator of the redox state of the deposition environment. However, the Cr, Mo, U, V, Ni and Cu, which are the redox indicators that can help measure and differentiate the authigenic and non-authigenic enrichments of Al, do not all converge. As such, no distinct depository environment between continental and marine appears to be the main feature of this field section (figure 5-10).

The P (figure 5-11 and figure 5-12) was measured against LREEs, HREEs and Th. And like Al, no key indication seems to differentiate its enrichment in continental or marine environments. Just as the

composition of Fe (Fe_2O_3 and FeO) theoretically deduced from the weight of the Fe_{total} measured by ICP-MS, does not allow to differentiate the ferric Fe from the ferrous Fe, which would have helped to place the Fe in a particular context of environment (figure 5-13, figure 5-14 and figure 5-15).

Overall, relative Mn enrichments do not appear to be a direct consequence of diagenesis in the Sirab Formation (figure 5-16). Moreover, even if diagenesis proved to be equally effective for the entire Sirab Formation, the absence of oxygenation within the sediments would not have allowed the development of manganese carbonates from soluble Mn^{2+} which should be mobilized by the diagenesis redox parameter. As such, the proper indication for relative Mn concentration remains the transfer of Elements from Mn-rich detrital geologic materials. Furthermore, the average composition of carbonates in Sirab diverges on the one hand between the compositions of the Geochemical Elements in andesite and in marine limestone (figure 5-17).

In other sections of Sirab including Wadi Shuram WS9, Wadi Aswad WA1 and Wadi Aswad WA2, anoxia continues (figure 5-20). There is no positive Eu/Eu* anomalies in all the sections of the field studied in this thesis (figure 5-4, figure 5-7 as well as figure 5-19). The REEs measured against the percentage of Major Elements diverge from one section to another and also diverge according to the percentage of the

Element analysed (figure 5-21, Figure 5-22 as well as figure 5-23). Here again, it seems from the REEs/Major Elements correlation ratios, that the distributions of the REEs in relation to the sediment environment did not record a single environmental parameter, although the profile of the LREEs was corroborated at profiles of Major Elements in the typical section of the Sirab (figure 5-8). Logically, in the absence of environmental fluctuations such as the Y/Ho ratios (mainly between >26 and <45) on all the sections of Sirab analysed in this thesis, the measurements of the REEs in relation to the Major Elements should display certain correlation constancies.

LREEs seem to be an intrinsic feature of continental rock weathering. As such, the rocks of the crust including shales (PAAS) are generally enriched in REEs. Because, the more the weathering of the rocks occurs, the more the minerals that contain the REEs are released into the sediments where they subsequently participate in the enrichment of the chemostratigraphy of the bed levels in the sediments. A good example which illustrates this phenomenon in this thesis is the STF 185 level. This unique petrographic mud sample has on average (X50) more Fe, Al, Mn, P content, and on average (X100) more than REEs content compared to the rest of the other samples which are petrographically superior to the sludge (e.g. table 5-2 and Table 5-3). However, compared to PAAS, REEs are poorly enriched in the Sirab Formation, specifically in the Wadi Shuram WS9, Wadi Aswad WA1 and Wadi Aswad WA2 sections (figure 5-24). This seems to prove that, the carbonates in the Sirab Formation were contaminated by

terrigenous fractions but that in all equal proportions and petrography included, their contaminations cannot calibrate the level of enrichment of the REEs in the crust.

6 ***Sixth chapter***: *Traces and REEs Elements.*

6.1 Introduction.

The sedimentology in chapter 1 as well as the petrography in chapter 3 of this thesis agrees with the nomenclatures of the sediments. Among the samples analyzed, whether in the type section or in other field sections, we find dolomites (grainstone, packstone and wackstone size) and dolomicrite (mudstone size). The dolomites are thicker than the dolomicrites and are mainly present at the lower Ramayli while the dolomicrites are reported at the upper Ramayli for example or at the STF 185 level among the samples analyzed in this thesis. In the present study, the particle size analysis was not carried out on the selected samples. However, the results of geochemical analyzes indicate that the contents of certain Elements in the samples are more enriched than others (example: Ca, Mg, Fe, Al, Mn, P as well as K, Na, etc.).

On a completely different chapter, the global correlations of the isotopic indicators of carbon and oxygen in chapter 4, of the Y/Ho ratio, of the Ce* anomaly, indicate that there is no significant redox change on the environment of carbonates deposition, with the sole exception of a temporary change in carbon isotopes during the passage of the upper Shital which, however, does not modify the anoxia in the sediment nor the signature of the oxygen isotopes. The constancy of the environmental redox parameter seems to be confirmed by the absence of any significant trace of diagenesis in relation to the Mn content throughout the Formation (figure 5-10).

The precipitation of carbonates appears to be independent of the constituent size of the grains. Since in coarse or fine grained horizons, dolomite remains the main carbonate composition. However, the sample from the STF 185 level (dolomicrite) contains more Ca, Mg, Fe, Al, Mn, P (Major Elements) than in the other samples from the coarse-grained levels. As such, the grain size of the sediment, although independent of the redox parameter, of the accumulation of carbonates, can nevertheless indicate a change in detrital inputs during the deposition of the sediments. Thus, the Major Elements detected in the Sirab Formation stratigraphy can ideally serve as indicators to scrutinize the state of the depositional environment in relation to paleoecology as some Major Elements such as (Fe, Al, Mn and P) can lead to discriminate the type of the environment deposition.

Moreover, to avoid doubts about the influence of the size of the grains on the palaeo-ecological analysis of the Sirab Formation, it was necessary to resort to the geochemistry of Elements incompatible with short residence times in the water of sea which are independent of grain size. To do this, the use of Elements that escape petrographic requirements (grain size of the sediment) such as Rare Earth and Trace Elements are essential. Th is largely independent of factors such as grain size. Thorium concentrations relative to other Elements such as Ti, Zr, and U content can therefore help filter the chemostratigraphy of deposits in addition to the analyzes already developed in previous chapters.

Veizer (1983a) finds that diagenetic modification of Ti, Th and Zr concentrations is unlikely in carbonate rocks. On the other hand, the REEs profiles published in different types of environments are currently better known and better documented throughout the world so that by crossing the REEs profiles with respect to known environments while adding the excursions of Th, Ti, Zr and U in relation to their affinities of terrestrial or marine concentrations that one can reconstruct the palaeo-ecology of the Formation.

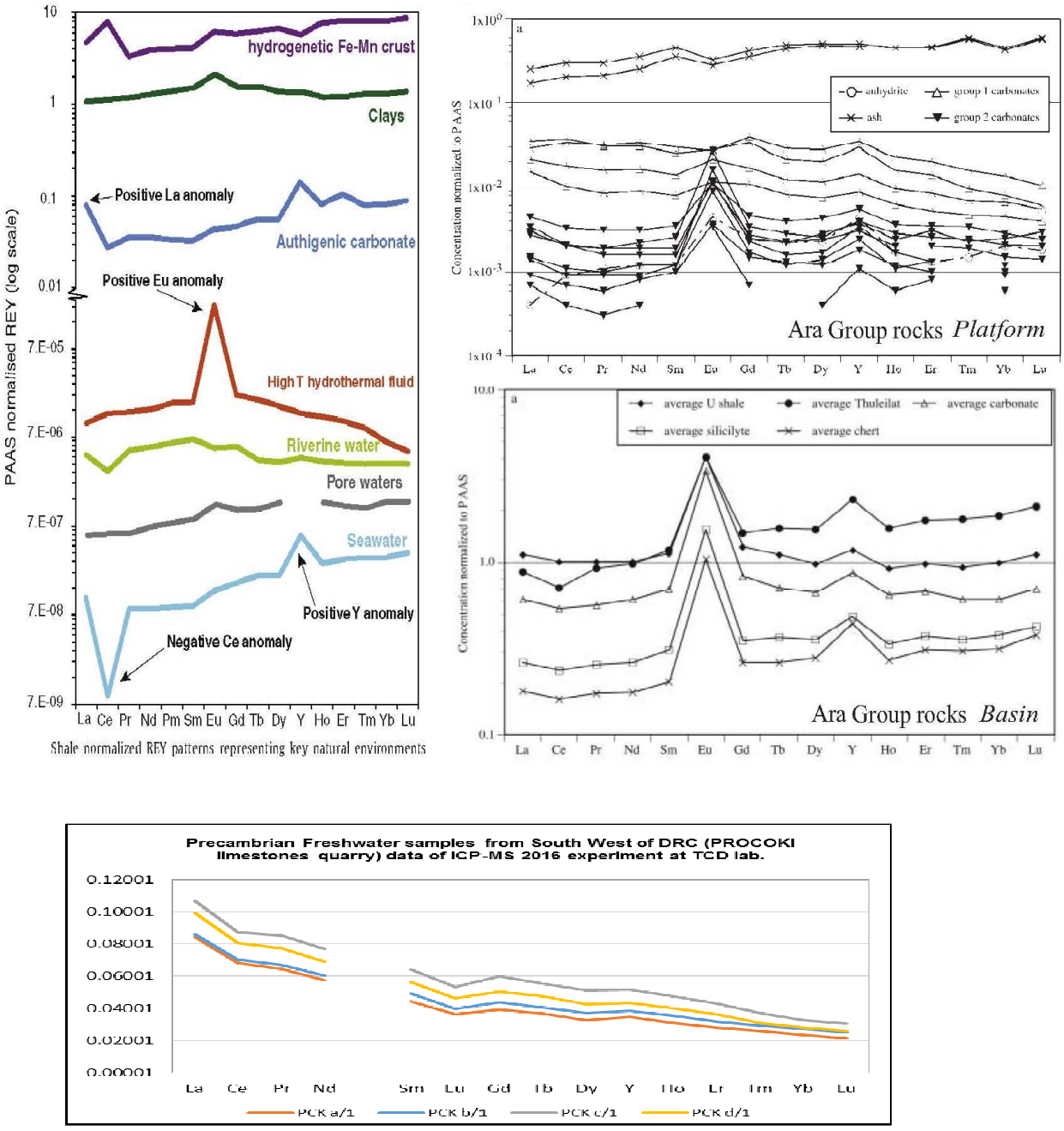

Figure 6-1: *different profiles of REEs according to the deposit ramp and basin environments known throughout the world. On these data, PASS normalised REY for different types of environement are from data Tostevin, Graham et al. (2016), Ara Group platform and basin are from Schroder and Grotzinger (2007) and Precambrian freshwater Procoki are from TCD lab (2016) also exeperimented by Mangoni (2020).*

Figure 5-1 illustrates a number of known environments and sedimentation basins around the world. This figure provides a glimpse of the characteristic features of different types of environment. Using the example taken from Tostevin, Graham et al., (2016), the profiles of (hydrogenic Fe-Mn crust, clays, authigenic carbonate, elevated hydrothermal fluid, river water, interstitial waters as well as seawater) are included. This example makes it possible to compare the results of the REEs in relation to the Sirab Formation.

Gold (2010) assigns the Sirab Formation an approximate and/or equivalent age to that of the Ara Group in the SOSB. However, she will recommend in the conclusion of her thesis, to continue high-precision chemostratigraphic studies to determine the architecture of the sedimentary facies of the Sirab Formation, mainly the study of the facies encountered in the Aswad Member.

Schroder and Grotzinger (2007) undertook the chemostratigraphic study of the Ara group from the caratts of the probes carried out in the Ara platform (Birba) as well as in the parts of the basin (U as the basal Formation of the basin, Athel as the intermediate Formation as well as than Thuleilat as an upper basin Formation). Sedimentological and chemostratigraphic correlations of Sirab to the Ara group and other geologic environments on the Ediacaran-Cambrian time boundary are presented in the general discussion of this study. REEs profiles in the Ara group platform and parts of the basin can be exploited for further

chemostratigraphic correlation between the Ara Group and the Sirab Formation.

In addition, towards the south-west of the DRC, Neoproterozoic limestones outcrop in the quarry called Procoki. The geological descriptions of the quarry as well as the petrographic nature of the rocks encountered are described in appendix 5 to the volume 2 of this thesis. In summary, freshwater stromatolites (Y/Ho ~ 29) abound on the outer Procoki limestone ramp and the Rare Earth profile of southwestern DRC can also be used for chemostratigraphic correlation with sediments from Sirab which throughout this study, presented mostly Y/Ho ratios greater than 26 and less than 45.

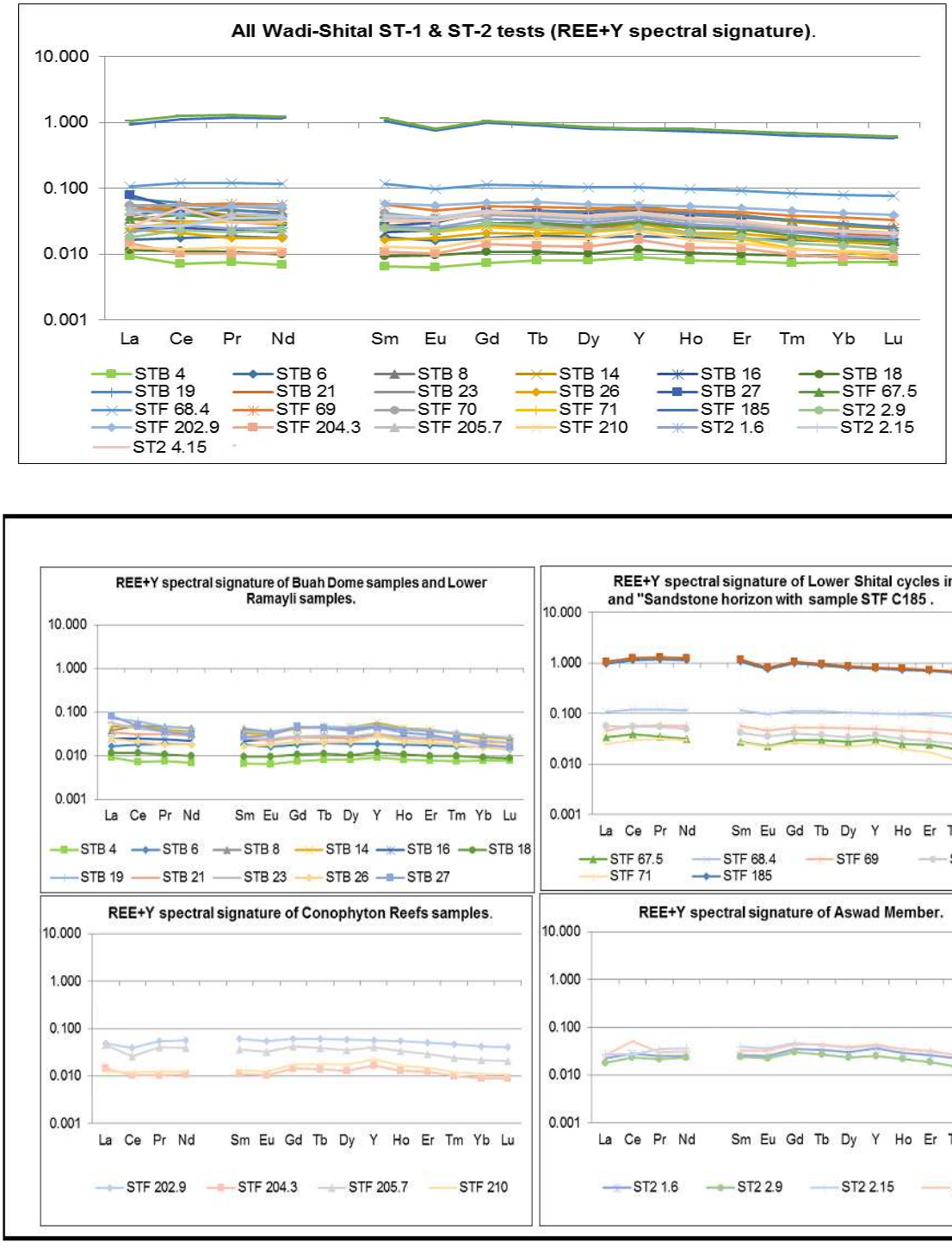

Figure 6-2: *REE + Y spectral signature of Wadi Shital ST-1 & ST-2 carbonates.*

Analysis of samples from the mainly Sirab section indicates that the REEs have an almost flat distribution profile (figure 6-2). Here, the Y/Ho ratios which imply an enrichment of the LREEs rather seem to show that the latter are in fact relatively enriched compared to the MREEs and HREEs. Taylor and McLennan (1985), Banner et al., (1988), report that in the platform and basin of the Ara group, the samples of dolomites located at A4C and those located in the shales of the basin (U and Thuleilat), show flat patterns of REEs. The models of the REEs of the platform and the Basin of the Ara Group do not allow correlating the latter with the ancient marine carbonate rocks.

In figure 6-1, the rocks of group 1 belonging to the carbonates of the Platform are those located above the ash level of the Ara Group. These rocks have the flat REEs signatures and as the stratigraphy rises from A4C, the carbonate rocks of group 2 gradually lose the flat REE signals. In the Basin, Schroder and Grotzinger (2007) admit that the positive (Eu*) anomalies observed in the figure are erroneous anomaly values because the level of volcanic ash located in the platform below the A4C, is the only one to to have some. In the Basin, the anomalies measured in the rocks of the U and Thuleilat shales as well as in the Athel silicilites are analytical interfaces due to barium. Their eliminations (positive Eu*) should therefore reduce the profiles of the curves of the REEs to flat shapes.

Moreover, neither in the Sirab Formation nor in the Ara group, the Y/Ho ratios retain the marine water signature globally. In these two Formations, Yttrium (Y) has a slightly positive profile in platform carbonates, basin shales for the Ara group as well as in carbonates of the Sirab Formation. (Y) slightly positive may be further evidence for dilution of the original seawater signature by detrital solutions. Although the amount of contamination from the original marine carbonates varies depending on the terrigenous fractions that are transferred into the chemical composition of the marine water. In figure 6-1, the graph from Tostevin, Graham et al., (2016), in which different types of environment are illustrated according to profiles in REEs, the sediment-water interface records a positive Y signature coupled with negative celerium (Ce) as typically seawater signature.

Walter et al., (2000), Kimura and Watanabe (2001), recall that anoxia is a characteristic of carbonates of the Ara Group and in laboratory analyses of this study, this characteristic was also encountered in carbonates of the Sirab Formation, while the same anoxic condition has been recognized in other world environments that cross the Ediacaran-Cambrian time boundary. However, apart from the lack of sediment oxygenation which leads to positive Ce* anomaly values, laboratory analytical errors can also lead to similar results. Therefore, to check for true Ce* anomalies, the laboratory values of this Element must be checked against the corresponding Pr/Pr* ratio values.

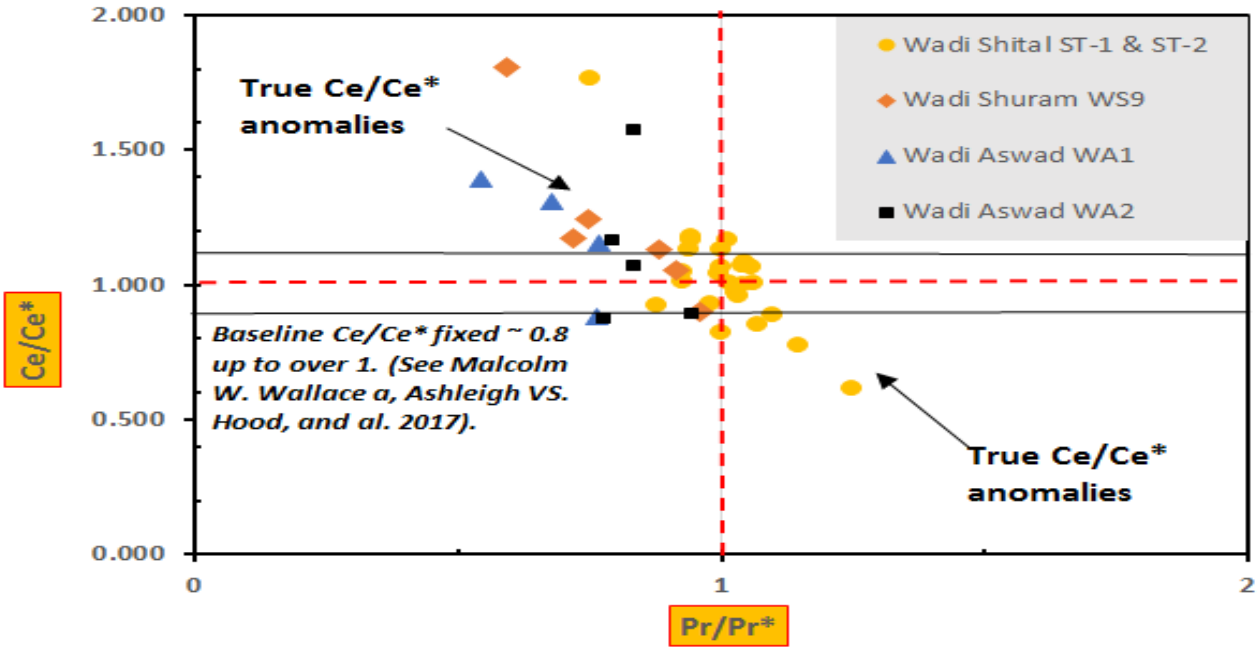

Figure 6-3: *Ce* Trues anomalies in Sirab Formation (sections Wadi Shital ST-1 & ST-2, Wadi Shuram WS9, Wadi Aswad WA1 and Wadi Aswad WA2).*

Compared to anoxic conditions and true Ce* anomalies, Mn is a good indicator of the redox state of the environment as the Element can become enriched in Mn oxides under oxic conditions while its reduction by diagenetic pathway produces Mn^{2+} which becomes soluble at the water-sediment interface and diffuses away from the reduction site (Morford et al., 2001). The relatively high Mn contents in the Sirab Formation vary considerably from the contents of the same Element reported in the platform and basin shales of the Ara Group by Schroder and Grotzinger (2007). In the platform, the Mn is in the order of 200 - 300 ppm while in the basin it is 200 - 800 ppm. In the analysis of this study, the measured percentages of MnO (%) on the section Wadi Shuram WS9 as well as Wadi Aswad WA1 and

WA2 appear much lower than those of carbonates (CaO% and MgO%) or about X100 less, moderately lower to SiO_2, Al_2O_3 and Fe_2O_3 (%) or about X10 less. The concentrations of MnO (%) approach those of (Na_2O% and K_2O %) in the majority of the samples. Measurements of Mn (ppm) by weight in the Wadi Shital ST-1 & ST-2 section remain lower than the weights of Ca, Mg, Fe and Al (ppm). But compared to those measured in the Ara group for the carbonates of the platform and the Basin, the Mn concentrations in the Sirab Formation are of the order of 600 to 2000 ppm as obtained on the typical section of Shital ST- 1 & ST- 2. These values are higher than those of the carbonates of the Ara group although the enrichment of this Element cannot be expressed at this stage as being the effect of a general diagenesis or even less, the effect of capture of Mn^{2+} ions by oxygenation in sediments.

However, Banner and Hanson (1990) consider that it is difficult to determine more precisely the results of the processes of diagenetic and redox enrichment in Mn to the water-sediment interaction. Nevertheless, in this study, the geochemical indicators (Mn/Sr, Mn/$\delta^{13}C$, and Mn/$\delta^{18}O$) which can help to scrutinize the enrichment in Mn in sediment by diagenetic way are not correlated with the lithology of the Formation.

It seems obvious that the profiles of the REEs in the Precambrian fresh water of the Procoki quarry as well as in the environments and in the minerals proposed by Tostevin, Graham et al., (2016), has been of little use in matching REEs profiles of the Sirab Formation, outside of Ara Group excursions. Nevertheless, an apparent contradiction remains in the Ara Group as well as in the Sirab Formation regarding the absence of a marine signature, or the evidence of widespread marine involvement for the Sirab Formation. Furthermore, the profiles of REEs in the two Formations of more or less equivalent age (Ara Group and Sirab Formation) recall a moderate involvement of terrigenous fractions in the dilution of seawater. Indeed, a high concentration of terrigenous fractions close to PAAS in the composition of carbonates in the Ara Group and Sirab Formation should lead to a profile characteristic of LREEs such as that observed in the Procoki quarry in the south west of the DRC (figure 6-1). For proof, Mattes and Morris 1990, Schroder et al., (2005) believe that the Ara Group Platform was weakly contaminated compared to PAAS, while the shales of the basin (U and Thuleilat) are contaminated by values close to those of PAAS.

6.2 Trace Elements and redox-sensitive correlation.

Th, Zr, Mo, U, V, as well as Ti were used as Trace Elements in this study to measure the change of redox signals.

Th: Th is present as a Minor Element in a range of heavy detrital minerals such as zircon, allanite, titanite and apatite (Deer et al., 1983; Mange and Maurer, 1992; Hermann, 2002; Salminen et al., 2005) but is generally present in greater abundance in the Th-rich phosphate mineral monazite. During weathering process, Th is transferred to the sediment via detrital heavy minerals. Authigenic sediments are generally poorly enriched in Th and this is inherited from the weathering of rocks before being transferred to the authigenic sediments. The control of Th in relation to the REEs makes it possible to overcome the enrichments of authigenic origin of this Element resulting from the degradation of the heavy and phosphate rocks which contain it.

A phosphate mineral such as monazite contains more Th so the low occurrence of this mineral in sediments can help correlate Th with possible detrital sources. On the other hand, Th can also be present in a range of secondary minerals such as thorite, huttonite, thorogummite as well as brockite and grayite (hydrated Th minerals; rhabdophane group phosphate) which are formed by chemical weathering of stable primary minerals such as apatite and allanite (Banfield and Eggleton, 1989; Berger et al., 2008). At the beginning of diagenesis, authigenic

monazite can also form by dehydration of rhabdophan but these mineral phases are considerably smaller than detrital minerals (<10μm) and are difficult to identify (Sawka et al., 1986; Milodowski and Zalasiewicz, 1991). However, the scanning electron microscope is generally required for the analysis of this mineral and to quantify their influence in the sediment (Banfield and Eggleton, 198; Berger et al., 2008). In summary, if detrital Th-bearing minerals are likely to exert a control on Th enrichment, the influence of authigenic phases should also not be entirely excluded.

Zr: Although Zr is present in traces in certain heavy minerals such as ilmenite, rutile, pyroxene and amphibole (Salminen et al., 2005), it is most often present in greater abundance in zircon (Deer et al., 1983; Mange and Maurer, 1992). Zircon is an ultrast0able heavy mineral and as such its correlation with Th depends on the types of Rare Earths that characterize Th enrichment. Logically, the predominance of fractionated HREEs within REEs favors a positive correlation of Zr and Th However, the influence of Th inherited from LREEs-rich fractions should not be negligible.

Mo: In sedimentary rocks, Mo is associated with a range of common sulphide minerals, such as pyrite, galena and sphalerite, but it is present in greater abundance in molybdenite (Salminen et al., 2005; Tribovillard et al., 2006). Molybdenite is a redox sensitive mineral and is commonly enriched in black shales deposited in theminic

environments (Tribovillard et al., 2006). On the other hand, molybdenum has very high seawater concentrations relative to crustal values and can record seawater conditions even with high clastic input (Piper, 1994; Crusius et al., 1996). Immobilization occurs when ambient HS activity exceeds threshold values, causing reactive behavior to Mo particles and entrapment by organics and/or iron-containing particles (e.g. sulphides, Helz et al., 1996; Zheng et al., 2000). Molybdenum entrapment appears to occur near the sediment-water interface and in the water column, and enrichment is believed to coincide with theminic conditions (Crusius et al., 1996; Lyons et al., 2003).

U: Rivers are the only major source of uranium in the oceans (Klinkhammer and Palmer, 1991). The Element is immobilized in sediment with active reduction of sulphates by diffusion of U^{6+} in the sediment, reduction to U^{4+}, followed by adsorption and precipitation (Cochran et al., 1986, Klinkhammer and Palmer, 1991; Jones and Manning, 1994; Morford et al., 2001). Additional uranium can be provided by direct precipitation from a body of anoxic water (Piper and Isaacs, 1995). Diagenetic re-oxidation has been suggested to cause loss of uranium in sediments (e.g. Cochran et al., 1986), but downward diffusion of mobilized uranium is more likely (e.g. Thomson et al., 1993). Authigenic uranium is calculated as $U_{aut} = U_{tot} - Th/3$ with Th/3 as the estimate of the detrital uranium fraction (Wignall and Myers, 1988; Jones and Manning, 1994).

V: Vanadium is frequently used with Cr to monitor redox conditions in the nitrate reduction zone. The Elements are immobilized as hydroxides near the lower limit (V) and the upper limit (Cr) of the nitrate reduction zone, respectively (Jones and Manning, 1994; Piper, 1994). Denitrification characterizes dysoxic conditions (Froelich et al., 1979). Usually V is associated with organic matter, but part of it can also be related to silicate minerals (Jones and Manning, 1994). Due to analytical problems with Cr, only V concentrations were taken into account in this study.

Ti: Ti is present in a range of heavy minerals containing Ti such as rutile, brookite, anastase, titanite, pyroxene, amphibole, ilmenite, magnetite, garnet and mica (Deer et al., 1983; Mange and Maurer, 1992; Salminen et al., 2005). However, it is likely that the common polymorphs of TiO_2 rutile and anastase have the strongest control over bulk geochemical values, as they contain Ti in greater abundance.

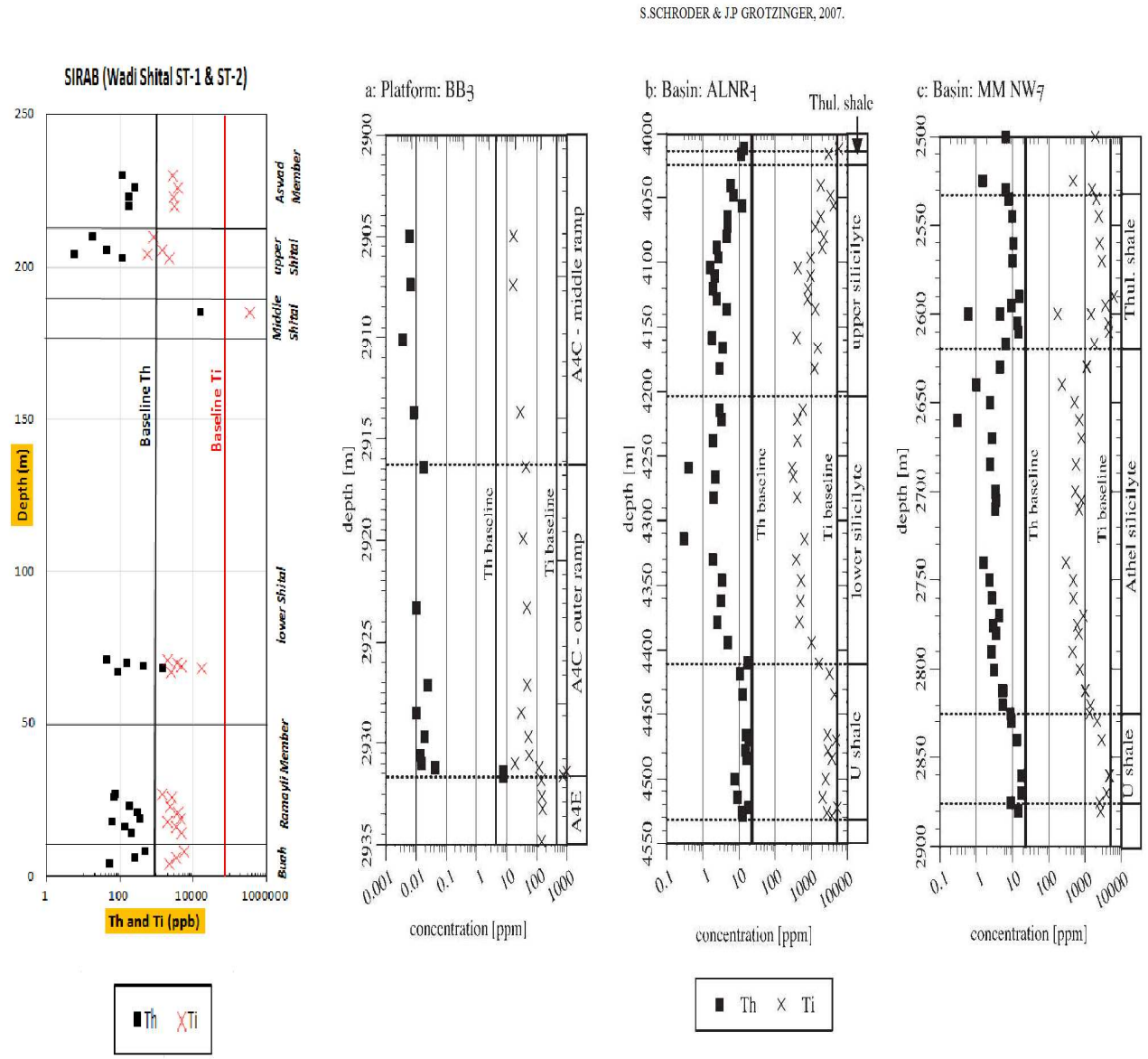

Figure 6-4: *Chemostratigraphic correlation of redox sensitive elements Th, Ti of type section of Sirab Formation (Wadi Shital ST-1 & ST-2) analysed in this study with Ara Group Platform BB-3 and Ara Group basin ALNR-1 and MM NW-7, data form Schroder and Grotzinger (2007).*

Redox-sensitive Trace Elements Th and Ti were measured in ppm in earlier work by Schroder and Grotzinger (2007), for the Ara Platform carbonates and the Ara basin carbonates. In Sirab Formation, the Elements were measured in ppb at the laboratory of Trinity College Dublin. Anyway, using a standard conversion, the ppb values can be roughly estimated in ppm by dividing by 1000 the original values obtained in ppb. The results of the comparison of sensitive redox Trace Elements show a near similarity between the Sirab Formation at Wadi Shital ST-1 and ST-2 (type section) and the Platform of the Ara Group (BB-3). Indeed, the ppm values of Th and Ti in the Ara Group platform have a scale range between 0.01 and > 1 ppm with the majority of the values plotted at the scale of 0.01 to 0, 1 ppm for Th while the range for Ti is 10-100 ppm. The two groups of carbonates from two logs of the Basin show a clear resemblance in the Trace Element scale range. For ALNR-1 and MM NW7, Th has a range of 0.1-10 ppm while Ti has a higher range ~500-10,000 ppm. Compared to the standard conversion of results obtained on the Sirab Formation, the carbonates show Th values between 10 and 10,000 ppb, with the majority of samples having a range of 50 to 300 ppb. Divided by 1000 as standard values, this sends Sirab carbonates to values close to the Ara Group Platform (BB-3) range with Th concentrations around 0.05 to 0.3 ppm. Regarding Ti in Wadi Shital ST-1 & ST-2, this Element has concentrations between 1000 and 6000 ppb which return after conversion to values of about 1-6 ppm. These values are again close to those of the BB-3 Platform

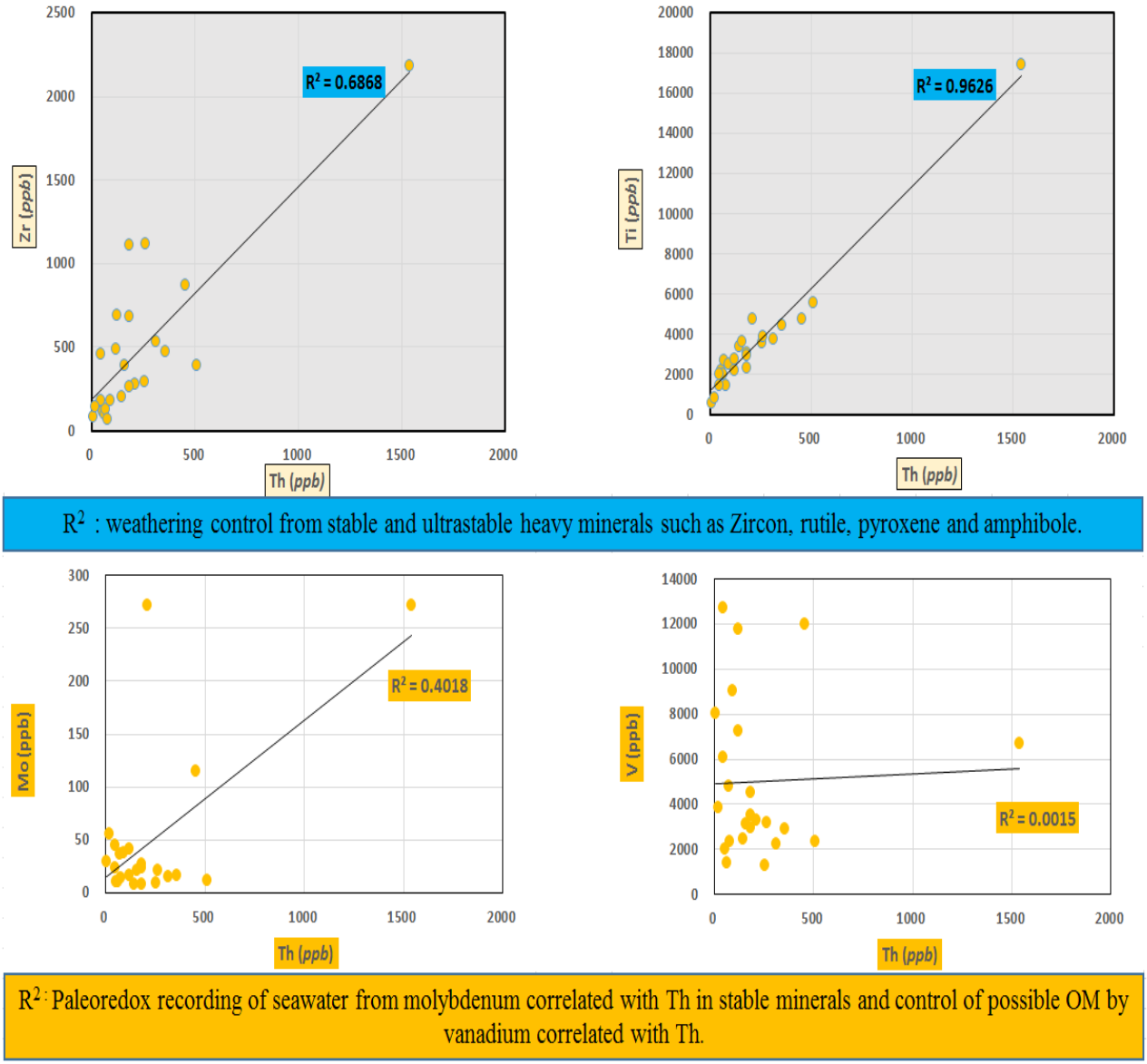

Figure 6-5: *Evolution of the redox chemistry deduced from stable minerals with respect to Th for the Zr/Th correlation; Ti/Th, recording of redox chemistry of seawater versus Mo/Th, and analysis of maintaining the state of dysoxic conditions versus V/Th, in the main field section of Sirab Formation at Wadi Shital ST-1 and ST-2.*

The dysoxic condition which can be defined as an absence of oxygen in the water-sediment interface and/or a low but stable presence of oxygen in the depositional environment is repeatedly confirmed in this study on the Sirab Formation while the V/Th ratio may mean less OM involvement. The impact of the alteration could have been minimal according to the correlation of Zr which is very abundant in the ultrastable mineral as well as in the stable mineral. The same is true for Ti which also has a positive correlation probably due to a stable mineral unaffected or less affected by weathering while Th from which Zr and Ti are correlated to determine impact-derived Rare Earth fractionation alteration can both (Zr and Ti) be present in the authigenic and detrital contributions. A more characteristic correlation factor is the palaeo-marine redox sensitivity to Mo/Th. Molybdenum is known to strongly record a trace of marine sensitivity even with high clastic input (Piper, 1994; Crusius et al., 1996). In figure 6-5, molybdenum clearly shows no satisfactory correlation with Th.

In the event that the Sirab Formation could be assumed to have been chemically mixed into the composition of the sediment by clastic and authigenic fractions along the mixing zone, the Y/Ho ratio should logically be zipped. Those Y/Ho raportes should occasionally showing clear recordings of the marine signature alternating with the freshwater signature. Unfortunately, this is not the case for the majority of Sirab samples which have intermediate Y/Ho values between the seawater and freshwater signature. At the stage of this

study, the concentrations of sea salt ions in seawater are not determined with great precision.

However, the analysis of this thesis only refers to general scientific reports approved for dissociating seawater from freshwater such as the Y/Ho ratio and data on Rare Earth concentrations. In mixed areas, the mass of stagnant water which may be located in an isolated lake or on an arm of a lagoon located in the hinterland after it has been disconnected from its junction with the sea, can lead to such a modification of the redox chemistry of the water which did not register either the marine signature and even less the signature of freshwater.

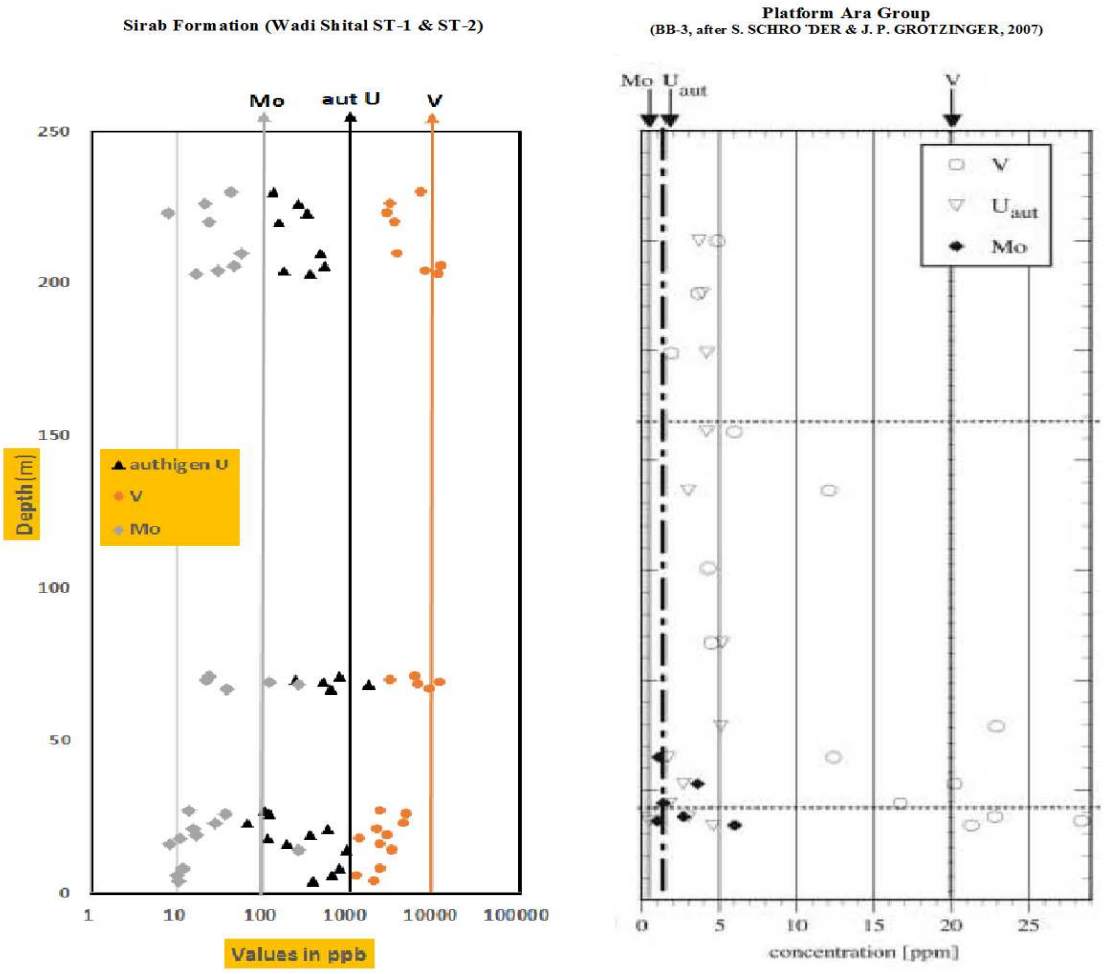

Figure 6-6: *Correlation of redox-sensitive trace elements including U authigen (U_{auth}) , V and Mo within carbonates of the type section of the Sirab Formation (Wadi Shital ST-1 & ST-2) with carbonates of the Ara Group Platform (BB -3). The data of the Ara Group come from Schroder and Grotzinger (2007).*

Using the diagram in figure 6-6 shows a close similarity between the Sirab carbonates of the type section (Wadi Shital ST-1 and ST-2) and the Ara Group carbonates of the platform (BB-3). Carbonate values in the Sirab Formation are given in ppb. Dividing them by 1000 to translate it in a standard way to ppm leads to a range of average Trace Element values below:

- 0.01– 0.2 ppm (Molybdenum);
- 1 - 7 ppm (Vanadium);
- ≤5 ppm ($U_{authigen}$).

These values are close to those of the Ara Group, see Figure 6-6:

- < 1 ppm (Molybdenum);
- 1 – 20 ppm (Vanadium);
- ≤ 1 ppm ($U_{authigen}$).

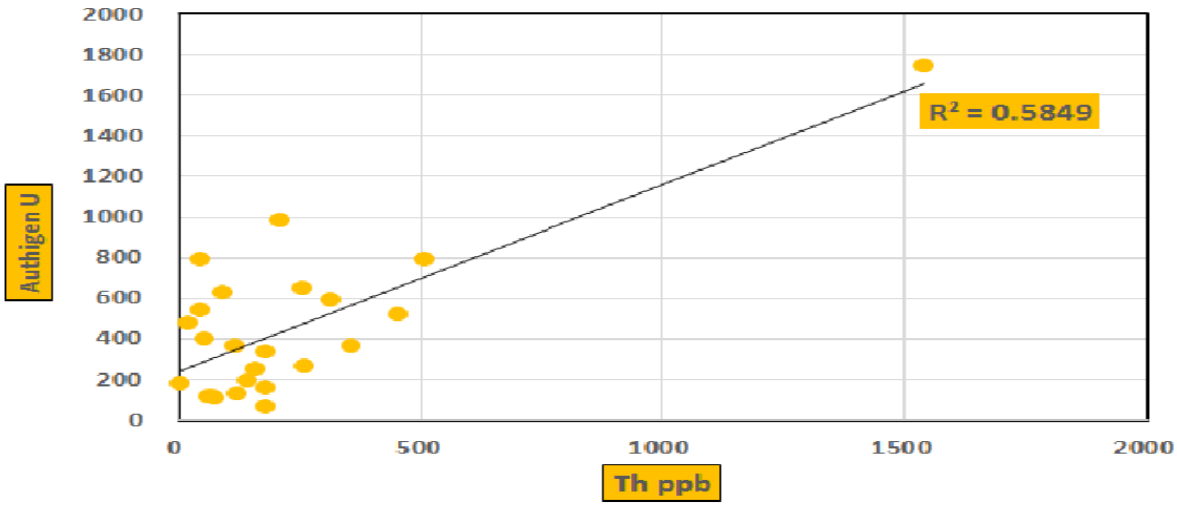

Figure 6-7: *Redox sensitivity correlation of $U_{authigen}$ and Th.*

Authigen U values correlate with Th in the Sirab Formation while compared to the Ara group basin (U and Thuleilat) these values remain very low. The original data from the Trinity College Dublin laboratory is given in ppb. Converting them to ppm in a standard way, the average uranium values do not exceed 3 ppm for the Wadi Shital ST-1 & ST-2 section of the Sirab Formation. The majority of the samples have values at < 1 ppm. On the other hand, a positive correlation of authgen uranium with Th could signify the presence of direct precipitation of U from anoxic water (Piper & Isaacs, 1995). Indeed, diagenetic reoxidation can lead to loss of uranium in sediments (eg Cochran et al., 1986). However, downward diffusion of mobilized uranium is more likely (eg, Thomson et al., 1993).

7 *Discussion and data interpretation.*

- **Evidence of carbonate ramp.**

Debate persists over the exact palaeo-geographic position and structural regime of part of Oman during the Ediacaran-Cambrian transition. But it seems probable that in Oman, within the framework of the Arabian plate, this region occupied a marginal position in a Gondwana in expansion around 600 Ma such that present-day Oman was juxtaposed between India and Pakistan to the south-east (Powell and Pisarevsky, 2002). The Al-Huqf region is today traversed by a series of NS-dominated faults, with a complex history of movement. It can be shown that these faults were active before and after the deposition of the Sirab Formation (Nicholas and Gold, 2012). Less common are NW-trending faults, which are a relic of the Late Neoproterozoic Pan-African Orogeny (Najd event). NE-trending structures, such as the Dome of Khufai, and other faults throughout the region appear to follow basement terranes and their sutures, respectively.

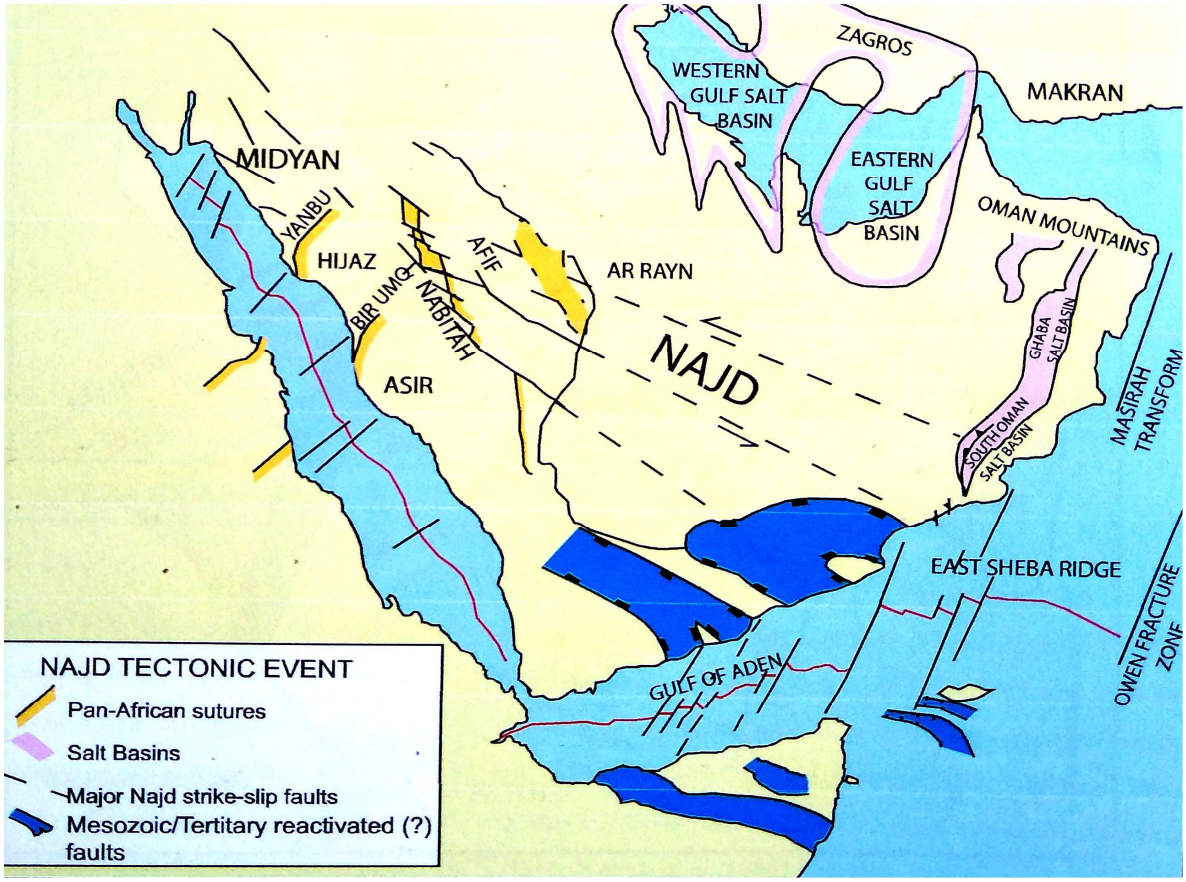

Figure 7-1: *The Arabian Peninsula, with Precambrian terranes (Midyan, Hiyaz, Asir, Nabitah, Afif and Ar Ryan) in the Arabian Shield zone with the Neoproterozoic-Cambrian slide fault system. The boundaries of the microplates are those from Stoeser and Camp (1985). Other data are from Looserveld et al., (1996).*

A) Ramayli Member

Relatively uniform mid- to upper-ramp grainstone, ooid and peloid shoal lithofacies occur regionally throughout the top of the Buah Formation and are overlain in all exposed sections of the Ramayli Member by fine-grained carbonates that evolve into carbonate muds with dispersed evaporite mineral growth (Gold, 2010). The lower part of the Ramayli Member represents shallow depth and restricted water circulation, with facies changes that suggest shallow, low-energy lagoon environments with the presence of lagoon(s) marked by the brief inflow ooids, peloids, oncoids (Nicholas and Gold, 2012). Silica is ubiquitous in carbonates and evaporites, and this mineral is defined as a substitute for evaporite in the mixing zone between meteoric and marine interstitial waters in peritidal environments (Milliken, 1979). The contribution of terrigenous siliciclastics is also present in certain sections close to the base of the Formation. Where siliciclastic terrigenous influxes occur, the lower unit of the Ramayli Member registers a fine oscillation of eustatic sea level rise and fall towards a generally shallow trend (Gold, 2010).

The lowering of the "marine" water trance through the Ramayli Member is accompanied by significant growth of microbial mats with patches of stromatolite Domes. The appearance of siliciclastic siltstone and mudstone deposits in the upper unit of this Member marks a new evolution of the filling of the Formation. The growth of low, "stubby" Stromatolite Domes in a single marker horizon around

Buah Dome indicates that water depths were extremely restricted, limiting the vertical growth of mat communities to only a few centimeters (Nicholas and Gold, 2012). At B-NW3 on the figure 1-5, the interval above the 'squat' stromatolite marker horizon is dominated by fissile red mudstones with pseudomorphic anhydrite rosettes. Microbial mat beds are sparse while emergent surfaces with breccia and chert crusts are regular. This led to hinting at a supratidal deposit environment and a sabkha framework for interpreting this interval.

There are dissolution and collapse beds at B-NW3, and lateral equivalent beds of halite at Wadi Shital. At the top of the Ramayli Member, sedimentary facies of extremely restricted evaporite deposits were reported and this feature was defined as a period of "marine" flooding of the sabkha environment which forms evaporite unit 1 (figure 1-13) from Gold (2010). Furthermore, Mattes and Conway Morris (1990) believe that salt deposition occurred during the Ediacaran-Cambrian interval as far east as the Al-Huqf and was not limited to the north and south of the region.

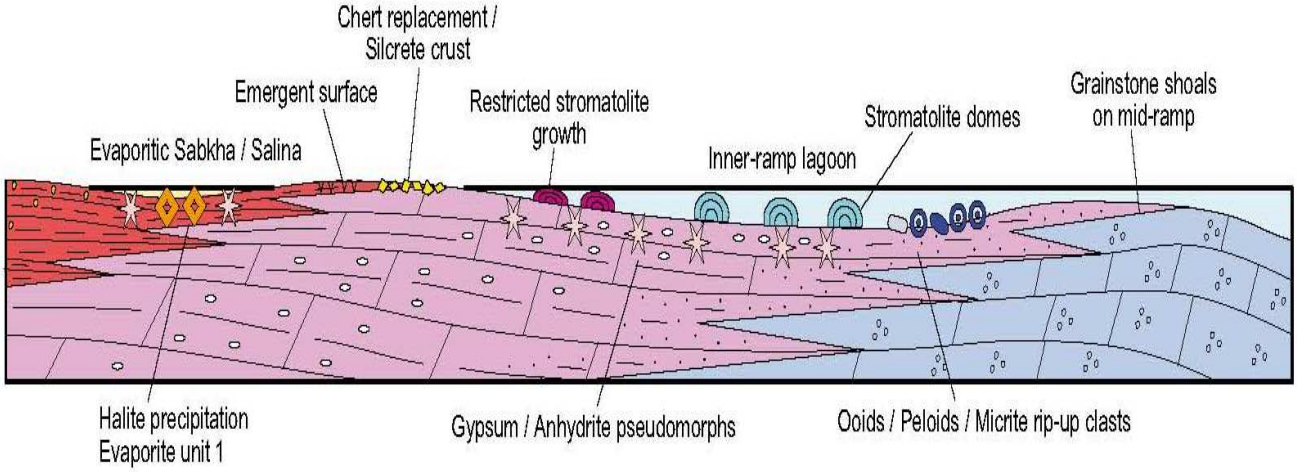

Figure 7-2: *conceptual cartoon model for depositional sequence (DS) settings and facies of Ramayli Member, during the Ediacaran-Cambrian (EC). The cartoon represents more at les the general deposition of the Member throughout Al-Huqf region. The cartoon is not strict paleo-geographic cross-section as such, or drawn to scale, but is an attempt to summarise the facies observations from a variety of localities for a particular time interval, such as reported by Nicholas and Gold (2012). In this figure, Lagoonal and sabkha facies of the Ramayli Member prograding over the underlying Buah Formation inner and mid ramp grainstones and ooid shoals to fill all available accommodation space during highstand. The bases of section refer to sections around the Buah dome and ST-1; see as well Figure 1-5.*

In essence, the progradation and/or retrogradation within the Ramayli Member should be provoked according to the filling of the Formation. Essentially, the pre-existing paleotopography should have played a role in the progressive accommodation of the whole of Sirab and the lithofacies developed were engendered depending on the filling, the detrital inputs, the chemical composition of the water and the moments of immersion-emergence of sediments, see figure 1-5.

In underground exploration wells near the Al-Huqf area such as Miqrat-1 to the north, the interval of part of the Buah Formation is interpreted as the truncated Ara group with a high logarithmic gamma response. Nicholas and Gold (2012) believe that this high gamma response interval corresponds to the red mudstones and siltstones of the upper Ramayli unit since in the Sirab Formation this upper Ramayli interval is dominated by fine siliciclastics.

B) <u>Salutiyyat Member.</u>

The Salutiyyat Member outcrops in a NE trending area through Al-Huqf, from Wadi Salutiyyat to Wadi Shuram. The samples of this section were not analyzed in this study considering that the lithofacies of the section correspond to more or less lateral variations of the lower units of the Ramayli whose samples were analyzed in the type section of Sirab (Wadi Shital ST -1 & ST-2). However, the existence of the Member and its basal unconformity indicate that there must have been a series of palaeo-highs across the Al-Huqf during the early Sirab deposition. Thus, the Nafun group is subaerial exposed by erosion as Salutiyyat Member lies wether above Buah Formation or Shuram Formation both belong to Nafun Group.

Subaerial erosion then makes it possible to describe in a few words the position of the Nafun group at Wadi Salutiyyat and Wadi Shuram. Thanks to this, it is therefore possible to imagine an ancient hollow relief having existed on the whole of Sirab. As the dominant paleotopographic landform normally contains a ridge, the linear geometry of this suggests that the paleo-ridge was bounded by faults because in Oman the Nafunt Group coincides exactly with a basement terrane and sutures. On the other hand, the movement on the faults flanking the NE-SW ridge after the start of the Ramayli deposition is considered to be the origin of the shallow trough along this axis. This would have allowed temporary flooding and filling of Member Salutiyyat until all accommodation spaces were filled (Nicholas and Gold, 2010). Subsequent basin-wide fault subsidence would then have allowed the rhythmic cycles of the Member to be deposited over all of the previous stratigraphy. Given the structural condition of the Saluttiyat section throughout the Al-Huqf region (figure 1-5), this Member may represent the initial localized stages of what became the general regional subsidence in the Haushi -Huqf controlled by faults. This led Gold (2010) to conclude that this Member would be a possible vestige of a hollow palaeo-relief.

Wadi Shuram contains some of the thickest sequences of the Sirab Formation, clearly indicating that it was an important depocenter during the accumulation of the Formation. However, the thick ridges of the Sirab Formation, which outcrop from WS-8 to WS-1 and further southwest, have been deposited on the paleo-ridge of the

Nafun Group, indicating that what was a palaeo-high before the beginning of the deposition of Sirab, then became an important palaeo-low during its accumulation. Far to the southwest along these ridges, the Shital Member appears to unconformably overlie the ridges of the Shuram Formation with little or no Salutiyyat Member in between [UTM 550725, 2220630]. The dramatic topographic inversion from the beginning of the Sirab deposition to its end at this locality was interpreted as likely caused by fault movement on the ridge sides. While other outcrops were located just north of the Mukhaibah Dome in the south of the area, where upper Shital Member beds including the buff sandstone marker horizon directly overlie the siltstones and layered sandstones of the Formation of Shuram and show then the proof of the existence of a raised palaeo-relief.

From field observation at Wadi Salutiyyat, there is an interval of low exposure directly below the first appearance of Shital Member cycles. A single bed in this interval is composed of dolospathic rhombuses, which in other sections have always been found in association with evaporite units such as the halite beds at Wadi Shital ST-1 (figure 1-5 and figure 1-13). Lithostratigraphic correlation suggested that this level of evaporite found on Wadi Salutiyyat beneath the cycles of the Shital Member represented the lateral temporal equivalent of the same cycles in neighboring sections. The horizon of the evaporite unit in the Salutiyyat Member has been defined as evaporite unit 1, which is equivalent to the beds of the upper Ramayli unit which occurs at Wadi Shital ST-1. On the other hand, the main depositional controls acting

at this time were considered not to be eustatic sea level changes but faulting movement causing localized hanging wall subsidence and uplift (Nicholas and Gold, 2012).

C) Lower Shital Member.

The characteristic of the Shital Member is the couplets of beds which repeat on a scale of 1 to 2 m, over tens to hundreds of meters of stratigraphy. This occurs particularly in the lower half of the Member (figure 1-13). The lithology of these couplets suggests that each bed represents a deepening sequence ranging from peritidal carbonates to temporarily emerging evaporites. The thicker main bed of each couplet is composed of a light gray or caramel-colored, well-weathered laminated dolomite (often clearly microbially rippled). Across the bed are large bird's eye windows which are common. These appear to have been generated by the gases released from the microbial mats at the bottom of the bed. This somehow indicates that lithification only occurred after each mud bed had accumulated (Gold 2010).

The occurrence of fine carbonate muds through the sediment bed, the development of microbial mats and stromatolite Domes; indicate a lagoonal to shallow intertidal environment (Nicholas and Gold, 2012). Chert replacement along lamellae is present in all beds and particularly towards the top of the lithostratigraphy.

The development of chert-replaced lamellae as well as chert-replaced breccias suggested that sediment bed was not only deposited in shallow lagoon environments but also in shallower parts of the lagoon between high tides and basses (Nicholas and Gold, 2012). The associated pockets of dissolution and collapse breccias within the beds also indicate repeated periodic post-lithification emergence of the upper bedding surfaces to allow the onset of karst dissolution.

The second bed of each verse may vary depending on localized environments. It is usually a thin weathered bed 10 to 20 cm thick and composed of fine red dolospar after anhydrite in chicken wire or dolomicrite in chicken wire from the dissolution of gypsum. In both cases, there are thin caps of evaporite on the main bed, more massive, below each couplet. These evaporite plugs are generally poorly exposed, but are clearly absent in some sections that presumably had less accommodation space or were not restricted enough for the bicarbonate supply to be depleted (e.g. half top of section WA-1; see also Figure 2-1). Conversely, at Wadi Sidr to the south (figure 1-5), these evaporite caps are about 20 to 40 cm thick and are composed of recrystallized yellow dolospar. At Wadi Shital, this type of coarse blocky dolomite was found in association with halite and it is possible that the evaporite caps were better developed and thicker in the south of the Al-Huqf area.

Field observations show that the lithofacies developed at the top of the Ramayli Member are highly variable laterally because all remaining accommodation space has been filled around the paleotopographic tops of the Nafun group. However, the lower Shital Member, wherever encountered in the field, is always composed of repetitive cycles of couplets of carbonate-evaporite peritidal beds, and is therefore remarkably uniform in lithofacies across the entire Al-Huqf region. Each rhythm pair is not only remarkably uniform in thickness as it repeats across stratigraphy, but is also laterally continuous with little or no change in bed thickness. These field descriptions showed that there was no evidence in the field of gradual and diachronous eustatic transgressive flooding across the top of the Ramayli Member. Instead, the flood appears to have occurred simultaneously, in geological terms, in all sections. This indicated a finely balanced interaction between progressive fault-controlled basin subsidence and minor fluctuations in eustatic sea level due to sub-Milankovitch cyclicity, such as Dansgaard-Oeschger events or bond cycles (see figure 1-2 and figure 7-1 relating to tectonic maps). Each time 1-2 m of accommodation space was created, the deposits would take over and fill the space with a wedge of peritidal dolomicrite, followed by evaporites as the shrinking water mass was isolated from the marine influence (Nicholas and Gold, 2012). Once the water evaporated, the top surface of the bed was exposed until the next flood and the next cycle of deposition began.

The layout of the stratigraphy indicates that the regional control faults bounding the fill structure of the Sirab Formation became active during the early deposition of the Shital Member. The fact that this Member is at least 150m thick (and in areas such as Wadi Shuram easily over 250m thick for sections WS9 and WS10 together). On the other hand, facies cyclization features can be found in sections up to the top of the Member in other locations (e.g. WA-1; figure 2-1). This indicates that the faults remained active and controlled deposition in the Al-Huqf area. Field data detailed by Gold (2010), and Nicholas and Gold (2012) indicate that while being a structural high during the Ediacaran-Cambrian, the Al-Huqf region (more precisely the Haushi-Huqf) had not always been exposed subaerially since within this regional anticyclone, the Shital Member deposits show the development of a localized symmetrical or slightly asymmetrical graben. The presence of cyclic carbonates of the lower Shital Member from Wadi Aswad in the north to Wadi Sidr in the south, over a distance of about 85 km, makes a north-south trend very likely. This corresponds well with the trend of pre-existing faults across the Al-Huqf and it appears that the trough structure of the Sirab was reversed after the infilling of the Formation. This probably during the Angudan Unconformity, accompanied by karstification and later incision by basal clastics of the Haima Super group. (Erosion of the entire Buah Dome Formation during this time indicates that over 250 m of carbonates were removed prior to deposition from Haima (Nicholas and Gold, 2012).

Recrystallized red dolospar and mudstones associated with dissolution breccias approximately 70-100 m from the base of the Shital Member have been reported in sections from Buah Dome to Wadi Sidr (Gold, 2010). These lithologies and bedforms are clearly associated with the deposition and emergence of evaporites when observed in good exposures, such as at the summit of the Ramayli Member at Wadi Shital ST-1. They indicate that there is a second evaporite unit present at this level throughout the area (figure 1-13). Sufficient accommodation space was created for a restricted body of water to develop and deposit an evaporite unit possibly due to eustatic rise in "sea" level which had been followed by floods. The remaining interval to the base of the quartz sandstone marker horizon is poorly exposed in many sections, while it appears that the deposition of peritidal cycles of carbonate and evaporite resumed after the deposition of the evaporite unit 2 (Gold, 2010).

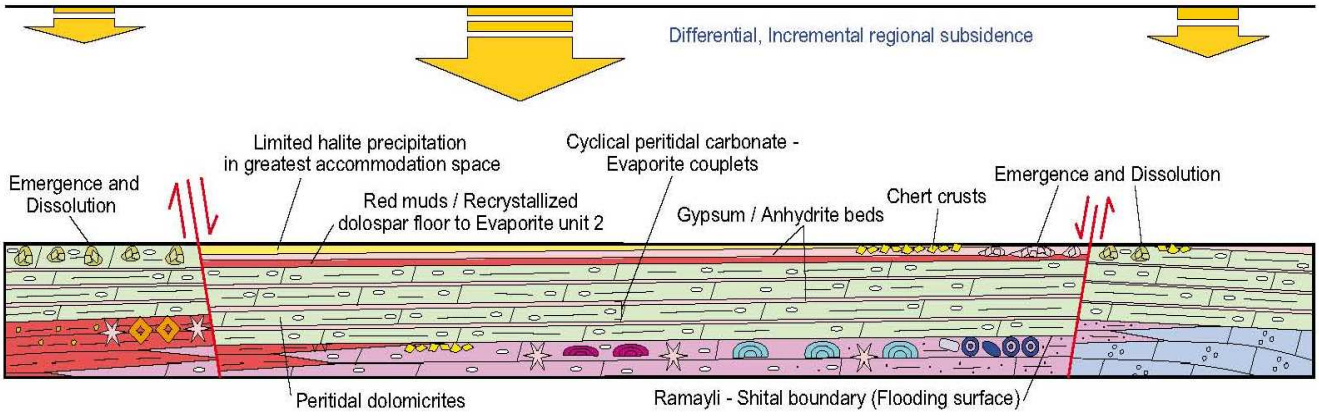

Figure7-3: *conceptual cartoon model for depositional sequence (DS) settings and facies of Lower Shital Member fault controlled transgression to Evaporite unit 2, during the Ediacaran-Cambrian (EC). Initiation of regional, basin-bounding fault-controlled subsidence causing differential accommodation space between individual fault blocks, Incremental fault movement and/or Milankovitch cyclicity causes repetition of cyclical peritidal carbonate-evaporite couplets, from Nicholas and Gold (2012).*

D) <u>upper Shital Member</u>.

The presence of a thin unit of quartz sandstone about 2 to 4 m thick from north to south across the Al-Huqf (figure 1-13), tried to be justified by a subsidence episode across the region that would have provided enough accommodation space for the accumulation and preservation of said unit (Gold, 2010). It was reported at the field observation that the above-mentioned quartz sandstone unit was overlain in Wadi Aswad and Wadi Shital by an evaporitic unit which apparently confirms the creation of a space similar to that of the evaporite unit 2.

Furthermore, the base of the sandstone was interpreted as a correlable flood surface. Analysis of the terrain's sedimentology attributed to this horizon of the lithostratigraphy a unique influx of siliciclastics of continental origin which would have been mixed with carbonates so as to mark the entire sandstone horizon as a robust regional marker of the Sirab Fromation.

Another change in post-'Evaporite unit 2' subsidence style was reported at the top of upper Shital. At Wadi Aswad to the north, the deposition of cyclic peritidal carbonates resumes until it passes into an interval of "tufted mats" upwards (figure 1-5). But in Wadi Shital and Wadi Shuram, there seems to have been a significant deepening which would therefore have allowed the development of mounds or microbial reefs whereas in Wadi Shital, the development of mounds or microbial reefs takes the form of accumulations of Conophyton and possibly surmounted by Thrombolites. This sedimentary facies above evaporite unit 2 at Wadi Shital has been considered to have formed in a "subtidal" environment (Donaldson, 1976; Grotzinger, 1989).

In Wadi Shuram there are good examples of small individual Thrombolite mounds as well as large Domal Stromatolitic Thrombolites. The upper Shital lithofaciè in Wadi Shital and Wadi Shuram revealed more open "marine" conditions that had not been considered for the peritidal-evaporite couplets. This provided evidence for more general subsidence in the Wadi Shuram area during the

deposition of the upper Shital. Nicholas and Gold (2012) concluded that this Sirab trough would have developed into low angle fringing carbonate ramps plunging towards a deposit on a NE-SW axis between the Wadi-Shital - Wadi Shuram zones.

Broadly, it was reported that four carbonate-evaporite cycles could be recognized from the base of the Sirab Formation to the top of the Shital Member. The lowest of them corresponds to the Ramayli Members and its lateral equivalent Salutiyyat. However, where the Salutiyyat is extremely thin or missing on the crest of the Nafun group paleo-shoal topographic eg southwest in Wadi Shuram, the Salutiyyat Member overlies the Nafun Group unconformably. Evaporite units 2 and 3 subdivide the Shital Member into two individual carbonate-evaporite cycles while the fourth is represented by the upper Shital Member (see Gold 2010 for details; figure 1-5).

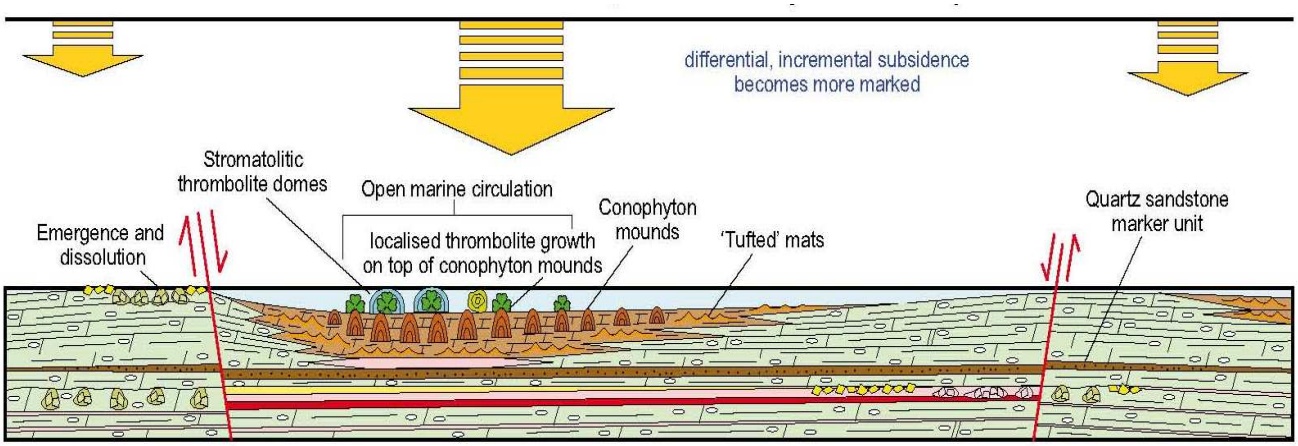

Figure 7-4: *Conceptual cartoon model for depositional sequence (DS) settings and facies of upper Shital Member subsidence in localised depocentres, during the Ediacaran-Cambrian (EC). Upper Shital more marked differential subsidence creates depocentres with more accommodation space allowing microbial build-ups to develop; initially conophyton reefs, followed by stromatolitic thrombolites, Fom Nicholas and Gold (2012).*

E) Aswad Member

The Aswad Member appears to represent a relatively uniform facies across all field sections that contain it (no internal subdivision; figure 1-1). The entire Member was defined as the result of progressive flooding that became general and uniform on a regional scale. This sits just above the upper Shital Member Increased differential sagging (Nicholas and Gold, 2012). Although the surviving stratigraphy of the Aswad Member is relatively thin (≤ 30 m), there is little change in its gross litho- and bio-facies from Wadi Aswad to the southern tip of its southern exposure of the region of Sirab, over a distance of about 60 km (see, sedimentological description in chapter 1).

The association between framestone Thrombolites, laminated Thrombolites and Oncoids is complex and gradual both laterally and vertically. Laminated stromatolitic Thrombolites have been reported to transition laterally upwards into larger Thrombolitic reef beds. As such, these latter beds would probably constitute the stage before full reef development (Schröder, 2000). Thrombolite reef beds themselves constitute high primary porosity sediment between mesoclots (Gold, 2010). Some of these beds have been clogged with calcite. The existence of a gradation of coagulated tissue towards Oncoids was reported by Nicholas and Gold (2012), with patches where Oncoids appear to have stuck together followed by the development of coagulated tissue. The development of extensive beds of Oncolite at this time seems to indicate that the Al-Huqf area had developed into a

shallow and geographically extensive "marine" ramp where the lapping of the "tides" rolled continuously from the banks of microbial balls between the "fields" of Thrombolite framework stone beds and a more localized bioherm. To the south of Wadi Shital, field data estimated that water depth was sufficient for microbial folded laminites to form around the flanks of such a localized Thrombolite mound. Conversely, at Wadi Aswad, the Oncolite layers contain an organic matter component not observed in the Wadi Shital region. And these oncoids were considered to have developed in slightly deeper, but current-dominated waters than those of Wadi Shital.

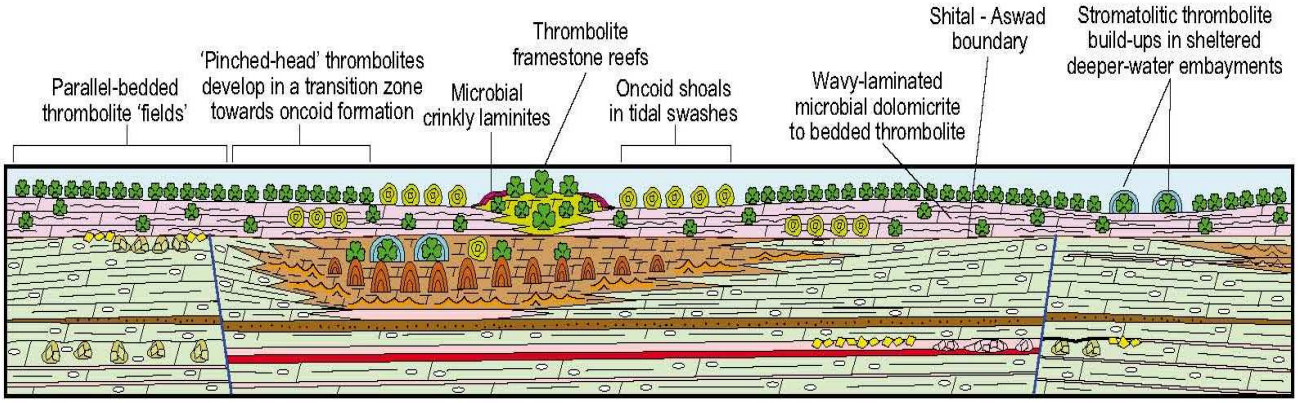

Figure 7-5: *conceptual cartoon model for depositional sequence (DS) settings and facies of Aswad Member more uniform flooding across ramp, during the Ediacaran-Cambrian (EC). More uniform regional fault-controlled subsidence gradually floods across the area accompanied by deposition of the Aswad Member. Connexion with open-marine conditions prevail across north and probably north east part of the Al-Huqf region, encouraging laterally extensive, parallel-bedded, thrombolite 'fields', punctuated by occasional build-up of thrombolite patch-reef framestones, from Nicholas and Gold (2012).*

- **Diagenesis in relation to the palaeo-environment of Sirab Formation.**

The demonstration of an active and generalized diagenesis throughout the Sirab Formation remains a difficult task. However, the scientific analyzes of tangible evidence of the involvement of diagenesis (Mn/Sr, Mn/Sr ratios versus $\delta^{13}C$, $\delta^{18}O/\delta^{13}C$, $Mn/\delta^{13}C$) have not been conclusive with regard to the results of this study for the Sirab Formation. However, these same reports above have nevertheless made it possible to demonstrate the existence of a few cases of early diagenesis which would have occurred across certain horizons of the stratigraphy of the Formation (see complete discussion of diagenesis in Chapter 4).

The typical Sirab section is significant of the whole Formation since it contains all the Members of the Sirab except for the lateral variation at the base of the Formation which occurs in certain localities such as at Wadi Shuram and Wadi Salutiyyat. In these localities, the base of the Sirab Formation unconformably overlies either the Buah Formation or the Shuram Formation belonging to the Nafum group. This angular discrepancy in the stratigraphic continuity between the Nafum group and the Sirab Formation led to the admission at the base of Sirab of a regionally distinct Ramayli unit depending on whether it concordantly overlies the Nafum group at the top of the Buah Formation (Ramayli Member) or in a discordant way between the Formation of Buah or Shuram (Salutiyyat Member). However, these two units (Ramayli and

Salutiyyat) have been recognized as lateral variations of the same facies.

Usually in carbonates manganese (Mn) enrichment is interpreted as expected from efficient diagenesis. The Mn concentration levels at Sirab are much higher than all those encountered in the Ara Group, whether for the carbonates of the platform (Birba) or those of the basin (U and Thuleilat). The majority of Sirab samples analyzed in this study indicate values of 600 - 2000 ppm Mn against only about 200 ppm for platform carbonates and 800 ppm for those of the Ara Group Basin (Schroder and Grotzinger 2007). Neither in the platform nor even less in the basin, the evidence of an active diagenesis was highlighted in the carbonates unequivocally. Although Mn ranks sixth in the list of Major Elements after (Calcium, Magnesium, Silicon, Fe and Aluminum) as analyzed by ICP-MS/OES, the relatively high enrichments of this Element in the Sirab Formation compared at concentrations of the same Element in the Ara Group, arouses great curiosity and seems in apparent contradiction due to the manifest absence of diagenesis.

Morford et al. (2001) found that manganese becomes enriched in Mn oxides (MnO) under oxic conditions while diagenesis reduction produces soluble Mn^{2+}, which diffuses away from the site of reduction. Normally, in an open Basin, soluble M^{2+} ions at the water-sediment interface can circulate freely out of their concentration sites

and then re-precipitate to form manganese carbonates in the presence of O_2 when the alkalinity of the medium is high. . Furthermore, Mn is generally depleted in sediments undergoing anoxic diagenesis, whereas it seems obvious that the recycling of Elements beyond the redox limits can be important (Calvert and Pedersen, 1996; Morford et al., 2001).

In connection with the previous paragraph, real Ce* anomalies have been proven for the Sirab Formation (figure 6-3). This strengthens the argument that there were persistent anoxic conditions in Sirab and in the Ara Group during carbonate deposition.

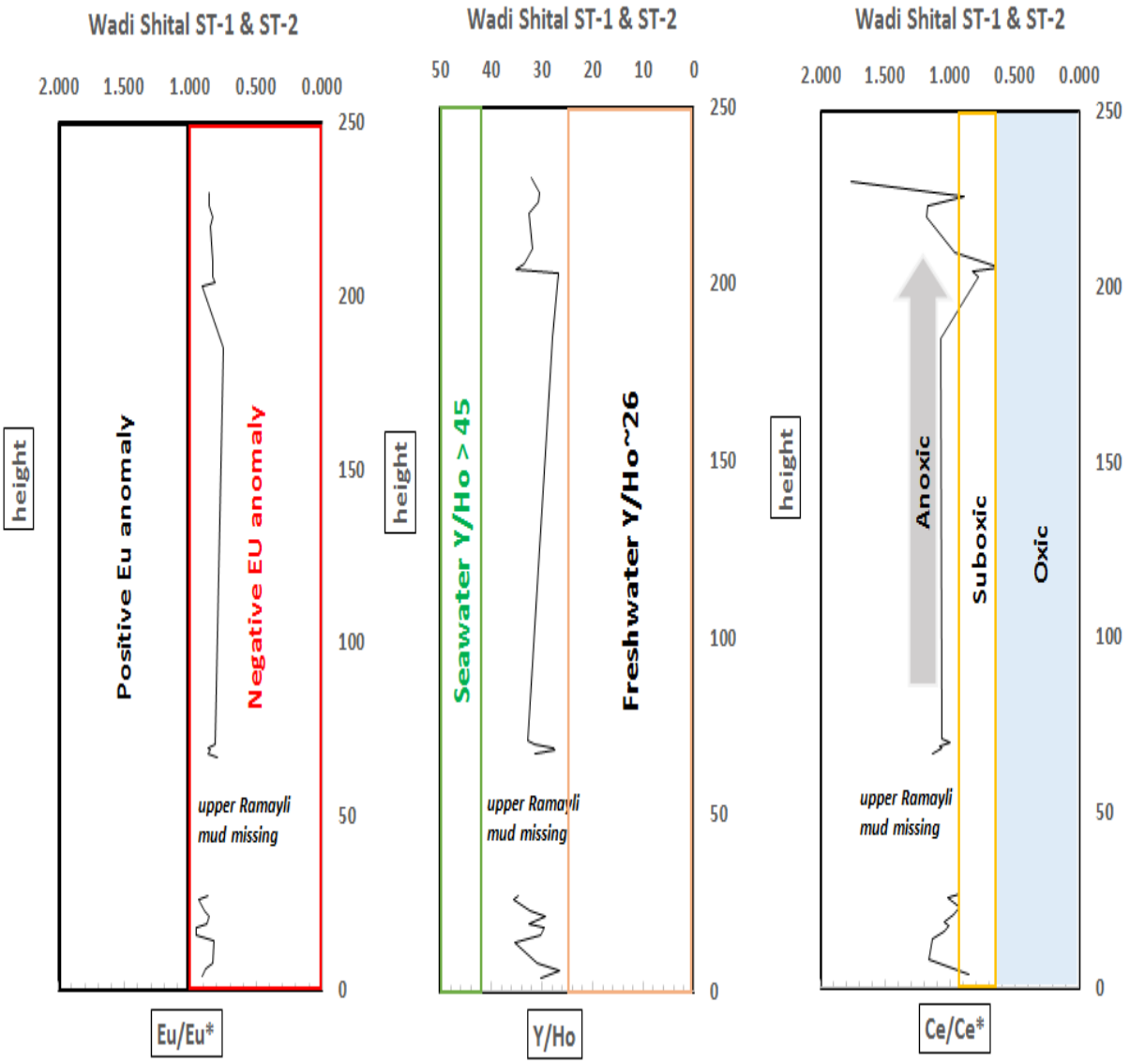

Figure 4-11: *Eu/Eu*, Y/Ho, Ce/Ce* diagrams plotted on the height of the stratigraphy, for the different outcrop levels of the type section of the Sirab (Wadi Shital ST-1 and ST-2).*

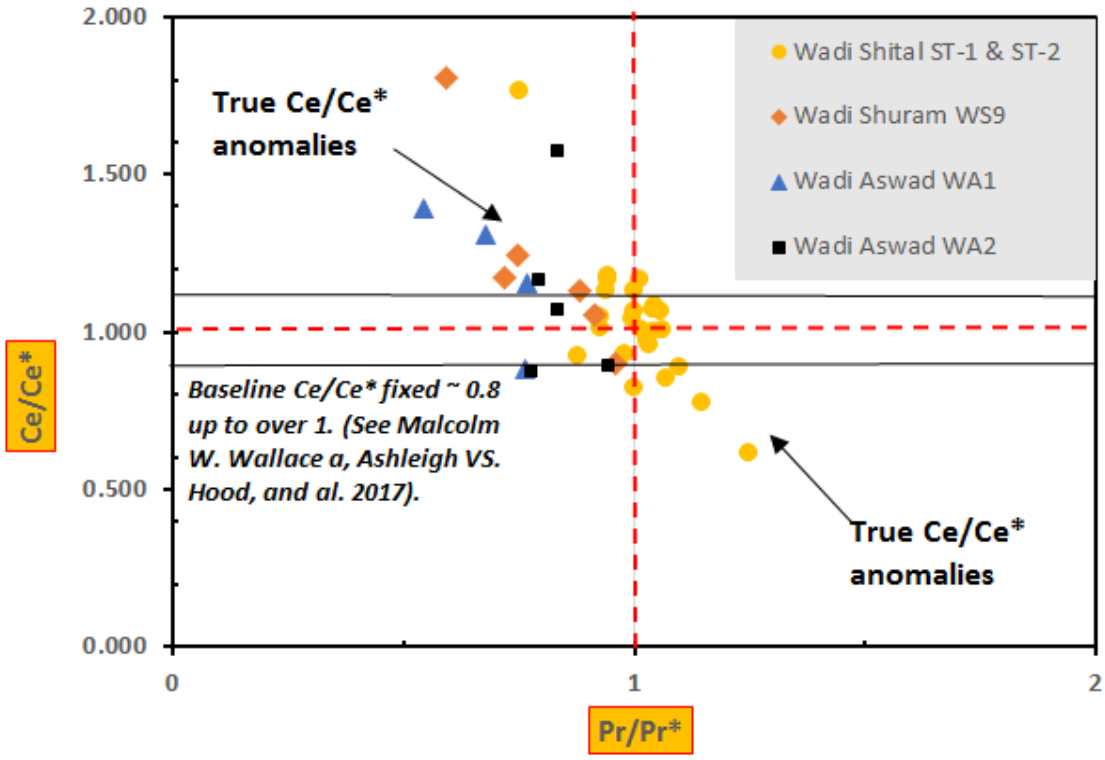

Figure 6-3: *Ce* trues anomalies in Sirab Formation (sections Wadi Shital ST-1 & ST-2, Wadi Shuram WS9, Wadi Aswad WA1 and Wadi Aswad WA2).*

However, in the Ara Group, the eastern flank of the shelf at log BB-3 is connected to Basin units (logs: ALNR-1, MM NW-7, AL-1; see Schroder and Grotzinger (2007). The Mn having concentrations 3 to 4 times lower in the carbonates of the Platform compared to those of the Basin, can result from the entrainment of a circulation of Mn^{2+} ions from the external ramp at the level of birba, up to at the depths of the basin where thereafter, the Mn^{2+} was trapped so that at any redox fluctuation of the environment, the manganese begins to precipitate and accumulate in the Basin.

In the Sirab Formation, the palaeo-geographic configuration of the ramp suggests the existence of a graben dominated by paleotopographic shoals as in the locality of Wadi Shuram. Nicholas and Gold (2012), describe this structure of the Sirab carbonate ramp as anticyclonic structural. If this had been the case, then the environmental conditions linked to anoxia during the filling of the Sirab, although penalizing for the manganese to concentrate in the sediments, would nevertheless have benefited from the structural form in the Al-Huqf or the Sirab was satisfied. Because, a structural hollow such as the "graben" in the Sirab which would be deprived of connection with the circulation of "sea" water or even fresh water, would cause a mass of permanent flood water which would dry up over time depending on environmental fluctuations (weather condition). As a result, the Mn^{2+} ions would find themselves trapped inside the graben with the effect of restricting their lateral circulation outside the ramp or "graben" which contained them. Only the vertical circulation of magnesium ions had to be more active so that all the quantities of manganese transferred in the sediments during the creation of the openings of the new accommodation spaces to allow the filling of the basin, are then definitively trapped in the Al-Huqf and only waiting to be deposited later in the sediment beds according to possible redox fluctuations such as repeated drying out of the water body from which three (3) cycles of evaporites have been recognized in the Sirab (figure 1-5). Seen from this angle, it would then have been likely to lead to concentrations of Mn in the sediment.

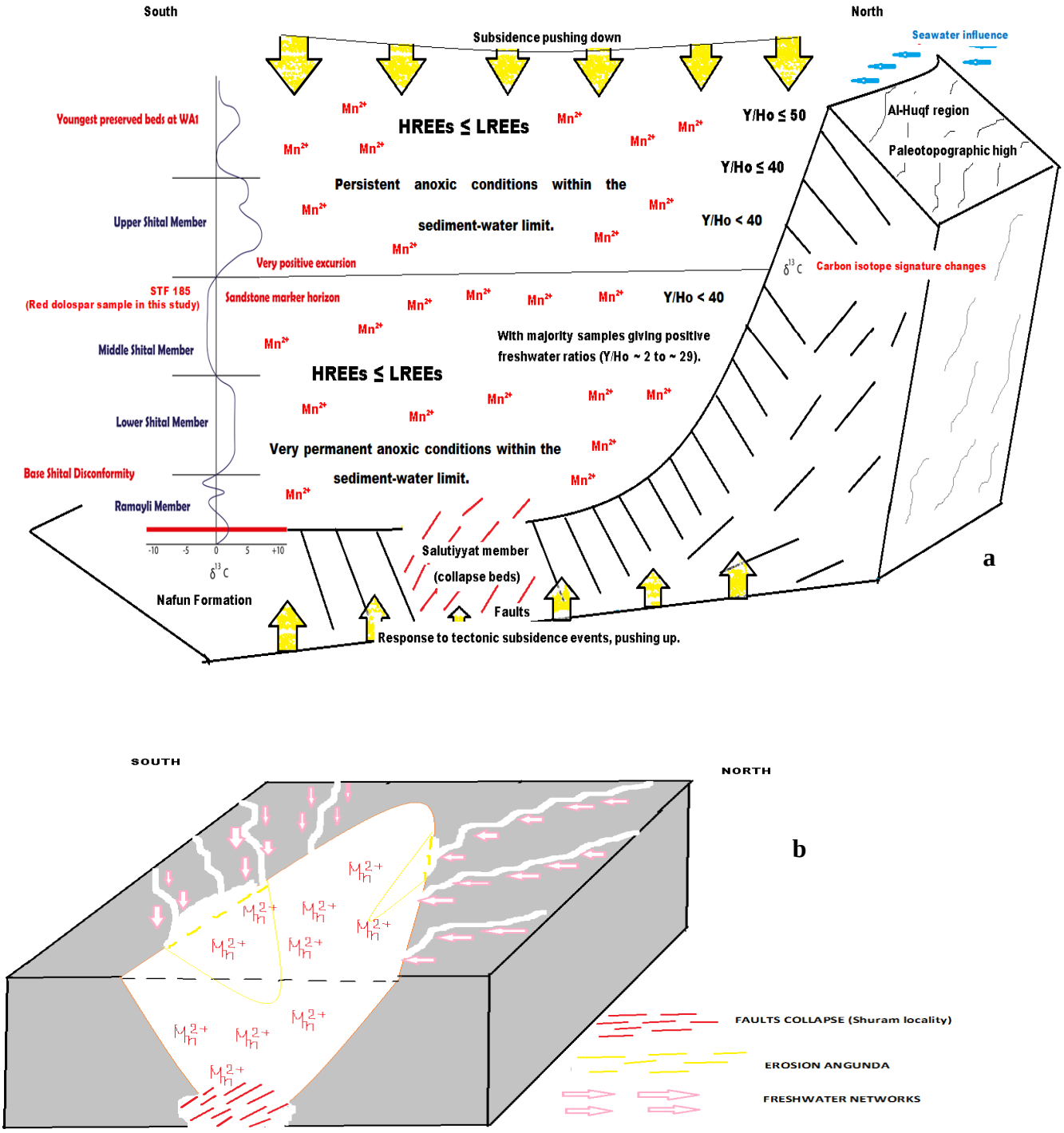

Figure 7-6: *Simplified sketch of a hollow structural form within which the "Graben" might have extended; with filling of the ramp with carbonates. Illustration of the Sirab Formation. This is a conceptual model built with the aim of imagining the reason for the high manganese contents of the Sirab Formation.*

The Y/Ho ratios in the majority of the samples do not indicate a marine water signature (figure 3-43, figure 4-11, figure 5-2 and figure 5-18). However, the loss of the marine signal in the chemical composition of the water can also result from the contamination of carbonates by terrigenous (clastic) fractions. For, even minute amounts of detrital minerals can alter the original seawater signature in carbonates, as Rare Earth concentrations are much higher in detritus than in seawater (Taylor and McLennan, 1985; Webb and Kamber, 2000). Table 7-1 illustrates the Y/Ho values recorded in carbonates of the Sirab Formation in comparison with the Y/Ho values of carbonates in seawater and freshwater.

- Marine limestones Y/Ho ratios knew > 45 (Zhang and Nozaki, 1996);
- Freshwater Y/Ho ~26 (Lawrence et al., 2006; Bolhar and Van Kranendonk, 2007);
- Precambrian freshwater Procoki Y/Ho ~ 29 (experimented in TCD lab 2016) appendix 5.

Y/Ho for Sirab (Wadi-Shital ST-1 & ST-2).

Sample	STB 4	STB 6	STB 8	STB 14	STB 16	STB 18	STB 19	STB 21	STB 23
Y/Ho	30.14	26.58	30.94	35.37	30.22	29.57	32.56	29.39	32.28
Sample	**STB 26**	**STB 27**	**STF 67.5**	**STF 68.4**	**STF 69**	**STF 70**	**STF 71**	**STF 185**	**STF 202.9**
Y/Ho	35.68	34.74	31.39	27.53	27.60	31.35	32.81	27.93	26.73
Sample	**STF 210**	**STF 204.3**	**STF 205.7**	**ST2 1.6**	**ST2 2.9**	**ST2 2.15**	**ST2 4.15**		
Y/Ho	35.06	33.58	31.86	32.57	30.60	30.38	32.04		

Y/Ho for Wadi Shuram WS9 and Wadi Aswad WA1 and WA2.

Wadi Shuram WS9						
Sample	**WS9-144**	**WS9-151.5**	**WS9-157.5**	**WS9-171**	**WS9-177.3**	**WS9-190**
Y/Ho	27.5	40	35	26.7	40	30
Wadi Aswad WA1						
Sample	**WA1-82.5**	**WA1-84.5**	**WA1-85.5**	**WA1-87**		
Y/Ho	30	30	25	36		
Wadi Aswad WA2						
Sample	**WA2-0.5**	**WA2-4**	**WA2-9**	**WA2-15.5**	**WA2-21.75**	
Y/Ho	45	50	35	37.5	35.5	

Table 7-2: *Values of ratios Y/Ho for all tested Wadi-Shital ST-1 & ST-2, Wadi Shuram WS9, Wadi Aswad WA1 and Wadi Aswad WA2 samples.*

The table of Y/Ho values of all samples from this study shows that all of Sirab across the Al-Huqf region should be favourable to the presence of fresh water rather than seawater. However, two samples from the Wadi Aswad WA2 section located north of the Al-Huqf region and lithostratigraphically at the top of the Sirab Formation have Y/Ho values of seawater. This seems to be logical because the description of the lithofacies of the Aswad Member made by Gold (2010), mentions this member as being a relic of the passage of marine waters at the level of the Formation. In apparent contradiction

with the upper Shital level in the sections of Wadi Shuram S8, WS9 and WS10 (deeper water where the presence of marine water had also been suspected by Nicholas and Gold (2012), there is in the number of samples used in this study in connection with Wadi Shuram WS9, no presence of marine water. Two samples nevertheless have Y/Ho ratios = 40 against 3 which are favorable to fresh water, among which 2 are strictly fresh water for a number of the 6 samples analysed.

To justify the presence of the sandstone marker horizon throughout the Al-Huqf region, the cyclicity of carbonates in the lower Shital Member, the inundation of the carbonate ramp in Wadi Shuram WS8, WS9 and WS10, the presence palaeo-topographic shoals in Wadi Shuram; Nicholas and Gold (2012) argue for a regional subsidence of the Sirab structure in the form of a basin. If such a hypothesis existed during the filling of the Sirab, it would have gradually given more access to accommodation surfaces through what currently constitutes a "graben". Thus, it is likely that the deep parts of the Sirab Formation would then have been totally trapped in the trough of the Al-Huqf topography during the Ediacaran-Cambrian. As new sediment deposits filled the entire structural hollow region, the summit deposits (located north of the region at Wadi-Aswad) may have penetrated at times in connection with the "sea".

The effects of the dilution of the original "sea" water by the current chemical composition at the water-sediment interface in Sirab Formation would have spread a little further from the connection point to the north. As such, the sections south of Al-Huqf, such as WS9, subsequently recorded Y/Ho values > 30. It is also apparent from Table 7-1 that Y/Ho values are generally slightly elevated from Member upper Shital, around Y/Ho ~ 30 on average. The STF 202.9 level which lies lithostratigraphically close to the Sandstone horizon (figure 1-13) continues to show the relict of a freshwater supply source (Y/Ho = 26.73) as evidence of the gradual dilution of the chemical composition of the water at the water-sediment interface.

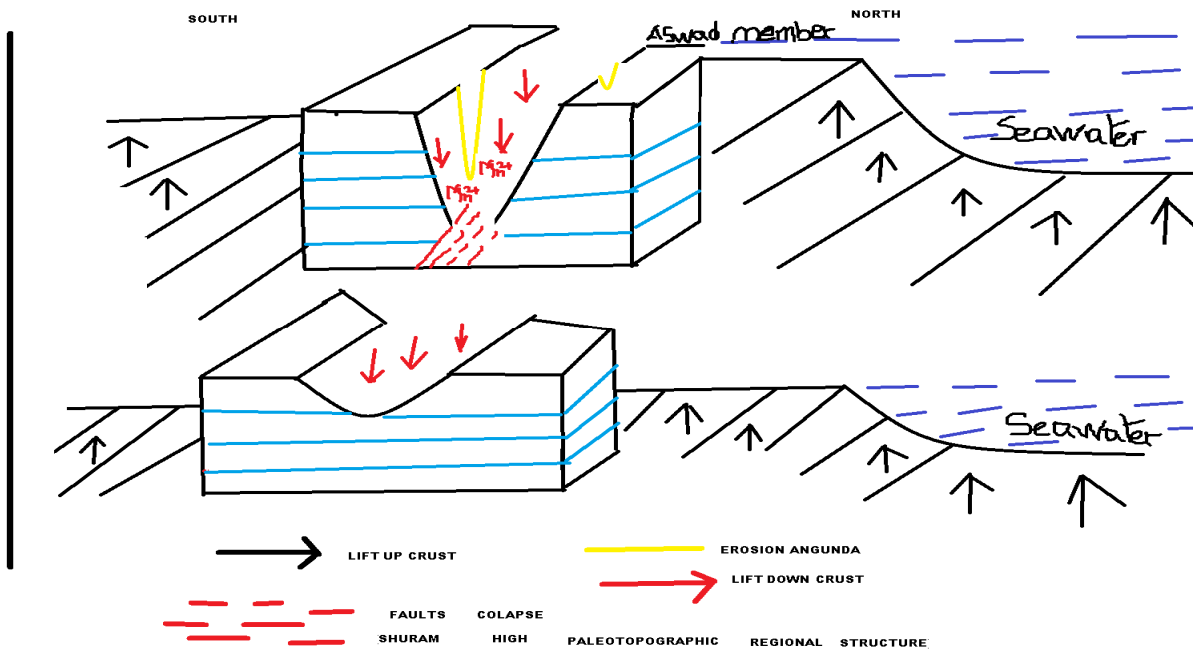

Figure 7-7: *Sketch showing sea level rise (eustatic) along with subsidence in the Al-Huqf region in which the field sections of the Sirab Formation currently reside.*

There is an apparent contradiction encountered in the analyzes of this study in relation to the chemical composition at the water-sediment interface during the Precambrian in the Sirab Formation. Indeed, the freshwater signature seems to predominate in the number of samples of this study as well as the fractionation into LREEs. Among nine (9) samples from Wadi Aswad sections WA1 and WA2, only 2 samples have Y/Ho ratios favorable to "sea" water. However, for these same samples, their means in composition REEs compared to PAAS (sections WA1, WA2 and even for WS9) indicate that the chondrites in the samples of these sections are depleted in Y/Ho against Zr, Th and REE+Y compared to the average concentrations in the crust. The detection limits of the REE+Y seem to confirm the hypothesis that the sediments coming from Sirab were relatively less contaminated by the original geochemical compositions of the Elements of the crust, because the continental detritus is more enriched in REEs compared to carbonates. Only Cerium and Yttrium have values that calibrate in some samples (2 ppm) while the majority of them have REEs < 1.

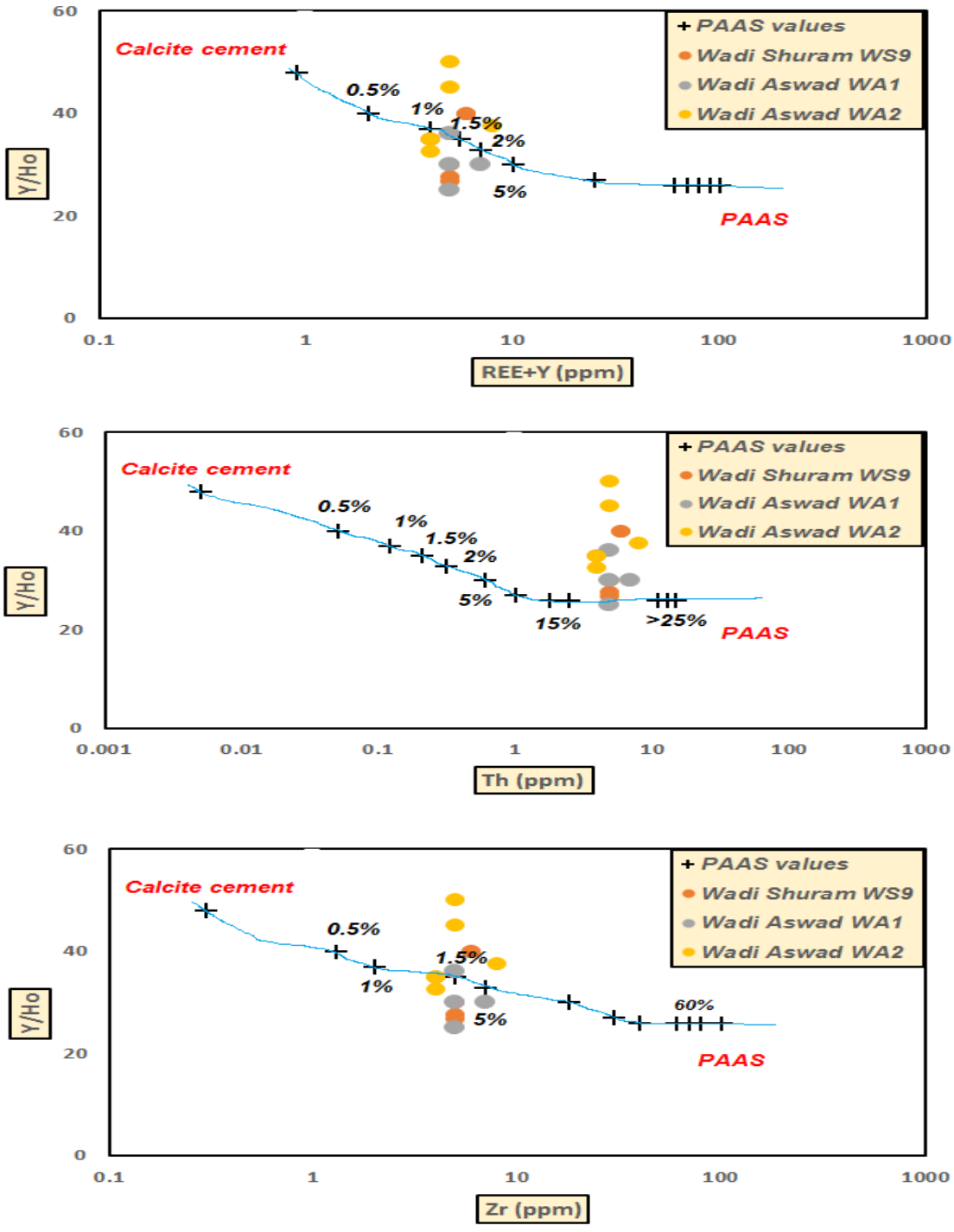

Figure 5-24: *Conservative mixing lines between sections Wadi Shuram WS9, Wadi Aswad WA1 as well as Wadi Aswad WA2 on Y/Ho versus. Zr, Th, and ΣREE+Y data plus Calcite cement, modified from Nothdurft et al. (2004) and PAAS by Taylor and McLennan (1985).*

The typical section of Sirab at Wadi Shital ST-1 & ST-2 confirms the result that, comparing the pattern of REEs that occur on Sirab with those obtained on the Ara Group (figure 6-1) and the pattern of REEs of limestones from the Procoki quarry in the south-east of the DRC, it appears that the Sirab Formation has REE profiles similar to those of the Ara Group in the Birba Platform (borehole BB-3). The Platform carbonates that have REEs similar to the Sirab carbonates are A4C. In the Sirab Formation, the profiles of the REEs remain almost unchanged from the base of the Ramayli Member Formation to the top of the Aswad Member Formation. In a way, this directly implies an almost constant palaeo-ecology of the environment of the deposit. The water-sediment interface of the Sirab Formation appears to have been chemically homogeneous or chemically very little variable.

In the A4C, several redox parameters such as authigenic Uranium, Vanadium, Molybdium (figure 6-6); Thorium and Titanium (figure 6-4), are correlated with Wadi Shital ST-1 & ST-2 data from the Sirab Formation. Manganese concentrations exceed due to the explanations provided at the very top of this discussion of diagenesis in relation to the Element Mn and structural landform across the region during the Ediacaran era. These include the absence of horizontal circulation of Mn^{2+} ions which would be followed by their trapping in the hollow of the palaeo-topographic structure.

Another evidence of lesser detrital influence in carbonate contamination of Sirab comes from its master section Wadi Shital ST-1 & ST-2. In the typical section of Sirab as well as in the Ara Group, the detritus has weakly influenced the composition of the carbonates according to the analysis of the profiles of the REEs. The REEs analysis of freshwater limestone from the Procoki quarry presented in detail in appendix 5 of volume 2, made it possible to better compare the contamination profile of this carbonate strongly influenced by continental detritus compared to authigenic sediments or little contaminated with clastic materials. Sediments uncontaminated or only slightly contaminated by continental clastic inputs generally retain their primary REEs compositions. For example, the Sirab Formation and the Procoki Quarry have in common carbonate sediments of relatively similar ages (Precambrian - Infracambrian) but their REEs profiles diverge. As a reminder, the Sirab Formation is geographically located in Oman at Al-Huqf through the Al-Huqf region, in the center of the desert located in the south-east of the region. While the Procoki quarry is located in the south-western DRC and its geolocation places it about 300 km off the African Atlantic coast while the carbonate facies found there at Procoki are closely mixed with volcanic episodes and significant clastic contributions (Kampunzu and al., 1991). This is the reason for the profile of the REEs of Procoki whose contribution by continental detritus is superior to that of the Sirab Formation and the Ara Group. The LREEs are sloping increased in the Procoki while the HREEs are regularly

exhausted. The carbonates of the Ara Group Platform and those of the Sirab indicate flat REEs, relatively weakened compared to the PAAS.

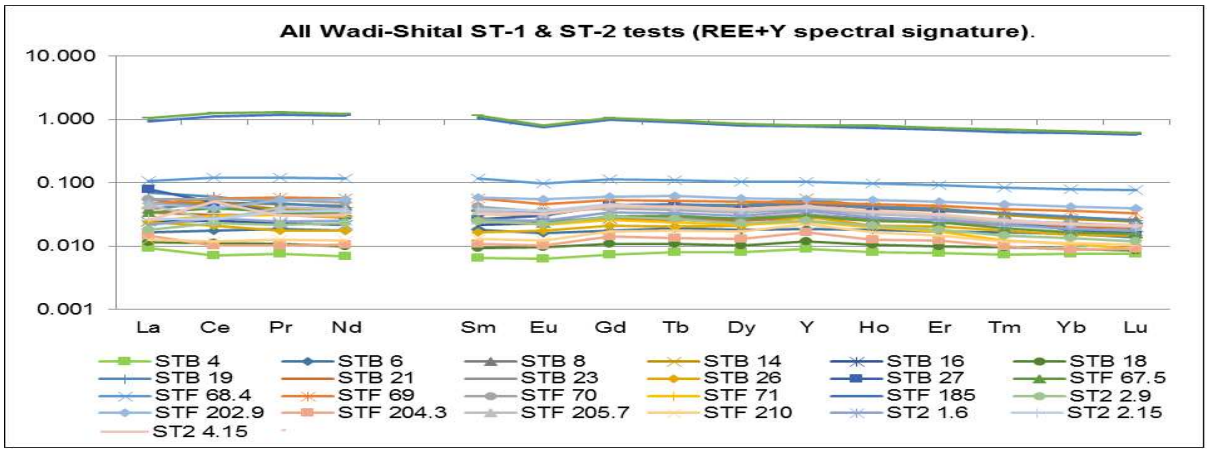

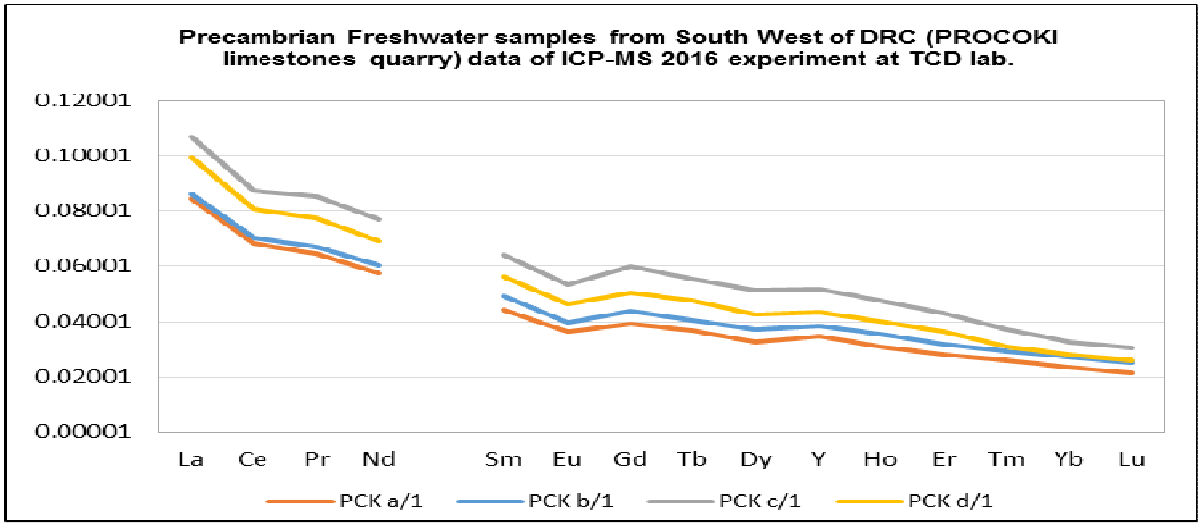

Figure 7-8: *Model of the carbonates of the ramp less influenced by terrigenous detritus with high LREEs potential and those strongly influenced by fractions LREEs (relative to Precambrian age).*

- **Sirab Formation in Wadi Shital ST-1 & ST-2.**

Sirab Formation: Internal Ramp, Y/Ho mostly favorable to freshwater. More or less flat REEs profile. No preferential splitting of REEs (contains in balance LREEs, MREEs and HREEs). Possible structural shape of the ramp: ± closed (endoreic network and/or possible stagnant water). No connection with the open marine environment from the base of the Formation to approximately the upper Shital Member, weak marine presence reported north of the region at Wadi Aswad with regard to the screening of the samples. Geolocation of the carbonate ramp: central part of the southeastern desert of Oman (Al-Huqf).

- **Precambrian Freshwater Procoki**.

Procoki limestones: internal ramp, Y/Ho fresh water ~29. Very pronounced LREEs profile, exhaustion in HREEs. No marine connection (see appendix 5, intention 2). Structural form of the ramp: hinterland, ±300Km from the African Atlantic coast.

However, besides the manganese content, there is yet another chemostratigraphic Element of differences between the Ara and Sirab group platform. These are the excursions of the $\delta^{13}C$ carbon. This difference is especially marked during the passage of the upper Shital where, the $\delta^{13}C$ marks a characteristic positive peak in all the analyzes

of the different sections of the Sirab (VPDB +5 to +8 ‰) while the levels which precede the upper Shital oscillate between values positive and negative $\delta^{13}C$ (VPDB -3 to +3‰), see Figure 4-1. In A4C and its equivalents in the Ara Group basin, δ13C is strictly negative with a characteristic curve (Schroder and Grotzinger 2007). The biomarker in A4C is documented and the earliest tabular limestone *Claudina* and possible *Namacalathus* fossils are recognized in Platform strata in the Ediacaran-Cambrian period. However in the Sirab, these fossils have not been demonstrated unequivocally (Gold, 2010). Possibly, the carbonate composition of Ara and Sirab partly depended on the water circulation between the platform and the basin for the Ara group while it differed in the Sirab considering of the horizontal restriction of the free circulation of the mass of water in the hollow paleotopography of Sirab which existed in Al-Huqf. The filling of the Sirab Formation having taken place gradually (Nicholas and Gold, 2012), the units at the base of the stratigraphy would not have or very little undergone the weak chemical fluctuations (Y/Ho) at the water-water interface-sediments. While during the brief period of possible marine linkage to the north of the region, the units above the stratigraphy from the upper Shital and Aswad Member would have recorded the water chemistry dilutions of " sea" (Y/Ho) and at the same time, the Mn^{2+} ions could then momentarily circulate freely between the structural trough of the Al-Huqf region and the "sea" to the north? Could it be that the litofacies characteristic of the upper bioherm of Shital then developed under the dependence of the mixture between the original chemical composition of the Sirab water and the

influence of “seawater”? However, even in the Ara Group, below A4, positive $\delta^{13}C$ values are also encountered (Schroder and Grotzinger 2007) while these occur stratigraphically from A0 – A3, where somewhere in A3 a level of volcanic ash is recognized. This could also constitute in the Ara Group, the equivalence of a redox parameter influencing $\delta^{13}C$ at the upper level of A4C?

In addition, a strong persistent presence of gamma signal was reported in the A4 as well as in the rocks of the Basin. This ratio was interpreted as coming from potassium. Potassium data was not available for Sirab type section at Wadi Shital ST-1 & ST-2. However on the sections of WS9, WA1 as well as WA2, potassium was analyzed as a Major Element with percentages in the samples of order K_2O (%) <0.01 to 0.04 ppm. Perhaps further correlation studies in the future between these two Formations will successfully correlate gamma signals from the Sirab Formation and the Ara Group.

Figure 7-9: *comparative Ara Group Platform and Basin carbonate rocks with Sirab Formation carbonates Rocks.*

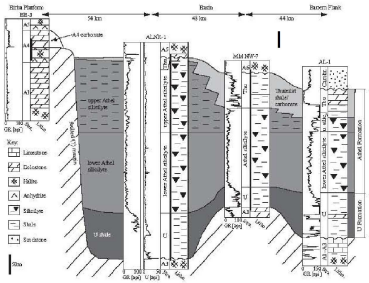

I Cross-section from Birba Platform through the central Athel Basin to the Eastern Flank (indicated by dashed line in figure II). Stratigraphic column uranium response (where available) and stratigraphic subdivisions for the wells; the black bars next to the stratigraphic subdivisions indicate comparative sections in each well; well AL-1 has been added as a representative for the Eastern Flank from the original work of S.SCHORDER & J.P. GROTZINGER., 2007

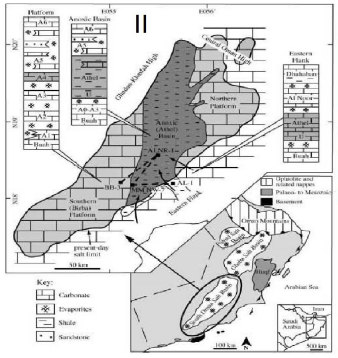

II. Geological setting of the general geology of Oman (after Loosveld et al. 1996). The detailed setting of South Oman Salt Basin is enlarged in the upper down map.

Individual stratigraphic columns are given for the Birba Platform, Athel Basin and Eastern Flank. In each column, the comparative interval is highlighted in grey.

Arrows on the map illustrate the dominant sources of detrital sediment (clastics input). Black squares and the dashed line indicate wells and the cross-section in figure **I**.

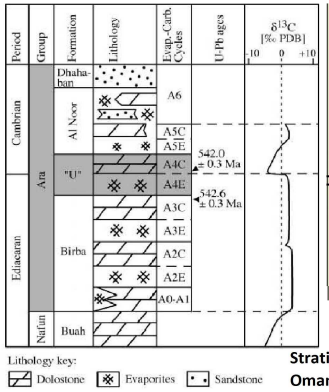

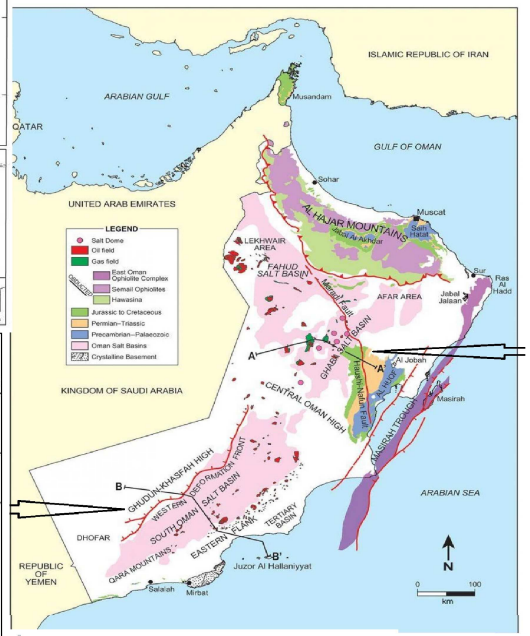

Ara Group

Stratigrapny or the Ara Group in the south Oman Salt basin (platform areas). The comparative interval A4C to Sirab Formation is highlighted in grey. Each Ara Group cycle contains an evaporitic unit (e.g. A4E) and a carbonate unit (e.g. A4C). Thicknesses are not scale. The younger Ara Group ash bed coincides with a negative δ13C anomaly (adapted from Loosveld et al., 1996; Amthor et Al., 2003).

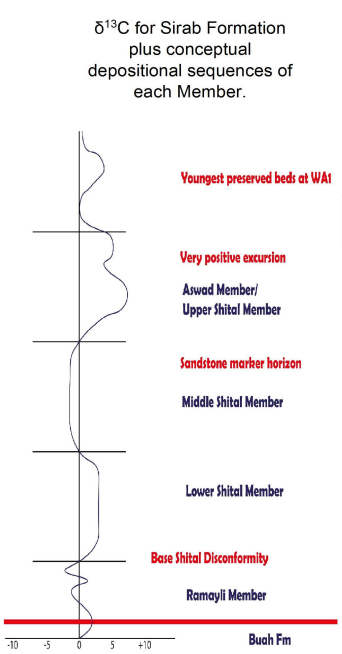

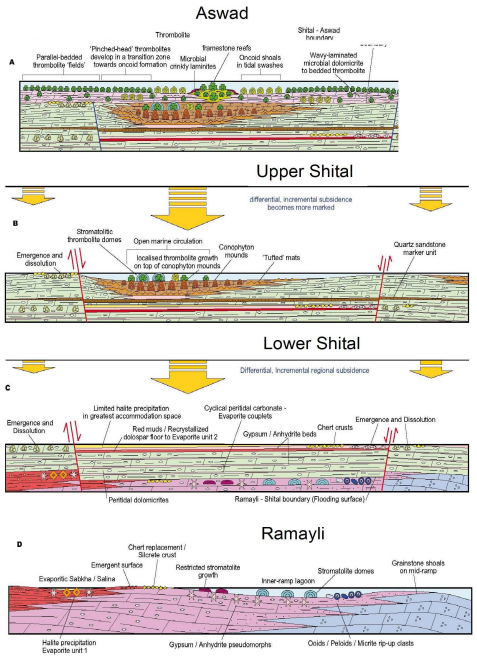

Geochemical parameter	Platform: well BB-3	Basin: well ALNR-1	Basin: well MM NW-7
Detrital proxies: Th	Depleted relative to average carbonate; peak in ash samples, decreasing up section	Near crustal values in U shale and Thuleilat shale, depleted in silicilyte; increasing up section to Thuleilat shale	
Detrital proxies: Ti	Depleted relative to average carbonate; peak in ash samples, ± constant up section	Same as Th above	
Detrital proxies: Zr	Same as Ti above	Same as Th and Ti above	
REE profile and ∑REE	∑REE decreases up section ; (1) ash: ∑REE *c.* half of PAAS, slight HREE enrichment (2) group 1: ∑REE *c.* two orders of magnitude < PAAS, strong HREE depletion, slight MREE enrichment (3) group 2: ∑REE *c.* three orders of magnitude < PAAS, flat profile	Mostly flat profiles with minor variation; silicilyte and chert samples are almost indistinct and tend towards slight HREE enrichment ; ∑REE in U shale and Thuleilat shale similar to PAAS, *c.* one order of magnitude smaller in silicilyte LREE enrichment in U shale	HREE enrichment most pronounced in Thuleilat shale
REE: Ce anomaly	True positive Ce anomaly in two group 1 carbonate samples ($Ce/Ce^* = 1.09–1.10$)	True negative Ce anomalies common ($Ce/Ce^* = 0.57–0.93$), but no systematic variation with lithology or stratigraphic position ; single silicilyte sample of MM NW-7 with true positive Ce anomaly ($Ce/Ce^* = 1.23$)	
Redox: Mn	Increases gradually up section ; Mn/Th increases sharply at base of A4C, flattens out at values above average carbonate, again increases in middle ramp no correlation with detrital parameters	Concentrations < PAAS, tend to be higher and more variable in the shale units than in silicilyte (Fig. 10a); no vertical trends of Mn/Th, ratio smaller than or equal to Mn/Th in PAAS ; no correlation with detrital parameters	Peak at 2700–2705 m correlates with higher carbonate content
Redox: V	Peak near base of A4C, dropping to ≤5 ppm up section peak concentrations exceed average carbonate; V/Th increases sharply at base of A4C, flattens out at values above average carbonate ; no correlation with detrital parameters	Silicilyte concentrations similar to or slightly > PAAS, V is strongly enriched in shale units ; V/Th enriched above PAAS throughout succession (Fig. 10d); no correlation with detrital parameters, but silicilyte samples tend to be more tightly clustered	
Redox: U/Th	Increases up section , ratio above average carbonate (except ash samples)	Enriched > PAAS throughout succession, peak near base of succession, two intervals of pronounced enrichment in silicilyte	Mostly below PAAS, increasing through silicilyte to prominent peak near top of unit, which is strongly enriched > PAAS
Redox: U_{aut}	Highly variable, values ≤5 ppm ; no correlation with detrital parameters	Enriched > PAAS throughout succession, peaks in basal U shale and in Thuleilat, increasing through upper silicilyte ; no correlation with detrital parameters, but silicilyte samples tend to be more tightly clustered	
Redox: Mo	Absolute values and Mo/Th similar in behaviour to V, below detection limit above base; no correlation with detrital parameters	Mo/Th > PAAS; no correlation with detrital parameters, but silicilyte samples tend to be more tightly clustered No vertical trends of absolute concentrations; Mo/Th strongly enriched > PAAS in lower silicilyte	High absolute concentrations in shale units, drop in silicilyte ; no vertical trends of Mo/Th, few samples near top of silicilyte have Mo/Th < PAAS

Table 7-2: *Geochemical parameter of Ara Group, from Schroder and Grotzinger (2007). Group (1) are carbonate at base of A4C and group (2) are carbonate above A4C.*

Comparative Geochemical parameters of Ara Group and Sirab Formation			
Sirab Formation	Platform well BB-3	Basin well ALNR-1	Basin well MM NW-7
Detrital proxies Th, Ti, and Zr	Fit with carbonate group 1 (base of A4C) and carbonate group 2 (above of A4C); see Figure 5-24, Figure 6-4 and Figure 6-5.	Not fit with U and thuleilat formation. But Little close silicylite	Not fit with U and thuleilat formation. But Little close silicylite
REEs	Fit with carbonate group 1 and group 2 (REEs flat and ∑REEs between 2 and 3 order magnitude < PAAS; see Figure 5-24, Figure 6-2 and figure 7-3.	Not fit with U and thuleilat formation. But Little close silicylite	Not fit with U and thuleilat formation. But Little close silicylite
REE (Ce*) anomaly	True anomalies were among samples of Wadi Shital ST-1 & ST-2, Wadi Shuram WS9 and Wadi Aswad WA1 & WA2. Most of values above (Ce/Ce* = 0.8 – 0.9); see Figure 6-3.		
Redox Mn	Not fit average concentration of Platform two groups. Mn highly content in respect to Ara Group and less fluctuation across the members and not correlation with detrital parameter; see figure 5-16	Not fit with U and thuleilat formation. Higher than silicylite	
Redox V, Mo and U_{auth}	Data nearly to Ara group carbonates Platform but less fluctuation among samples; see Figure 6-5, Figure 6-6 and Figure 6-7.	Not fit with U and thuleilat formation. But Little close silicylite	Not fit with U and thuleilat formation. But Little close silicylite

Table 7-3: *Geochemical parameters to correlate Ara group Platform and carbonates rocks to Sirab Formation carbonates rocks.*

Conclusion

Sedimentological data and field investigations across Haushi-Huqf in Oman have proven the existence of outcropping sediments which are largely composed of carbonates and which overlie the Nafun group. These carbonates, currently called Sirab Formation, represent more or less an equivalent surface to the Ara Group, but few comparative studies of the chemostratigraphy between these two Formations are valid to date.

The absence of a clear presence of *Claudina* and possible *Namacalathus* biomarkers in Sirab Formation strata casts doubt on the correlation between the Sirab Formation and Ara Group, but REEs data as well as chemostratigraphy help overcome this and make comparisons between the paleo-ecology of these two geological Formations.

Indeed, anoxia is the main characteristic of the carbonates of the Sirab Formation, in particular with the ratios of real Ce*. It demonstrates that the environmental parameter of anoxia was permanent during the period of carbonate deposition in Sirab Formatin and this is also the case with the Ara Group in general. The presence of marine signature Y/Ho remains mixed in the Ara Group. Some authors such as Schroder and Grotzinger (2007) think that there was a loss of marine signature in the carbonates of the Ara Group whereas in view of the

geochemical data here in this thesis, the majority of the samples in relation to the Formation from Sirab have Y/Ho ratios lower than the value of sea water. This therefore indicates a similar trend of dolomitic carbonates with weak "marine" presence with respect to Y/Ho values between the Ara Group and the Sirab Formation. However, north of the Haushi-Huqf region in Wadi Aswad, some carbonates at the top of the Sirab Formation record the marine signature in the Aswad Member, showing then a very strong restriction of the marine connection in the Ediacaran - Cambrian era for the Sirab Formation. The Th, Ti and Zr detrital proxies of the Ara Group BB-3 carbonate platform which include carbonate group 1 and carbonate group 2 (base and top of A4C) are common with those of the Sirab Formation. The REEs signatures are depleted compared to the PASS in the carbonate Platform (BB-3 well) and in the carbonates of the Sirab Formation. The Redox V, Mo and U_{authi} in the Ara Group in Platform and the Sirab Formation show similarities.

Less common is the average Mn concentration in the Sirab Formation. In fact, this Geochemical Element is much more concentrated in the Sirab Formation than in the Ara Group basin and platform. It appears that the structural shape of the basin relief of the Sirab Formation may have encouraged Mn trapping while the involvement of diagenesis is less evident. As such, Mn^{+2} ions could be trapped in the endoreic region with restriction to the marine connection. The presence of the Salutiyyat Member, the tectonic stretching and contractions of the Arabian Plate terranes during the Gondwana-wide Najd Event may

have been a consequence of the creation of a hollow relief in the hinterland (Sirab Formation).

Future studies of the exact structure of the Al-Huqf relief during the Ediacaran-Cambrian era in Oman could help to better understand the reason for the unconformity at the base of the Sirab Formation and the Nafun Group that occurs in Wadi Salutiyyat and Wadi Shauram, and this evidence may also confirm the trapping of Manganese ions according to the shape of the existing landform.

Bibliography

Al-Husseini. (2000). Origin of the Arabian Plate structrures: Amar collision and Najd rift. GeoArabia., 527-542.

Al-Husseini, M. (2010). Middle East Geologic Time Scale 2010: Early Cambrian Asfar Sequence. GeoArabia, v. 15,, p. 137-160.

Allen. (2007). The Huqf Supergroup of Oman: Basin development and context for Neoproterozoic glaciation. Earth Science Reviews, 84 (3-4), 139-185.

Al-Siyabi, 2. (2005, October 01). Digital characterization of thrombolite stromatolite reef distribution in a carbonate ramp system (terminal Proterozoic, Nama Group, Namibia. AAPG Bulletin, pp. 1293–1318.

Al-Siyabi, 2. (2005, October 01). Exploration history of the Ara intrasalt carbonate stringers in the South Oman Salt Basin. GeoArabia, pp. 39–72.

Al-Siyabi, 2. (2005, October 01). Exploration history of the Ara intrasalt carbonate stringers in the South Oman Salt Basin. GeoArabia, pp. 39–72.

Amthor et al., 2. (2003, MAY 01). Extinction of Cloudina and Namacalathus at the Precambrian-Cambrian boundary in Oman. pp. 431–434.

Aderson, T. &. (1983). Stable isotopes of oxygen and carbon and their application to sedimentologic and paleoenvironment problems. SEPM Shirt course, 10, p111-151.

Bau, M. &. (1996). Distribution of yttrium and Rare-Earth Elements in the Penge and Kuruman iron-formations, Transvaal Supergroup, South Africa. Precambrian Research, 79, 37–55.

Beales, F. &. (1980). Criteria for the recognition of diverse dolomite types with an emphasis on studies on host rocks for Mississipi Valley-type ore deposits. concepts and Models of Dolomitization. Soc. Econ.Paleontologists Mineralogists, Spec.Pub, 28, 155-161.

Beherens, E. &. (1972). Subtidal Holocene dolomite, Baffin Bay, Texas. J Sediment. Petrol, 42, 155-161.

Bowring, S. G. (2007). Geochronologie constraints on the chronostratigraphic framework of the Neoproterozoic Huqf Supergroup, Sultanate of Oman. American Journal of Science.

Brand, U. &. (1980). Chemical diagenesis of a multicomponent carbonate system : 1. Trace Elements. Journal of Sedimentary Petrology, 50(4)., p1219-1236.

Brand, U. &. (1980). Chemical diagenesis of a multicomponent carbonate system: 1. Trace Elements. Journal of Sedimentary Petrology, 50 (4), 1219-1236.

Brasier, M. (1992.). Global ocean-atmosphere change across the Precambrian-Cambrian transition. Geologicla Magazine, 129 (2), 161-168.

Corfield, R. (1995). An introduction to the techniques, limitations and landmarks of carbonate oxygen isotope palaeothermometry. Geological Society London, Special Publications, 83 (1), 27.

Cozzi and Al-Siyabi, 2. (2004). Sedimentology and play potential of the late Neoproterozoic Buah Carbonates of Oman. GeoArabia, 11-36.

Dickson. (1966). Carbonate identification and genesis as revealed by staining. Journal of Sedimentary Research (1966) 36 (2), p 491–505.

Droste, 1. (1997, October 01). Stratigraphy of the Lower Paleozoic Haima Supergroup of Oman. GeoArabia, pp. 419–472.

Droste, H. (1997). Stratigraphy of the Lower Paleozoic Haima Supergroup of Oman. GeoArabia, 2 419-72.

Dunham. (1962). Classification of Carbonate Rocks According to Depositional Textures. AAPG Special Volumes, abstract, p 108-121.

Elderfield, G. &. (1990). Application of the Ce anomaly as a paleoredox indicator: The ground rules. Paleoceanography and Paleoclimatology, P 823-833.

Fairchild, J. M.-S. (1990). Stratigraphic shifts in carbon isotopes from Proterozoic stromatolitic carbonates (Mauritania): Influences of primary mineralogy and diagenesis. American Journal of Science, 290, 46-79.

Folk's. (1952). course notes.

Folk's. (1962). Classification of Carbonate Rocks According to Depositional Textures. AAPG Special Volumes, p 108-121.

Forbes, G. H. (2010). Lexicon of Oman subsurface stratigraphy: Reference guide to the stratigraphy of Oman's hydrocarbon basins. GeoArabia Special Publication 5, 371 p.

Fortey, R. (1995). Cambrian fossils and stratigraphy in the Sultanate of Oman. Midlle East petroleum geosiences, GEO, 387-393.

Gorin et al, 1. (1982). Late Precambrian-Cambrian Sediments of Huqf Group, Sultanate of Oman1. AAPG Bulletin, 2609–2627.

Gorin et al., 1. (1982, December 01). Late Precambrian-Cambrian Sediments of Huqf Group, Sultanate of Oman1. Research Article, pp. 2609–2627.

Grotzinger and Amthor, 2. (2002, March 10-13). Facies and Reservoir Architecture of solated Microbial Carbonate. AAPG Annual Meeting.

Grotzinger and Amthor, 2. (2002, March 10-13). Tectonically – Driven Evaporite-Carbonate Transitions in a Precambrian/Cambrian Saline Giant: Ara Salt Basin of South Oman. AAPG Annual Meeting, p. 1.

Grotzinger, J. (2005). Chemostratigraphy of Carbonates Stringers. Internal PDO report.

Grotzinger, S. &. (,2007). Evidence for anoxia at the Ediacaran–Cambrian boundary: the record of redox-sensitive trace elements and rare earth elements in Oman. Journal of the Geological Society, London, Vol. 164, 2007,, pp. 175–187.

Hargrove et al., 2. (December). How juvenile is the Arabian–Nubian Shield? Evidence from Nd isotopes and pre-Neoproterozoic inherited zircon in the Bi'r Umq suture zone, Saudi Arabia. ScienceDirect, 308-326.

Hoefs, J. (2008). Stable isotope geochemistry. Springer.

Hughes Clarke, 1. (1988, January). STRATIGRAPHY AND ROCK UNIT NOMENCLATURE IN THE OIL-PRODUCING AREA OF INTERIOR OMAN. JPG journal of Petroleum Geology, pp. 5-60.

Hussein, 1. (1989). Geochronology of the late Precambrian Hamisana shear zone, Red Sea Hills, Sudan and Egypt. Geological Society, 1017-1029.

James, K. a. (1986). Thrombolites and Stromatolites: two distinct types of microbial structures. . Palaios, 492-503.

Jarvis, K. G. (1989). Avoidance of spectral interference on europium in inductively coupled plasma mass spectrometry by sensitive measurement of the doubly charged ion. J. Anal. At. Spectrom. 4, 743–747.

Jasmine B.D.Jaffrés., G. A. (2007). The oxygen isotope evolution of seawater: A critical review of a long-standing controversy and an improved geological water

cycle model for the past 3.4 billion years. Earth-Science Reviews; Volume 83, Issues 1–2, July , P 83-122.

Johnson, P. R. (2003). Post-amalgamation basins of the NE Arabian shield and implications for Neoproterozoic III tectonism in the northern East African orogen. ScienceDirect, 321-337.

Kattan, J. a. (2001). Implications of SHRIMP and microstructural data on the age and kinematics of shearing in the Asir terrane, southern Arabian Shield, Saudi Arabia. USGS, 172-173.

Kattan, J. a. (2001). Implications of SHRIMP and microstructural data on the age and kinematics of shearing in the Asir terrane, southern Arabian Shield, Saudi Arabia. USGS, 172-173.

Kattan, J. a. (2001). Oblique sinistral transpression in the Arabian shield: the timing and kinematics of a Neoproterozoic suture zone. ScienceDirect, 117-138.

Kattan, J. a. (2003). Post-amalgamation basins of the NE Arabian shield and implications for Neoproterozoic III tectonism in the northern East African orogen. ScienceDirect, 321-337.

Kattan, J. a. (2003). Post-amalgamation basins of the NE Arabian shield and implications for Neoproterozoic III tectonism in the northern East African orogen. ScienceDirect, 321-337.

Kaufman, A. &. (1995). Neoproterozoic variations in the C-isotopic ccomposition of seawater: stratigraphic and biogeochemical implications. . Precambrian Research, 73 (1-4), 27-49.

Kaufman, A. J. (1993). The vendian record of Sr and C isotopic variations in seawater: Implications for tectonics and paleoclimate. Earth and Planetary Science Letters, 120 (3-4), 409-430.

Klovan, E. &. (1971). Course notes.

Land, L. (1985). The origin of massive dolomite. J.Geol.Educ, .33 (2), p112-125.

Lawrence, M. G. (2006). Rare Earth Element and Yttrium Variability in South East QueenslandWaterways. Aquat. Geochem. 12, 39–72.

Leather, J. A. (2002). Neoproterozoic snowball Earth under scrutiny: evidence from the Fig glaciation of Oman. Geology, 30 (10), 891.

Lee, Y. &. (1987). Deep-burial dolomitization in the Ordovician Ellenburger Group carbonates, West Texas and southeastern New Mexico. Journal of Sedimentary Petrology, 57 (3), 544-557.

Marshall, J. (1992). Climatic and oceanographic isotopic signals from the carbonate rock record and their preservation. Geological Magazine, 129 (2), 143-160.

McCarron, M. (2000). The sedimentology and chemostratigraphy of the Nafun Group, Huqf Supergroup, Oman.

McCormick, D. &. (2001). Digital Mapping of Neoproterozoic Thrombolite-Grainstone Facies Architecture in Namibia: Analog for Intrasalt Reservoirs in South Oman Salt Basin. American Association of Petroleum Geologists, Annual.130.

McLennan, S. (1989). Rare earth elements in sedimentary rocks: influence of provenance and sedimentary processes. In: Lipin, B.R. & McKay, G.A. (eds); Geochemistry and Mineralogy of Rare Earth Elements. Mineralogical Society of America, Reviews in Mineralogy, 21, 169–200.

Mclennan, S. (1989). Rare Earth Elements in sedimentary rocks; influence of provenance and sedimentary processes. Reviews in Mineralgy and Geochemistry, 21(1), 169-200.

Mclennan, S. (2001). Relationships between the trace element composition of sedimentary rocks and upper continental crust. Geochemistry geophysics geosystems, 21 (1), 1021.

Meyer, E. Q. (2012). Trace and rare earth elemental investigation of a Sturtian cap carbonate, Pocatello, Idaho: evidence for ocean redox conditions before and during carbonate deposition. Precambrian Res. 192–195, 89–106.

Meyer, E. Q. (2012). Trace and rare earth elemental investigation of a Sturtian cap carbonate, Pocatello, Idaho: evidence for ocean redox conditions before and during carbonate deposition. Precambrian Res. 192–195, 89–106. http://dx.doi.org/10.1016/j.precamres.2011.09.015.

Morrow, D. C. (1986). Manetoe facies-a gas-bearing, megacrystalline, Devovian dolomite, Yukon and Northwest Territories, Canada. American Association of Petroleum Geologists Bulletin, 70 (6), 702-720.

Nicholas and Brasier, 2. (2000). Outcrop equivalent of the subsurface Precambrian–Cambrian Ara Group in Oman. GeoArabia, 151-152.

Nicholas, C. J., & Gold, S. E. (2012). Ediacaran–Cambrian Sirab Formation of the Al Huqf region, Sultanate of Oman. GeoArabia (2012) v. 17 no. 1, p. 49-98.

Nozaki, Z. a. (1996). Rare earth elements and yttrium in seawater: ICP-MS determinations in the East Caroline, Coral Sea, and South Fiji basins of the western South Pacific Ocean. ScienceDirect Volume 60, Issue 23, December , P 4631-4644.

Quick, J. 1. (1991). Late proterozoic transpression on the Nabithah fault system implications for the assembly of the Arabian Shield. Precambrian Research , 119-147.

R. McCabe et al. (2019). A multidisciplinary approach for the quantitative provenance analysis of siltstone: Mesozoic Mandawa Basin, southeastern Tanzania. Geological Society, London, Special Publications, 484, 275-293,

Rabu, D. (. (1988). Geologie de l'Autochtone des montagnes d'Oman: la fenetre du Jabal Akhdar. Document du Bureau de Recherches Géologiques et Minières (BRGM), Orléans, France, no. 130, 630 p.

Radke, B. &. (1980). On the formation and occurence of saddle dolomite. Journal of Sedimentary Petrology, 50(4), 1149-1168.

Roedder, E. &. (1968). Experimental evidence that fluid inclusion do not leak. Economic Geology, 63 (7), 715.

Romine, K. &.-S. (2003). Regional Seismic Interpretation.: West Deformation Front, South Oman Salt Basin, SRK Project. Internal PDO Report.

Romine, K. S.-S. (2004). North Oman Haima-Huqf Tectononostratigraphy Study, SRK Project. Internal PDO Report .

RosalieTostevin., G. A. (2016). Effective use of cerium anomalies as a redox proxy in carbonate-dominated marine settings. Chemical Geology; Volume 438, 2 November, Pages 146-162.

Schroder, S. (2000). Reservoir quality prediction in Ara Group carbonates of the South Carbonate Platform, South Salt Basin.

Sophia Gold, 2. (2010). Ediacaran–Cambrian Sirab Formation of the Al Huqf region, Sultanate of Oman. GeoArabia, 49–98.

Stuart-Smith, P. &. (2003). Regional Tectonostratigraphy of Oman: An Intergrated Potentiel Field Interpretation Study SRK Project . Internal PDO Report.

Tucker, M. &. (1990). Carbonate Sedimentology. Blackwells. Oxford.

Tucker, M. (1983). Diagenesis, geochemistry, and origin of a Precambrian dolomite; the Beck Spring Dolomite of eastern California. Journal of Sedimentary Research, 53 (4), 1097-1119.

Tucker, M. (1986). Formerly aragonitic limestones associated with tillites in the Late Proterozoic of Death valley, California. Journal of Sedimentary Research,56 (6), 818-830.
Veizer, J. (1983b). Trace elements and isotopes in sedimentary carbonates. Reviews in Mineralogy and Geochemistry, 11 (1), 265-299.

Veizer, J. C. (1992). Geochemistry of Precambrian carbonates: IV. Early Paleoproterozoic (2.25 ±0.25 Ga) seawater. Geochim. Cosmochim. Acta, 56, 875-885.

Zhang, J. L. (1997). Carbon isotope profiles and their correlation across the Neoproterozoic-Cambrian boundary interval on the Yangtze Platform, Chine. Bulletin of National Museum of Natural Science, 10, 107 - 116.

Zhum, M. B. (2006). Advances in Cambrian stratigraphy and paleontology: Integrating correlation techniques, paleobiology, taphonomy and paleoenvironmental reconstruction. Palaeoworld, 15 (3-4), 217-222.

Zhum, M. Z. (2004.). Evolution of C isotopes in the Cambrian of China: implications for Cambrian subdivision and trilobite mass extinctions. Geobios, 37 (2), 287-301.